INAUGURAL–DISSERTATION

zur
Erlangung der Doktorwürde
der
Naturwissenschaftlich-Mathematischen Gesamtfakultät
der
Ruprecht-Karls-Universität
Heidelberg

vorgelegt von

Biologe Marcelo de Araujo Carvalho, MSc

aus Rio de Janeiro

2001

Paleoenvironmental reconstruction based on palynological and palynofacies analyses of the Aptian-Albian succession in the Sergipe Basin, northeastern Brazil

Gutachter: Prof. Dr. Peter Bengtson
Priv.–Doz. Dr. Eduardo A. M. Koutsoukos

Promotionsdatum 12.06.2001

For my daughter Dominique
and my mother Marly

Acknowledgements

This study has been carried out at the Institute of Geology and Paleontology of the University of Heidelberg and supported by a German Academic Exchange Service (DAAD) scholarship, which is gratefully acknowledged. My special thanks go to *Frau* Helga Wahre.

I wish to express my sincere appreciation to Prof. Dr. Peter Bengtson for his supervision and guidance of my doctoral research. My thanks also go to Priv.-Doz. Dr. Eduardo A. M. Koutsoukos (Petrobras, Brazil), my co-supervisor, for discussions and advice throughout the research.

I would like to express my gratitude to C. C. Lana, MSc (Petrobras, Brazil), Prof. Dr. Below (University of Cologne, Germany) and M. Regali (Petrobras, Brazil) for their help in solving taxonomic and biostratigraphic problems. Special thanks go to E. Pedrão, MSc (Petrobras, Brazil) for her invaluable help.

I wish to thank Dr. H. Jäger (Universität of Heidelberg, Germany) for comments and suggestions about the palynofacies.

I would like to express my gratitude to Priv.-Doz. Dr. Noor Farsan (University of Heidelberg, Germany) for his help.

I would like to express my thanks to the Petrobras geologists in Sergipe (Brazil), G. A. Hamsi Jr., P. C. Galm, .P. R. Santos, and in particular Dr. W. Souza Lima for discussions about geological problems.

I also wish to thank the Petrobras geologists of the Section for Biostratigraphy and Paleoecology (Rio de Janeiro, Brazil), Dr. M. C. Vivers, Dr. R. Antunes, Dr. R. Dino, M. Arai, MSc and J. Guzzo, MSc. Special thanks go to Valéria C. Condé, MSc (Petrobras, Brazil) and to Geochemistry Section of Petrobras (Rio de Janeiro, Brazil) for providing the geochemical analyses.

I would like to express my thanks to M. A. Medeiros, MSc (Universidade Estadual do Rio de Janeiro) for his assistance on sequence stratigraphy matters.

I am particularly grateful to G. Li, Dr. S. Walter, P. Schlicht, Sattler, D. and my Brazilian friends Dr. G. Fauth, S. Becker Fauth and E. Andrade. Special thanks go to Susana Bengtson for her inestimable help.

Very special thanks go to Dr. J. Seeling for his cooperation and many helpful discussions.

Last but not least, my love and thanks to my daughter Dominique for her patient wait for her father to return home to Brazil.

Abstract

Palynological and palynofacies analyses were carried out on 272 core samples from two wells (GTP-17-SE and GTP-24-SE) in the Sergipe Basin with the aim of reconstruction the paleoenvironment of the upper Aptian–middle Albian interval.

The succession studied comprises the Muribeca and Riachuelo formations. The Muribeca Formation (Ibura and Oiteirinhos members) represents the transitional phase between the continental and marine regime and the Riachuelo Formation (Angico and Taquari members) the open marine phase.

The palynomorphs were identified, recorded (qualitative analysis) and counted (quantitative analysis). Paleoecological investigations were carried out using on multivariate statistical methods (cluster analysis and Pearson correlation) to determine the ecological similarity between palynomorph assemblages of different depositional settings. In addition, Palynological Marine Index (PMI), the Peridinioid to Gonyaulacoid ratio (P/G ratio) and paleoclimatic analyses were employed.

For the palynofacies analysis the kerogen categories were counted and submitted to cluster analyses (r and q-mode). In addition, geochemical study (Total Organic Carbon determination, Rock-Eval pyrolysis and fluorescence) based on a total of 140 samples from well GTP-24-SE was carried out. For a detailed marine environmental analyses, kerogen distribution trends and parameters were applied, based on percentages of kerogen categories.

The succession studied yielded a rich palynomorph assemblage, in particular terrestrial components. Altogether 17 genera and 19 species of spores, 24 genera and 31 species of pollen grains, 17 genera and 20 species of dinocysts were identified. Moreover, one genus of Acritarcha and one genus of fresh-water algae were recorded.

The preservation of the palynomorphs is variable, ranging from moderately to well preserved for the miospores and from poorly to moderately preserved for the dinocysts.

The sections are clearly dominated by the pollen group, in particular gymnosperms, which is by far the most abundant group in the two wells studied. This group forms 84.7% in GTP-17-SE and 61.8% in GTP-24-SE of the total palynomorph assemblage. In well GTP-17-SE the second most abundant group is the spores which reach a value of 8.9% of all palynomorphs. Well GTP-24-SE is characterized by a relatively high abundance of marine palynomorphs with 31.7% of the total palynomorphs. Fresh-water palynomorphs are rare, although less so in well GTP-24-SE (0.1%).

The upper Aptian *Sergipea variverrucata* Zone, *Equisetosporites maculosus* and *Dejaxpollenites microfoveolatus* sub-zones and middle Albian *Classopollis echinatus* Zone were recognized. The absence of the *Cardiongulina elongata*, *Brenneripollis reticulatus* and *Retiquadricolpites reticulatus* sub-zones and the *Steevesipollenites alatiformis* Zone of the uppermost Aptian to lower middle Albian indicates a possible hiatus.

The cluster analysis based on the abundance and composition of all 60 palynomorph genera revealed four superclusters, which represent different palynological assemblages. The stratigraphic distribution of these assemblages allowed the definition of seven ecophases.

The relative abundance of spores and the genus *Classopollis* indicates for a predominantly arid paleoclimate. However, these conditions tend to decrease upwards in sequence, changing to tropical climates.

The stratigraphic distribution of palynofacies associations that defined eight palynofacies units in well GTP-17-SE and ten in well GTP-24-SE reflects a continuous terrestrial influx (moderate to very high abundances of phytoclasts) throughout the succession. The amorphous organic matter (AOM) and palynomorph groups show moderate to high abundances, in particular in well GTP-24-SE. The increase in abundance of these groups indicates a transgression or a decreasing terrestrial influx in the area.

The palynological and palynofacies analyses of the successions studied allowed detailed environmental reconstruction. The succession is characterized by a long-term transgressive trend, recognizable in the ecophases and palynofacies units. Six depositional environments were recognized: a brackish lagoonal to lagoonal coastal plain environment, intertidal-nearshore (GTP-17-SE) and shallow-neritic (GTP-24-SE), intertidal to shallow marine (GTP-17-SE) and shallow-neritic (GTP-24-SE), shallow marine (GTP-17-SE) and middle-neritic (GTP-24-SE), and intertidal to shallow marine (GTP-17-SE) and shallow-neritic (GTP-24-SE). The paleoenvironmental evolution reflects the progressively increasing marine influence into the area. The results confirm that the change from a brackish lagoon to open marine environment was controlled by sea-level during the deposition of the Muribeca Formation, and predominantly by a progressive sea-level rise during the beginning of the deposition of Riachuelo Formation.

Kurzfassung

Anhand von 272 Proben aus zwei Bohrungen (GTP-17-SE und GTP-24-SE) im Sergipe-Becken wurden palynologische und palynofazielle Untersuchungen durchgeführt. Ziel war eine Rekonstruktion der Umweltverhältnisse des Intervals vom oberen Apt bis mittleren Alb.

Die Abfolge umfasst die Muribeca Formation und die Riachuelo Formation. Die Muribeca Formation (Ibura und Oiteirinhos Member) repräsentiert hierbei die Übergangsphase zwischen kontinentalen und marinen Bedingungen, während die Riachuelo Formation (Angico und Taquari Member) unter offen marinen Bedingungen abgelagert wurde.

Die Palynomorphen wurden identifiziert und sowohl qualitativ als auch quantitativ analysiert. Palökologische Untersuchungen wurden mit Hilfe von Methoden der multivariaten Statistik (Kluster-Analyse, Pearson-Korrelation) durchgeführt, um ökologische Zusammenhänge zwischen dem Auftreten der Palynomorphen und den verschiedenen Ablagerungsräumen zu finden. Darüberhinaus wurden der *Palynological Marine Index* (PMI), das Peridinoid zu Gonyaulacoid Verhältnis und die Paläoklima Analyse benutzt.

Für die Palynofazies-Analyse wurden die Kerogen-Kategorien gezählt und einer Kluster-Analyse unterzogen (r- und q-mode). Daneben wurden geochemische Untersuchungen durchgeführt (TOC, Pyrolyse, Floureszenz), die auf 258 Proben der Bohrung GTP-24-SE basieren. Für die umfassende Analyse der Umweltbedingungen wurden die Kerogenverteilungen und –charakteristika herangezogen, wobei die prozentualen Anteile der Kerogen-Kategorien zu Grunde gelegt wurden.

Die Abfolge beinhaltet eine reiche Vergesellschaftung von Palynomorphen, innerhalb derer die terrestrische Komponenten überwiegen. Insgesamt wurden 17 Gattungen und 19 Arten von Sporen, 24 Gattungen und 31 Arten von Pollen und 17 Gattungen mit 20 Arten von Dinoflagellatenzysten unterschieden. Daneben konnte eine Acritarchen Art und eine Gattung von Süßwasseralgen identifiziert werden. Der Erhaltungszustand der Palynomorphen ist sehr variabel. Er reicht von mäßig bis sehr gut bei den Miosporen und von schlecht bis mäßig bei den Dinoflagellatenzysten.

Die Profile werden von Pollen dominiert, insbesondere von Gymnospermen, der mit Abstand häufigsten Gruppe in beiden Bohrungen. Sie stellen 84,7% der gesamten Palynomorphen in GTP-17-SE und 61,8% in GTP-24-SE. In Bohrung GTP-17-SE bilden Sporen mit einem Anteil von 8,9 % die zweithäufigste Gruppe. Bohrung GTP-24-SE ist durch eine große Häufigkeit (31,7%) von marinen Palynomorphen gekennzeichnet. Süßwasser Formen sind sehr selten, aber etwas häufiger in GTP-24-SE (0,1%).

Die *Sergipea variverrucata* Zone, die *Equisetosporites maculosus* und die *Dejaxpollenites* microfoveolatus Subzonen des oberen Apt und die *Classopollis equinatus* Zone des mittleren Alb wurden nachgewiesen. Das Fehlen der *Cardiongulina elongata* , *Brenneripollis reticulatus* und der *Retiquadricolpites reticulatus* Subzonen und der *Steevesipollenites alatiformis* Zone des obersten Apt bis unteren Mittel-Alb deuten auf einen möglichen Hiatus hin.

Die Kluster-Analyse, basierend auf der Häufigkeit und der Zusammensetzung aller 60 Gattungen von Palynomorphen, erzeugte vier Superkluster, die verschiedene palynologische Vergesellschaftungen repräsentieren. Die stratigraphische Verbreitung dieser Vergesellschaftungen ermöglichte die Definition von sieben Ökophasen. Die relative Häufigkeit von Sporen und der Gattung *Classopollis* weisen auf ein vorwiegend arides Klima hin. Dies nimmt zum Hangenden hin ab und wechselt zu eher tropisch warmen Bedingungen.

Die stratigraphische Verbreitung der Palynofazies-Vergesellschaftungen, die durch acht Palynofazies-Einheiten in Bohrung GTP-17-SE und zehn in Bohrung GTP-24-SE repräsentiert werden, zeigen einen kontinuierlich terrestrischen Einfluß (mäßige bis sehr große Häufigkeiten von Phytoklasten) durch die gesamte Abfolge hindurch. Die amorphen organischen Bestandteile und die Palynomorphen zeigen mäßige bis große Häufigkeiten, insbesondere in Bohrung GTP-24-SE. Der Anstieg der Häufigkeiten dieser Gruppen weist auf eine Transgression oder auf einen abnehmenden terrestrischen Einfluß auf das Gebiet hin.

Die palynologische und palynofazielle Untersuchung der Bohrungen erlaubte eine detaillierte Rekonstruktion der Ablagerungsverhältnisse. Durch die Abfolge der Palynofazies-Einheiten und der Ökophasen ist ein langanhaltender transgressiver Trend erkennbar. Sechs sedimentäre Einheiten können unterschieden werden: brackisch-lagunär, küstennah-lagunär, intertidal–tiefes supratidal (GTP-17-SE) und flach-neritisch (GTP-24-SE), intertidal bis flach-marin (GTP-17-SE) und flach-neritisch (GTP-24-SE), flach-marin (GTP-17-SE) und mittel-neritisch (GTP-24-SE), und intertidal bis flach-marin (GTP-17-SE) und flach-neritisch (GTP-24-SE).

Die Entwicklung innerhalb der Abfolge macht den sich zunehmend verstärkenden marinen Einfluß auf das Untersuchungsgebiet deutlich. Die Ergebnisse bestärken, daß der Wechsel von brackisch-lagunären zu offen marinen Verhältnissen auf Meeresspiegelschwankungen während der Ablagerung der Muribeca Formation zurück zu führen ist. Der Beginn der Ablagerung der Riachuelo Formation wurde ebenfalls durch einen progressiven Meeresspiegelanstieg gesteuert.

Resumo

Análises palinológicas e de palinofácies de dois poços perfurados na Bacia de Sergipe foram realizadas usando 272 amostras de testemunhos do intervalo Aptiano superior–Albiano médio.

Nas seções estudadas foram registradas duas formações: Muribeca (membros Ibura e Oiteirinhos), que representa a fase transicional; Riachuelo (membro Angico e Taquari) o início da fase marinha aberta.

A análise palinológica foi baseada na identificação, registro (análise qualitativa) e contagem (análise quantitativa) dos palinomorfos. Os palinomorfos foram usados na investigação paleoecológica realizada através da métodos estatísticos (análise de agrupamento e correlação de Pearson) com o objetivo de identificar similaridades ecológicas entre as associações de palinomorfos de diferentes sistemas deposicionais. Além disso, foram usados o *Palynological Marine Index* (PMI), razão entre peridinióides e gonialacóides (P/G) e análises paleoclimáticas.

Para a análise de palinofácies, as categorias de querogenos foram contadas e submetidas à análise de agrupamento (modo R e Q). Além disso, foram realizadas análises de geoquímica (Carbono Orgânico Total, pirólise e fluorescência) baseadas em 140 amostras do poço GTP-24-SE. Para uma análise de palinofácies mais detalhada foram usadas as tendências e parâmetros de palinofácies.

Foram registrados 17 gêneros e 19 espécies de esporos, 24 gêneros e 31 espécies de polens, 17 gêneros e 20 espécies de dinoflagelados. Além disso um gênero de Acritarca e um gênero de alga dulcícola foram registrados.

A análise quantitativa palinológica mostra claramente que a seção é dominada pelo gimnospermas que formam 84,7% do total de palinomorfos no poço GTP-17-SE e 61,8% no GTP-24-SE. No poço GTP-17-SE o segundo grupo mais abundante são os esporos (8,9% de todos os palinomorfos). A seção do poço GTP-24-SE é caracterizada palinológicamente pela abundância dos palinomorfos marinhos (37,7% de todos os palinomorfos).

Neste estudo foram reconhecidas a Zona *Sergipea variverrucata* e as subzonas *Equisetosporites maculosus* e *Dejaxpollenites microfoveolatus* correspondentes à idade neo-Aptiano e a Zona *Classopollis echinatus* correspondente ao Albiano médio. A ausência das subzonas *Cardiongulina elongata*, *Brenneripollis reticulatus* and *Retiquadricolpites reticulatus* e a Zona *Steevesipollenites alatiformis* do intervalo do topo do Aptiano superior–Albiano inferior indica um possível hiato.

A análise de agrupamento baseada na abundância e composição de todos os gêneros de palinomorfos, revelou quatro super-agrupamentos que representam os diferentes tipos de associações. A distribuição estratigráfica destes tipos permitiu definir sete ecofases.

A abundância relativa dos esporos e de polens de *Classopollis* é evidência de um paleoclima predominantemente árido durante a deposição da seção estudada. No entanto, essas condições tendem a diminuir, mudando para um clima tropical.

A distribuição estratigráfica de associações de palinofácies que definiu oito unidades palinofaciológicas no poço GTP-17-SE e dez no poço GTP-24-SE, indica um influxo contínuo de material terrestre em toda seção.

Os grupos de materia orgânica amorfa (AOM) e palinomorfos mostram, principalemnte no poço GTP-24-SE, uma abundância moderada a alta. O aumento da abundância desses dois grupos indica uma provável transgressão ou diminuição do influxo terrígeno na área estudada.

As análises palinológica e de palinofácies na seção estudada permitiu uma reconstrução detalhada dos ambientes.

A seção é caracterizada por uma tendência transgressiva reconhecida nas ecofases e nas unidades palinofaciológicas. Seis ambientes deposicionais foram reconhecidos: laguna a planície costeira de laguna; intermaré a proximal para o poço GTP-17-SE e nerítico raso no GTP-24-SE), intermaré a marinho raso (GTP-17-SE) e marinho raso (GTP-24-SE); marinho raso (GTP-17-SE) e nerítico médio (GTP-24-SE) e intermaré a marinho raso (GTP-17-SE) e nerítico raso (GTP-24-SE). A evolução paleoambiental da seção estudada reflete a preogressiva influência marinha na área Os resultados obtidos confirmam que a mudança de um ambiente lagunar para marinho aberto foi controlado pelas mudanças do nível do mar e pelo tectonismo relacionado à separação dos continentes africano e sul-americano.

ACKNOWLEDGEMENTS

ABSTRACT

KURZFASSUNG

RESUMO

CHAPTER 1 INTRODUCTION **1**

CHAPTER 2 THE SERGIPE BASIN **3**

2.1 LOCATION 3
2.2 STRUCTURAL FRAMEWORK 4
2.3 TECTONIC-SEDIMENTARY EVOLUTION AND LITHOSTRATIGRAPHY 4
2.4 CRETACEOUS SEQUENCE STRATIGRAPHY OF THE SERGIPE BASIN 7

CHAPTER 3 MATERIAL AND METHODS **11**

3.1 MATERIAL 11
3.2 METHODS 12
3.2.1 Sampling *12*
3.2.2 Palynological analysis *12*
3.2.3 Paleoecological analysis *13*
3.2.4 Palynofacies analysis *16*
3.2.5 Geochemical analysis *23*

CHAPTER 4 STRATIGRAPHY AND LITHOFACIES **25**

4.1 LITHOSTRATIGRAPHY 25
4.2 EVOLUTION OF DEPOSITIONAL ENVIRONMENTS 26
4.2.1 Transitional phase *26*
4.2.2 Open marine phase *30*
4.3 LITHOFACIES 32

CHAPTER 5 PALYNOLOGY **34**

5.1. QUALITATIVE ANALYSIS 34
5.2. SYSTEMATIC PALYNOLOGY 34
5.3 QUANTITATIVE ANALYSIS 49
5.3.1 Palynomorph abundance *49*

CHAPTER 6 BIOSTRATIGRAPHY **57**

6.1 PALYNOMORPH ZONATION 59

CHAPTER 7 PALEOECOLOGY **64**

7.1 PALYNOLOGICAL ASSEMBLAGES 64
7.2 ECOPHASES 68
7.3 PALYNOLOGICAL MARINE INDEX (PMI) 72
7.4 P/G RATIO 72

7.5 PALEOCLIMATIC IMPLICATIONS 75

CHAPTER 8 PALYNOFACIES ANALYSIS 78

8.1 PALYNOFACIES ASSOCIATIONS 78

8.2 PALYNOFACIES UNITS 82

8.2.1 Palynofacies units of well GTP-17-SE........ 83

8.2.2 Palynofacies units of GTP-24-SE 93

8.3 EFFECTS OF LITHOLOGY ON THE KEROGEN DISTRIBUTION 107

CHAPTER 9 GEOCHEMICAL ANALYSIS 111

9.1 TOTAL ORGANIC CARBON (TOC) 111

9.1.2 TOC and lithology 112

9.2 HYDROGEN AND OXYGEN INDICES (ROCK-EVAL PYROLYSIS) 112

9.3 ORGANIC FACIES CHARACTERIZATION 113

9.4 KEROGEN FLUORESCENCE 113

CHAPTER 10 PALYNOFACIES AND SEQUENCE STRATIGRAPHY 116

10.1 PALYNOFACIES AND SEQUENCE STRATIGRAPHY 116

10.2 RESULTS 119

10.2.1 Sequence stratigraphic subdivision based on palynofacies........ 119

CHAPTER 11 PALEOENVIRONMENTAL INTERPRETATION 124

11.1 INTERPRETATION OF THE DEPOSITIONAL HISTORY 125

CHAPTER 12 CONCLUSIONS 133

CHAPTER 13 REFERENCES 136

PLATES

APPENDICES

CHAPTER 1
INTRODUCTION

The Sergipe Basin (Figure 1) contains one of the most extensive marine middle Cretaceous carbonate successions among the northern South Atlantic basins. The Aptian-Albian succession of the basin is represented by a mixed carbonate-siliciclastic platform system (Muribeca and Riachuelo formations), corresponding to a transitional phase between the rift phase and the beginning of the open marine phase. These phases reflect the progressive separation of the African and South American continents, which led to marine ingressions basins of the continental margin. However, on a short-term view variations of the sea-level curve are observed and hence variations in local paleoenvironments. The interpretation of these different paleoenvironments using palynology and palynofacies analyses is the main topic of the studies presented herein.

The study is based on the succession recovered from two wells (GTP-17-SE and GTP-24-SE) in the onshore part of the basin (Figure 2).

Palynology has several applications in geology, for example chronostratigraphy, biostratigraphy, and paleoclimatology. Among these applications, the use of palynomorphs and their paleoecology for paleoenvironmental reconstruction has been particularly developed.

Palynofacies analysis is an interdisciplinary approach in that not only the palynomorphs in the palynological slides are investigated, but the entire organic content of the slides. The particles are viewed as sedimentary components that reflect original conditions in the source area and the depositional environments. In this study palynofacies and their distribution were analyzed to understand the evolution of the paleoenvironments. Special attention was paid to the interpretation of changes in sea-level and possible links with climatic changes. Moreover, the palynofacies distribution from the two studied wells (GTP-17-SE and GTP-24-SE) is supplemented by investigations based on palynology, its ecological significance, geochemical characterization, and sequence stratigraphy.

The objective of this study was to reconstruct the paleoenvironment on the basis of integration of palynology and palynofacies analysis. To achieve these aims following palynological investigations were carried out:

- Determination of the stratigraphically diagnostic palynomorphs, in particular the dinoflagellates.

- Paleoecological study based on palynomorphs.

- Paleoclimatic reconstruction based on palynomorphs.

- Palynological kerogen classification, to support the identification of palynofacies.

- Identification of palynofacies intervals in the studied.

- Integration of palynology, sedimentology and palynofacies data.

CHAPTER 2
THE SERGIPE BASIN

2.1 Location

The Sergipe Basin, which forms the southern part of the Sergipe-Alagoas Basin in northeastern Brazil, is a structurally elongated marginal basin between latitude 9° and 11°30 S, and longitude 37° and 35 ^{o} 30 W. Onshore the basin is 16-50 km wide and 170 km long and covers an area of 6000 km^{2} and the offshore portion comprises an area of ca. 5000 km^{2} (Figure 2.1).

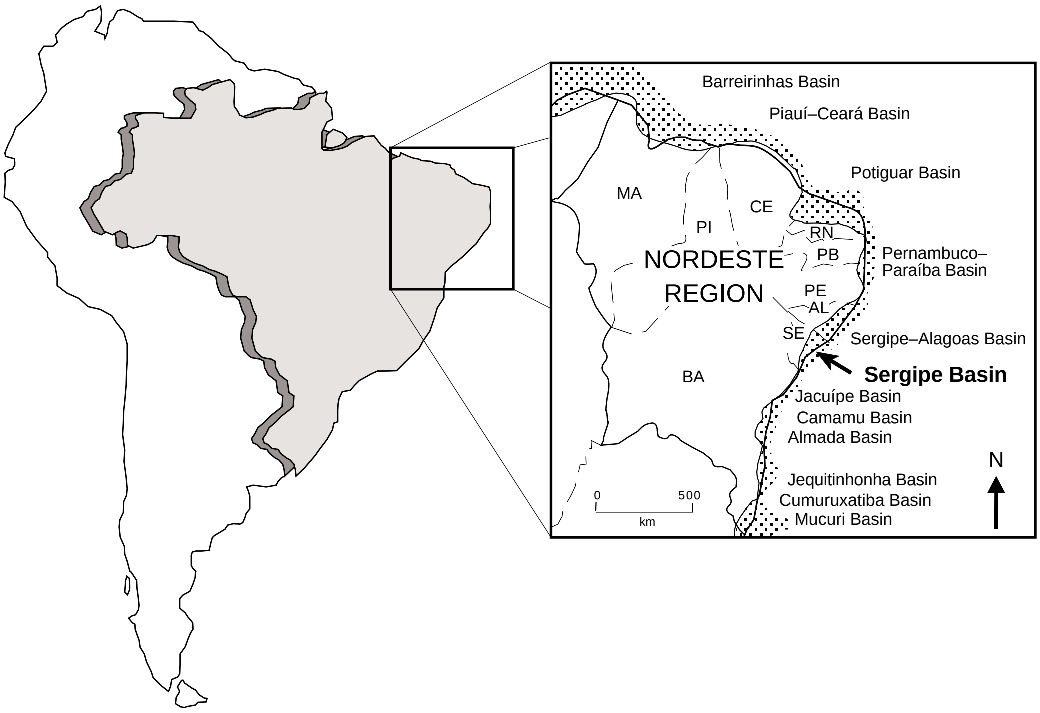
Barreirinhas Basin
Piauí–Ceará Basin
Potiguar Basin
MA
CE
PI
RN
PB
Pernambuco–Paraíba Basin
NORDESTE REGION
PE
AL
SE
Sergipe–Alagoas Basin
Sergipe Basin
BA
Jacuípe Basin
Camamu Basin
Almada Basin
N
Jequitinhonha Basin
Cumuruxatiba Basin
Mucuri Basin
0
500
km

Figure 2.1. Location map of the marginal basins of northeastern Brazil (from Seeling 1999).

The basin is limited on the continent by a system of normal faults, and offshore by the continental slope; by the Japoatã-Penedo High to the north and by the Jacuípe Basin to the south. In the southwest lies the Estância platform (Figure 2.2), where only a thin sedimentary record of Cretaceous marine deposits is found (Schaller, 1970; Bengtson, 1983; Koutsoukos *et al.*, 1991).

2.2 Structural framework

The principal structural feature of the Sergipe Basin is a series of half-grabens with a regional dip averaging 10° to 15° to the southeast (Ojeda & Fugita, 1976). These are bounded by faults with an overall N-E and N-S orientation. The faults were formed during the Early Cretaceous as consequence of the rupture of the African-South American continent. The structural framework of the basin consists of large-scale tilted fault blocks with a N-S trend, which originate the structural lows and highs in the basin (Figure 2.2).

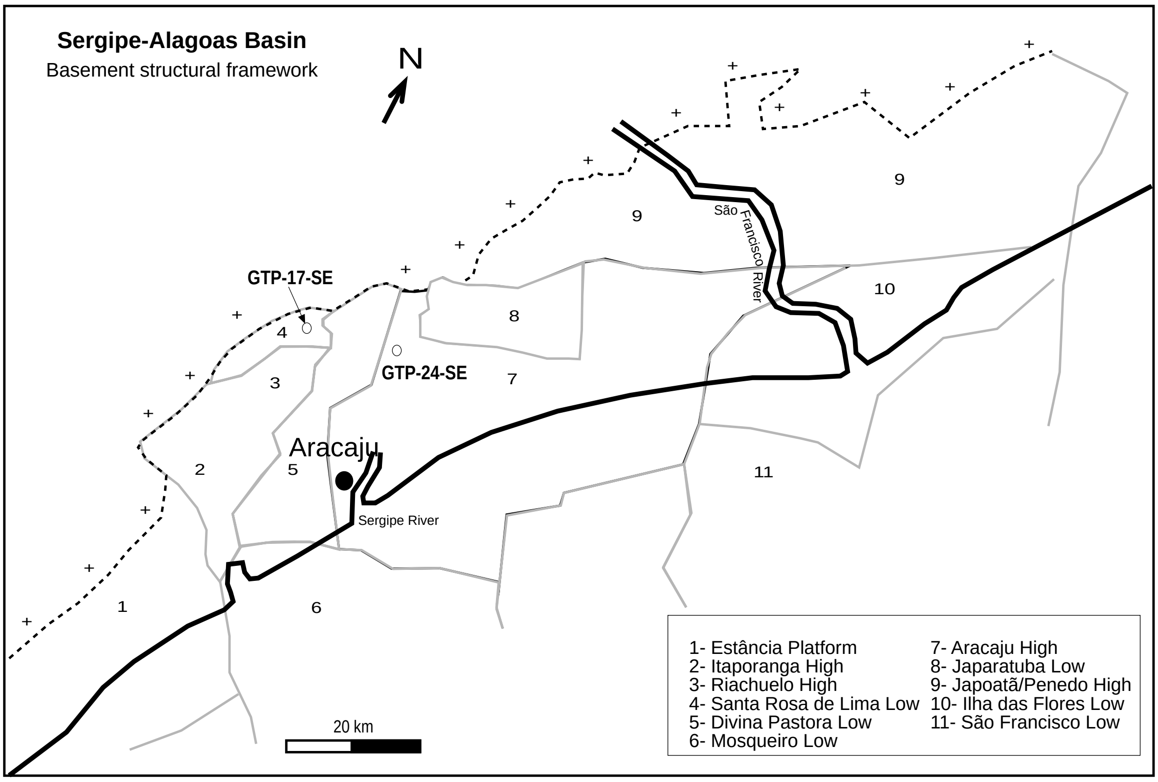
Sergipe-Alagoas Basin
Basement structural framework
N
GTP-17-SE
GTP-24-SE
Aracaju
São Francisco River
Sergipe River
1
2
3
4
5
6
7
8
9
9
10
11
20 km
1- Estância Platform
2- Itaporanga High
3- Riachuelo High
4- Santa Rosa de Lima Low
5- Divina Pastora Low
6- Mosqueiro Low
7- Aracaju High
8- Japaratuba Low
9- Japoatã/Penedo High
10- Ilha das Flores Low
11- São Francisco Low

Figure 2.2. Basement structural framework of the Sergipe Basin and southern part of Alagoas Basin (adapted after Cainelli *et al*., 1987, and Koutsoukos *et al*., 1991).

2.3 Tectonic-sedimentary evolution and lithostratigraphy

The Sergipe Basin belongs to the class of sedimentary basins related to passive continental margins. The evolution of the basin has attracted the attention of many workers, for example Ojeda & Fugita (1976), Ojeda (1982), Chang *et al*. (1988) and Lana (1990).

According to Ojeda & Fugita (1976) and Ojeda (1982) the tectonic evolution of the Sergipe Basin can be divided into five main phases: intracratonic (Permo-Carboniferous), pre-rift (late Jurassic (?) to earliest Cretaceous), rift (earliest Cretaceous to early (?) Aptian), transitional (Aptian), and a marine drift phase (late Aptian to Recent) (Figure 2.3). The lithostratigraphic units formed during these phases are shown in Figure 2.3.

Intracratonic phase: Sedimentation began in the Carboniferous-Permian with coarse-grained glacial and fluvial clastics of the Igreja Nova Group, which rest on Pre-Cambrian basement.

Pre-rift phase: This phase is associated with crustal uplift and development of marginal depressions that antecede the rifting of the continental crust (Ojeda, 1982). During this phase the sediments of the Perucaba Group were deposited: fluvial fine to medium-grained sandstones of the Candeeiro Formation; lacustrine shales and claystones of the Bananeiras Formation, and medium to coarse arkoses and sandstones of the Serraria Formation deposited by fluvial systems with aeolian reworking.

Rift phase: This phase is characterized by the development of faults that were formed before the opening of the South Atlantic during the Early Cretaceous. The Igreja Nova Group is overlain by a megasequence, the Coruripe Group, deposited under tectonically unstable conditions, typical of rift phases. This megasequence is composed of five formations: the lower part consists of fluvial sandstones (Penedo Formation) and fine-grained clastics (Barra de Itiuba Formation) deposited in lagoonal environments. In the proximal portion of the basin coarse-grained sandstones were deposited by alluvial fans (Rio Pitanga Formation). Furthermore, in lagoonal environments clastic sediments were deposited (Coqueiro Seco and Ponta Verde formations).

Transitional phase: This phase represents the first marine ingressions in the area, beginning in the early Aptian with deposition of evaporites, clastics and carbonate sediments (Muribeca Formation) under relatively quiet tectonic conditions (Ojeda, 1982). The sediments were deposited in lagoonal-evaporitic environments. This transitional phase began with the conglomerates of Carmópolis Member deposited in a system infilled paleotopographic depressions and deltas fans (Koutsoukos, 1989). The Ibura Member, which overlies the Carmópolis Member, is represented by a succession of bituminous shales, soluble salts (anhydrite, halite, tachyhydrite, carnallite, and sylvinite) and dolomitic limestones (Koutsoukos, 1989). The Ibura evaporites reflect a transgressive facies, when large eroded areas were inundated and evaporitic basins developed (Ojeda, 1982). According to Della Fávera (1990), the evaporites were deposited in shallow-marine areas and on sabkha plain environments. The Oiteirinhos Member consists of intercalations of grey to black bituminous shales, limestones and siltstones. The Maceió Formation was deposited by alluvial fans to the SE of the basin. The sediments consist of arkoses intercalated with shales and halites.

		Groups and Formations (Feijó 1995)	Members (Feijó 1995)	Tectonic Phases (Feijó 1995)
Quaternary		Barreiras Formation		Open marine phase
Neogene	Pliocene			
	Miocene	Piaçabuçu Group		
Paleogene	Oligocene			
	Eocene			
	Paleocene			
Cretaceous	Maastrichtian			
	Campanian			
	Santonian			
	Coniacian	Cotinguiba Formation	Sapucari Aracaju	
	Turonian			
	Cenomanian			
	Albian	Riachuelo Formation	Maruim Taquari Angico	
	Aptian	Muribeca Formation Maceió Formation	Oiteirinhos Ibura Carmópolis	Transitional phase
	"Bahian"	Coruripe Group		Rift phase
Jurassic		Perucaba Group		Pre-rift phase
Carboniferous–Permian		Igreja Nova Group		Intracratonic

Figure 2.3. Summary of tectonic-sedimentary evolution of Sergipe Basin (adapted from Seeling 1999).

Open Marine phase (drift): As a result of the progressive separation of the African and South American continents, an open marine regime was established with the deposition of the Riachuelo Formation. This formation is represented by the Angico, Taquari and Maruim members.

The Angico Member is characterized by very fine-grained sandstones to conglomerates, interbedded with siltstones, shales and rare thin beds of limestone (Koutsoukos, 1989), deposited nearshore by cyclical flows of shallow siliciclastic turbidities (delta fans) (Koutsoukos *et al.* 1991).

Eastwards the Angico Member grades into the Taquari Member, which consists of rhythmically bedded, organic-rich, calcareous black shales and calcilutites. Fine-grained sediments of this member were deposited in lagoonal environments, near patch reefs and relatively distant from the coarse-grained siliciclastic deposits of the Angico Member. The fine carbonate sediments of this environment are composed of micritic mud formed by abrasion of the carbonate grains from patch reefs or produced by calcareous algae. The grainstone/packstone sedimentation in this area occurred through turbidity flows. The turbidities probably originated in patch reefs, by slumping or remobilizations caused by storms (Mendes, 1994).

The Maruim Member consists of carbonate packstones/wackestones, oolitic-oncolotic-peloidal grainstones and red algal patch-reefs.

The Riachuelo Formation is overlain by carbonates of low-energy environments of the Cotinguiba Formation. These sediments were deposited mainly in bathyal to abyssal depths (Feijó, 1995). The Cotinguiba Formation is overlain by the Piaçabuçu Group represented by shales (Calumbi Formation), calcarenites (Mosqueiro Formation) and medium to coarse-grained sandstones (Marituba Formation). The continental clastics of the Barreiras Formation cover much of the Cretaceous sedimentary record of the Sergipe Basin.

2.4 Cretaceous sequence stratigraphy of the Sergipe Basin

Sequence stratigraphy has been applied by a few workers to the Cretaceous of the Sergipe Basin, e.g. Feijó (1995), Mendes (1994), Pereira (1994) and Hamsi Junior *et al.* (1999). For the subdivision of the entire Cretaceous interval, based on depositional sequences, two models have been proposed, by Pereira (1994) and Feijó (1995), respectively.

Pereira (1994) established a stratigraphic framework for five continental marginal basins of Brazil, based on data from 100 wells and 5000 km of seismic lines. He subdivided the Cretaceous of Sergipe into eleven depositional sequences. The Albian-Maastrichtian interval was studied in more detail and 23 system tracts were distinguished. The sequences established by Pereira (1994) are summarized in Figure 2.4.

Stage	Sequences	Interpretation
lower Maastrichtian - uppermost Maastrichtian	MAiC-Ks	HST(?) TST LST
lower Campanian - upper Campanian	CAi/MAiC	HST(?) TST LST
upper Turonian - lower Campanian	TsC/CAi	HST(?) LST (slope fan) or LST/TST LST (basin floor fan)
middle Cenomanian - upper Turonian	CNm/TsC	HST TST
upper Albian - middle Cenomanian	ABsC/CNm	HST TST
middle Albian - upper Albian-lower Cenomanian	ABm/ABsC	LST HST TST(?)
upper Aptian-lower Albian - middle Albian	ALs/ABm	HST LST/TST
lower Aptian - upper Aptian-lower Albian	SBL/ALs	HST TST LST
upper Barremian - lower Aptian	Bs/SBL	HST TST
Hauterivian-lower Valanginian - upper Barremian	SBH-V/Bs	
Upper Jurassic - Hauterivian-lower Valanginian	JS-SBH/V	

Figure 2.4. Depositional sequences proposed by Pereira (1994) for the Cretaceous of the Sergipe Basin.

Feijó (1995) subdivided the Cretaceous succession into four major tectono-sedimentary sequences: pre-rift, rift, transitional and passive margin (Figure 2.5). He further subdivided these into twelve second-order sequences (K10-K120), which were subsequently subdivided using unconformities and correlative conformities. His work is the most recent summary on depositional sequences for the entire Cretaceous of the Sergipe Basin.

Stages	Major sequences	2nd-order sequences
Maastrichtian Santonian	Passive margin	K90 - K120
Santonian Cenomanian		K80
Cenomanian Albian		K60 - K70
upper Aptian	Transitional	K50
lower Aptian upper Barremian	Rift	K40
Barremian Hauterivian		K20 - K30
Valanginian Upper Jurassic	Pre-Rift	J- K10

Figure 2.5. Depositional sequences proposed by Feijó (1995) for the Cretaceous of the Sergipe Basin.

Mendes (1994) and Hamsi Junior *et al*. (1999) studied part of the Cretaceous interval and subdivided the succession on the basis of sequence stratigraphy. Mendes (1994) subdivided the uppermost Aptian-lowermost Cenomanian succession into three third-order sequences separated by three regional discontinues (D1-D3) (Figure 2.6). These sequences and their boundaries are also recognized in the wells studied herein (see Chapter 4).

Stages	Sequences	Lithostratigraphy
lower Cenomanian	III	
upper Albian		Riachuelo Formation
middle Albian lower Albian	II	
lower Albian upper Aptian	I	

Figure 2.6. Depositional sequences proposed by Mendes (1994) for part of the Cretaceous of the Sergipe Basin (modified from Mendes, 1994)

The most recent study using a sequence stratigraphic approach for the middle Cretaceous of the Sergipe Basin was carried out by Hamsi Junior *et al*. (1999). They assigned large-scale stratigraphic framework to the Marine Carbonate Megasequence, considered to be first-order cycle. According to Hamsi Junior *et al*. (1999) this megasequence ranges from the upper Aptian to the Coniacian. Within this megasequence, two second-order sequences are recognized, K60 and K70, including the systems tracts KM1, KM2, KM3 and KM4 of third order (Figure 2.7). The sequences were separated on the basis of regional discontinuities or major flooding surfaces identified in well logs and through biostratigraphic and geochemical data.

The KM1 sequence was interpreted by Hamsi Junior *et al*. (1999) as a transgressive systems tract (TST) in the upper Aptian (Muribeca Formation) possibly bounded below by an unconformity and above by a maximum flooding surface (mfs). KM2 represents the highstand systems tract (HST) of the second-order sequence K60. KM3 was interpreted as the TST of the second-order sequence K70, and KM4 is represented by a HST deposited discordantly over KM3.

Stages	Lithostratigraphy	Sequences		Systems tracts	Interpretation
Coniacian	Cotinguiba Formation	Marine Carbonate Megasequence	K70	KM4	Highstand Systems Tract
Turonian				KM3	Transgressive Systems Tract
Cenomanian					
Albian	Maruim Member, upper part of Taquari and Angico members		K60	KM2	Highstand Systems Tract
upper Aptian	Taquari Member, lower part of Angico Member			KM1	Transgressive Systems Tract
	Muribeca Formation				

Figure 2.7. Depositional sequences proposed by Hamsi Junior *et al*. (1999) for part of Cretaceous.

CHAPTER 3
MATERIAL AND METHODS

3.1 Material

The study was carried out using 272 core samples from two wells drilled by Petromisa/Petrobras (the Brazilian state-owned oil company) in the Santa Rosa de Lima and Taquari-Vassouras (between Rosário do Catete and Carmópolis cities) areas in Sergipe (Figure 3.1). The cores are stored at Petrobras, SEAL (Aracaju, Sergipe).

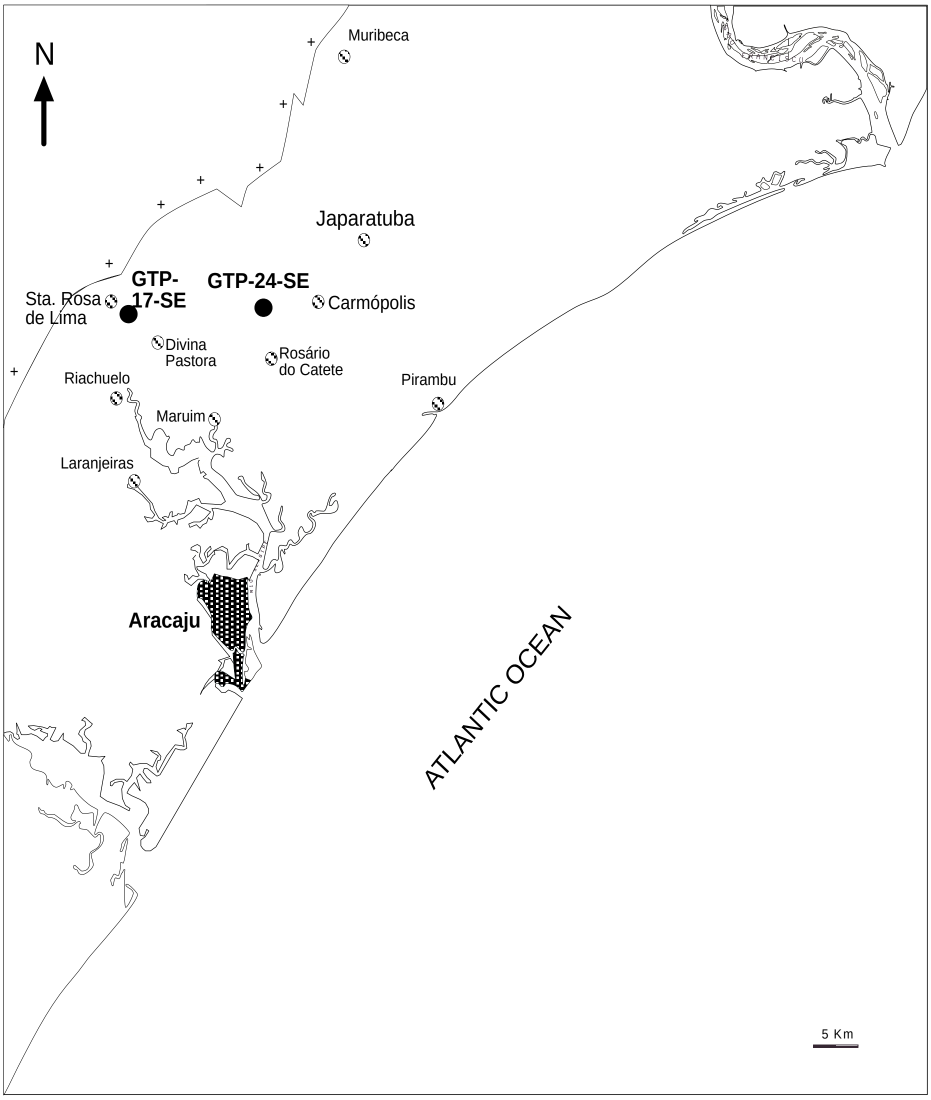
N
Muribeca
Japaratuba
GTP-17-SE
GTP-24-SE
Sta. Rosa de Lima
Carmópolis
Divina Pastora
Rosário do Catete
Riachuelo
Pirambu
Maruim
Laranjeiras
Aracaju
ATLANTIC OCEAN
5 Km

Figure 3.1. Map of Sergipe Basin showing the location of the two studied wells.

Although the basin contains a large number of wells, the two studied wells were selected because they are cored throughout (Table 3.1).

Table 3.1. Summary of data on the studied wells.

Well name	Coordinates (UTM)	Area	Samples (no.)	Thickness (m)
GTP-17-SE	x= 8.821.540 y= 698.950	Santa Rosa de Lima	159	452.95
GTP-24-SE	x= 8.822.240.52 y= 714.950.96	Taquari/Vassouras	113	397.26

3.2 Methods

3.2.1 Sampling

The cores were sampled at approximately every 3.9 m in well GTP-17-SE and every 2.5 m in GTP-24-SE (Figure 3.1). At important intervals, such as sequence boundary (based on Mendes, 1994) and the inferred Aptian–Albian boundary, two or more samples were collected per meter. In additions, samples were collected from all lithological varieties to enable the palynofacies analyses.

3.2.2 Palynological analysis

3.2.2.1 Sample preparation

The samples were prepared at the Research Center of Petrobras (CENPES), Rio de Janeiro, Brazil. The method applied of palynological preparation used by Petrobras was compiled by Uesugui (1979) after, e.g., Erdtman (1949), Erdtman (1969), and Faegri & Iversen (1966).

The objective of the palynological preparation is to destroy the mineral constituents by acids. As the samples were not oxidized, the same slides were used for palynological and palynofacies analyses. The following procedure was employed for all samples:

- Dilute hydrochloric acid (HCl) (32%) was added to the sample to remove any carbonate. After 3 hours when the reaction ceased, the acid was siphoned off and the sample was washed three times with distilled water to free it from HCl.

- Dilute cold hydrofluoric acid (HF) (40%) was added to the sample to remove any silicates. After 12 hours the residue was then washed several times.

- Dilute HCl (10%) was added to dissolve the fluorides, which might have formed in the residue.

The remaining residue was then sieved through a 10 µm nylon sieve prior to mounting on slides.

3.2.2.2 Qualitative analysis

The qualitative analysis consisted basically of the identification and recording of the palynomorphs in the samples. For this analysis 253 samples were used, a total of 101 from GTP-17-SE and 152 from GTP-24-SE. The samples were analyzed under a transmitted light microscope (Leitz Labor Lux S). The photographs were taken with an AXIOPLAN Zeiss with differential interference contrast (DIC) coupled to a MC 100 SPOT.

3.2.2.3 Quantitative analysis

The quantitative analysis was based on the first 200 palynomorphs counted for each slide. This analysis was the basis for the establishment of the palynomorph distribution. The number of palynomorphs that should be counted is controversial. Some authors (e.g., Dino, 1992; Hashimoto, 1995; Lana, 1997) follow proposals by Chang (1967), who first statistically demonstrated that the greater the number of counted individuals is, the better the sample is represented. However, as mentioned by Lana (1997, p. 11) when more than 100 palynomorphs are counted the standard deviation is not significantly altered. According to Chang (1967) the minimum number that must be counted for each sample is 30 individuals; therefore samples that did not reach this number were not used for quantitative analysis.

3.2.3 Paleoecological analysis

The paleoecological analysis was carried out using multivariate statistical methods (cluster analysis and Pearson correlation) to identify the ecological similarity between palynomorph assemblages from different depositional settings. In addition, the Palynological Marine Index (PMI), the Peridinioid to Gonyaulacoid ratio (P/G ratio) and paleoclimatic analysis were employed.

3.2.3.1 Cluster analysis

Cluster analysis was employed based on abundance and composition, in order to establish groupings and to recognize the relationship between the taxa (palynological analysis) and kerogens (palynofacies analysis). To identify the divisions of the studied succession based on palynology and the palynofacies approach, Q- and R-mode cluster analyses were performed on counts of palynomorphs and kerogen categories. This cluster analysis forms discrete groupings that are based on the characteristics (abundance) of the objects. The results are clearly displayed in dendrograms which, when combined, allowed assessment reasons for clustering.

3.2.3.2 Pearson coefficients

The Pearson coefficient (+/- 1) obtained from the relative abundance of palynomorphs, is used to yield a correlation matrix and to identify the relationship between the taxa. This coefficient reflects the presence or absence of similarity among the taxa. If coefficient approaching 1 implies a positive correlation and approaching -1, a negative correlation among the palynomorphs. Only the numerically and paleoecologically important taxa were used herein.

3.2.3.3 Paleoclimatic analysis

According to Lima (1983), in Cretaceous times the floras were significantly different from modern ones. Therefore, paleoclimatic reconstructions are based on the few species that survive to the present and on those extinct species that are closely related to extant ones.

The paleoclimatic investigations were based on selected palynomorphs that are well-known indicators of Cretaceous times. Moreover, the investigations were also based on abundance of the pollen grains of the genus *Classopollis* and fern spores. High abundance of *Classopollis* has been found to be related to arid environments (Srivastava, 1976; Vakhrameev, 1981; Doyle *et al.*, 1982; Lima, 1983). Vakhrameev (1981) proposed climatic belts based on abundance of *Classopollis*, where a low abundance (1-10%) of the genus indicates a temperate climate, 20-50% warm subtropical, and 60-100% semi-arid to arid conditions. In contrast, high abundance of fern spores reflects nearshore environments under humid conditions. This hypothesis is directly related to the importance of humidity on the reproductive-cycle of modern pteridophytes (Doyle *et al.* 1982; Lima, 1983).

3.2.3.4 Palynological Marine Index (PMI)

This index was created by Helenes *et al.* (1998) to support in the interpretation of depositional environments. PMI is calculated using the formula: PMI= (Rm/Rt + 1)100, where Rm is richness of marine palynomorphs (dinoflagellates, acritarchs and foraminiferal test linings) and Rt is the richness of terrestrial palynomorphs (pollens and spores) counted per sample. In the present study, the Rm and Rt were expressed as number of genera per sample. The genus level preferred because genera are more easily identified than species and the genera identified herein show the same environmental significance as species. The high values of PMI are interpreted as indicative of normal marine depositional conditions. When the samples have no marine palynomorphs the PMI value is 100.00.

3.2.3.5 Peridinoid to Gonyaulacoid ratio (P/G)

The peridinoid to gonyaulacoid ratio (P/G) introduced by Harland (1973) has been used to recognize paleosalinity variations and proximity to shorelines. The peridinioid-dominated assemblage reflects low salinity and nutrient-rich conditions (Jaminski, 1995) related to nearshore environments (lagoonal, brackish water). In contrast, low values of the ratio, i.e. gonyaulacoid-dominated assemblages indicate open marine environments. However, salinity is not the only factor that controls the dinoflagellate assemblage composition. According to some studies (e.g., Wall *et al.* 1977; Bujak, 1984; Powell *et al.* 1990; Lewis *et al.* 1990) the increase of peridinoid dinoflagellates is also attributed to upwelling. Lewis *et al.* (1990) mentioned that the P/G ratio is a useful indicator of upwelling strength.

The ratio is used herein the manner described by Lewis *et al.* (1990), using the formula **P-G/P+G**, where **P** is the number of peridiniacean cysts and **G** the gonyaulacacean cysts. According to them, a ratio approaching 1 implies dominance of peridiniacean cysts, and approaching -1, dominance of gonyaulacacean cysts.

3.2.4 Palynofacies analysis

3.2.4.1 Kerogen classification

A preliminary international classification of organic matter was discussed during a workshop on “Organic Matter Classification” in Amsterdam (Lorente & Ran 1991). In this workshop the organic matter was designated Palynological Organic Matter (POM). The POM was divided into four major groups: palynomorphs, structured debris, amorphous matter and indeterminate matter. These were then subdivided into several categories.

In the first monographic work on palynofacies Tyson (1995) revised (and reevaluated) the palynofacies terms. This author presented an informal classification (Tyson, 1995, p.350) close to the proposal presented in the workshop in Amsterdam. This classification is used herein (Figures 3.2-3.4) and kerogen categories are illustrated in Figure 3.5.

3.2.4.2 Kerogen categories

Amorphous Organic Matter (AOM) group

According to Tyson (1995) the AOM group consists of structureless particles that are observed under light microscopy. This group is composed of ‘AOM‘ and resin. The characteristics of the two subgroups are shown in Figure 3.2.

AOM Group	Origin	Description
"AOM"	Derived from phytoplankton or degradation of bacteria.	Structureless material. Color: yellow-orange-red; orange-brown; grey. Heterogeneity: homogeneous; with "speckles"; clotted; with inclusions (palynomorphs, phytoclasts, pyrite. Form: flat; irregular; angular; pelletal (rounded eleongate/oval shape).
Resin	Derived from higher plants of tropical and subtropical forest.	Structureless particle, hyaline, homogeneous, non-fluorescent, rounded, sharp to diffuse outline.

Figure 3.2. Classification of the amorphous organic matter (AOM) group used in this study (based on Tyson, 1995).

Phytoclast group

The phytoclast group consists of structured particles. This group is subdivided into two major subgroups: opaque and translucent. The opaque subgroup is subdivided into opaque-equidimensional (O-Eq) and opaque-lath (O-La). The translucent subgroup is subdivided into fungal hyphae (Fh), wood tracheid with visible pits (Wp), wood tracheid without visible pits (Ww), cuticles (Cu) and membranes (Mb) (Figure 3.3).

Zooclast group

The zooclast group consists of animal-derived fragments. According to Tyson (1995) most zooclast fragments include arthropod exoskeletal debris, organic linings from bivalve shells and ostracode carapaces.

Phytoclast Group		Origin	Description
Opaque	Equidimensional (O-Eq)	Derived from the ligno-cellulosic tissues of terrestrial higher plants or fungi.	Black particle from wood material. Long axis less than twice the short axis. Without internal biostructures.
	Lath (O-La)		Black particle from wood material. Long axis more than twice the short axis. Without internal biostructures.
Translucent	Wood tracheid with pits (Wp)		Brown particle from wood tracheid with visible pits.
	Wood tracheid without pits (Ww)		Brown particle from wood tracheid without visible pits.
	Cuticle (Cu)		Thin cellular sheets, epidermal tissue, in some case with visible stomates
	Membranes (Mb)		Thin, non-cellular, transparent sheets of probable plant origin.
	Fungal hyphae (Fh)	Derived from fungi	Individual filaments of mycelium of vegetative phase of eumycote fungi.

Figure 3.3. Classification of the phytoclast group used in this study (based on Tyson 1995).

Palynomorph group

The palynomorph group is subdivided into the sporomorph subgroup (Sm), which is further subdivided in spores and pollen grains; the phytoplankton subgroup (Pl), which consists of organic-walled microplankton and the zoomorph subgroup, composed of foraminiferal test linings (FTL) and scolecodonts (Figure 3.4).

3.2.4.3 Kerogen count

For a detailed paleoenvironmental study based on palynofacies, a count of the kerogen found in the slides is necessary. This count is presented as percentage (Appendix 3). According to Tyson (1995), the ideal count is 500 particles per sample using transmitted light microscopy.

In this study a total of 284 samples (117 samples from GTP-17-SE and 165 from GTP-24-SE) were studied. In each sample 500 particles were counted using transmitted light microscopy.

Palynomorph group		Origin	Description
Sporomorph subgroup	Spores	Terrestrial palynomorph produced by pteridophyte plants and fungi.	Triangular or circular palynomoph; Trilete spore with 3 laesurae (Y-mark); Monolete spore single laesura; varied ornamentation
	Pollen grains	Terrestrial palynomorph produced by Gymnosperm and Angiosperm plants.	*Palynomorphs with complex to simple morphology; usually spherical to subspherical shapes; with several ornamentation types; apertures may be present.
Zoomorph subgroup	Foraminiferal test linings	Organic linings of benthic foraminifera.	Chitinous linings; brown coloured; inner smaller chambers often darker.
	Scolecodonts	Mouth parts of some polychaete worms (mostly marine).	Chitinous tooth-like jaw, dark brown; size 100-1000 µm.
Phytoplankton subgroup	Acritarchs	Small microfossils of unknown and probably varied biological affinities.	Central cavity enclosed by a wall of single or multiple layers; fossils with various form and sculpturing, ranging from types resembling dinoflagellates to those resembling chitinozoans; Size 5-240 µm
	Dinoflagellate cysts	Resting cysts produced during the sexual part of the life cycle of Class Dinophyceae survives.	Main feature is the paratabulation which divides the theca and cyst in rectangular or polygonal plates separated by sutures; 3 main morphologies: proximate, cavate and chorate; often with an opening (arceopyle) through which excystment occurs.
	Prasinophytes	Fossilising structures produced by small quadriflagellate algae (Division Pyrrhophyta).	Most, like Tasmanites, are spherical; diameter 50 to 2000 µm, smooth and thick-walled.
	Chlorococcale algae	Exclusively colonial freshwater algae (*Botriococcus* and *Pediastrum*)	*Botriococcus:* irregular globular colonies; size 30 to 2.000 µm, sometimes with several lobes; orange-brown. *Pediastrum*: radially-symmetrical colonial green algae; mostly 30-200 µm in diameter and with one or two horns on the outermost ring of cells. Inner cells may be irregularly-shaped with spaces between cells, or closely packed.

Figure 3.4. Classification of the palynomorph group used in this study (based on Tyson, 1995).

3.2.4.4 Kerogen distribution

In marine environments the proximal-distal trend is one of the most important controls on kerogen distribution. For a detailed marine environmental analyses several kerogen distribution trends and parameters have been used (cf. Tyson, 1993, 1995) (Figure 3.6). These trends and parameters are based on percentages of kerogen categories.

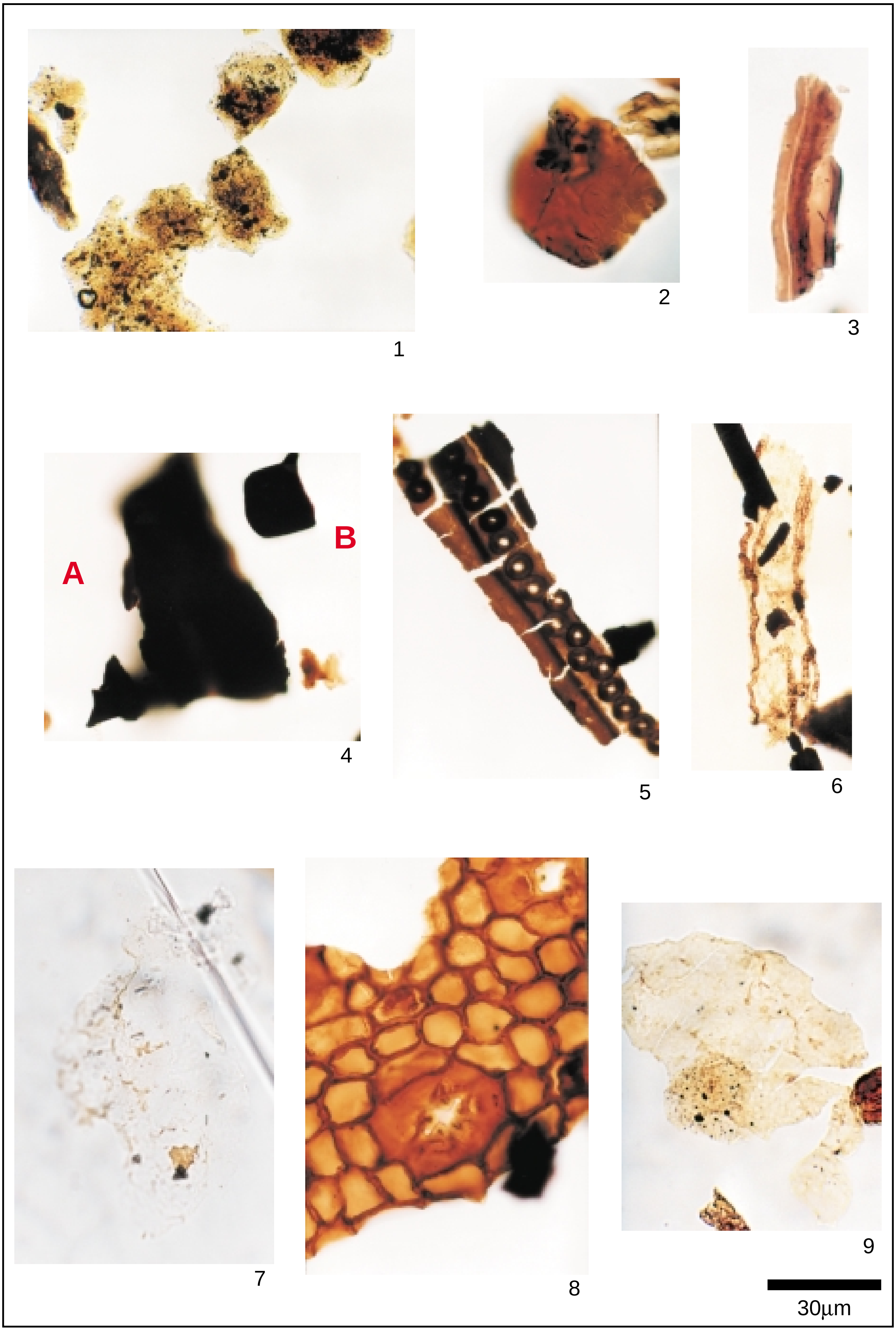

Figure 3.5. Kerogen categories. 1) AOM; 2) Resin (Re); 3) Wood tracheid without pits (Ww); 4) A- opaque lath (O-La), B- opaque equidimensional (O-Eq); 5) Wood tracheid with pits (Wp); 6) Fungal hyphae (Fh); 7) Membrane (Mb); 8) Cuticle; 9) Zooclast.

3.2.4.5 Kerogen trends

Percentage of ‘AOM‘ (of total kerogens)

A large amount of ‘AOM‘ results from a combination of high preservation rate and low-energy environments. The preservation of ‘AOM‘ is directly related to dysoxic conditions and consequently, but not necessarily, correlated to high primary productivity (Tyson, 1993). According to Tyson (1993) in carbonate facies the ‘AOM’ may be the only kerogen available for preservation.

Percentage of phytoclasts (of total kerogens)

High percentages of components the phytoclast group are mostly related to proximal depositional conditions. The main controlling factor is the short transport of the particles. Other factors, such as oxidizing conditions and the relative resistance of lining tissues are also associated with the proximity of the source area (Mendonça Filho, 1999). Generally, large amounts of phytoclast particles are deposited by rivers in estuaries and delta environments, both close to shorelines. However, deposition also occurs in deep waters, by turbidity currents (Habib, 1982).

Parameters	Environmental factors		
	Proximal-distal trend	Distal anoxic facies	Upwelling (with arid hinterland)
% phytoclast/kerogen	▶	▲	▲
% AOM/kerogen	◀	▲	▼
% palynomorph/kerogen	◀	▲	▼ ?
Opaque : translucent phytoclasts	◀	▼	▼ ?
% cuticle/ phytoclasts	▶	negligible	▲
% sporomorphs/palynomorphs	▶◀	▼	▲
Frequency of tetrads	▶	▼ ?	▲
% microplankton/palynomorphs	◀▶	▲	▼
Peridinoid : gonyulacoid dinocysts	▶	▲ ?	▼
Dinocyst species diversity	◀	▲	▲
Absolute dinocyst abundance	◀▶	▲	▼
Frequency of foraminiferal lining	▶	▲	▼

high-low ▶ high-low-high ▶◀ decreases ▲ may increase ▼ ?
low-high ◀ low-high-low ◀▶ increases ▼ may decrease ▲ ?

Figure 3.6. Some parameters used in palynofacies analysis (adapted from Tyson 1995).

Percentage of palynomorphs (of total kerogens)

The palynomorph group is the least abundant of the three main groups, therefore its occurrence is controlled by ‘AOM‘ and phytoclast dilution (Tyson, 1993). Large amounts of palynomorphs, dominated by sporomorphs, indicate proximity of terrestrial sources associated with oxygenated environments. Consequently, a small amount of ‘AOM‘ is observed as a result of low preservation rates. With moderate proximity to land large amounts of palynomorphs can also be found, although without dilution of phytoclasts (Tyson, 1995). If microplankton dominates the palynomorph group, the environment may be of a distal shelf, with adjacent land areas being generally arid, oxygenated and with low ‘AOM‘ preservation but high productivity.

The abundance of microplankton is inversely related to that of the sporomorphs (Tyson, 1993). Depending on the type of microplankton the ratio of sporomorphs to phytoplankton reflects the proximal-distal trend. The ratio of peridionioid to gonyaulacoid dinocysts (P/G ratio) also reflects the nearshore-offshore trend (see Chapter 7).

3.2.4.6 Ratios and Parameters

The palynofacies parameters and ratios used herein follow Tyson (1995). He suggested that for the ratios the sum of the two components must to be at least 50 particles. The ratios of opaque to translucent phytoclasts (O:TR) and of equidimensional to lath (O-Eq:O-La) opaque phytoclasts should be plotted as log graphs, because the values give more symmetrical plots (Tyson, 1995). For the palynomorph parameters the tetrad abundances and PMI values were employed.

Ratio of opaque to translucent phytoclasts (O:TR)

According to Tyson (1993) opaque phytoclast particles derive mainly from oxidation of translucent material, which has been transported over a prolonged period of time. In contrast, translucent particles are deposited in nearshore environments without a prolonged transport. Therefore, the ratio between these two categories could indicate the proximal-distal trend.

Ratio of equidimensional to lath opaque phytoclast (O-Eq:O-La)

This ratio also indicates a proximal-distal trend. A large amount of equidimensional particles suggests close proximity as a result of short transport. These equidimensional particles are sorted according to their buoyancy, where smaller particles are deposited in distal environments (Steffen & Gorin, 1993a). This interpretation is applied especially when the equidimensional particles are larger than the lath ones.

Abundance of tetrads

Tetrads consist of clusters of four pollen grains or spores. High amounts of tetrads indicate short duration of transport and consequently deposition in nearshore environments. Theoretically, a prolonged transport would cause disaggregation of the tetrads. However, tetrads are also found in deep water, especially when the pollen grains are small (for example *Classopollis*). Clusters of more than four pollen grains can also be found, sometimes containing up to 15 grains or more. These aggregates clearly indicate a short transport from their place of origin.

Palynologycal Marine Index (PMI)

As the PMI is based on the palynomorph diversity of terrestrial and marine palynomorphs; therefore, it was used as a substitute for terrestrial:marine ratio. The application of PMI has already been described.

3.2.4.7 Influence of lithology on kerogen groups

The relationship between lithology and kerogen distribution has been discussed by Tyson (1995), Mendonça Filho (1999), and Piper (1996), among others. According to Piper (1996) the sediment grain size influences the distribution of kerogen because of hydrodynamic equivalence or post-depositional oxidation. Changes in kerogen distribution due to environmental variations may be confused with changes of lithology, making it important to identify and separate these lithological influences on kerogen distribution. To this end Tyson (1995) suggested a comparison of samples with similar granulometric composition. The lithological data is best evaluated at two levels of scale: first the lithology of each sample and then the dominant lithology of the interval where this sample was taken. This detailed lithological investigation suggested by Tyson (1995) is applied herein (Appendix 1).

3.2.5 Geochemical analysis

The geochemical study was based on a total of 140 samples from well GTP-24-SE processed for geochemical analyses in the Geochemistry Section of Petrobras, Rio de Janeiro, Brazil. The geochemical methods employed in this study included Total Organic Carbon (TOC) determination, Rock-Eval pyrolysis and fluorescence.

The accumulation of organic matter (OM) in sediments is estimated using TOC analysis. According to Tyson (1995) TOC analysis is a convenient method to determine the abundance of OM in sediments. The accumulation of OM is controlled by major factors such as primary productivity, water depth, and sediment grain size. The TOC is always controlled by three main variables: input of organic matter (OM), preservation of the supplied OM, and dilution of the OM by sediment accumulation (Tyson, 1995). The results of the TOC and sediment grain size analyses are presented here. The values of TOC in marine rocks range from ca. 0.1% (deep-sea pelagic deposits) to 94% (coals) (Tyson, 1995).

Rock-Eval pyrolysis involves the measurement of parameters such as hydrogen and oxygen indices, (HI) and (OI), respectively, S1 (free hydrocarbons), S2 (residual petroleum potential), S3 (generate CO_2), and Tmax (temperature of maximum hydrocarbon evolution from kerogen, ^{o}C). These parameters are useful to characterize the organic matter and source rock potential. For this study only the HI (measured in units of mg hydrocarbon/g total organic carbon, mgHC/gTOC) and OI (measured in units of $mgCO_2/gTOC$) (Miles, 1989) indices were used.

The diagram HI versus OI, also known as a "modified van Klevelen diagram", was employed to characterize the organic matter type. This characterization is based on four kerogen types that are based purely on chemical composition of the kerogen; i.e. on the C, H and O content (Miles, 1989) and identified in the diagram (Table 3.2). In fact, these four kerogen types are based only on the hydrogen content and not on morphology. Types I and II are characterized by well-preserved AOM and Types III and IV by woody material (phytoclasts).

Table 3.2. Kerogen types. Data from Tyson 1995 and Miles 1989.

Kerogen Type	Origin	Main environment
I	algal or cynobacterial materials	Anaerobic, in particular lacustrine
II	mixture of phytoplankton, zooplankton and bacterial material	Anaerobic to dysaerobic, marine
III	predominantly contiental plants and vegetal debris	Oxic, marine, deltaic
IV	continental plants	Oxidized in subaerial environments and/or recycled from older sediments

A total of 164 samples were analyzed to estimate the fluorescence parameters. This parameter, based on the qualitative preservation scale of Tyson (1995, p. 347) (Figure 3.7), was used to estimate the thermal maturity. The different fluorescence colors are indicative of the level of maturity of the organic matter. This (kerogen) shows autofluorescence when excited by ultra-violet (UV) light through a fluorescence microscopy. According to Bordenave (1993), the fluorescence is caused by the emission of photons by fluorophores when excited by electromagnetic radiation.

	Characteristics of organic matter under fluorescence
1	Kerogen is all non-fluorescent (except perhaps for rare fluorescent palynomorphs, such as algae, or cuticles). 1a. AOM very rare (<5%) or absent. 1b. AOM present (common to abundant).
2	Most palynomorphs fluoresce, but the matrix of autochthonous (plankton-derived) AOM remains predominantly non-fluorescent. 2a. Palynomorphs show dull orange-yellow fluorescence. 2b. Palynomorphs show dull yellow-green fluorescence.
3	Most palynomorphs fluoresce and a matrix of autochthonous AOM shows dull fluorescence.
4	As 3, but AOM matrix shows moderate and heterogeneous fluorescence (i.e. visible but clearly less than that of *in situ* palynomorphs).
5	As 3, but AOM matrix shows strong but heterogeneous fluorescence (intensity approaches nearly to *in situ* palynomorphs).
6	Matrix of autochthonous AOM shows fairly homogeneous and very strong fluoresecence (bright yellow, like telalginite).

Figure 3.7. Qualitative preservation scale of the organic matter (adapted from Tyson 1995, p. 347).

CHAPTER 4
STRATIGRAPHY AND LITHOFACIES

4.1 Lithostratigraphy

The succession studied in wells GTP-17-SE and GTP-24-SE comprises part of the Muribeca and Riachuelo formations (Figure 4.1). The Muribeca Formation represents the transitional phase and includes the Ibura and Oiteirinhos members. The Riachuelo Formation, deposited during the open marine phase, is represented by the lower part of the Angico and the Taquari members (see Figure 2.3).

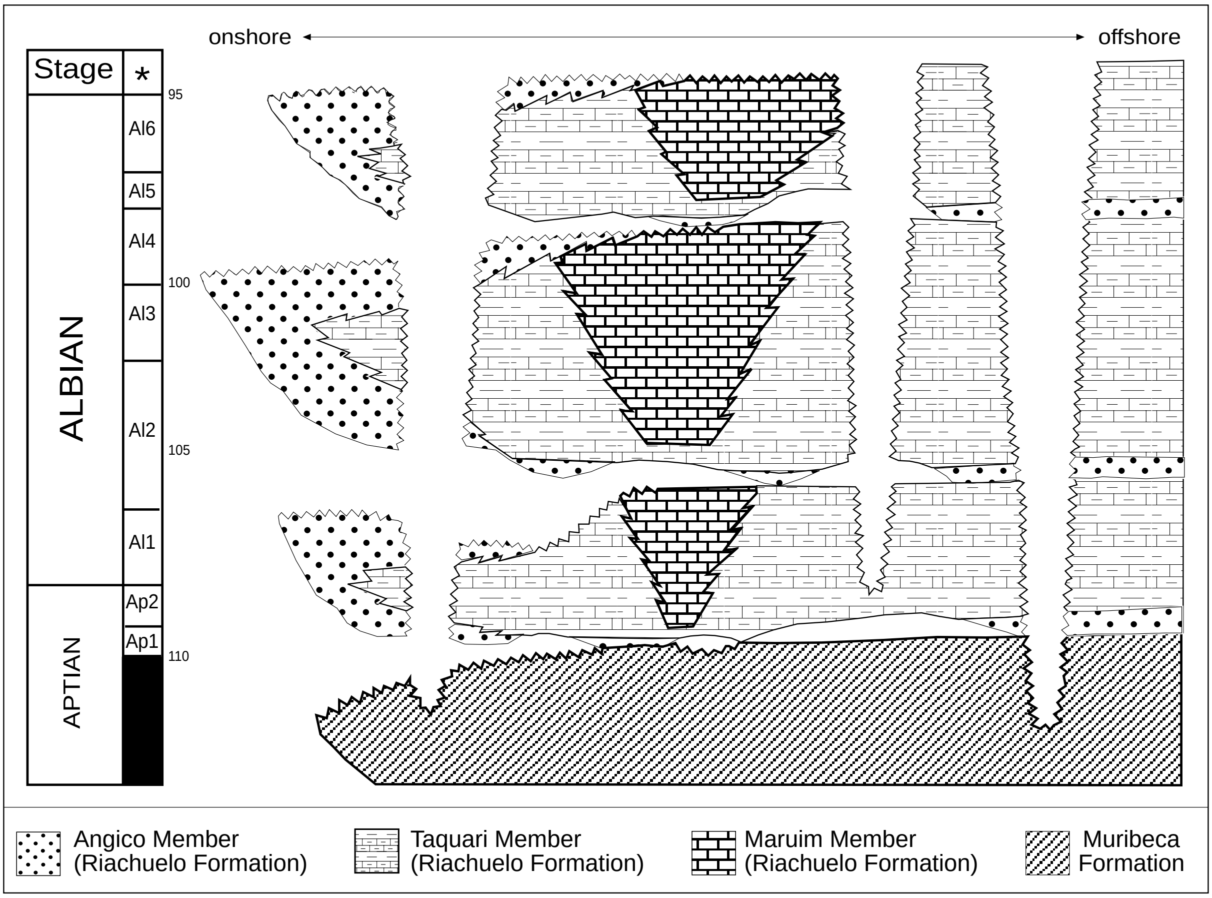
onshore
offshore
Stage
*
ALBIAN
APTIAN
Al6
Al5
Al4
Al3
Al2
Al1
Ap2
Ap1
95
100
105
110
Angico Member (Riachuelo Formation)
Taquari Member (Riachuelo Formation)
Maruim Member (Riachuelo Formation)
Muribeca Formation

Figure 4.1. Lithostratigraphic scheme for the Aptian–Albian of the Sergipe Basin (adapted from Mendes, 1994). * Foraminiferal biozonal scheme from Koutsoukos (1989).

In well GTP-17-SE (Figure 4.2) the succession has a thickness of ca. 450 m and is subdivided into: (1) the Muribeca Formation, represented by the Ibura Member (63 m) and the Oiteirinhos Member (80 m); and (2) the Riachuelo Formation, represented by the Angico Member (312 m).

In well GTP-24-SE (Figure 4.3), the succession reaches 400 m and is subdivided into (1) the Muribeca Formation, with the Ibura Member (26.9 m) and the Oiteirinhos Member (126.9 m); and (2) the Riachuelo Formation with the Taquari Member (247 m).

The two wells are situated on a W-E axis, extending from the Santa Rosa de Lima Low area (GTP-17-SE) to the Aracaju High area (Taquari-Vassouras) (GTP-24-SE) (see Figure 2.2). This axis also reflects a proximal-distal trend. The thicknesses of the formations and their corresponding depths from ground level are taken from Petrobras (1978a-b).

4.2 Evolution of depositional environments

4.2.1 Transitional phase

The upper Aptian to Albian deposits in the Sergipe Basin consist of a mixed carbonate-siliciclastic platform system (Muribeca and Riachuelo formations). At the end of the rift phase, followed by tectonic quiescence, sediments of the Muribeca Formation were laid down (Figure 4.4).

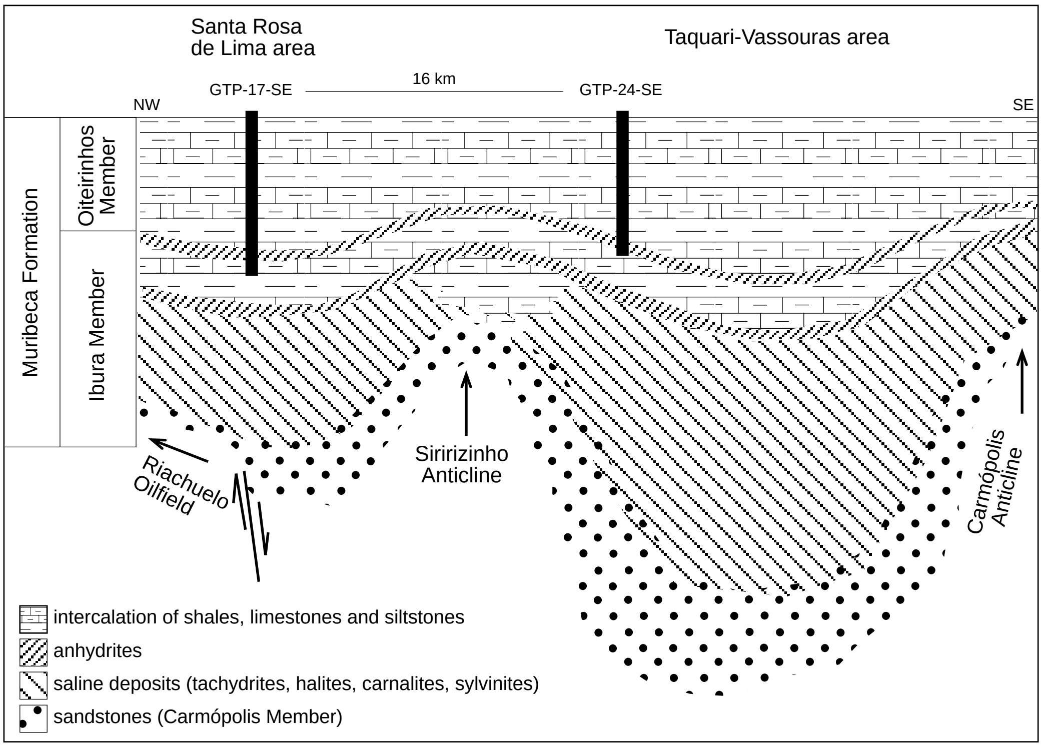
Santa Rosa de Lima area
Taquari-Vassouras area
16 km
GTP-17-SE
GTP-24-SE
NW
SE
Muribeca Formation
Oiteirinhos Member
Ibura Member
Riachuelo Oilfield
Siririzinho Anticline
Carmópolis Anticline
intercalation of shales, limestones and siltstones
anhydrites
saline deposits (tachydrites, halites, carnalites, sylvinites)
sandstones (Carmópolis Member)

Figure 4.4. Geological cross-section of the Muribeca Formation (adapted from Borchert, 1977).

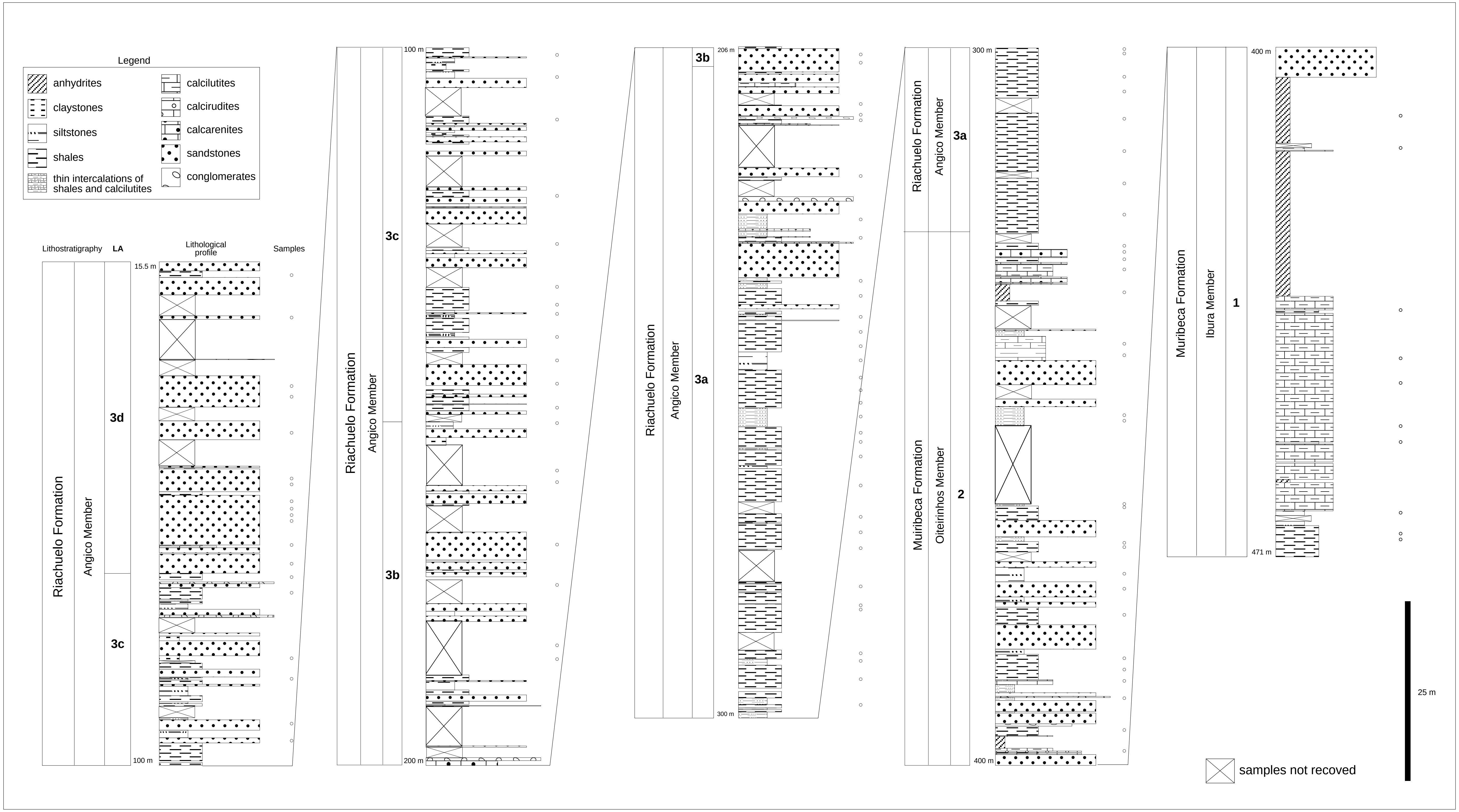
Legend
anhydrites
claystones
siltstones
shales
thin intercalations of shales and calcilutites
calcilutites
calcirudites
calcarenites
sandstones
conglomerates
Lithostratigraphy
LA
Lithological profile
Samples
15.5 m
100 m
Riachuelo Formation
Angico Member
3d
3c
100 m
200 m
3c
3b
206 m
300 m
3b
3a
300 m
400 m
Riachuelo Formation
Angico Member
3a
Muiribeca Formation
Oiteirinhos Member
2
400 m
471 m
Muribeca Formation
Ibura Member
1
25 m
samples not recoved

Figure 4.2. Stratigraphic profile of well GTP-17-SE. For description of lithofacies, see Chapter 4.3. LA=lithofacies association.

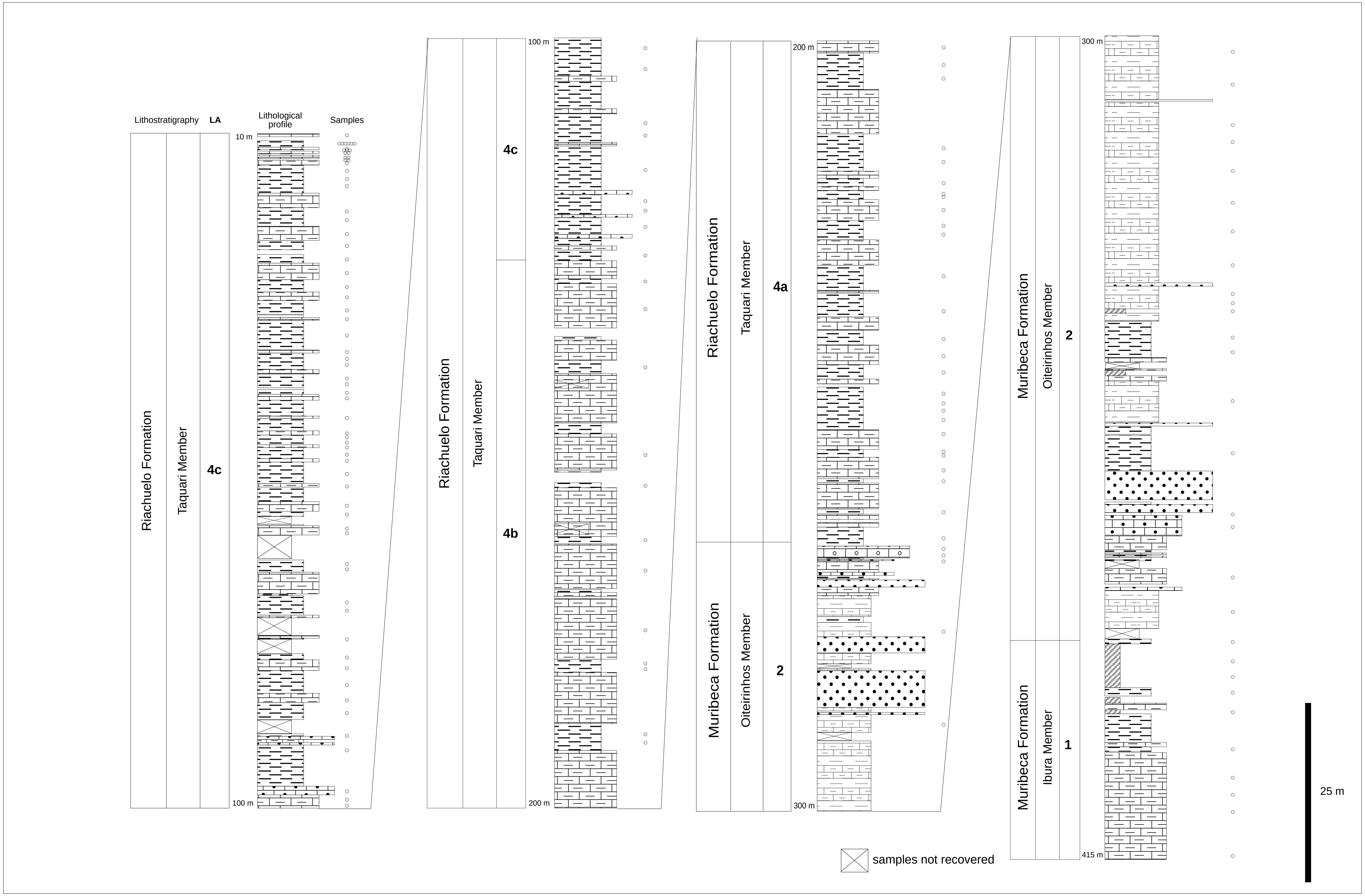
Lithostratigraphy
LA
Lithological profile
Samples
10 m
100 m
Riachuelo Formation
Taquari Member
4c
100 m
200 m
Riachuelo Formation
Taquari Member
4c
4b
200 m
300 m
Riachuelo Formation
Taquari Member
4a
Muribeca Formation
Oiteirinhos Member
2
300 m
415 m
Muribeca Formation
Oiteirinhos Member
2
Muribeca Formation
Ibura Member
1
samples not recovered
25 m

Figure 4.3. Stratigraphic profile of well GTP-24-SE. LA= lithofacies associations For description of lithofacies, see Chapter 4.3. For lithological symbols, see Figure 4.2.

Data about the depositional environments of the Muribeca Formation are from Feijó (1980), who subdivided the formation into eight depositional intervals (Table 4.1).

Feijó (1980) referred the intervals IVb and IVa to the Ibura Member. The sediments of interval IVb were deposited uniformly throughout almost the whole basin. The anhydrite nodules recognized in this interval suggest a sea-level fall. Interval IVa is characterized by the intensive growth of these anhydrite nodules, an event designated as the "principal anhydrite" of the Muribeca Formation. Deposition during this interval was on a sabkha plain.

Table 4.1. Depositional environments of the Muribeca Formation (adapted from Feijó, 1980).

Interval	Lithology	Depositional environment	Main characteristics
I	Intercalation of shales and massive calcilutites	Open marine	Marine fossils
II	Siltstones, fine-grained sandstones intercalated with shales and laminated calcilutites	Slightly deeper lagoon	Strong subsidence with sea-level rise
IIIa	Laminated calcilutites intercalated with shales, massive calcilutites, anhydrite nodules	Open lagoon	Two envents of strong anhydritization (electric marker "two peaks")
IIIb	Laminated calcilutites, siltstones, fine-grained sandstones	Open lagoon	
IVa	Laminated-massive calcilutites, intensive growth of anhydrite nodules	Coastal plain	"Principal anhydrite" of Muribeca Formation
IVb	Massive calcilutites; anhydrite nodules	Shallow lagoon	
IVc	Laminated calcilutites, shales	Shallow lagoon	
IVd	Laminated calcilutites, shales, anhydrites, halites	Shallow lagoon	First salt deposition in the Atlantic

The Oiteirinhos Member was subdivided into intervals IIIb, IIIa II and the lowermost part of interval I.

Interval IIIb consists of limestones, shales and fine-grained sandstones deposited in open lagoonal environments. This interval shows great lithological variation; however, calcilutite deposition predominates, suggesting a transgression. Interval IIIa is characterized by a feature called "two peaks", observed in the gamma-ray profile. This marker is related to two clear events of anhydrite deposition. The anhydrites were generate due to an intense exposition of the calcilutites that overlie large parts of the area studied.

Interval II is characterized by rapid subsidence, which allowed the deposition of fine-grained sediments such as siltstones and shales, in the slightly deeper water of a lagoon; however, burial events are observed. In the upper part of this interval, wave ripples were recognized indicating progressively shallower conditions.

Interval I is the uppermost unit proposed by Feijó (1980). Its upper limit lies within the Riachuelo Formation (Taquari Member). Ammonites, echinoderms and benthic and planktonic foraminifera indicate that the sediments were deposited under open marine conditions (Feijó, 1980).

4.2.2 Open marine phase

After the transitional phases (evaporitic, proto-marine) represented by the Muribeca Formation and the base of the Riachuelo Formation, the open marine phase began (Figure 4.5). The information about the development of this phase is from Koutsoukos *et al*. (1991) and Mendes (1994).

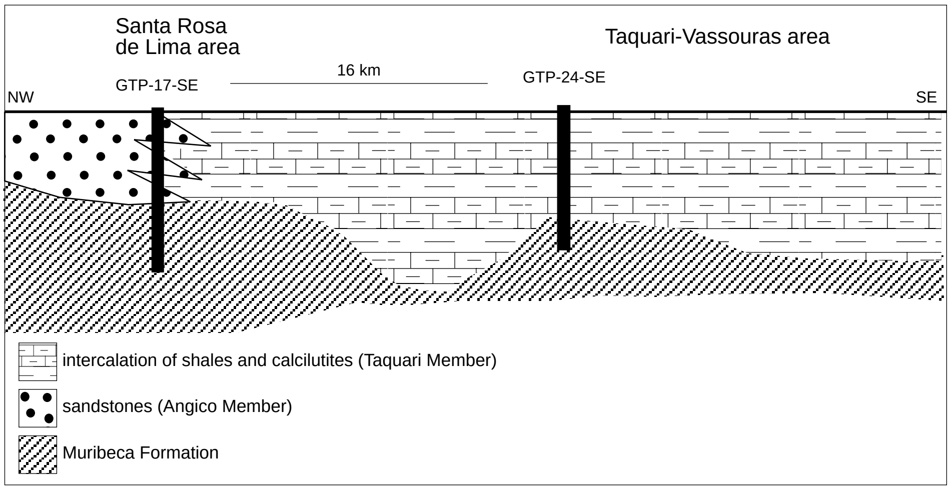
Santa Rosa de Lima area
Taquari-Vassouras area
16 km
GTP-17-SE
GTP-24-SE
NW
SE
intercalation of shales and calcilutites (Taquari Member)
sandstones (Angico Member)
Muribeca Formation

Figure 4.5. Geological cross-section of the base of the Riachuelo Formation (adapted from Borchert, 1977).

Mendes (1994) subdivided the Riachuelo Formation into three depositional sequences (see Figure 2.6). In the two studied wells, he identified sequences I and II.

Using percentage maps for coarse siliciclastics (sandstones and conglomerates) and carbonates and the siliciclastic/carbonate ratio (Figures 4.6 and 4.7), Mendes (1994) identified the areas of occurrence of these facies. This provides the base for interpretation of the sedimentary evolution of the sequence.

The lower limit of Sequence I is marked by discontinuity D1 that separates the Muribeca and Riachuelo formations. In well GTP-17-SE this discontinuity was recognized by Mendes (1994) at 327 m, and in well GTP-24-SE at 253 m. Using percentage maps of the sedimentary rocks, he observed that where well GTP-24-SE is located, occurs a predominance of carbonates, chiefly mudstones and wackestones. However, siliciclastic facies predominate in the whole area studied. The upper limit of Sequence I is marked by the discontinuity and in part correlative conformity D2 at 195 m in GTP-17-SE and at 125 m in GTP-24-SE.

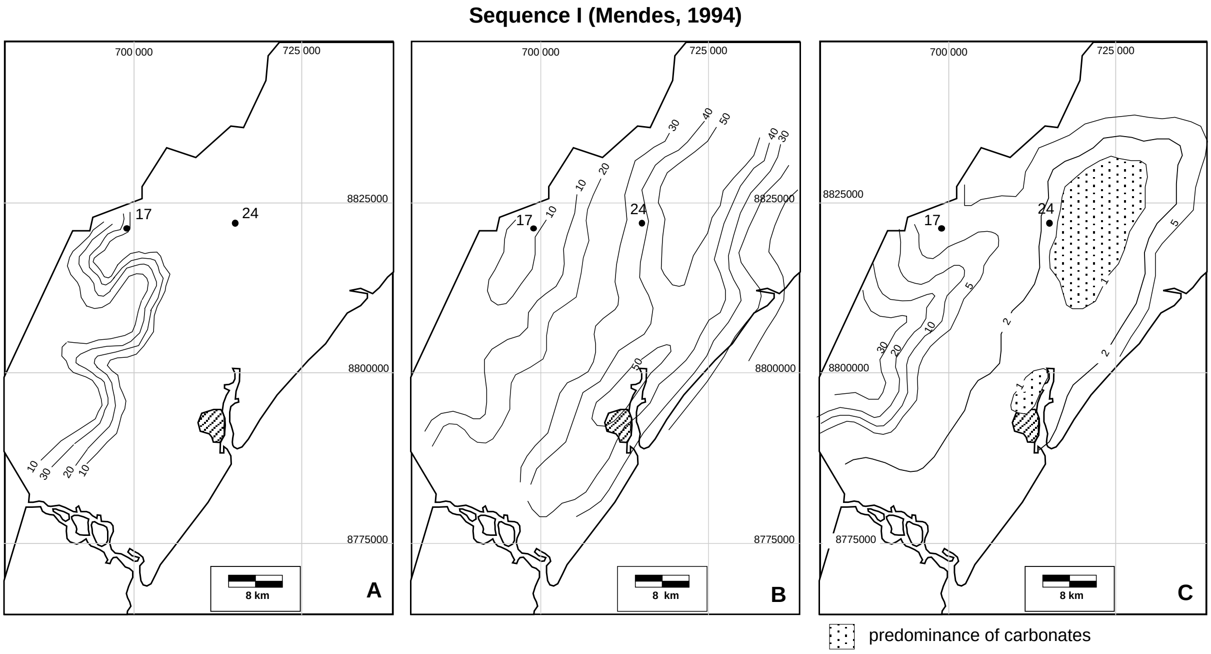

Sequence I (Mendes, 1994)

Figure 4.6. A) Percentage map of sandstones and conglomerates; B) Percentage map of carbonates; C) Map of the ratio of siliciclasts/carbonates. Modified after Mendes (1994).

The base of sequence II is defined by D2 and the top by discontinuity 3 (D3). The latter was not recognized by Mendes (1994) in the studied wells. In Sequence II a major proportion of sediments derived from patch reefs is recognized. In the areas where the path reefs occurred there was limited deposition of coarse-grained clastics. Sequence II shows the same characteristics as Sequence I, where the siliciclastic sediments predominate, except in the area of the carbonate banks (see Figure 4.7). The carbonate banks in the northeastern part of the area studied by Mendes (1994) are clearly oriented towards the center of the onshore part of the basin (NE/SW) where well GTP-24-SE is located. Through analysis of the percentage maps, Mendes (1994) identified a lagoonal/inner shelf environment between the carbonate banks and the margin of the basin. In this area the deposition of coarse-grained siliciclastics (Angico Member) dominated. The paleogeography of this sequence is illustrated in Figure 4.7.

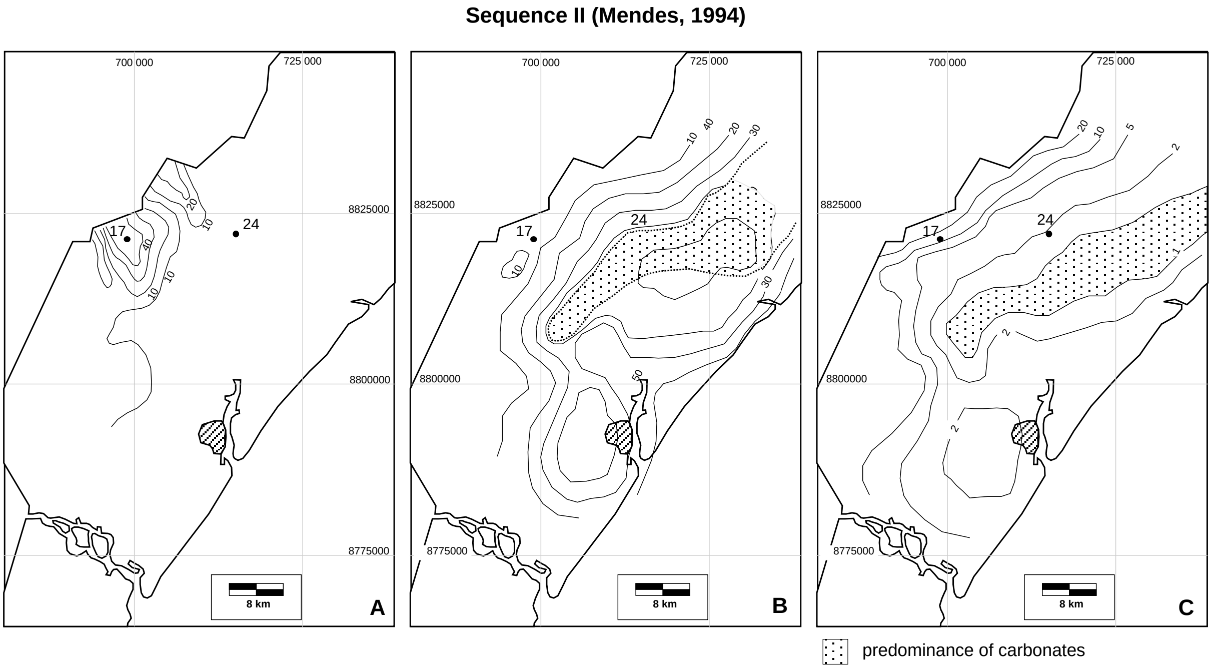

Figure 4.7. A) Percentage map of sandstones and conglomerates; B) Percentage map of carbonates; C) Map of the ratio of siliciclasts/carbonates. Modified after Mendes, 1994).

4.3 Lithofacies

Four broad lithofacies associations were distinguished in the succession of wells GTP-17-SE and GTP-24-SE (Figures 4.2 and 4.3): (1) mixed calcilutites/shales/anhydrites; (2) mixed calcilutites, shales, siltstones, sandstones and anhydrites; (3) mixed sandstones and shales; (4) mixed calcilutite and shales. The background information for this subdivision of lithofacies was taken from Petrobras (1978a-b).

Lithofacies association 1 is present in both wells. It comprises laminated medium-grey calcilutite beds, with fragments and dissemination of organic matter, carbonaceous dark-grey shale beds and grey anhydrites. This lithofacies association is characterized by common occurrence of anhydrite beds. Lithofacies association 1 corresponds to the Ibura Member. In well GTP-17-SE this lithofacies association extends from 471 to 407 m and in well GTP-24-SE from 415 to 383 m.

Lithofacies association 2 is composed of laminated cream to brownish calcilutites and medium-dark grey shales, with very thin intercalations of fine-grained, light grey sandstones. Anhydrite beds are present and occasional ooids occur. This heterolithic nature is characteristic of the Oiteirinhos Member, which occurs in both wells. In well GTP-17-SE lithofacies association 2 occurs from 407 to 327 m and in well GTP-24-SE from 383 to 257 m.

Lithofacies association 3 consists predominantly of sandstones, with locally thick intercalations of shales and siltstones. This lithofacies association is present only in well GTP-17-SE, from 327 to 15 m. It is related to the Angico Member. Lithofacies association 3 was subdivided into four lithofacies.

Lithofacies 3a contains mainly fine to conglomeratic sandstones, with thin beds of dark grey shales and medium grey siltstones. The sandstones are very porous and poorly consolidated. This lithofacies occurs from 327 to 215 m.

Lithofacies 3b contains fine to conglomeratic sandstones intercalated with greenish grey shales and greenish grey siltstones. This lithofacies occurs from 215 m to 147 m.

Lithofacies 3c is more pelitic than lithofacies 3a, containing fine to conglomeratic sandstones. In this facies increase gradually the frequency and thickness of the greenish grey shales and greenish grey siltstone beds. Lithofacies 3c extends from 147 to 70 m.

Lithofacies 3d is characterized by a predominance of fine-grained sandstones, although ranging from very fine to conglomeratic. The sandstone beds are locally intercalated with very thin beds of greenish grey shales and greenish grey siltstones. Lithofacies 3d occurs from 70 to 15 m.

Lithofacies association 4 is subdivided into three lithofacies, consisting of intercalations of shales and calcilutites. It occurs only in well GTP-24-SE (Taquari Member), from 257 to 12 m.

Lithofacies 4a consists of parallel laminated light to medium grey calcilutites intercalated with medium to dark grey shales. This lithofacies occurs from 257 to 205 m.

Lithofacies 4b consists of massive light grey calcilutites and greenish grey shales. This lithofacies occurs from 205 to 125 m.

Lithofacies association 4c is characterized by parallel laminated dark grey to black shales and massive medium grey calcilutites. This lithofacies occurs from 125 to 12 m.

CHAPTER 5

PALYNOLOGY

All slides are kept in the palynological collections of Section for Biostratigraphy and Paleoecology, Cenpes, Petrobras (Rio de Janeiro, Brazil),

5.1. Qualitative analysis

Of the 253 samples used in this study (see Chapter 3), only eleven were barren. Despite the rich palynomorph assemblage no new species are recorded and all the species encountered have a worldwide distribution. As most of the species are well known and have already been exhaustively described in the literature, only their systematic position is provide in the ensuing section

The miospores identified in this study are arranged according to their presumed botanical affinity, after Singh (1971) and Ravn (1995). Some palynomorphs could only be assigned to genus because only a few poorly preserved specimens could be recovered.

For the dinoflagellates the current classification of fossil and living dinoflagellates of Fensome *et al*. (1998) was used.

The miospore assemblage is composed of 17 genera and 19 species of spores, 23 genera and 31 species of pollen grains and four spore types. The dinocysts include 17 genera and 20 species. Acritarchs are represented by one genus and three types. Among the fresh-water algae only one genus was recorded.

The preservation of the palynomorph is variable. The miospores are moderately to well-preserved and the dinocysts poorly to moderately preserved, often with surface corrosion.

5.2. Systematic palynology

Division BRYOPHYTA
Order Sphagnales
Family Sphagnaceae
Genus *Antulsporites* Archangelsky & Gamerro, 1966

Antulsporites baculatus Archangelsky & Gamerro, 1966
Plate 1, Figure 1

Holotype: Archangelsky & Gamerro (1966), p. 203, Plate 1, Figures 12-14.

Division PTERIDOPHYTA
Order Filicales
Family Schizaeaceae
Genus *Cicatricosisporites* Potonié & Gelletich, 1933, emend. Pflug & Thomson, 1953

Cicatricosisporites avnimelechi Horowitz, 1970
Plate 1, Figure 6

Holotype: Horowitz (1970), p. 164, Figures 4-6.

Cicatricosisporites microstriatus Jardiné & Magloire, 1965
Plate 1, Figure 11

Holotype: Jardiné & Magloire (1965), p. 202, Plate 1, Figures 18-19.

Genus *Klukisporites* Couper, 1958

Klukisporites foveolatus Pocock, 1964
Plate 1, Figure 7

Holotype: Pocock (1964), p. 194, Plate 7, Figures 5, 6.

Klukisporites pseudoreticulatus Couper, 1958
Plate 1, Figure 4

Holotype: Couper (1958), p.138, Plate 19, Figures 8-10.

Genus *Microfoveolatosporis* Krutzsch, 1959, emend. Potonié 1956

Microfoveolatosporis daukiensis Kar & Singh, 1986
Plate 1, Figure 3

Holotype: Kar & Singh (1986), p. 106, Plate 8, Figures 11-13.

Family Matoniaceae
Genus *Matonisporites* Couper, 1958

Matonisporites silvai Lima, 1978
Plate 1, Figure 14

Holotype: Lima (1978), pp. 165-166, Plate 12, Figures 4-6.

Family Cyatheaceae or Dicksoniaceae
Genus *Cyathidites* Cookson, 1947,emend. Potonié, 1956

Cyathidites spp.
Plate 1, Figure 2

Remarks: Several species are present in the succession, although only one is illustrated in Plate 1, Figure 2.

Order Selaginellales
Family Selaginellaceae
Genus *Echinatisporites* Krutzsch, 1959

Echinatisporites varispinosus (Pocock, 1962) Srivastava, 1977
Plate 1, Figure 5

Holotype: Pocock (1962), p. 36, Plate 1, Figures 18-19.

1962 *Acanthotriletes varispinosus* Pocock, p. 36, Plate 1, Figures 18-20.
1977 *Echinatisporites varispinosus* Srivastava, p. 39.

Order Lycopodiales
Family Lycopodiaceae
Genus *Leptolepidites* Couper, 1953

Leptolepidites psarosus Norris, 1966
Plate 1, Figure 18

Holotype: Norris (1966), p. 586, Plate 103, Figures 2-5.

Genus *Perotriletes* (Erdtman, 1945) Couper, 1953

Perotriletes spp.
Plate 1, Figure 16

Remarks: Several species are present in the succession, although only one is illustrated in Plate 1, Figure 16.

Genus *Retitriletes* van der Hammen, 1954, emend. Döring *et al.*, in Krutzsch, 1963

Retitriletes sp. 3 Regali, 1989
Plate 1, Figure 15

Order Marsileales
Family Marsiliaceae
Genus *Collarisporites* Kaiser, 1976

Collarisporites fuscus Deák, 1964
Plate 1, Figure 17

Holotype: Déak (1964), p. 99.

Genus *Crybelosporites* Dettmann, 1963

Crybelosporites pannuceus (Brenner, 1963) Srivastava, 1977

Plate 1, Figure 10

Holotype 1963 *Perotriletes pannuceus* Brenner, p. 66, Plate 18, Figure 3.

1965 *Perotriletes perinopustulosus* Jardiné & Magloire, p. 203, Plate 3, Figures 3-4.
1977 *Crybelosporites pannuceus* (Brenner) Srivastava, p. 35

Genus *Foveosporites* Balme, 1957

Foveosporites canalis Balme, 1957

Plate 1, Figure 8

Holotype: Balme (1957), p. 17.

Division PTERIDOPHYTA – Incertae sedis

Genus *Clavatriletes* (van der Hammen, 1954) Herbst,1965

Clavatriletes spp.

Plate 1, Figure 12

Genus *Pilosisporites* Delcourt & Sprumont, 1955

Pilosisporites trichopapillosus (Thiegart, 1949) Delcourt & Sprumont, 1955

Plate 1, Figure 19

Holotype: Thiegart (1949), p. 22, Plate 4-5, Figure 18.

1949 *Sporites trichopapillosus* Thiegart, p. 22, Plate 4-5, Figure 18.
1955 *Pilosisporites trichopapillosus* Delcourt & Sprumont, p. 35, Plate 3, Figure 3.

Genus *Reticulosporis* Krutzsch, 1959

Reticulosporis foveolatus (Pierce, 1961) Skarby, 1964

Plate 1, Figure 9

Holotype: Pierce (1961), p. 81.

1961 *Reticulosporis foveolatus* Pierce, p. 81.
1964 *Reticulosporis foveolatus* Skarby, p. 72.

Genus *Verrucosisporites* (Ibrahim, 1932) Potonié & Kremp, 1954

Verrucosisporites spp.

Plate 1, Figure 13

Remarks: Several species are present in the succession, although only one is illustrated in Plate 1, Figure 13.

Division GYMNOSPERMAE
Order Cycadales
Family Cycadaceae
Genus *Bennettitaepollenites* Thiegart, 1949, emend. Potonié, 1958

Bennettitaepollenites regaliae Dino, 1996
Plate 2, Figure 16

Holotype: Dino (1996), p. 262, Plate 4, Figures 1, 6.

Family Cheirolepidaceae
Genus *Classopollis* Pflug, 1953, emend., Pocock & Jansonius, 1961

Classopollis classoides Pflug, 1953, emend. Pocock & Jansonius, 1961
Plate 2, Figure 9

Holotype: Pflug (1953), p. 91, Plate 16, Figures 29-31.

1953 *Classopollis classoides* Pflug, p. 91, Plate 16, Figures 29-31.
1961 *Classopollis classoides* Pocock & Jansonius, p. 443, Plate 1, Figures 1-9.

Genus *Cycadopites* (Wodehouse, 1958) Wilson & Webster, 1946

Cycadopites spp.
Plate 2, Figure 17

Remarks: Several species are present in the succession, although only one is illustrated in Plate 2, Figure 17.

Order Coniferae
Family Taxodiaceae, Taxaceae and Cupressaceae
Genus *Uesuguipollenites* Dino, 1996

Uesuguipollenites callosus Dino, 1996
Plate 2, Figures 6-7

Holotype: Dino (1996), p.258, Plate 1, Figures 1-7.

Family Araucariaceae
Genus *Araucariacites* Cookson, 1947 ex Couper, 1953

Araucariacites australis Cookson, 1947
Plate 2, Figure 2

Holotype: Cookson (1947), p. 130, Plate 13, Figure 3.

Genus *Callialasporites* Dev, 1961, emend. Potonié, 1966

Callialasporites segmentatus (Balme, 1957) De Jersey, 1963

Plate 2, Figure 10

Holotype: Balme (1957), p. 33, Plate 9, Figures 93, 94.

1957 *Zonalapollenites segmentatus* Balme, p.33, Plate 9, Figures 93, 94.
1961 *Callialasporites segmentatus* Dev, p.48.
1963 *Callialasporites segmentatus* De Jersey, p. 12.

Order Caytoniales
Family Caytoniaceae
Genus *Vitreisporites* Leschik, 1955

Vitreisporites pustulosus Regali, 1987

Plate 2, Figure 11

Holotype: Regali, p. 649, Plate 1, Figures 3-4.

1974 *Caytonipollenites*? sp. 1 Regali, Uesugui & Santos, p. 286, Plate 5, Figure 2.
1987b *Vitreisporites pustulosus* Regali, p. 649, Plate 1, Figures 1-5.

Order Gnetales
Family Ephedraceae
Genus *Equisetosporites* Daugherty, 1941, emend. Singh, 1964

Equisetosporites albertensis Singh, 1964

Plate 2, Figure 15

Holotype: Singh (1964), p. 133, Plate 17, Figures 17-18

Equisetosporites concinnus Singh, 1964

Plate 2, Figure 23

Holotype: Singh (1964), p. 133, Figures 10-15.

Equisetosporites maculosus Dino, 1996

Plate 2, Figures 13-14

Holotype: Dino (1996), p. 259, Plate 2, Figures 1-5.

Equisetosporites ovatus (Pierce, 1961) Singh, 1964

Plate 2, Figure 19

Holotype: Pierce (1961), p. 45, Plate 3, Figure 80.

1961 *Strianinaperturites ovatus* Pierce, p. 45, Plate 3, Figure 80.
1964 *Equisetosporites ovatus* Singh, p. 133.

Family Gnetaceae
Genus *Gnetaceaepollenites* Thiergart, 1938, emend. Jansonius, 1962

Gnetaceaepollenites chlatratus Stover, 1964
Plate 2, Figure 20

Holotype: Stover (1964), p. 149, Plate 1, Figures 12-17.

Gnetaceaepollenites diversus Stover, 1964
Plate 2, Figure 22

Holotype: Stover (1964), p. 147, Plate 1, Figures 1-11.

Gnetaceaepollenites jansonii (Pocock, 1964) Lima, 1980
Plate 3, Figure 1

Holotype: Pocock (1964), p. 149, Plate 1, Figures 26-27.

1964 *Ephedripites jansonii* Pocock, p. 149, Plate 1, Figures 26-27.
1968 *Equisetosporites lajwantis* Srivastava, Figures 10, 11.
1968 *Ephedripites jansonii* Muller, p. 9, Plate 2, Figure 9
1980 *Gnetaceaepollenites jansonii* (Pocock) Lima, p. 35, Plate 3, Figure 11.

Gnetaceaepollenites uesuguii Lima, 1978
Plate 2, Figure 21

Holotype: Lima (1978), p. 242, Plate 22, Figures 2-3.

Family Gnetaceae or Ephedraceae
Genus *Steevesipollenites* Stover, 1964

Steevesipollenites binodosus? Stover, 1964
Plate 2, Figure 18

Holotype: Stover (1964), p. 151, Plate 2, Figures 7-9.

Division Gymnospermae – Incertae sedis
Genus *Complicatisaccus* Pautsch, 1971

Complicatisaccus cearensis? Regali, 1987
Plate 2, Figure 12

Holotype: Regali (1987), p. 648, Plate 1, Figures 15-17.

Genus *Elaterosporites* Jardiné, 1967

Elaterosporites klaszi (Jardiné & Magloire, 1965) Jardiné, 1967
Plate 3, Figures 2-4

Holotype: Jardiné & Magloire (1965), p. 205, Plate 4, Figures 3a-3b.

1965 *Galeacornea klaszi* Jardiné & Magloire, p. 205, Plate 4, Figures 3a-3b.
1967 *Elaterosporites klaszi* Jardiné, p. 246, Plate 2, Figures h-m.

Genus *Sergipea* Regali, Uesugui & Santos, 1974, emend. Regali, 1987

Sergipea naviformis Regali, Uesugui & Santos, 1974
Plate 2, Figure 5

Holotype: Regali, Uesugui & Santos (1974), p. 273, Plate 4, Figures 10-11.

Sergipea simplex Regali, 1987
Plate 2, Figure 8

Holotype: Regali, (1987a), p. 619, Plate 1, Figures 24-25.

Sergipea variverrucata Regali, Uesugui & Santos, 1974, emend. Regali, 1987
Plate 2, Figures 3-4

Holotype: Regali, Uesugui & Santos (1974), p. 273, Plate 4, Figure 12.

1974 *Sergipea variverrucata* Regali, Uesugui & Santos, p. 273, Plate 4, Figure 12.
1987a *Sergipea variverrucata* Regali, p. 616, Plate 1, Figures 1-16.

Division ANGIOSPERMAE
Order Geraniales
Family Euphorbiaceae
Genus *Stellatopollis* Doyle in Doyle, van Campo & Lugardon, 1975

Stellatopollis barghoornii Doyle, 1975
Plate 3, Figure 22

Holotype: Doyle (1975), p. 426; Plate 7, Figure 18; Plate 8, Figures 1-5; Plate 9, Figures 1-4.

Stellatopollis dubius Jardiné & Magloire, 1965, emend. Lima, 1978
Plate3, Figure 23

Holotype: Jardiné & Magloire (1965), p. 203, Plate 4, figs 4-5.

1965 *Stellatopollis dubius* Jardiné & Magloire, p. 203, Plate 4, figs 4-5.
1976 *Crotonipollis dubius* Lima, p. 17, Plate 1, Figures 16-20.
1978 *Stellatopollis dubius* Lima, p. 274, Plate 25, Figures 4-5.

Stellatopollis sp.1. Doyle *et al.*, 1977
Plate 3, Figure 24

Order Salicales
Family Salicaceae
Genus *Rousea* Srivastava, 1969

Rousea georgensis Brenner, 1963, emend. Dettmann, 1973
Plate 3, Figure 8

Holotype: Brenner (1963), p. 91-92.

1963 *Rousea georgensis* Brenner, p. 91-92.
1973 *Rousea* georgensis Dettmann, p. 14-15.

Order Tubiflorae
Family Solanaceae
Genus *Striatopollis* Krutzsch, 1959

Striatopollis reticulatus Regali, Uesugui & Santos, 1974, emend. Dino, 1996
Plate 3, Figure 21

Holotype: Regali, Uesugui & Santos (1974), p. 279. Plate 8, Figure 2.

1974 *Striatopollis reticulatus* Regali, Uesugui & Santos, p. 279. Plate 8, Figure 2.
1996 *Striatopollis reticulatus* Dino, p. 264, Plate 5, Figures 4-7.

Order Principes?
Family Gunneraceae
Genus *Afropollis* Doyle *et al*., 1982

Afropollis aff. *jardinus* Doyle, Jardiné & Doerenkamp, 1982
Plate 3, Figure 5

Holotype: Brenner (1968), p. 381, Plate 10, Figures 5-6.

1968 *Reticulatasporites jardinus* Brenner, p. 381, Plate 10, Figures 5-6.
1973 *Reticulatasporites jardinus* (Brenner) Herngreen, p. 536, Plate 2, Figure 9.
1982 *Afropollis* aff. *jardinus* Doyle, Jardiné & Doerenkamp, p. 47, Plate 5, Figures 1-7.

Afropollis operculatus Doyle, Jardiné & Doerenkamp, 1982
Plate 3, Figure 7

1977 "*Reticulatasporites*" *jardinus* Doyle *et al*., pp. 457-458, Plate 2, Figures 1-4.
1981 *Reticulatasporites jardinus* (Brenner) Hochuli, p. 339, Plate 1, Figures 5-6.
1982 *Afropollis operculatus* Doyle, Jardiné & Doerenkamp, p. 47, Plate 6, Figures 1-7.

Genus *Brenneripollis* (Brenner, 1963) Juhász & Góczán, 1985

Brenneripollis reticulatus Brenner, 1963, emend. Juhász & Góczán, 1985
Plate 3, Figures 11-12

Holotype: Brenner (1963), p. 94.

1963 *Brenneripollis reticulatus* Brenner, p. 94.
1985 *Brenneripollis reticulatus* Juhász & Góczán, p. 151.

Genus *Retimonocolpites* (Pierce 1961) ex Pierce 1966

Retimonocolpites textus? (Norris, 1967) Singh, 1983
Plate 3, Figures 6, 10

Holotype: Norris (1967) p. 106, Plate 16, Figures 21-25.

1967 *Liliacidites textus* Norris, p. 106, Plate 16, Figures 21-25; Plate 17, Figures 1, 2.
1983 *Retimonocolpites textus* (Norris) Singh, p. 188.

Genus *Tricolpites* (Cookson, 1947) ex Couper, 1953, emend. Belsk, Boltenhagen & Potonié, 1965

Tricolpites spp.
Plate 3, Figure 13

Remarks: Two or three species are present in the succession, although only one is illustrated in Plate 3, Figure 13.

Division Angiospermae – Incertae sedis
Genus *Dejaxpollenites* Dino, 1996

Dejaxpollenites foveoreticulatus Dino, 1996
Plate 3, Figures 14-16

Holotype: Dino (1996), p. 261, Plate 3, Figures 6-10.

Dejaxpollenites microfoveolatus Dino, 1996
Plate 3, Figure 17

Holotype: Dino (1996), p. 261, Plate 3, Figures 1, 5.

Genus *Retitricolpites* (van der Hammen, 1954) ex van der Hammen & Wijmstra, 1964

Retitricolpites spp.
Plate 3, Figure 9

Remarks: Two or three species are present in the succession, although only one is illustrated in Plate 3, Figure 9.

Genus *Schrankpollis* Regali & Santos, 1996

Schrankpollis reticulatus? sensu Regali & Santos, 1996
Plate 3, Figure 18

Holotype: Regali & Santos (1996), p. 5, Plate 3, Figures 5-6.

Genus *Quadricolpites* Wingate, 1980

Quadricolpites reticulatus? Wingate, 1980
Plate 3, Figures 19-20

Holotype: Wingate (1980), p. 44, Plate 16, Figures 12-16.

Division PYRRHOPHYTA
Order Peridiniales
Family Ceratiaceae
Genus *Circulodinium* Alberti, 1961

Circulodinium spp.
Plate 4, Figure 1

Remarks: Two or three species are present in the succession, although only one is illustrated in Plate 4, Figure 1.

Genus *Cyclonephelium* Deflandre & Cookson, 1955, emend. Stover & Evett, 1978

Cyclonephelium spp.
Plate 4, Figures 2-5

Remarks: Several species are present in the succession, although only three are illustrated in Plate 4, Figure 2-5.

Genus *Odontochitina* Deflandre, 1935, emend. Davey, 1970

Odontochitina operculata (Wetzel, 1933) Deflandre and Cookson, 1955
Plate 4, Figures 6, 7

Holotype: Wetzel, p. 170, Plate 11, Figure 21.

1933 *Ceratium* (*Euceratium*) *operculatum* Wetzel, p. 170, Plate 11, Figure 21
1935 *Odontochitina silicorum* Deflandre, p. 234, Plate 9, Figures 8-10
1946 *Odontochitina operculata* Deflandre, cards 1016-1019.
1955 *Odontochitina operculata* (Deflandre) Deflandre and Cookson, p. 291, Plate 3, Figures 5, 6.

Genus *Pseudoceratium* Gocht, 1957

Pseudoceratium securigerum? (Davey & Verdier, 1974) Bint, 1986
Plate 4, Figures 9

Holotype: Davey & Verdier (1974), Plate 91, Figure 3

1974 *Aptea securigerum* Davey & Verdier, pp. 642-643, Plate 91, Figures 2-3.
1986 *Pseudoceratium securigerum* Bint 1986, p. 145.

Family Gonyaulacaceae
Genus *Apteodinium* Eisenack, 1958 emend. Lucas-Clark, 1987

Apteodinium granulatum Eisenack 1958 emend Lucas-Clark 1987
Plate 5, Figures 2-3

Holotype: Eisenack (1958), p. 386, Plate 23, Figure 9.

1958 *Apteodinium granulatum* Eisenack, p. 386, Plate 23, Figure 9.
1987 *Apteodinium granulatum* Lucas-Clark, p. 170 and 172.

Genus *Cribroperidinium* Neale & Sarjeant, 1962 emend. May, 1980

Cribroperidinium tensiftense Below, 1981

Plate 5, Figure 1

Holotype: Below (1981), pp. 41-42, Plate 1, Figures 10, 11a-b; Plate 13, Figures 3a-e, 4-5.

Genus Dinopterygium? Deflandre, 1935, emend. Stover & Evitt, 1978

Dinopterygium? spp.

Plate 5, Figure 5

Remarks: Two or more species are present in the succession, although only one is illustrated in Plate 5, Figure 5.

Genus *Exochosphaeridium* Davey *et al.*, 1966

Exochosphaeridium spp.

Plate 6, Figure 1

Remarks: Several species are present in the succession, although only one is illustrated in Plate 6, Figure 1.

Genus *Florentina* Davey & Verdier, 1973, emend. Duxbury, 1980

Florentina mantellii (Davey & Williams, 1966) Davey & Verdier, 1973

Plate 4, Figure 13

Holotype: Davey & Williams (1966), p. 66, Plate 6, Figure 6.

1966 *Hystrichosphaeridium mantellii* Davey & Williams, p. 66, Plate 6, Figure 6.
1967 *Hystrichosphaeridium stellatum* (Maier 1959) Clarke & Verdier, Plate 2, Figures 1-2
1969 *Hystrichosphaeridium mantellii* (Davey & Williams) Davey, p. 145, Plate 4, Figure 9
?1971 *Hystrichosphaeridium cooksoni* Singh, p. 329, Plate 51, Figure 7 and Plate 52, Figures 1-4.
1973 *Florentina mantelli* Davey & Verdier, p. 191.

Genus *Oligosphaeridium* Davey & Williams, 1966, emend. Davey, 1982

Oligosphaeridium albertense (Pocock, 1962) Davey & Williams, 1969

Plate 5, Figure 18

Holotype: Pocock (1962), p. 82, Plate. 15, Figure 226.

1962 *Hystrichosphaeridium albertense* Pocock, p. 82, Plate. 15, Figures 226-227.
1969 *Oligosphaeridium albertense* Davey & Williams, p. 5.

Oligosphaeridium complex (White 1842) Davey & Williams, 1966

Plate 5, Figure 17

Holotype: White (1842), p. 39, Plate 4, Figure 11

1842 *Xanthidium complex* White, p. 39, Plate 4, Figure 11.
1940 *Hystrichosphaeridium elegentulum* Lejeune-Carpenter, p. 22, Figures 11-12.
1946 *Hystrichosphaeridium complex* (White) Deflandre, p.11
1959 *Hystrichosphaeridium asterigerum* Gotch, p. 67, Plate 3, Figure 1 and Plate 7, Figures 1-4.
1966 *Oligosphaeridium complex* (White) Davey & Williams, p. 71, Plate 7, Figures 1-2 and Plate 10, Figure 3.

Oligosphaeridium irregulare (Pocock, 1962) Davey & Williams, 1969

Plate 5, Figure 13

Holotype: Pocock (1962), p. 82, Plate 15, Figures 228-229.

1962 *Hystrichosphaeridium irregulare* Pocock, p. 82, Plate 15, Figures 228-229.
1969 ?*Oligosphaeridium irregulare* Davey & Williams, p. 5.
1971 *Oligosphaeridium irregulare* (Pocock) (Davey & Williams), Brideaux, p. 90, Plate 26, Figure 62.

Oligosphaeridium poculum Jain, 1977

Plate 5, Figure 16

Holotype: Jain (1977), p. 181, Plate 1, fig 3.

Oligosphaeridium pulcherrimum (Deflandre & Cookson, 1955) Davey & Williams, 1966

Plate 5, Figure 14

Holotype: Deflandre & Cookson (1955), p. 270, Plate 1, Figure 8.

1955 *Hytrichosphaeridium pulcherrimum* Deflandre & Cookson, p. 270, Plate 1, Figure 8.
1966 *Oligosphaeridium pulcherrimum* Davey & Williams, p75, Plate 10, Figure 9 and Plate 11, Figure 5.

Oligosphaeridium totum Brideaux, 1971

Plate 5, Figure 15

Holotype: Brideaux (1971), pp. 88-89, Plate 25, Figures 53-55, 57.

Genus *Prolixosphaeridium* Davey *et al.*, 1966 emend. Davey, 1969

Prolixosphaeridium parvispinum (Deflandre, 1937) Davey *et al.*, 1969

Plate 4, Figure 14

Holotype: Deflandre (1937), p. 77, Plate 16, Figure 5.

1937 *Hystrichosphaeridium xanthiopyxides* var. *parvispinum* Deflandre, p. 77, Plate 16, Figure 5.
1958 *Hystrichosphaeridium parvispinum* Cookson & Eisenack, p. 45, Plate 8, Figures 10, 12.
1969 *Prolixosphaeridium parvispinum* (Deflandre) Davey, Downie, Sarjeant & Verdier, p. 17.

Genus *Systematophora* Klement, 1960, emend. Stancliffe & Sarjeant, 1990

Systematophora cretacea? Davey 1979

Plate 5, Figure 4

Holotype: Davey, p. 560, Plate 8, Figures 10, 13-15.

Genus *Spiniferites* Mantell, 1850, emend. Sarjeant, 1970

Spiniferites ancoriferus Cookson & Eisenack, 1974
Plate 5, Figure 9

Holotype: Cookson & Eisenack, (1974), p. 58, Plate 21, Figures 4-5.

Spiniferites bejuii Masure *et al*., 1998
Plate 5, Figure 12

Holotype: Masure *et al.* (1998), p. 266, Plate 3, Figures 3, 4, 6.

Spiniferites chebca Below, 1982
Plate 5, Figure 7-8

Holotype: Below (1982), p. 35, Plate 8, Figures 8a-c.

1982 *Spiniferites multibrevis* subsp. *chebca* Below, p. 35, Plate 8, Figures 7, 8a-c, 9.
1993 *Spiniferites chebca* (Below) Lentin & Williams 1993 p. 604.

Spiniferites lenzi Below, 1982
Plate 5, Figure 6

Holotype: Below (1982), p. 34, Plate 7, Figures 7a-b, Plate 8, Figures 3a-b, 6a-b.

Genus *Tanyosphaeridium* Davey & Williams 1966

Tanyosphaeridium spp.
Plate 4, Figure 12

Remarks: Two or three species are present in the succession, although only one is illustrated in Plate 4, Figure 12.

Genus *Trichodinium* Eisenack & Cookson, 1960, emend. Clarke & Verdier, 1967

Trichodinium castanea (Deflandre, 1935) Clarke & Verdier, 1967
Plate 6, Figures 2-3

Holotype: Deflandre (1935), p. 229, Plate 6, Figure 8.

1935 *Paleoperidinum castanea* Deflandre, p. 229, Plate 6, Figure 8.
1967 *Trichodinium castanea* Clarke & Verdier, p. 19, Plate 1, Figures 1-2.

Family Peridiniaceae

Genus *Palaeoperidinium* Deflandre, 1935, emend. Sarjeant, 1967

Palaeoperidinium cretaceum (Pocock, 1962) emend. Harding, 1990

Plate 4, Figure 8

Holotype: Pocock (1962), p. 80, Plate 14, Figure 219.

1962 *Palaeoperidinium cretaceum* Pocock, p. 80, Plate 14, Figures 219-221.
1970 *Astrocysta cretaceum* Davey, p. 359.
1986 *Palaeoperidinium cretaceum* (Pocock), Jansonius, p. 214, Plate 5, Figure 6.
1990 *Palaeoperidinium cretaceum* Harding, p. 44, Plate 1 Figures 1-9, Plate 2, Figures 1-9, Plate 3, Figures 1-9.

Genus *Subtilisphaera* Jain & Millepied, 1973 emend. Lentin & Williams 1976

Subtilisphaera senegalensis Jain & Millipied, 1973

Plate 4, Figure 11

Holotype: Jain & Millipied (1973), pp. 27-28, Plate 3, Figures 31-33.

Subtilisphaera trendallii? (Cookson & Eisenack, 1970) Lentin & Williams, 1976

Plate 4, Figure 10

Holotype: Cookson & Eisenack (1970), pp. 145-146, Plate 12, Figure 5.

1970 *Ascodinium trendallii* Cookson & Eisenack, pp. 145-146, Plate 12, Figures 5-6.
1976 *Subtilisphaera trendallii* Lentin & Williams, p. 120.

Division CHLOROPHYTA
Class Acanthophyceae
Family Botryococcaceae
Genus *Botryococcus* Kutzing, 1849

Botryococcus spp.

Plate 6, Figure 8

Group Acritarcha
Subgroup Sphaeromorphitae
Genus *Leiosphaeridia* Eisenack, 1958

Leiosphaeridia sp.

Plate 6, Figure 9

MISCELLANEOUS

Foraminiferal test linings

Plate 6, Figures 6-7

Scolecodonts

Plate 6, Figures 4-5

5.3 Quantitative analysis

The succession studied yielded a rich palynomorph assemblage, in particular of terrestrial components. However, the marine palynomorphs, notably in the upper part of the section of well GTP-24-SE, also show relatively high abundances. The results of counts (percentage) of each species for the two wells are given in Appendix 2.

The palynomorphs are divided into two major groups: (1) terrestrial palynomorphs, represented by spores from pteridophytes, pollens from gymnosperms, angiosperms and fresh-water algae; (2) and marine palynomorphs, composed of dinoflagellates (subdivided into ceratioid, gonyaulacoid and peridinoid), foraminiferal test linings, acritarchs and scolecodonts.

5.3.1 Palynomorph abundance

The succession is strongly dominated by terrestrial palynomorphs. The pollen group, in particular gymnosperms, is by far the most abundant taxa. This group forms 84.7% of the total palynomorph assemblage in GTP-17-SE and 61.8% in GTP-24-SE. In well GTP-17-SE the second most abundant group is the spores, which reach 8.9% of all palynomorphs. Well GTP-24-SE is characterized by a relatively high abundance of marine palynomorphs with 31.7% of the total palynomorphs. Fresh-water palynomorphs are rare, comprising less than 0.1% in both wells. The relative abundances are shown in Figure 5.1.

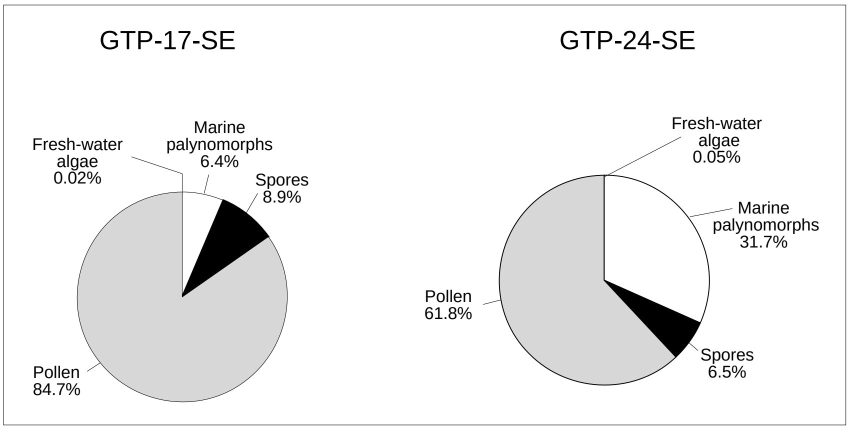

Figure 5.1. Relative abundance of the palynomorph groups for the studied wells.

The abundance of the palynomorphs is also influenced by hydrodynamic equivalence effects. Being the sizes of the palynomorphs equivalent to the fine fraction of the sediments, the palynomorphs are more abundant in sediments such as shales, calcilutites. Coarse sediments such as sandstones normally have low abundances of palynomorphs (Muller, 1959). Moreover, the nature of the sediments is also an important factor in the distribution of the palynomorphs. Being allochthonous sediments, generally the siliciclastic deposited in marine environments show higher abundances of terrestrial than marine palynomorphs. On the other hand, marine palynomorphs are more abundant in carbonate sediments (e.g. Traverse & Ginsburg, 1966; Groot & Groot, 1966; Lana 1997).

The results presented here support the relationship between the high frequency of terrestrial palynomorphs in siliciclastic rocks and of marine groups in carbonate sedimentation (Figure 5.2-5-4).

Lithology		%	Marine		Terrestrial		
			Df	FTL	Fwa	Pollen	Spores
anhydrites		7	24.9	7.8	0.1	61	6.3
carbonates	calcirudites	0.2	24.9	7.8	0.1	61	6.3
	calcarenites	1.3	13.1	4.9	-	77.3	4.7
	calcilutites	27.4	31.8	10.1	0.1	51.7	6.3
mean			***23.3***	***7.6***	***0.1***	***63.3***	***5.8***
siliciclastics	sandstones	15.2	13.4	2.3	-	74.5	9.7
	siltstones	3.7	4	2.4	-	88.4	5.2
	shales	37.8	14.7	5.4	-	73.4	6.5
	claystones	0.6	28.5	2	-	50.5	19
mean			***15.6***	***3***	-	***71.7***	***10.1***

Figure 5.2. Palynomorphs abundance vs. lithology in both wells.

In well GTP-17-SE the abundance of terrestrial palynomorphs is considerable, in particular gymnosperm pollen grains. They occur in siliciclastic as well as in carbonate rocks. A particular characteristic is that the terrestrial palynomorphs occur mostly in diverse types of siliciclastic deposits (Figure 5.3). However, the results of the spore distribution confirm the relation between the siliciclastic sedimentation and terrestrial palynomorphs.

In contrast to what is commonly reported elsewhere the marine palynomorphs are also observed in higher abundance in siliciclastic than in carbonate sediments (Figure 5.3).

Lithology		%	Marine		Terrestrial		
			Df	FTL	Fwa	Pollen	Spores
carbonates	calcarenites	1	3.2	4.5	-	88.2	4.2
	calcilutites	12.5	0.3	6.8	0.1	90.6	2.2
mean			***1.8***	***5.7***	***0.05***	***89.4***	***3.2***
siliciclastics	sandstones	32.1	14.4	2.5	-	72.8	10.3
	siltstones	8.9	4	2.4	-	88.4	5.2
	shales	22.3	7.1	5.4	0.1	64.2	6.3
	claystones	1.4	28.5	2	-	50.5	19
mean			***13.5***	***3.1***	***0.03***	***69***	***10.2***

Figure 5.3. Palynomorphs abundance vs. lithology in well GTP-17-SE.

The results from well GTP-24-SE, which is characterized by mixed sedimentation of shales and calcilutites, confirm that the marine palynomorphs are more abundant in carbonates and terrestrial palynomorphs in siliciclastics (Figure 5.4)

Lithology		%	Marine		Terrestrial		
			Df	FTL	Fwa	Pollen	Spores
	anhydrites	2.6	24.9	7.8	0.1	61	6.3
carbonates	calcirudites	0.4	28.5	2	-	50.5	19
	calcarenites	1.5	28	5.6	-	60.9	5.5
	calcilutites	37.7	35.6	10.4	0.1	47.1	6.8
mean			***30.7***	***6***	***0.03***	***52.8***	***10.5***
siliciclastics	sandstones	3.4	-	-	-	98	2
	shales	43.8	22.3	7.1	0.1	64.2	6.3
mean			***11.2***	***3.6***	***0.1***	***81.1***	***4.2***

Figure 5.4. Palynomorphs abundance vs. lithology in well GTP-24-SE.

5.3.1.1 Stratigraphic distribution of terrestrial palynomorphs

Pteridophyte spores

Pteridophyte spores are present in low to moderate abundances in the studied succession. This group averages 8.9% of all palynomorphs in GTP-17-SE but reaches 36.0% at 100.90 m. In well GTP-24-SE the spores make up 6.5% of all palynomorphs and show a peak in abundance of 32.5% at 22.88 m. In both wells the spores increase in abundance upwards; this trend is more pronounced in well GTP-17-SE (Figure 5.5). The most abundant pteridophyte genus is *Cicatricosisporites*, which in well GTP-17-SE reaches 56.0% of all pteridophytes.

Gymnosperm pollen

The gymnosperm group is the most abundant and diversified group in the studied succession. The high abundance resulted from a large amount of *Classopollis* and *Araucariacites* grains in the samples.

The gymnosperm group is also well represented by pollen grains from the ephedroid group, in particular by the genus *Equisetosporites*. In both wells *Classopollis* is by far the most abundant genus reaching 66.9% of the total palynomorphs in GTP-17-SE and 49.0% in GTP-24-SE. At 364.90 m of GTP-24-SE *Classopollis* is the only palynomorph present. Other important components are the saccate pollen grains. These are mainly represented by the monosaccate genus *Callialasporites*, which reaches 2.0% in some samples. Bisaccate pollen grains are rare such as all other genera no mentioned above.

Angiosperm pollen

The angiosperm group is characterized by low abundances and moderate diversity. The most abundant genus is *Afropollis*, although not exceeding 1.0% of all palynomorphs in the two wells. Most genera are represented only by a single grain.

Fresh-water algae (Fwa)

This group is represented by only the single genus *Botryococcus*, which is rare in both wells.

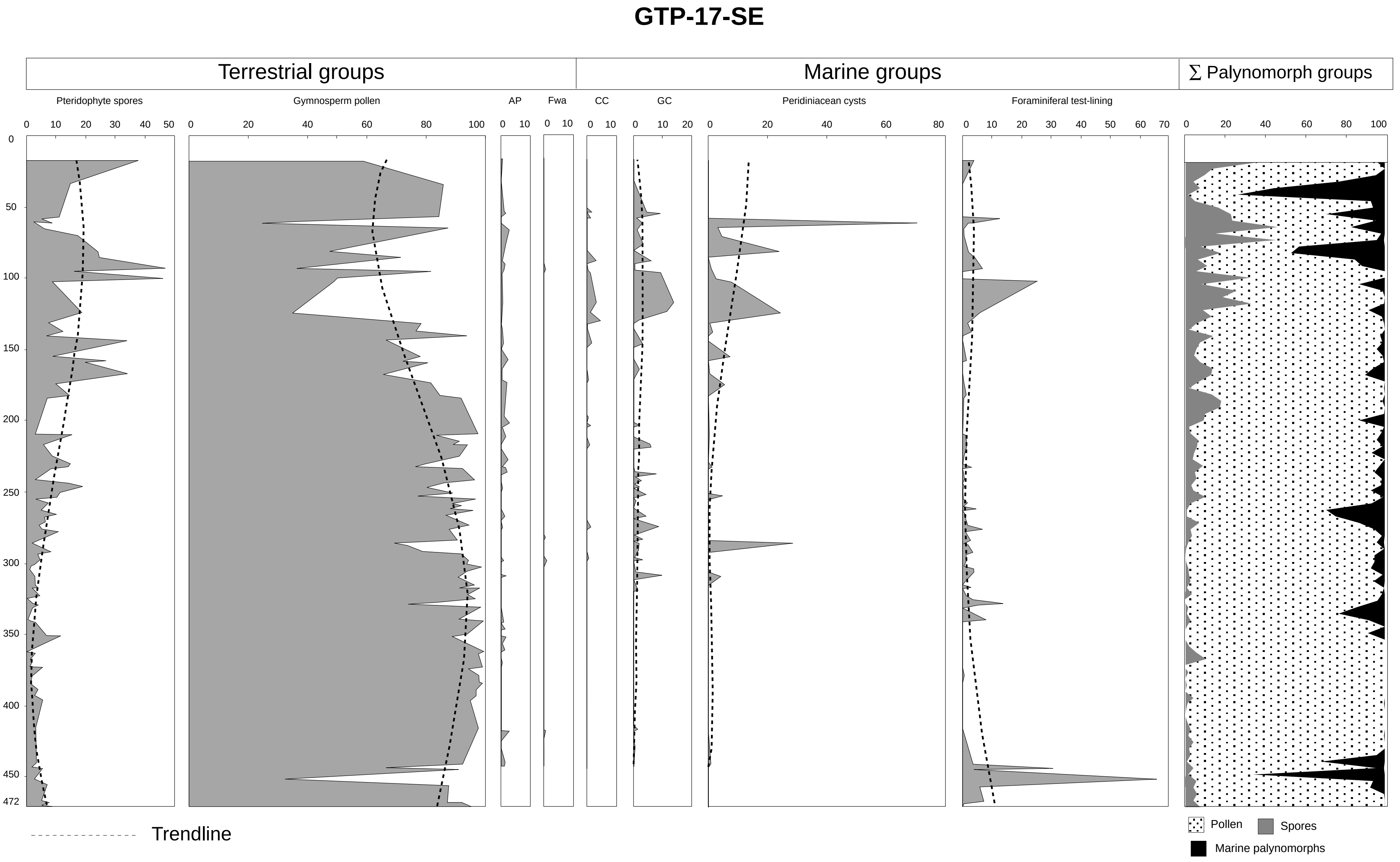

Figure 5.5. Stratigraphic distribution of the palynomorph groups in well GTP-17-SE. Acritarchs and scolecodonts are not included in the sum because of extremely low abundances. AP= angiosperm pollen; Fwa= fresh water algae; CC= ceratiacean cysts; GC= gonyaulacacean cysts.

5.3.1.2 Stratigraphic distribution of marine palynomorphs

Dinoflagellates (Df)

Ceratiacean cysts

Ceratiaceans are represented by four genera, *Circulodinium*, *Cyclonephelium, Odontochitina* and *Pseudoceratium*. This group shows moderate abundances, particularly in well GTP-24-SE, where *Cyclonephelium* is relatively common. The other genera are present in low numbers. The abundance curve shows that the ceratiacean cysts occur mainly in the upper part of the section (see well GTP-24-SE) (Figure 5.6).

Gonyaulacacean cysts

This dinoflagellate group is the most abundant and diversified group. It is composed of twelve genera and includes *Spiniferites,* the most abundant dinoflagellate genus. The abundance of gonyaulacacean cysts increases upwards in both wells. This is most clearly observed in well GTP-24-SE (Figure 5.5). In GTP-17-SE, the group shows a moderate abundance. In this well the dinoflagellates assemblage is dominated by peridinioid dinocysts (discussed below). In GTP-24-SE *Spiniferites* averages 8.8% of all palynomorphs, and at 268.50 reaches 54.5% of all palynomorphs (Figure 5.5). In well GTP-17-SE this genus is the second most abundant dinoflagellate after *Subtilisphaera*.

Other particularly numerous genera among the gonyaulacacean cysts are *Exochosphaeridium* and *Trichodinium*. *Exochosphaeridium* is relatively abundant in well GTP-24-SE, where it makes up 3.8% of all palynomorphs, but in well GTP-17-SE it is rare. In contrast, *Trichodinium* is less abundant in well GTP-24-SE than in GTP-17-SE. None of the other nine genera are common.

Peridiniacean cysts

This group of dinocysts (especially *Subtilisphaera*) is present in great abundances in the succession. However, it shows very low diversity with only two genera, *Palaeoperidinium* and *Subtilisphaera*. Although there are great fluctuations, the abundances of peridiniacean cysts generally increase upward (Figures 5.5-5.6).

Subtilisphaera is the most common peridiniacean genus and the second most abundant dinoflagellate in the succession (Figures 5.5-5.6). In well GTP-17-SE *Subtilisphaera* is the most abundant dinocyst (2.2% of all palynomorphs), at 61.70 m reaching 70.2% of all palynomorphs (Figure 5.5). In well GTP-24-SE, *Subtilisphaera* is the second most abundant dinoflagellate (5.5% of all palynomorphs), 13.25 m reaching 54.9% at.

The genus *Palaeoperidinium* is found only in well GTP-24-SE, where it is comparatively rare. However, at 124.40 m *Palaeoperidinium* shows a peak in abundance, reaching 9.1% of all palynomorphs.

Foraminiferal test linings (FTL)

Foraminiferal test linings are the most abundant marine palynomorphs, with relatively high abundances throughout the succession. FTL are more abundant in well GTP-24 than GTP-17-SE; however, they constitute 38.1% of all marine palynomorphs in well GTP-17-SE, and 24.1% in GTP-24-SE. Moreover, the abundance trend of FTL differs between the wells. In GTP-17-SE the trendline decreases slightly, whereas in GTP-24-SE the curve increases upward (Figure 5.5).

Acritarcha

Among the Acritarcha only the genus *Leiosphaeridia* has been identified. Acritarchs are rare in both wells, making up less than 1.0% of all palynomorphs.

Scolecodonts

This group is composed of few types that show very low abundances in both wells.

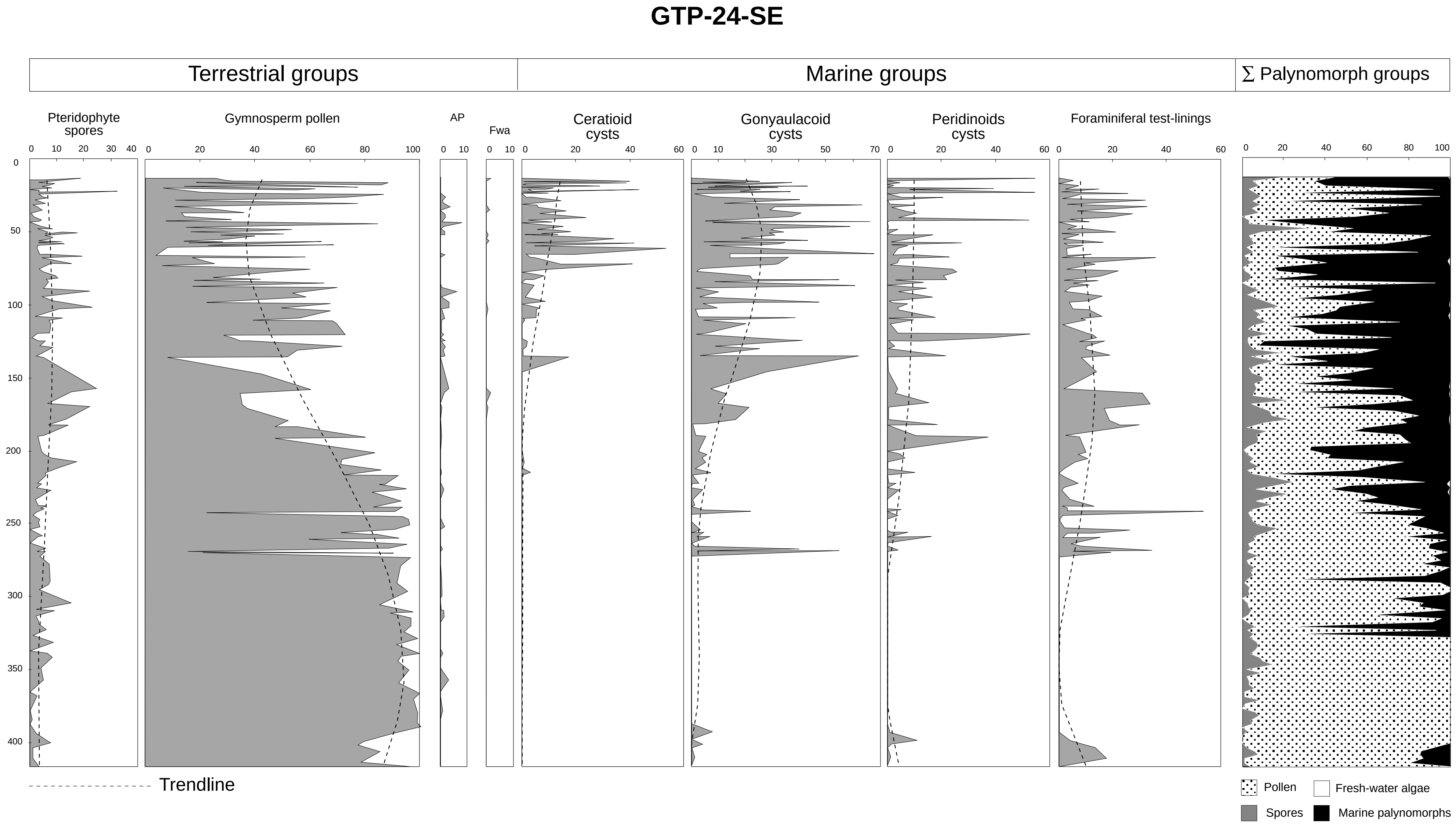

Figure 5.6. Stratigraphic distribution of the palynomorph groups in well GTP-24-SE. Acritarchs and scolecodonts are not included in the sum because of extremely low abundances. AP= angiosperm pollen; Fwa= fresh water algae.

CHAPTER 6
BIOSTRATIGRAPHY

The most recent and thorough palynostratigraphic study from the Sergipe Basin is that of Regali & Santos (1996) published as internal report. This study was published only as extended abstract Regali & Santos (1999). Based on nonmarine palynomorphs the upper Aptian–lower Albian sequence was subdivided into eight sub-zones (Figure 6.1).

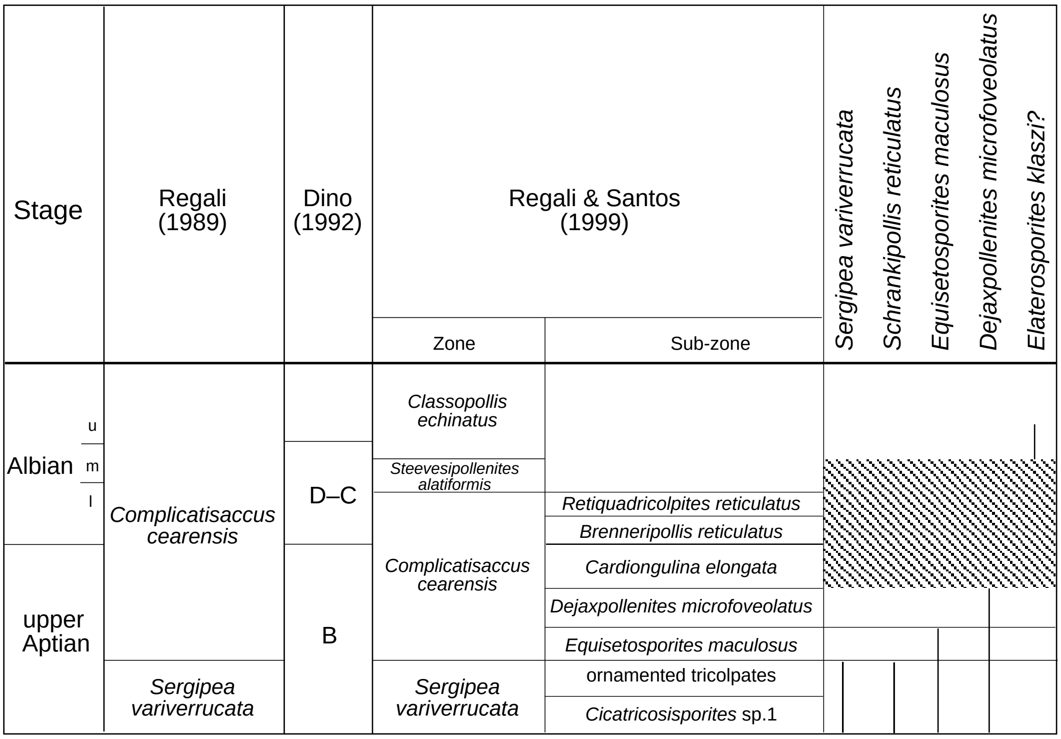
Stage
Regali (1989)
Dino (1992)
Regali & Santos (1999)
Zone
Sub-zone
Sergipea variverrucata
Schrankipollis reticulatus
Equisetosporites maculosus
Dejaxpollenites microfoveolatus
Elaterosporites klaszi?
Albian
u
m
l
upper Aptian
Complicatisaccus cearensis
Sergipea variverrucata
D–C
B
Classopollis echinatus
Steevesipollenites alatiformis
Complicatisaccus cearensis
Sergipea variverrucata
Retiquadricolpites reticulatus
Brenneripollis reticulatus
Cardiongulina elongata
Dejaxpollenites microfoveolatus
Equisetosporites maculosus
ornamented tricolpates
Cicatricosisporites sp.1

Figure 6.1. Correlation of the biostratigraphic zonation used herein (Regali & Santos 1999) with recent palynostratigraphic frameworks for the upper Aptian–Albian of the notheastern Brazilian basins

A number of biostratigraphic studies of the Aptian–Albian of the Sergipe Basin have been carried out, in particular using other microfossils, such as foraminifera (Koutsoukos, 1989, 1991), calcareous nannofossils (Scarparo & Koutsoukos 1998) and ostracodes (Viviers *et al.*, 2000). Koutsoukos & Bengtson (1993) proposed an integrated foraminifera-ammonite biostratigraphy for the Sergipe Basin and correlated this regional biostratigraphic scheme with the international standard zonation. They pointed out that the exact position of the Aptian–Albian boundary is difficult to determine in Sergipe because the upper Aptian *Hypacanthoplites jacobi* and the lower Albian *Leymeriella tardefurcata* ammonite zones of northwestern Europe cannot be recognized.

The first palynostratigraphic purpose for the Cretaceous of the Sergipe Basin was published by Müller (1966). On basis of abundance zones, he established 13 biozones ranging from the Aptian to the Santonian and correlated these with previous foraminifers and ostracodes schemes. The upper Aptian–Albian deposits correspond to his palynological zones i–m.

As the outcome of extensive studies on palynomorphs from the Brazilian sedimentary basins, Regali *et al*. (1974a) published the most relevant zonation for the Cretaceous. This interregional biostratigraphic framework subdivided the upper Aptian to middle Albian sequence into seven biozones based on nonmarine species. Subsequently, this zonation was re-examined and refined by Regali (1989), who also correlated this scheme with zonations proposed for several African basins (e.g. Herngreen, 1973; Doyle *et al*., 1982; Penny, 1986).

The Cretaceous stage boundaries were discussed in 1995 during the “Second International Symposium on Cretaceous Stage Boundaries” in Brussels. For the base of the Albian stage two sections were proposed as possible Global Boundary Stratotype Sections and Points (GSSP) (Hart, 1996). The first occurrence of the ammonite *Leymeriella schrammeni* was proposed to define the base of the Albian stage in the Vohrum section (North Germany). However, in this stratotype, few other biostratigraphic data are known. The Pol de Pré-Guittard (Vocontian Trough in southeastern France) was also suggested as an alternative stratotype section. This may be the most complete succession across the Aptian–Albian transition. From this section, biostratigraphic data on ammonites, calcareous nannofossils, planktonic foraminifera, dinoflagellates, and oceanic anoxic events are available. For the Aptian–Albian boundary Hart (1996) indicated extinctions of dinoflagellates such as *Hystrichosphaerina schindewolfii* and *Cerbia tabulata*, whereas *Nematosphaeropsis singularis*, *Pseudoceratium securigerum* and *Pseudoceratium eisenackii* had their first appearances at this level.

Kennedy *et al*. (2000) also reject the Vohrum section as a possible GSSP and suggest the Tartonne section (Alpes-de-Haute-Provence) in the Vocontian Trough, as a potential GSSP. The base of the Albian Stage suggested by them coincides with the first occurrence of the ammonite *Leymeriella* (*L*.) *tardefurcata*. According to them, the Pol de Pré-Guittard section, also in the Vocontian Trough, is unsuitable as a GSSP due to a hiatus at the critical level in the section.

6.1 Palynomorph zonation

The study presented herein was primarily limited to recognizing the zones and sub-zones proposed by Regali & Santos (1999) (Figure 6.1). The succession in the two wells studied by them was dated as late Aptian (*Equisetosporites maculosus* and *Dejaxpollenites microfoveolatus* sub-zones) (Marília Regali, Petrobras, Rio de Janeiro, person. comm. September 1999). However, the samples available to Regali & Santos (1999) are not from the same depths as those used in this study.

The recognition of the zonation proposed by Regali & Santos (1999) was based on the distribution of selected taxa, mainly from well GTP-24-SE. Recognition of the zonation in well GTP-17-SE is difficult owing to the low diversity of palynomorphs and the coarse grain sedimentation, in particular sandstones (discussed in 5.4).

Four successive biostratigraphic intervals are identified for the upper Aptian–middle Albian of the studied succession. These are mainly based on the biostratigraphic framework introduced by Regali & Santos (1999). A few changes were necessary, however, because of the diverging occurrences of palynomorphs in the studied wells compared to those examined by the above authors. According to them the sub-zones proposed are only locally applicable, although some of these sub-zones can be recognized in other basins in Brazil.

The *Sergipea variverrucata* zone and the *Equisetosporites maculosus* and *Dejaxpollenites microfoveolatus* sub-zones from the Regali & Santos (1999) were recognized herein (Figure 6.1).

The major difference from the study by Regali & Santos (1999) for the two studied wells, is the recognition of the middle Albian (*Classopollis echinatus* Zone) characterized by the first occurrence of *Elaterosporites klaszi*?. However, it was recorded from samples that were not studied by Regali & Santos (1999).

The dinoflagellate occurrence from studied succession are compared with schemes from the African basins (e.g.; Habib, 1975, 1977, 1978; Williams & Bujak 1985; Schrank & Ibrahim, 1995) (Figure 6.2).

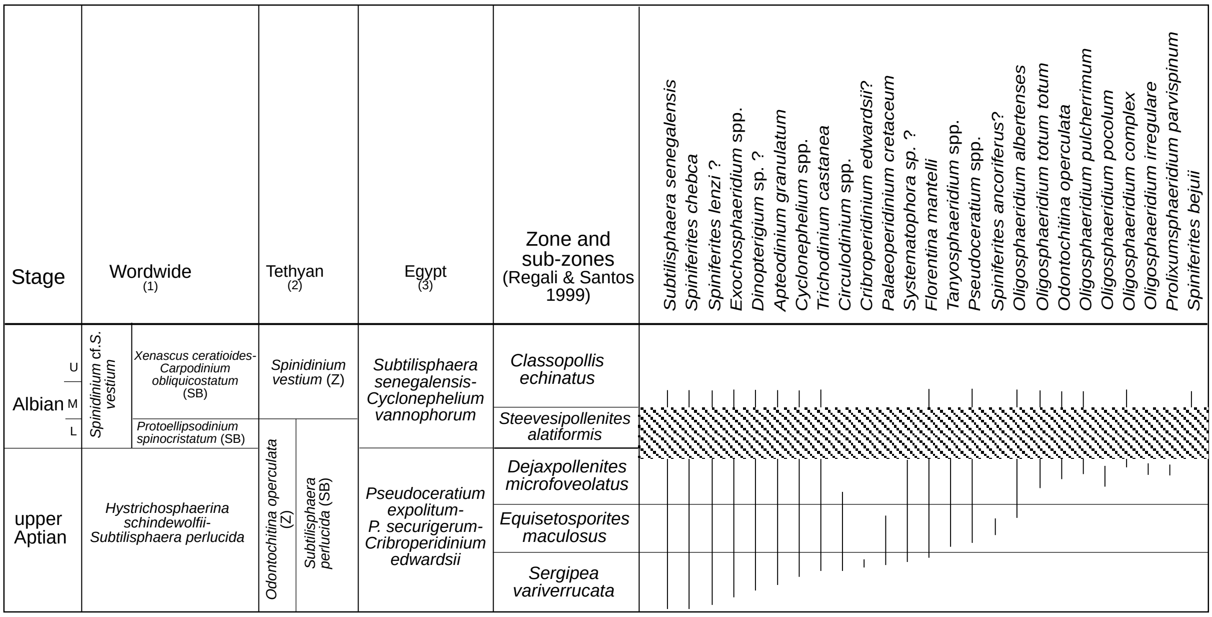

Figure 6.2. Correlation of the biostratigraphic zonation used herein (Regali & Santos 1999) and the recorded dinoflagellates in the succession with dinoflagellate zonation from (1) Williams & Bujak (1985); (2) Habib, (1975, 1977, 1978) (3) Schrank & Ibrahim (1995).

Sergipea variverrucata Zone (upper Aptian)

Definition: The top of this zone is defined by the last occurrence (LO) of *Sergipea variverrucata*.

Other characteristics: In this zone the local LOs (LLO) of *Cyathidites* spp., *Gnetaceaepollenites diversus*, *Klukisporites pseudoreticulatus*, *Stellatopollis dubius*, *Vitreisporites pustulosus* and *Cribroperidinium edwardsii* are observed.

Age and correlation: According to Regali (e.g., 1987a, 1989) the extinction of *Sergipea variverrucata* occurs within the upper Aptian but not at the Aptian–Albian boundary. However, Dino (1992) placed the *Sergipea variverrucata* extinction at the boundary. *Cribroperidinium edwardsii* is considered to be a long-ranging species, however, according to the zonation of Schrank & Ibrahim (1995), it is restricted to the Aptian.

***Observation**: Sergipea variverrucata* is recorded only in well GTP-24-SE. Due the absence of this species in well GTP-17-SE, the LLO of *Schrankipollis reticulatus* (ornamented tricolpates) was used to identified the upper zonal boundary (Figure 6.3). The LLO of *Schrankipollis reticulatus* coincides with the LO of *Sergipea variverrucata* (Figure 6.1) According to Dino (1992), the extinction of *Equisetosporites maculosus* coincides with the extinction of *Sergipea variverrucata*.

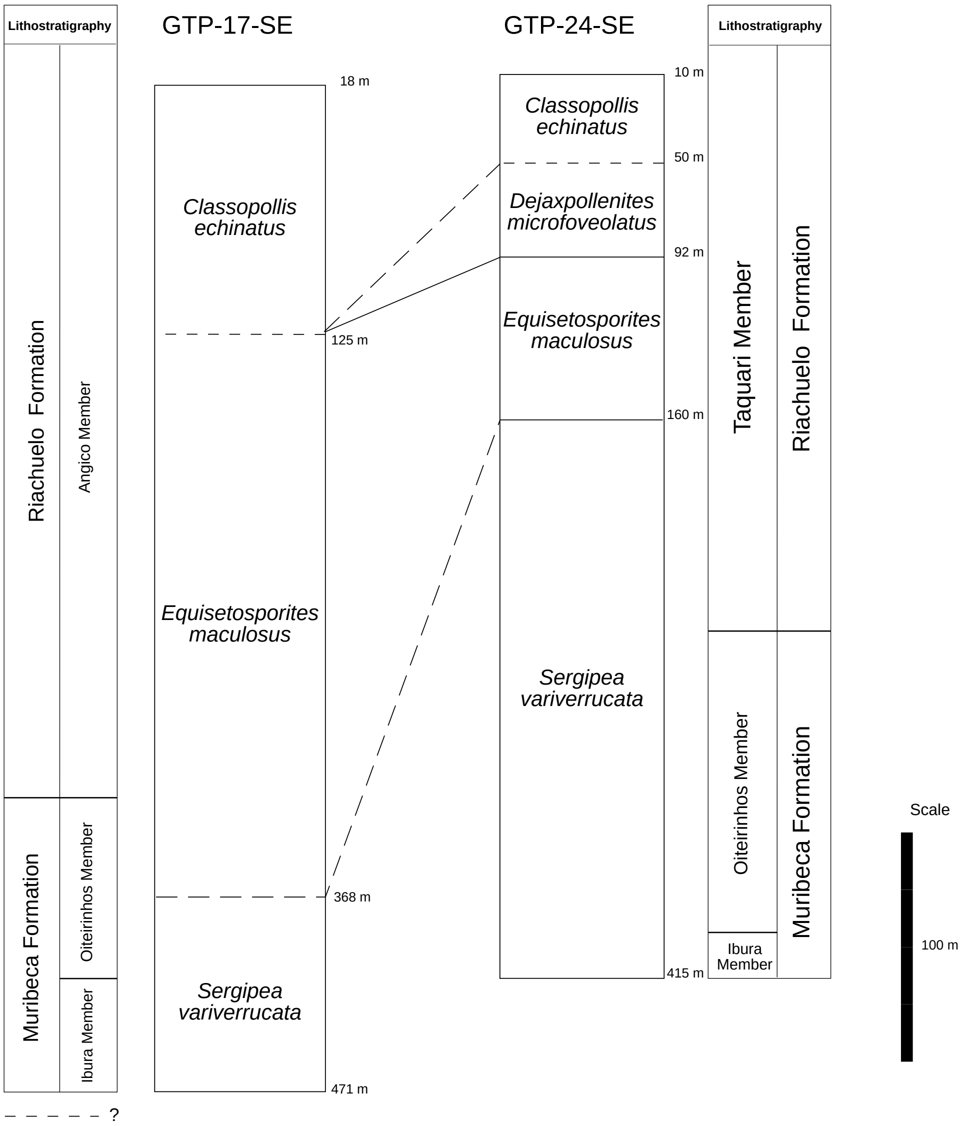
Lithostratigraphy
GTP-17-SE
GTP-24-SE
Lithostratigraphy
Riachuelo Formation
Angico Member
Muribeca Formation
Oiteirinhos Member
Ibura Member
18 m
Classopollis echinatus
125 m
Equisetosporites maculosus
368 m
Sergipea variverrucata
471 m
10 m
Classopollis echinatus
50 m
Dejaxpollenites microfoveolatus
92 m
Equisetosporites maculosus
160 m
Sergipea variverrucata
415 m
Taquari Member
Riachuelo Formation
Oiteirinhos Member
Ibura Member
Muribeca Formation
Scale
100 m
– – – – – ?

Figure 6.3. Correlation of the identified zones and sub-zones between the two studied wells

Equisetosporites maculosus Sub-zone (upper Aptian)

Definition: The base of this sub-zone is defined by the LO of *Sergipea variverrucata*. The upper boundary is defined by the local LO of *Equisetosporites maculosus*.

Other characteristics: the *Equisetosporites maculosus* sub-zone is characterized, among others, by the following local first occurrences (LFO): *Antulsporites* spp., *Brenneripollis reticulatus*, *Equisetosporites albertenses*, *Equisetosporites ovatus*, *Microfoveolatus daunkiensis*, and the LFO of the dinoflagellates *Pseudoceratium* spp., *Spiniferites ancoriferus*?, *Tanyosphaeridium* sp. and *Oligosphaeridium albertenses*. In this interval the LLOs of *Bennettitaepollenites regaliae*, *Gnetaceaepollenites chlatratus*, *Striatopollis reticulatus* and *Palaeoperidinium cretaceum* are observed.

Age and correlation: In this sub-zone the LFO of *Oligosphaeridium* spp. represented by *Oligosphaeridium albertenses* is recognized. This species has mainly been reported from the Barremian–Albian of Morocco (Below, 1982, 1983, and 1984). *Palaeoperidinium cretaceum* is recorded from the lower to upper Aptian by Torricelli (2000), and from the Barremian–Albian by Below (1981).

Dejaxpollenites microfoveolatus Sub-zone (late Aptian)

Definition: The base of this sub-zone is defined by the LLO of *Equisetosporites maculosus* and its top by the LLO of *Dejaxpollenites microfoveolatus*.

Other characteristics: In this sub-zone the local FFOs of *Oligosphaeridium complex*, *Oligosphaeridium totum* and *Odontochitina operculata* are observed. The LLOs of the palynomorphs *Tanyosphaeridium* sp., *Systematophora*? spp., *Circulodinium Uesuguipollenites callosus*, *Antulsporites* sp., and *Gnetaceaepollenites uesugui* and the dinoflagellates *Oligosphaeridium irregulare*, *Oligosphaeridium pocolum* and *Prolixosphaeridium parvispinum* are restricted into this sub-zone.

Age and correlation: According to Dino (1994), *Dejaxpollenites microfoveolatus* is also found in the Albian of his Biozone C (Figure 6.1). *Odontochitina operculata* has frequently been reported from the Aptian and less commonly from the Albian (Figure 6.2), whereas *Prolixosphaeridium parvispinum* has mainly been reported from Aptian strata (e.g., Davey, 1979; Hedlund & Beju, 1977; Davey & Verdier, 1974)

Observation: In this sub-zone only the LFOs of dinoflagellates are recorded. This reflects the marine influence in the upper part of the succession. The well-diversity of *Oligosphaeridium* and the LFO of *Odontochitina* support this conclusion. This sub-zone was not recognized in well GTP-17 (Figure 6.3).

Classopollis echinatus Zone (middle? Albian)

Definition: The base of this zone is defined by the LFO of *Elaterosporites klaszi*?

Age and correlation: An Albian age is indicate by the presence of elaterate-bearing species represented herein by the *Elaterosporites klaszi*?. Elaterates have been reported as typical of the Albian strata (Herngreen & Duenas-Jimenez, 1990). *Elaterosporites klaszi* is not known to occur below the middle Albian. This species is used to define the *Elaterosporites klaszi-Afropollis-Tricolporopollenites* Zone of the middle Albian of the Morocco (Schrank &

Ibrahim, 1995). Of particular stratigraphic interest is the local FO of the dinocyst *Spiniferites bejuii*. This species was described from the Coniacian–Santonian of the Côte d'Ivoire-Ghana transform margin. However, according to Cecília C. Lana (Petrobras, Rio de Janeiro, person. comm., September 1999) this species has also been reported from older strata. According to the zonation of Regali & Santos (1999), the species *Elaterosporites klaszi* occurs in this zone.

***Observation**: Classopollis echinatus* was not recorded in the samples studied. This interval overlies the *Dejaxpollenites microfoveolatus* sub-zone. The absence of forms indicating the *Cardiongulina elongata*, *Brenneripollis reticulatus* and *Retiquadricolpites reticulatus* sub-zones and *Steevesipollenites alatiformis* Zone of the uppermost Aptian–lower middle Albian indicates a possible hiatus comprising the stage boundary.

CHAPTER 7
PALEOECOLOGY

The paleoecological analysis provides data on the palynomorph composition that reflect the progressive increase in marine influence in the area. For this analysis, percentage data on palynomorph genera from wells GTP-17-SE and GTP-24-SE were used to investigate the relationship between the palynomorphs and their depositional environment.

7.1 Palynological assemblages

R-mode cluster analysis, based on the abundance and composition of all 64 palynomorph genera found in wells GTP-17-SE and GTP-24-SE, revealed four superclusters that represent the palynological assemblages (PA) 1-4 (Figure 7.1). The major break between clusters 1 and 2 reflects clearly the separation of marine and terrestrial palynomorphs.

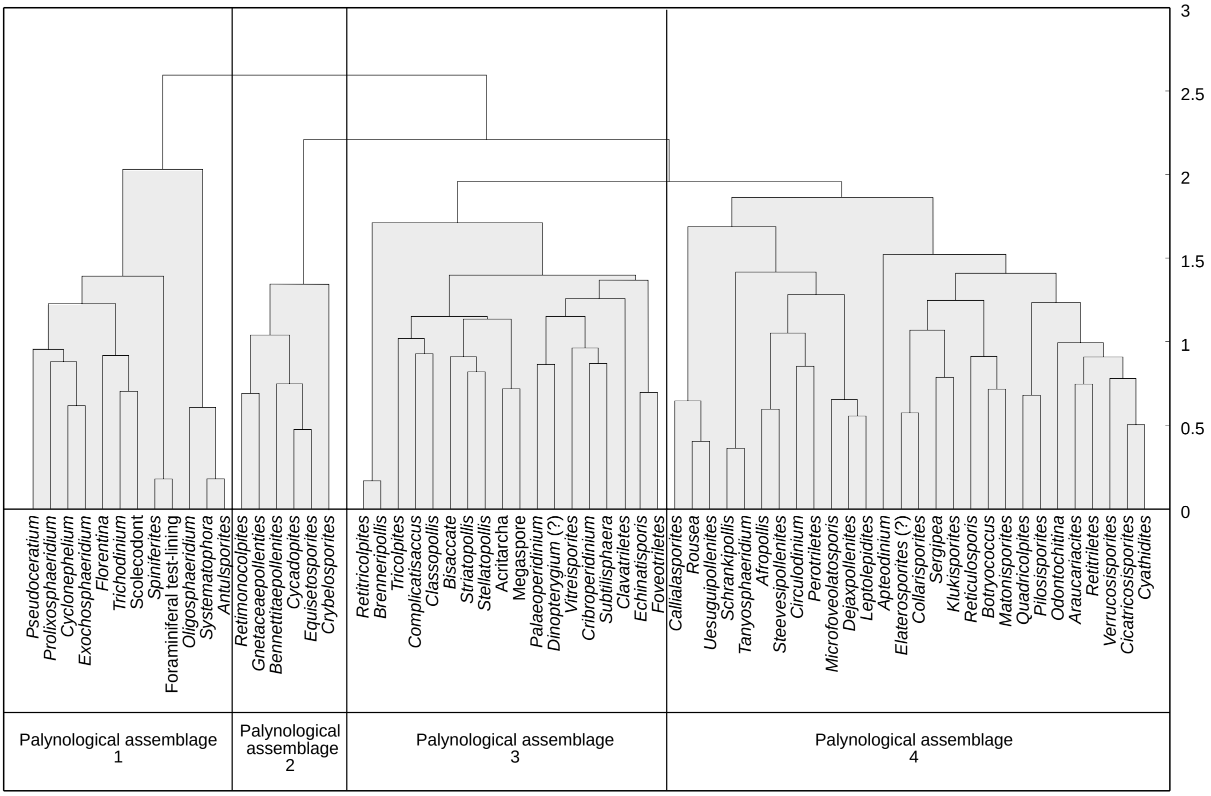

Figure 7.1. Dendrogram (r-mode) of 64 genera from the two wells studied showing the four palynological assemblages.

Palynological Assemblage 1

Palynological Assemblage 1 assemblage is composed of marine palynomorphs, with the exception of the fern spore genus *Antulsporites*. The assemblages contains *Pseudoceratium, Prolixosphaeridium Cyclonephelium, Exochosphaeridium, Florentina, Trichodinium,* scolecodonts*, Spiniferites,* foraminiferal test linings, *Oligosphaeridium*, *Systematophora* and *Antulsporites*.

Nine out of nineteen genera of the dinoflagellates recorded in the succession are included in this assemblage, the majority of them belonging to the gonyaulacoid group. Generally, these genera indicate an open marine environment (neritic setting). *Spiniferites* is the most abundant dinoflagellate and, together with associated dinoflagellates such as *Exochosphaeridium*, *Trichodinium* and, *Oligosphaeridium*, indicative of open neritic conditions (Downie *et al.*, 1971; Williams, 1977; Masure, 1984; Marshall & Batten, 1988; Lana, 1997). However, the most abundant marine palynomorph is the foraminiferal test lining group (FTL), which generally, is present in great abundance in nearshore environments (Tyson, 1995; Lana 1997). This supports the theory that most FTL are derived from benthic foraminifera (Tyson, 1993). According to some authors (e.g., Cross *et al.*, 1966; Melia, 1984; Tyson 1993) high abundances of this group is an indication of upwelling.

Like the FTL, *Cyclonephelium* is mainly recorded in nearshore environments (Eshet *et al.*, 1992; Lana, 1997). Moreover, high abundances of the genus *Cyclonephelium* are related to restricted marine environments under stress conditions.

	Psilatriletes	*Cicatricosisporites*	Megaspore	*Botryococcus*	Foraminiferal test-lining	*Spiniferites*	*Subtilisphaera*	*Exochosphaeridium*	*Cyclonephelium*	*Trichodinium*	*Palaeoperidinium*	*Oligosphaeridium*	*Classopolis*	*Equisetosporites*	*Gnetaceaepollenties*	*Araucariacites*	*Afropollis*	*Bisaccate*
Psilatriletes	1.0																	
Cicatricosisporites	**0.5**	1.0																
Megaspore	0.001	0.12	1.0															
Botryococcus	0.18	0.04	0.02	1.0														
Foraminiferal test-lining	-0.04	-0.11	-0.07	0.04	1.0													
Spiniferites	-0.04	-0.1	-0.06	0.06	**0.82**	1.0												
Subtilisphaera	-0.03	-0.02	-0.004	0.13	0.08	0.11	1.0											
Exochosphaeridium	0.05	-0.05	-0.02	0.11	0.17	**0.23**	0.01	1.0										
Cyclonephelium	0.05	-0.06	-0.05	0.05	0.09	0.13	-0.02	**0.38**	1.0									
Trichodinium	0.06	-0.06	-0.03	-0.03	0.09	0.09	-0.05	0.08	0.09	1.0								
Palaeoperidinium	-0.02	-0.01	-0.02	0.01	0.02	0.03	-0.004	0.01	-0.02	0.06	1.0							
Oligosphaeridium	0.01	-0.06	0	0.001	0.01	0.03	0.03	0.19	**0.36**	-0.04	-0.02	1.0						
Classopolis	*-0.31*	*-0.2*	0.01	-0.15	*-0.4*	*-0.42*	*-0.36*	*-0.47*	*-0.5*	*-0.24*	*-0.5*	*-0.26*	1.0					
Equisetosporites	-0.05	-0.07	0.04	0.02	-0.12	-0.1	-0.18	0.04	-0.05	-0.03	-0.004	-0.02	-0.15	1.0				
Gnetaceaepollenties	-0.06	-0.06	-0.04	0.02	-0.01	-0.03	-0.05	-0.01	0.03	-0.02	-0.05	-0.04	-0.19	*-0.29*	-0.1.0			
Araucariacites	**0.27**	**0.29**	0.06	-0.03	*-0.26*	*-0.27*	-0.08	-0.10	-0.11	-0.08	-0.05	0.02	*-0.3*	0.16	**0.2**	1.0		
Afropollis	-0.04	0.02	-0.01	0.02	0.07	0.11	0.12	0.11	-0.01	0.07	0.08	-0.07	*-0.24*	**0.31**	**0.25**	0.05	-0.1.0	
Bisaccate	0.09	0.16	0.1	0.03	-0.05	-0.06	-0.03	-0.05	-0.05	-0.04	-0.01	-0.04	0.06	-0.02	-0.06	-0.03	-0.01	1.0

Figure 7.2. Pearson correlation of selected paleoecologically significant genera from the two studied wells. Values in bold indicate significant positive correlation and those in italic negative correlation.

Palynological Assemblage 2

PA2 is composed only of terrestrial palynomorphs: *Retimonocolpites, Gnetaceaepollenites, Bennettitaepollenites, Cycadopites, Equisetosporites, Cyathidites* and *Crybelosporites*. This assemblage has the lowest palynomorph abundance of the assemblages, with ephedroid types (*Gnetaceaepollenties* and *Equisetosporites*) being the most abundant. Their pollen grains are related to the modern gymnosperms *Ephedra* and *Welwitschia* (Gnetales), which are found in arid to semi-arid environments (Doyle *et al*., 1982; Arai & Coelho, 1996). As observed by Doyle *et al*. (1982), the correlation of *Gnetaceaepollenites* and *Equisetosporites* with *Classopollis* is negative (Figure 7.2), which suggests that these genera are less tolerant of saline conditions than *Classopollis*.

Two pteridophyte genera, (*Cyathidites* and *Crybelosporites*), also are present in this assemblage, although in small numbers.

Palynological Assemblage 3

PA3 shows the highest palynomorph abundance among the assemblages, with a dominance of *Classopollis* grains. The assemblage consists of *Retitricolpites, Brenneripollis, Tricolpites, Complicatisaccus, Classopollis*, bisaccates, *Striatopollis, Stellatopollis*, Acritarcha, megaspore, *Palaeoperidinium, Dinopterygium*?, *Vitreisporites, Cribroperidinium, Subtilisphaera, Clavatriletes, Echitriletes*, and *Foveotriletes*. *Classopollis* was produced by the extinct conifer family Cheirolepidiaceae (Doyle *et al*., 1982) and dominated in regions with arid climates. *Classopollis* is most commonly recorded in nearshore marine-lagoonal environments and often associated with evaporites (Vakhrameev, 1970; Doyle *et al*., 1982; Hashimoto, 1995; Arai & Coelho, 1996). *Classopollis* shows low correlation with the other palynomorphs (Figure 7.2).

The presence of bisaccate (bisaccate-types and *Vitreisporites*) pollen in PA3 is contradictory because these pollen types are normally associated with temperate highland climates. However, Arai & Coelho (1996) investigated samples from the Aptian–Albian of the Araripe Basin (north of the Sergipe Basin) and observed a relatively high correlation between the bisaccate group and *Classopollis*. According to them, the bisaccates were transported by trade winds and that its abundance was influenced by a minor dilution in the arid periods (weaker terrestrial supply), whereas the terrestrial influx responsible for transport of the other palynomorphs was relatively weak. Lima (1983) suggested that the occurrence of the bisaccate pollen *Vitreisporites* and *Cedripites* in deposits where *Classopollis* predominates, could be attributed to short episodes of cooler (possibly subtropical) conditions.

The fern spores (megaspores, *Clavatriletes*, *Echinatisporis* and *Foveotriletes*) are also present in this assemblage, but in low abundances. The presence of megaspores reflects a nearshore environment. These spores are large, dense and thick-walled and not easily transported, so in general they are deposited near their source (Speelman & Hills, 1980).

Four genera of dinoflagellates are recorded in PA3 (*Palaeoperidinium, Dinopterygium*?, *Cribroperidinium,* and *Subtilisphaera*). Among them, the genus *Subtilisphaera* is by far the most abundant, being the second most abundant dinocyst genus in the assemblage. Generally, this genus is associated with marine environments with low salinity (Jain and Millepied, 1975). *Subtilisphaera* are abundant in assemblages of low diversity (Arai *et al.*, 1994; Lana, 1997). It represents 98% of the total of the four genera recorded in PA3, and correlation with other palynomorphs is very low (Figure 7.2). Arai *et al.* (1994, 2000) proposed *Subtilisphaera* ecozones for the Early Cretaceous of the proto-Atlantic Ocean. These ecozones were originally identified in the Aptian–Albian of the Ceará Basin (northern Brazil) and later in other continental marginal basins of Brazil. However, according to Arai *et al.* (op. cit.) this ecozone has not been confirmed in the Sergipe Basin. Within five ecozones, the *Subtilisphaera spp. diluted by terrestrial palynomorphs Ecozone* would be the most comparable with the PA3. *Subtilisphaera* and *Palaeoperidinium* are typical of restricted marine environments. *Dinopterygium*? and *Cribroperidinium* shows very low abundances.

Palynological Assemblage 4

PA4 is distinguished by the high diversity of fern spores and the high abundance of the genus *Araucariacites*. It is composed of *Callialasporites, Rousea*, *Uesuguipollenites, Schrankipollis, Tanyosphaeridium, Afropollis, Steevesipollenites*, *Circulodinium, Perotriletes, Microfoveolatosporis, Dejaxpollenites, Leptolepidites, Apteodinium, Elaterosporites*?, *Collarisporites, Sergipea, Klukisporites, Reticulosporis, Botryococcus, Matonisporites, Quadricolpites, Pilosisporites, Odontochitina, Araucariacites, Retitriletes, Verrucosisporites, Cicatricosisporites*, and *Cyathidites*.

Araucariacites is the second most abundant genus of the terrestrial palynomorphs. According to Doyle *et al.* (1982) it is related to a tropically-centered group, which are found in lowland deposits of the Early Cretaceous age. These authors mentioned that an increase in aridity resulted in a decline of *Araucariacites* abundance. This was also suggested by Arai & Coelho (1996), who mentioned the fact that *Araucariacites* is characteristic of humid and subtropical to tropical climates. The genus shows a negative correlation with *Classopollis* (Figure 7.2), thus confirming this hypothesis.

PA4 contains the highest number of pteridophyte genera with *Cicatricosisporites* and *Cyathidites* being the most abundant. The fern spores have been largely related to humid conditions, based on modern distributions of the pteridophytes (Doyle *et al.*, 1982; Lima, 1983; Arai & Coelho, 1996). Generally, high abundance of these spores is recorded in nearshore environments (Hughes & Moody-Stuart, 1967; Tschudy 1969, Heusser & Balsam 1977, Mudie 1982, Tyson, 1989). The genera *Cicatricosisporites* and *Cyathidites* have a negative correlation with *Classopollis* and ephedroid pollen (Figure 7.2).

Afropollis is the most abundant angiosperm pollen genus in the succession, although, it is recorded only in small amounts. This genus has been interpreted as typical of arid environments; however; just as the ephedroid group, *Afropollis* was less tolerant to saline soil conditions (Doyle *et al*. 1982). *Afropollis* also shows a negative correlation with *Classopollis* (Figure 7.2).

Four genera of dinoflagellates are found in PA4: *Tanyosphaeridium, Circulodinium, Apteodinium*, and *Odontochitina*, with *Apteodinium* being the most abundant. It has been interpreted as indicative of inner neritic conditions (Wilpshaar & Leereveld, 1994), but others have suggested it could be found in open marine environments (Leckie, 1990). *Circulodinium* is characteristic of restricted marine environments (Lana, 1997). The other two genera are rare.

In this assemblage is included the only fresh-water palynomorph found in the succession, the genus *Botryococcus*. This genus is characteristic of fresh-water lacustrine, fluvial, lagoonal and deltaic facies (Traverse, 1955; Pocock, 1972; Herngreen *et al.*, 1980 Batten & Lister, 1988; Williams, 1992). According to Tyson (1995), the abundance of *Botryococcus* in marine sediments is usually low.

7.2 Ecophases

The application of ecophases was first introduced by Schuurman (1977), who defined as a recognizable step of the successive development of a (palynological) assemblages (in Brugman *et al.*, 1994). According to Brugman *et al*. (1994) the ecophases are characterized by the distribution of palynomorph taxa that reflect developments in the local vegetation or phytoplankton communities.

The stratigraphic distribution of the palynological assemblages allowed the definition of seven ecophases (Figure 7.3-7.4). These are recognized in both wells, but with some differences that are discussed below.

Ecophase 1 is distinguished by a relatively high abundance of marine palynomorphs from the palynological assemblage 1 (PA1). In well GTP-17 a PA1 is composed essentially of FTL. In well GTP-24-SE FTL are also dominant, although dinocysts (*Spiniferites*) are present in moderate abundances.

The main characteristic of Ecophase 2 is the absolute dominance of PA3, in particular the genus *Classopollis*. Marine palynomorphs are rare, and are found only in the lower part of the ecophase.

The dominance of PA4, in particular by *Araucariacites* together with the highest abundance of the palynomorphs from PA2 characterizes Ecophase 3. This ecophase can be further distinguished by the rare occurrence of marine palynomorphs.

During Ecophase 4 the abundance of palynomorphs from PA3 increased again due mainly to *Classopollis*. The great abundance of these terrestrial palynomorphs from PA3 reflects a high proportion of fine siliciclastic sedimentation, especially shales.

Ecophase 5 is characterized by an increase in marine palynomorphs from PA1, mainly due to *Spiniferites*, *Exochosphaeridium*, and *Trichodinium* associated with fern spores (*Cyathidites* and *Cicatricosisporites*) and *Araucariacites* from PA4. Of all the dinoflagellates recorded in the succession, these marine components are the ones that are most clearly indicative of open marine environments. Therefore, their abundance in this ecophase is strong evidence of the beginning of a transgressive phase.

In Ecophase 6 the percentage of *Classopollis* (PA3) increases again, but remains lower than in ecophases 2 and 4. This, together with a moderate abundance of marine palynomorphs from PA1 (particular in well GTP-24-SE), indicates that the terrestrial influx was not as strong as in Ecophase 4. Moreover, in spite of the evidence of a moderate regression, the environment is still characterized as open marine.

Ecophase 7 is characterized by high abundance and diversity of marine palynomorphs from PA1 indicating an open marine environment. This is distinguished mainly in well GTP-24-SE. The abundance of PA1 in well GTP-17-SE is relatively low, with PA4 being the most abundant. In fact, in both wells *Araucariacites* pollen grains from PA4 are the most characteristic land-derived elements. The low abundances of PA1 in well GTP-17-SE are taken to reflect a proximal facies of the Angico Member.

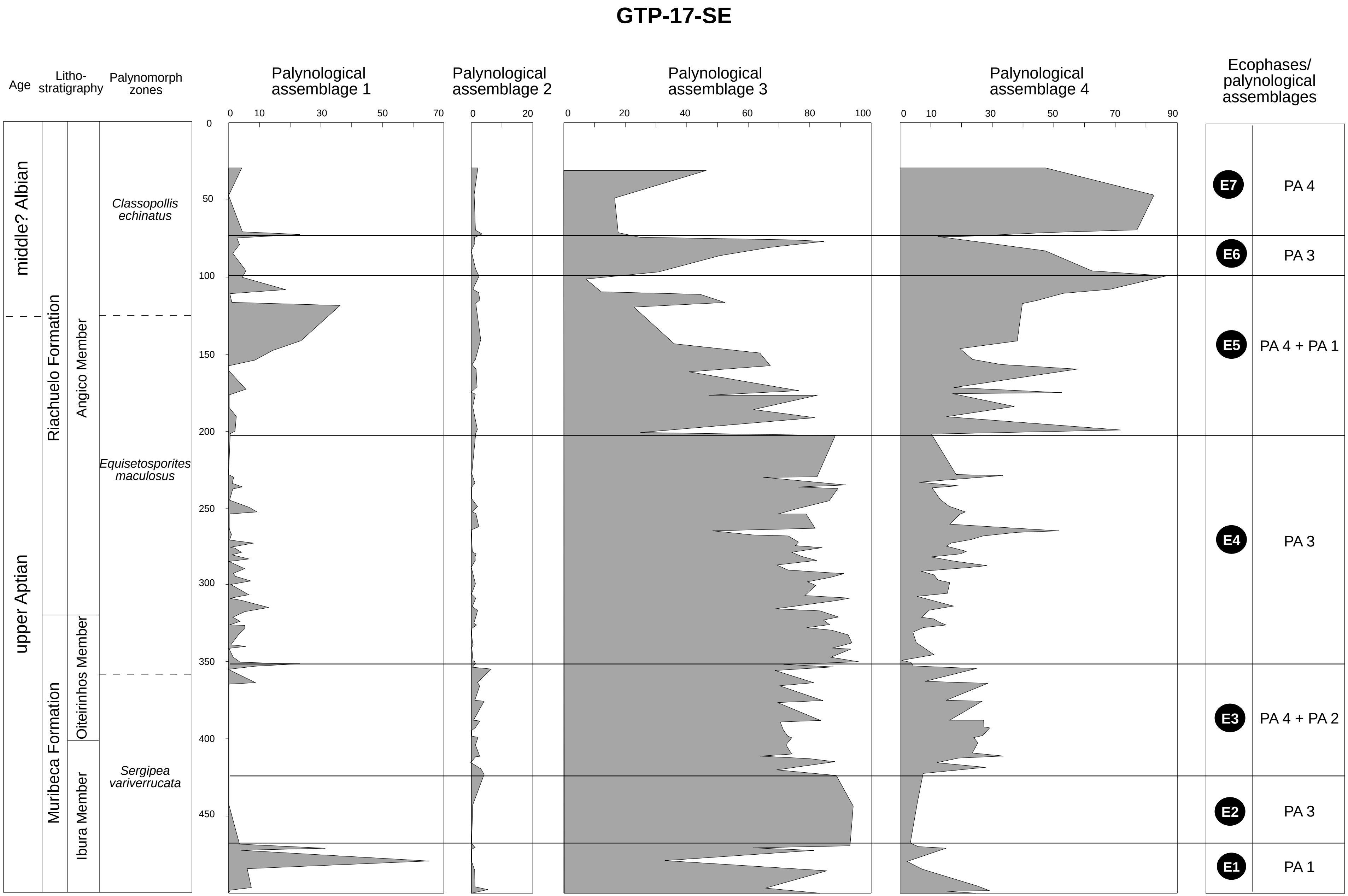

Figure 7.3. Stratigraphic distribution of palynological assemblages showing the ecophases for well GTP-17-SE.

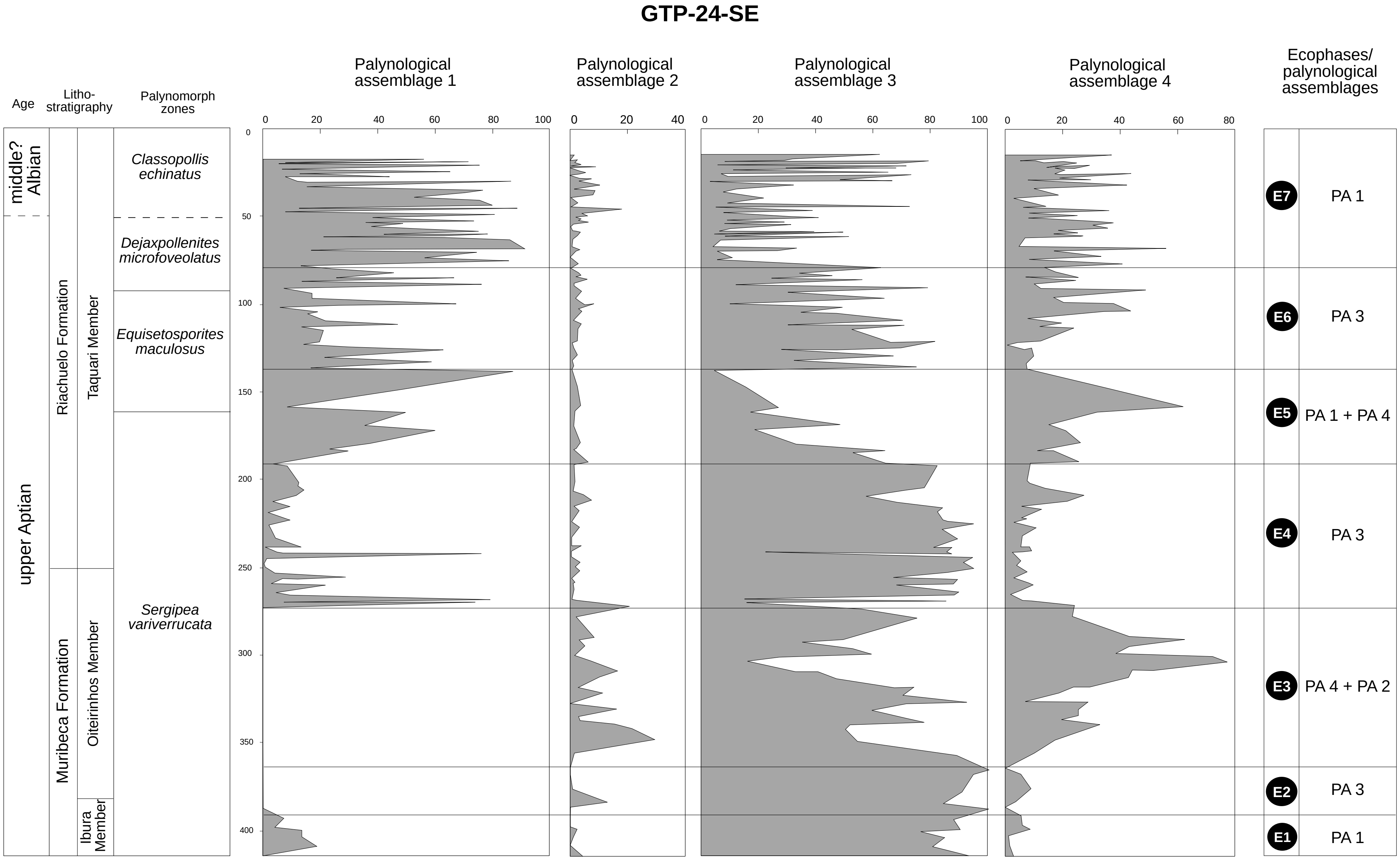

Figure 7.4. Stratigraphic distribution of palynological assemblages showing the ecophases for well GTP-24-SE

7.3 Palynological Marine Index (PMI)

The PMI curves of both wells show strong fluctuations. The index ranges from 100.0, where marine palynomorphs are absent to 250.00 (in GTP-24-SE). This fluctuation reflects the major (low PMI values) and minor (high PMI values) influx in the area. However, in both curves there is an increase in abundance of marine palynomorphs upward. The average abundance in well GTP-24-SE is higher (138.90) than in GTP-17-SE (122.90). Most peaks of the PMI from both wells are related to an increase in abundance of FTL and/or *Spiniferites*. However, in well GTP-17-SE some of these peaks are related also to the presence of *Subtilisphaera*.

High values of PMI are found in ecophases where PA3 shows moderate abundance (Figure 7.5). This is best observed in well GTP-17-SE (ecophases 1 and 5). In well GTP-24-SE high PMI values are also found in ecophases characterized by PA1 (e.g., ecophases 1, 4, 5 and 7) (Figure 7.6).

7.4 P/G ratio

The P/G ratio is characterized by strong fluctuations, but with a slight decrease upward (Figures 7.5-7.6). As for the PMI, this decrease also indicates a progressive marine influence in the area. However, terrestrial input into the this marine environment is indicated through major peaks of the P/G ratio that reflect the marked increase in abundance of the genus *Subtilisphaera*.

Comparison of PMI with the P/G ratio curves shows that the increase in PMI values is directly related to the decrease of the P/G ratio (Figures 7.5-7.6). It is not surprising that the highest values of the ratio are recognized in ecophases 4 and 6 characterized by PA3. However, in the lower part of Ecophase 5 of well GTP-17-SE *Subtilisphaera* is also very common (Figure 7.6).

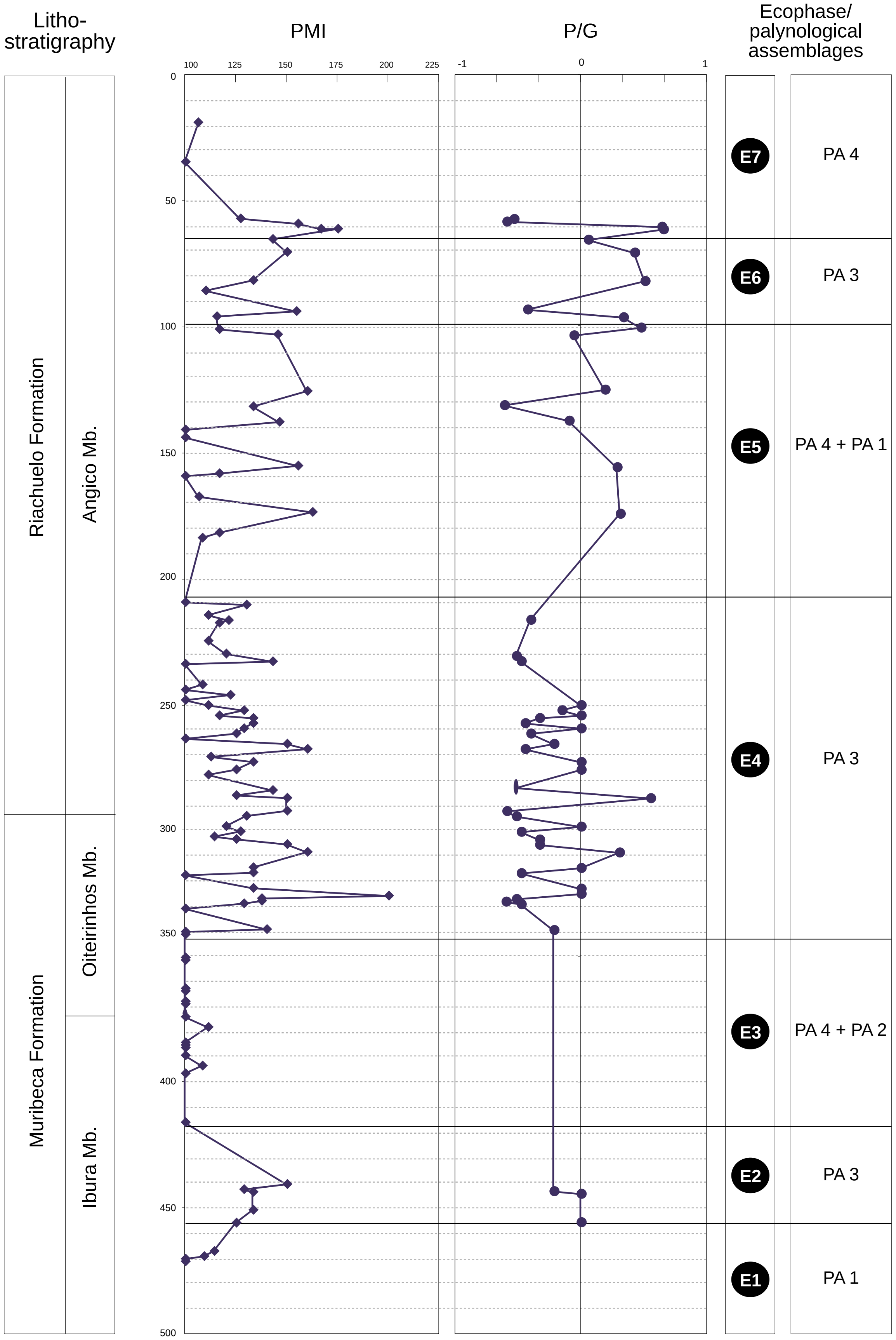

Figure 7.5. Stratigraphic distribution of PMI and P/G ratio for well GTP-17-SE showing the ecophases and their palynological assemblages.

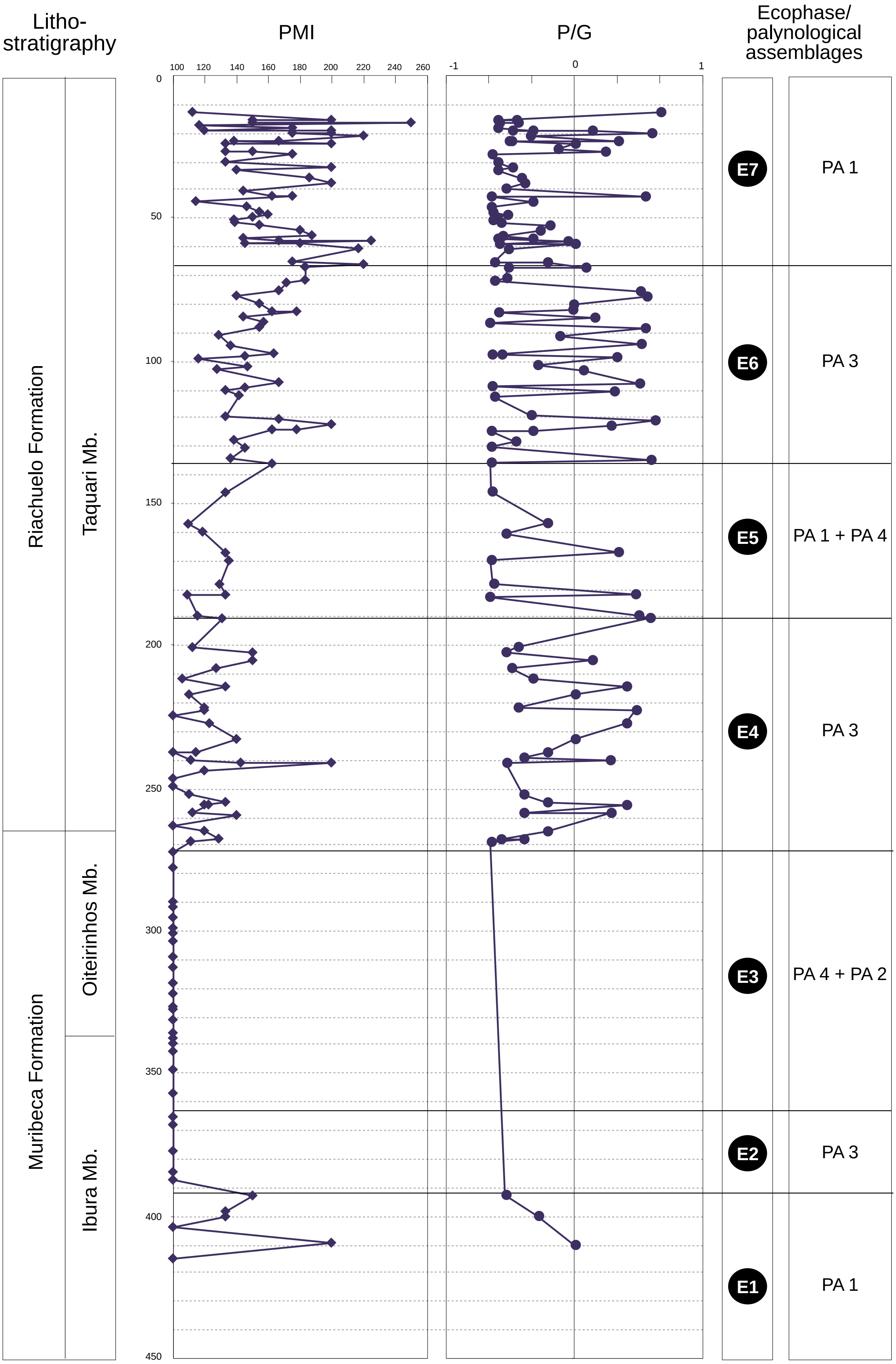

Figure 7.6. Stratigraphic distribution of PMI and P/G ratio for well GTP-24-SE showing the ecophases and their palynological assemblages.

7.5 Paleoclimatic implications

In both studied wells high abundances of *Classopollis* are observed, although the relative abundance decreases markedly upward, whereas fern spores increase. These trends reflect the progressive increase of humid conditions. However, *Classopollis* is conspicuously more abundant than the spores, making up 52.0% in well GTP-17-SE and 43.0% in GTP-24-SE. This indicates that in spite of the increase in humidity, the climate was semi-arid to arid. The abundance of *Classopollis* is higher in well GTP-17-SE than in well GTP-24-SE. This is possibly related to the proximal setting of GTP-17-SE and the relative high abundances of marine palynomorphs in GTP-24-SE.

In ecophases 5 and 7 there is a clear decrease in abundance of *Classopollis* with an average of 36.0% in well GP-17-SE and 23.0% in GTP-24-SE (Figures 7.7-7.8). These proportions suggest that the climate was slightly humid during deposition. This is also indicated by the relatively high abundances of *Araucariacites* grains.

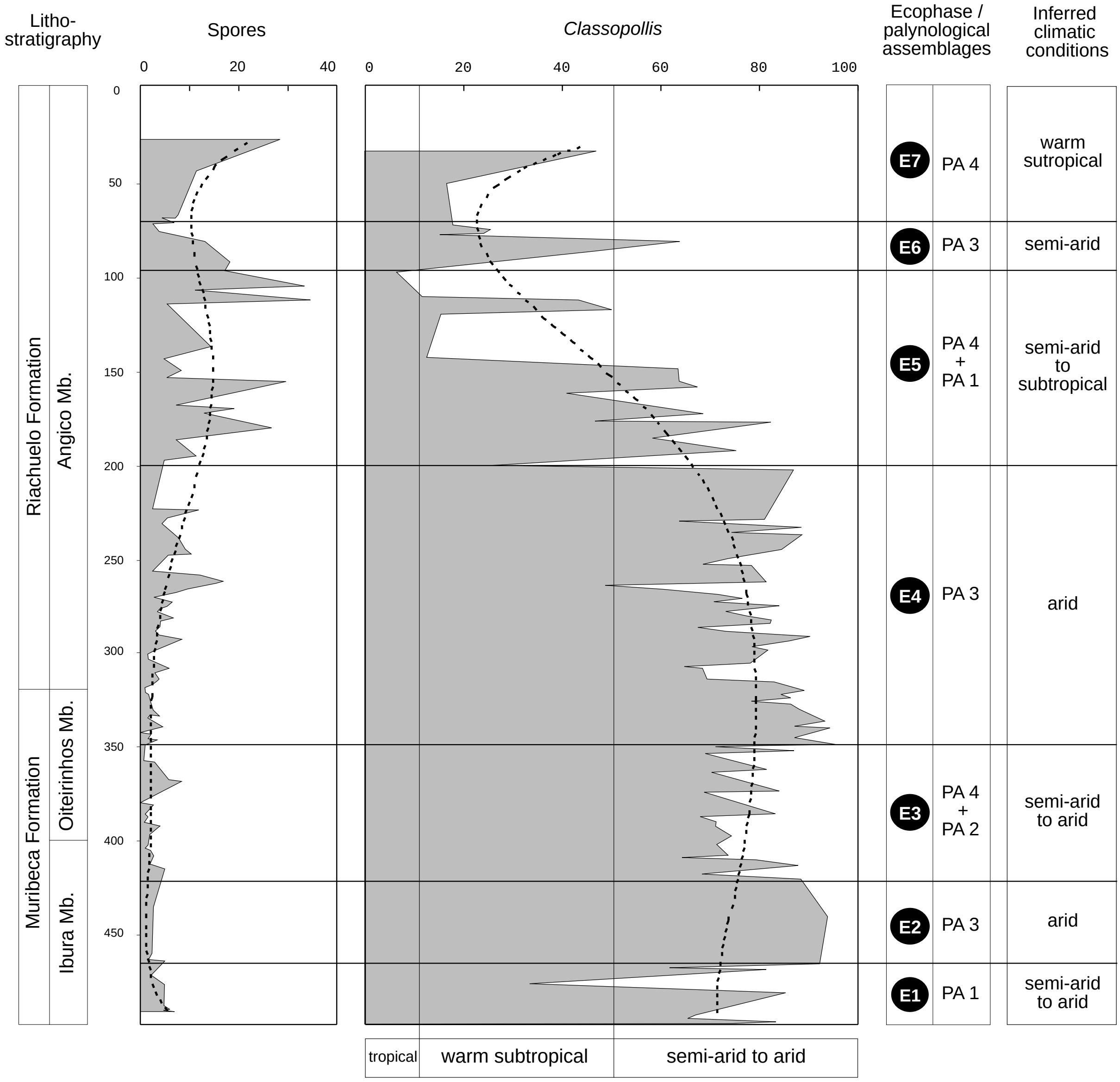

Figure 7.7. Relative abundances of spores and *Classopollis* in well GTP-17-SE, and inferred climatic conditions.

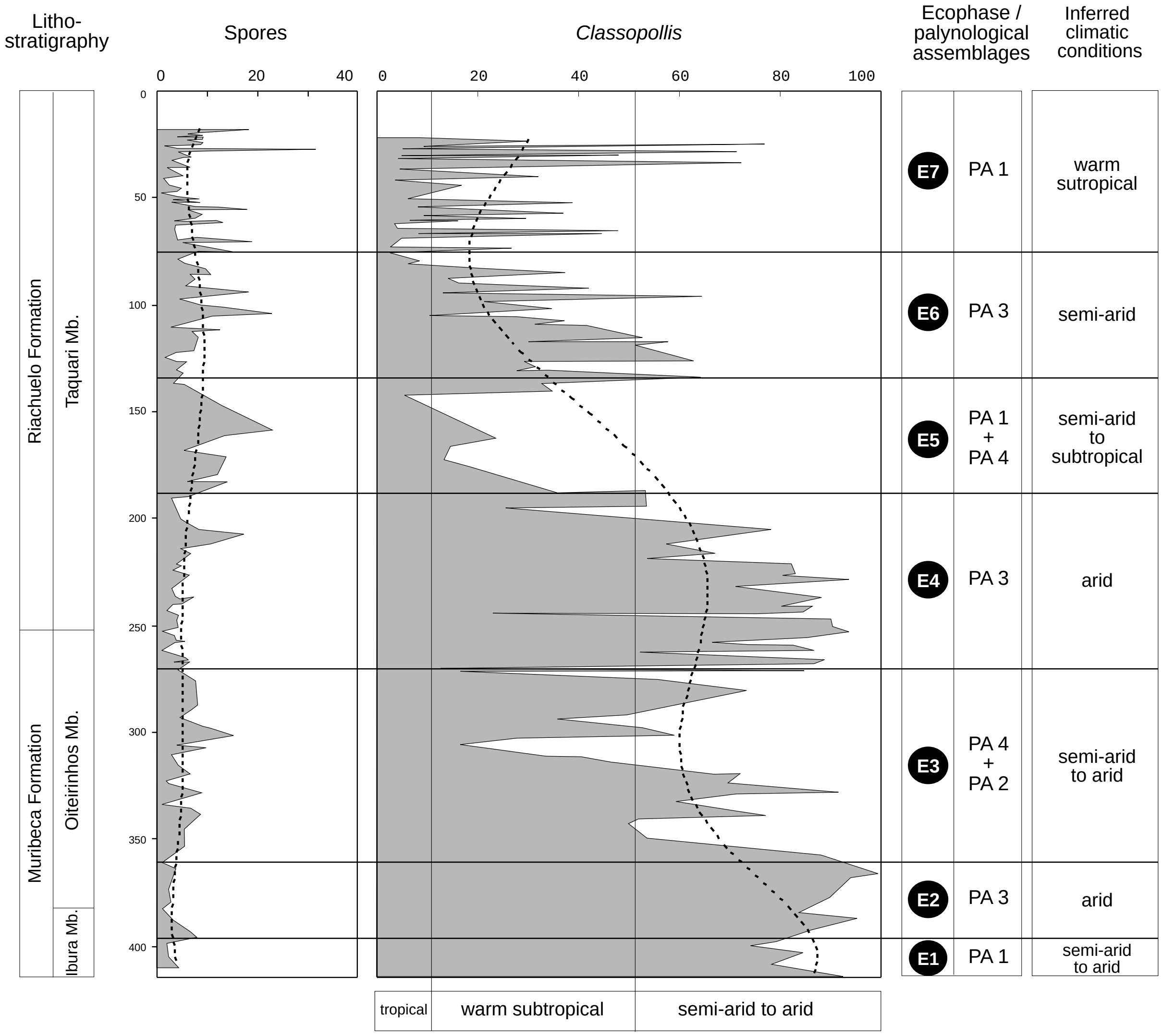

Figure 7.8. Relative abundances of spores and *Classopollis* in well GTP-24-SE, and inferred climatic conditions.

CHAPTER 8
PALYNOFACIES ANALYSIS

The term *palynofacies* was first introduced by Combaz (1964) to describe the “*total microscopic image of the organic components*”. The term became popular and detailed studies have subsequently been published. However, the definition varied between different authors. Some authors named the organic components “organic matter” (e.g., Gehmann, 1962; Lorente, 1990), others “palynodebris” (e.g., Alpern, 1970; Durand *et al.*, 1970; Boulter & Riddick 1986; Farr 1989; van der Zwan, 1990; Boulter 1994;) and still others “kerogen” (Tyson, 1995, 1996; Araujo, 1998; Mendonça Filho, 1999; Carvalho, 1999). The latter is today the most widely used term to describe the organic components (Tyson, 1993).

Tyson (1995) defined the term kerogen as “the particulate organic matter residue isolated from a sedimentary rock after complete dissolution of the rock matrix by HCL and HF (non-oxidative) acids”. The term palynofacies was defined by the same author as “a body of sediment containing a distinctive assemblage of palynological organic matter thought to reflect a specific set of environmental conditions, or to be associated with a characteristic range of hydrocarbon-generating potential”.

8.1 Palynofacies Associations

Five types of palynofacies are identified in the studied succession (Figure 8.1). These types were observed in all samples studied from the two wells. Owing to their low abundance, the zooclast groups are not used in the definition the palynofacies associations.

Palynofacies types	Description
Phy-o	Predominance of the phytoclast group with a high content of opaque particles.
Phy-t	Predominance of the phytoclast group with a high content of transluscent particles.
Pal-s	Predominance of the palynomorph group with a high content of sporomorphs.
Pal-mp	Predominance of the palynomorph group with a high content of marine palynomorphs.
AOM	Predominance of the AOM group.

Figure 8.1. Palynofacies types identified in the studied wells.

To assess the pattern of distribution of the palynofacies types, their abundances were submitted to cluster analysis by (r- and q-mode combined). The cluster for well GTP-17-SE, based on the abundance and composition of the kerogen groups (except the zooclast group), revealed two superclusters (Figure 8.2). These are: supercluster A, which is subdivided into A1, A2 and A3, and supercluster B, subdivided into B1 and B2. The combination of the r- and q-mode analyses shows that the phytoclast group is mainly included in cluster A (all samples up to 50.0%). A1 is composed mostly of phytoclasts and a moderate abundance of the AOM group (Phy/AOM); A2 of high abundances of phytoclasts combined with moderate to high abundances of palynomorphs (Phy/Pal); and A3 composed of very high abundances of phytoclasts (Phy). The palynomorph group shows high values at 103.30 m, which made it possible to separate this sample from the others. The high abundances of the AOM group occur in supercluster B. B1 is characterized by very high abundances of the AOM group. In B2 this group occurs with phytoclasts and, in particular with the palynomorph group (AOM/Pal).

The major break that occurred between clusters A and B is strongly related to the abundance of the phytoclast group. The cluster analysis by r-mode (Figure 8.2) clearly shows that the phytoclast group is separated from the palynomorph and AOM groups.

For well GTP-24-SE, the cluster analyses revealed four superclusters (A to D) (Figure 8.3). Supercluster A is composed of only one cluster distinguished by high abundances of phytoclast group (Phy). Supercluster B was subdivided into B1 and B2, in which cluster B1 is represented by a combination of high abundances of the phytoclast group, with moderate to high abundances of the AOM group (Phy/AOM), and B2, in which the phytoclast group is combined with moderate to high abundances of palynomorphs (Phy/Pal). Supercluster C is characterized by very high percentages of the palynomorph group (Pal). Supercluster D is represented by high abundances of the AOM group. This supercluster was subdivided into D1 and D2, based on the amounts of AOM. D1 presents very high abundances of the AOM group. The D2 cluster is a combination of high abundances of AOM with a moderate abundance of palynomorphs.

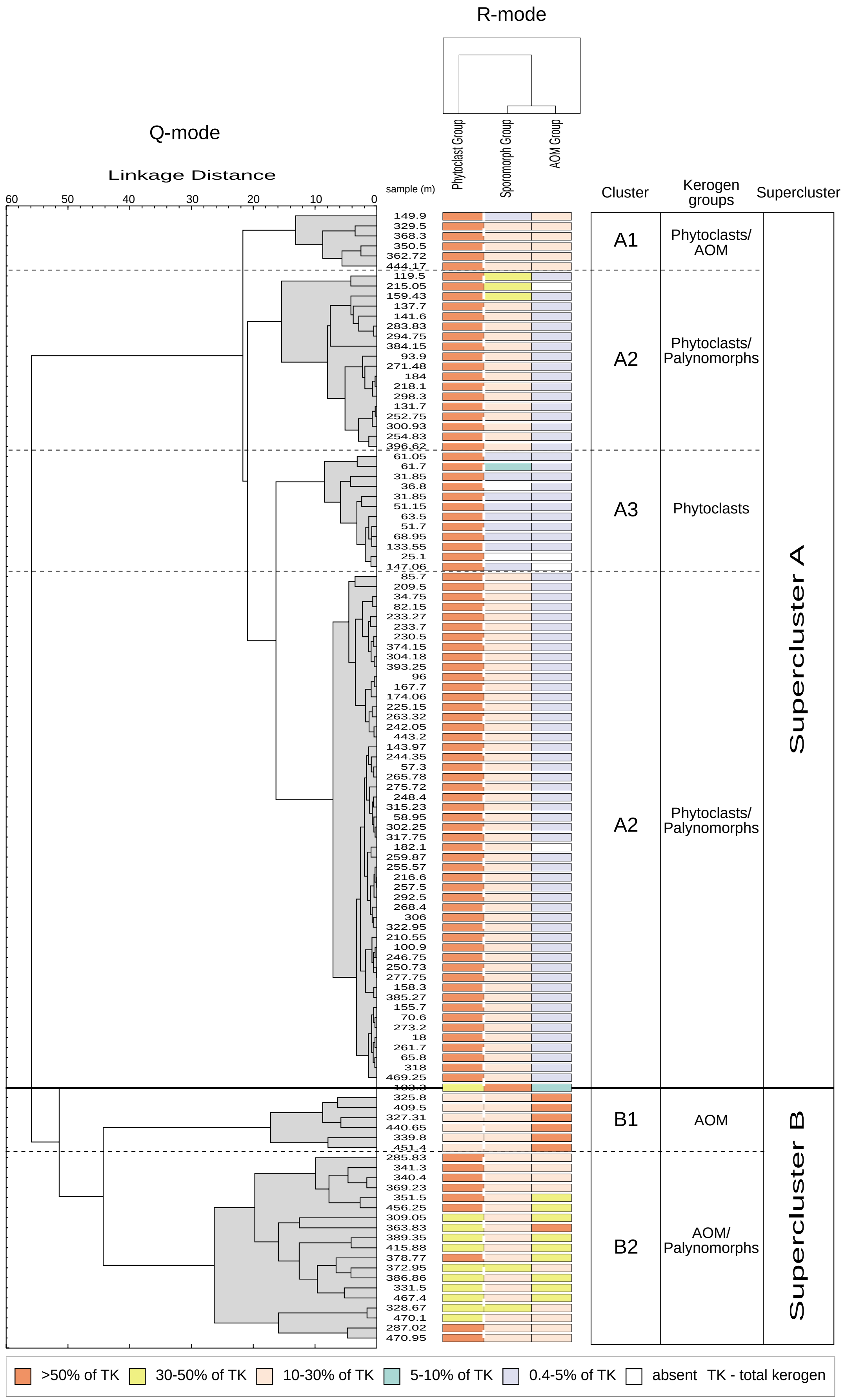

Figure 8.2. Dendrograms by r and q-mode of well GTP-17-SE showing the grouping of samples (q-mode) and kerogen groups (r-mode).

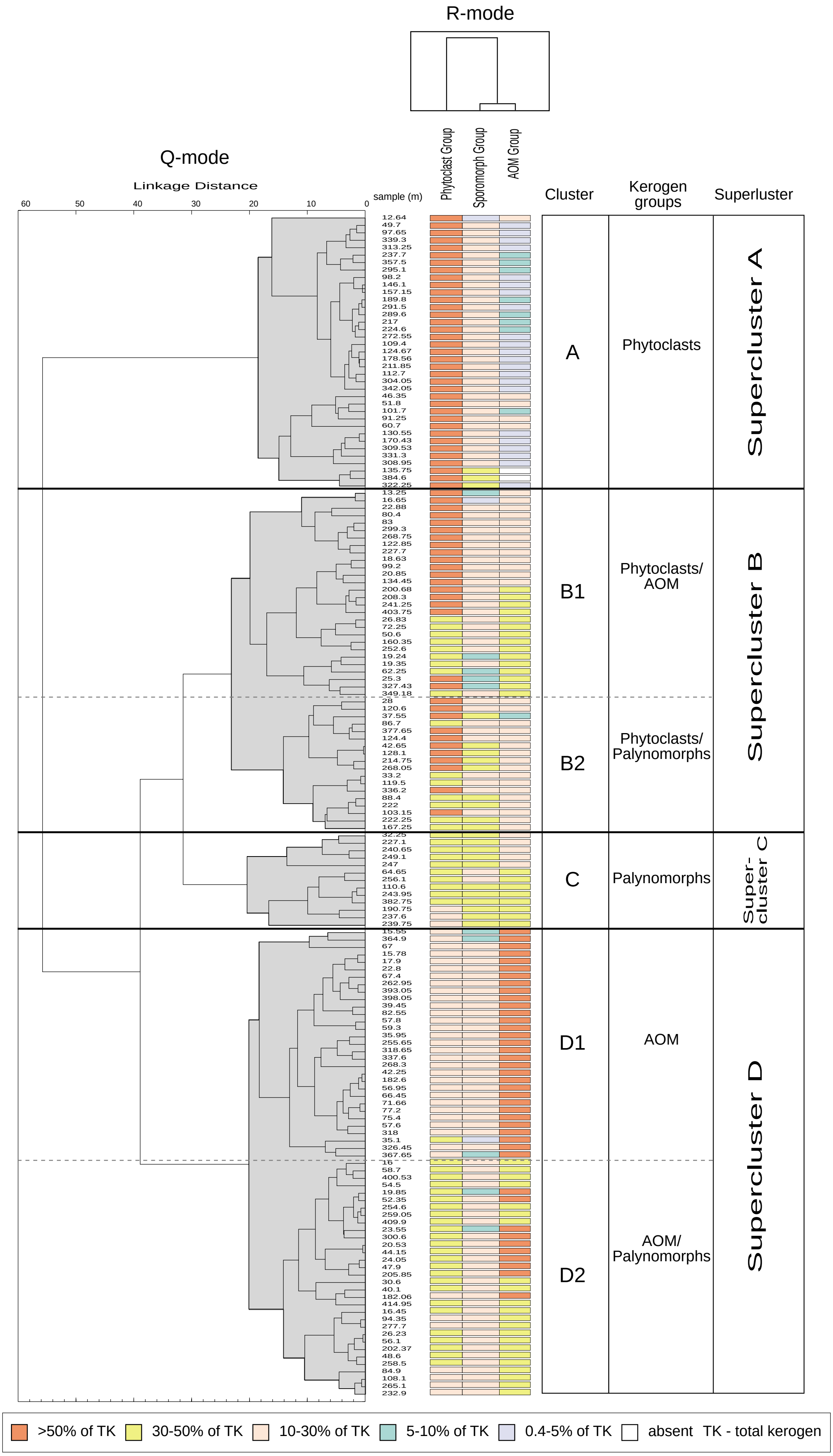

Figure 8.3. Dendrograms by r and q-mode of well GTP-24-SE showing the grouping of samples (q-mode) and kerogen groups (r-mode).

In this well the main break separates clearly the samples with high abundances of the AOM group from those with high abundances of phytoclasts (r-mode) (Figure 8.3). Based on the palynofacies composition, their abundance and the clusters, the types were grouped into nine **palynofacies associations** (Figure 8.4), which were used for the definition of palynofacies units

Palynofacies associations	Description
Phy-o	Predominance of the phytoclast group with a high content of opaque particles.
Phy-o/Pal-s	Predominance of the phytoclast group with a high content of opaque particles combined with sporomorphs.
Phy-o/Pal-mp	Predominance of the phytoclast group with a high content of opaque particles combined with marine palynomorphs.
Phy-o/AOM	Predominance of the phytoclast group with a high content of opaque particles combined moderate content of the AOM group.
Pal-s/Phy-o	Predominance of the palynomorph group with a high content of sporomorphs combined with opaque particles.
Pal-mp/Phy-o	Predominance of the palynomorph group with a high content of marine palynomorphs combined with opaque particles.
AOM/Phy-o	Predominance of the AOM group combined with opaque particles.
AOM/Pal-s	Predominance of the AOM group combined with sporomorphs.
AOM/Pal-mp	Predominance of the AOM group combined with marine palynomorphs.

Figure 8.4. Palynofacies associations identified after the cluster analyses.

8.2 Palynofacies units

The pattern of stratigraphic distribution of the palynofacies associations forms the base for the definition of palynofacies units. The variations reflect from environmental changes, mainly shoreline shifts that influenced the proximal-distal trend.

The palynofacies units were defined according to Brugman *et al.* (1994), who established units and subunits to Lettenkeuper of the Germanic Basin, based on quantitative data on total organic matter. They indicated that the stratigraphical subdivisions of the succession based on ecophases may allow interpretations of depositional environments, but at some intervals because of the lack of significant palynomorphs, the palynofacies units are very useful to interpret the paleoenvironments.

8.2.1 Palynofacies units of well GTP-17-SE

The sedimentary succession of GTP-17-SE is represented by a lower part characterized by moderate to high contents of ‘AOM‘ kerogen and an upper part with high to very high amounts of the phytoclast group. There is a progressive increase in phytoclast particles upward, in particular of opaque particles. The mean of entire succession (in this study used as **general mean**) of the kerogen categories is displayed in Figure 8.5. The succession of GTP-17-SE was subdivided into eight units (units A-17 to H-17) as illustrated in Figure 8.22.

	Kerogen groups				**Phytoclast Group**							**Palynomorph Group**				
					Opaque		Translucent					Marine		Terrestrial		
	AOM %	Ph%	Pa %	Zoocl %	O-Eq	O-La	Fh	Wp	Cu	Ww	Mb	Ftl	Df	Fwp	Pl	Sp
Max.	74.2	100	49.2	2.0	53.5	89.3	2.6	4.4	24.7	59.8	1.4	65.1	71.1	0.6	100	36.0
Min.	-	11.2	-	-	-	32.4	-	-	-	0.5	-	-	-	-	24.6	-
General mean	**10.9**	**73.7**	**15.2**	**0.3**	**12.5**	**59.4**	**0.2**	**0.7**	**3.3**	**23.8**	**0.1**	**2.8**	**4.5**	**0.02**	**85.9**	**6.8**

Figure 8.5. Palynofacies summary for well GTP-17-SE. Relative abundance (%) of kerogen groups from total of kerogen. Relative abundance (%) of the phytoclast group from total phytoclasts. Relative abundance (%) of the palynomorph group from total palynomorphs. AOM= amorphous organic matter; Ph= phytoclast; Pa= palynomorphs; Zoocl= zooclast; O-Eq= opaque equidimensional; O-La= opaque lath; Fh= fungal hyphae; Wp= wood tracheid with pits; Ww= wood tracheid without pits; Mb= membrane; FTL= foraminiferal test linings; Df= dinoflagellates; Pl= pollen; Sp= spores.

The values of the *ratios of opaque to translucent* (O:TR) for GTP-17-SE range from –0.27 to 1.9, with a mean of 0.47 (Table 8.1). The ratio curve is characterized by a slight long-term increasing trend upwards. The *ratios of equidimensional to lath particles* (O-Eq:O-La) range from 0.07 to –1.85 (mean = -0.79) and the ratio curve shows a marked increase upwards. The abundance of tetrads shows a slight decrease upward. The abundance values range from 0 to 23.5% (% of palynomorphs) with a general mean of 3.8%. The PMI values range from 100.00 (nonmarine palynomorphs) to 200.00, with a mean of 122.90. The results found in each unit are shown throughout this well section and the stratigraphic distribution of the palynofacies ratios and parameters are illustrated in Figure 8.23.

Table 8.1. Summary of palynofacies parameters of well GTP-17-SE. O= opaque; TR= translucent; O-Eq= opaque equidimensional; O-La= opaque lath.

	O:TR ratio (log10)	O-Eq:O-La ratio (log10)	Tetrad frequency (%)	PMI
Max.	1.90	0.10	23.50	200.00
Min.	-0.26	-1.90	-	100.00
General mean	**0.47**	**-0.79**	**3.80**	**122.90**

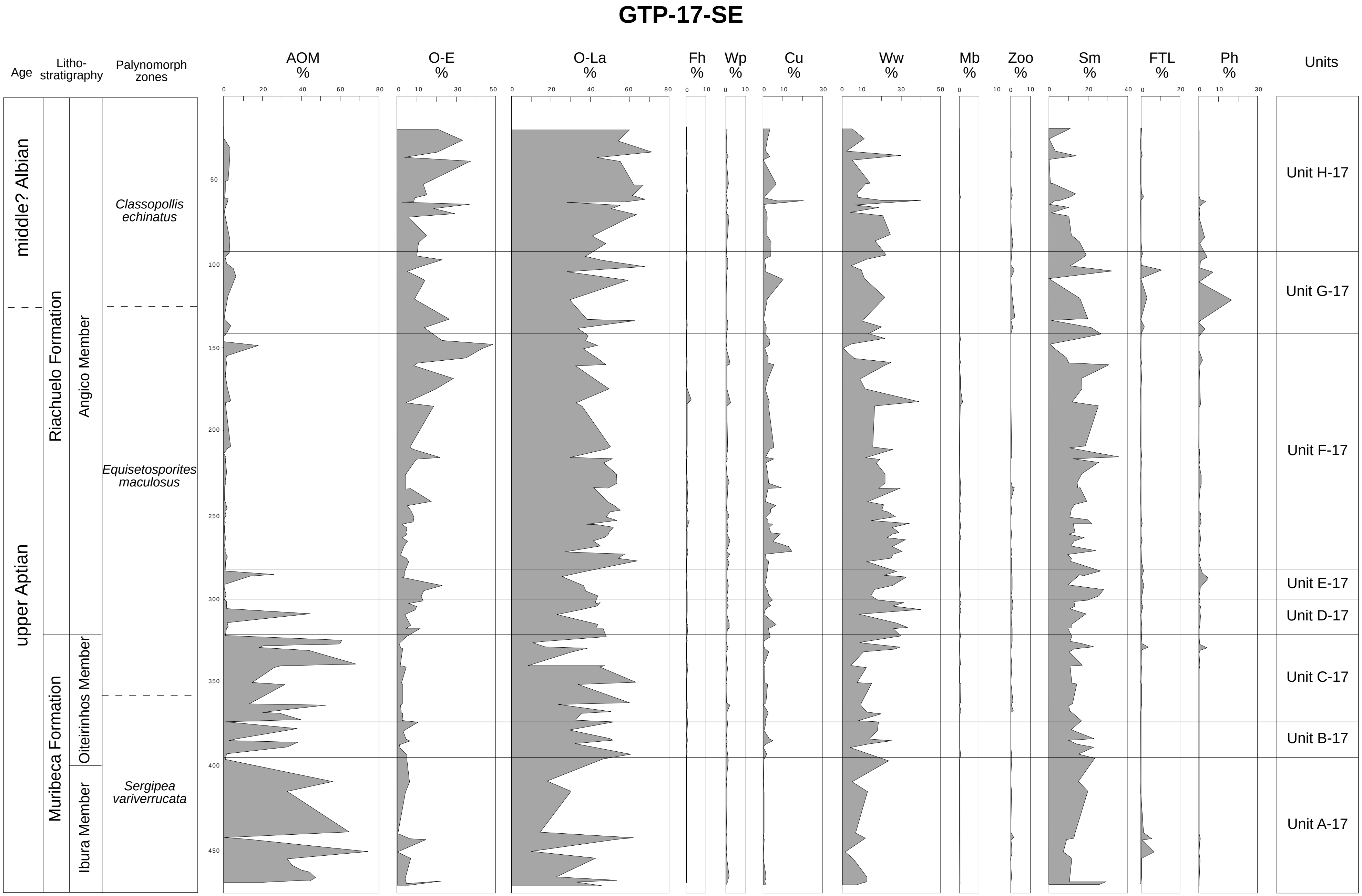

Figure 8.22. Stratigraphic distribution of kerogen categories in well GTP-17-SE. AOM= amophous organic matter; O-Eq= opaque equidimensional; O-La= opaque lath; Fh= fungal hyphae; Wp= wood tracheid with pits; Ww=wood tracheid without pits; Cu= cuticle; Mb= membrane; Zoo= zooclast; Sm= sporomorphs; FTL= foraminiferal test linings; Ph= phytoplankton.

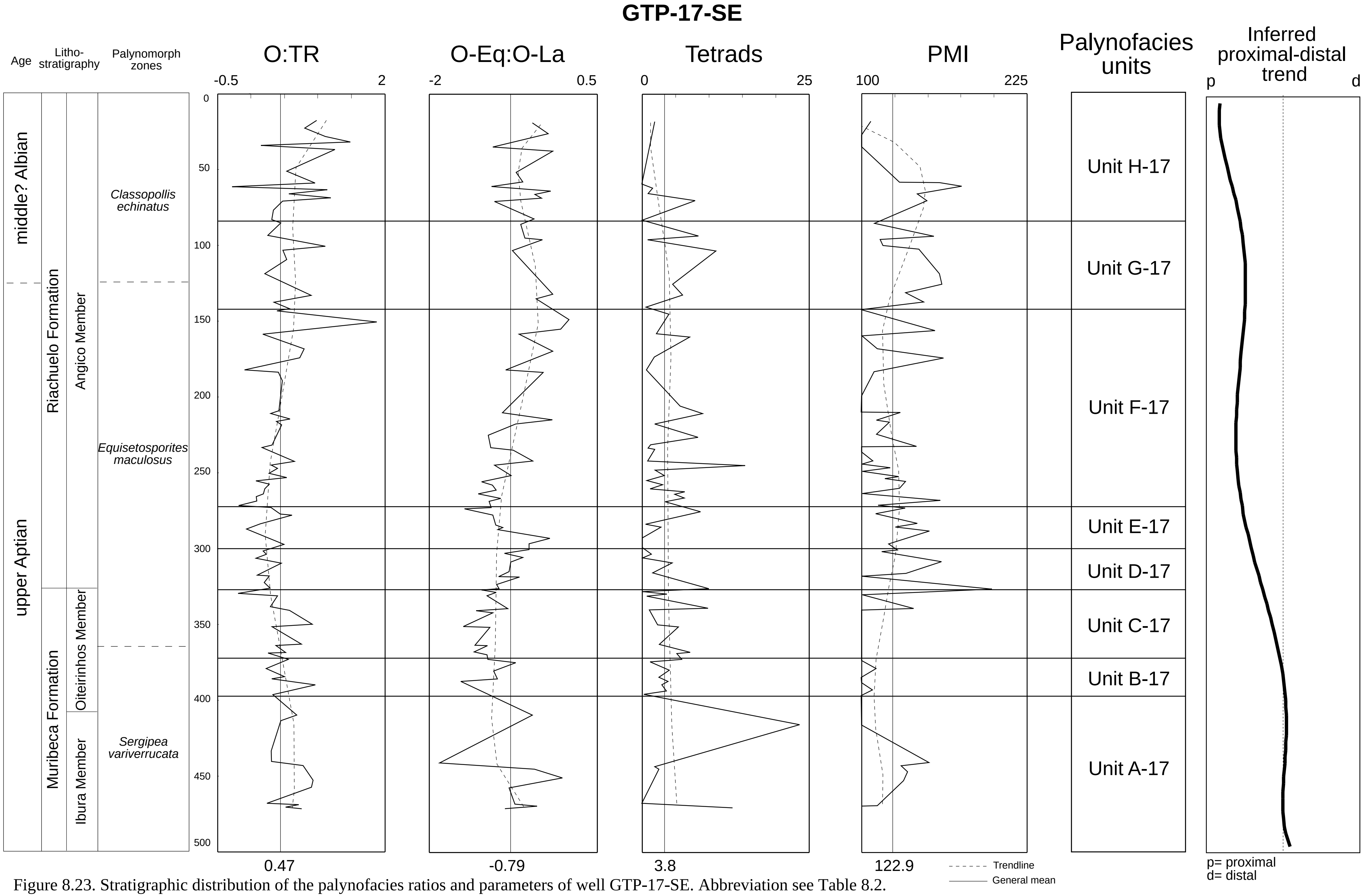

Figure 8.23. Stratigraphic distribution of the palynofacies ratios and parameters of well GTP-17-SE. Abbreviation see Table 8.2.

Unit A-17 (471-393 m) - Palynofacies association AOM/Pal-s

This unit is characterized by relatively large amounts of the AOM group, which are combined with a moderate abundance of terrestrial palynomorphs (sporomorph subgroup). However, marine palynomorphs, in particular foraminiferal test linings (FTL), are present. Despite the large amount of phytoclasts, this unit is characterized by the AOM group because its average abundance (32.3%) in this unit is much higher than its general mean (10.9%) (see Figure 8.6). The AOM group reaches high values (up 70% of total kerogen). Its abundances decrease towards the top, where they make up only 0.4% of the kerogen. The phytoclast group contains mainly opaque-lath particles. The trendline of this group decreases upwards. Translucent particles are present in moderate amounts throughout the succession.

		Kerogen groups				**Phytoclast Group**							**Palynomorph Group**				
						Opaque		Translucent					Marine		Terrestrial		
		AOM %	Ph%	Pa %	Zoocl %	O-Eq	O-La	Fh	Wp	Cu	Ww	Mb	Ftl	Df	Fwp	Pl	Sp
Unit A-17	Max.	74.2	89.4	29.3	1.2	25.1	89.3	-	3.3	3.3	31.1	-	65.1	1.0	0.5	97.5	7.0
	Min.	0.4	11.2	10.0	-	-	54.5	-	-	-	10.3	-	-	-	-	32.5	1.5
(AOM/ Pal-s)	Mean	32.3	51.1	16.5	0.2	11.1	69.1	-	0.7	0.9	18.1	-	11.6	0.3	0.1	84.0	4.2
General mean		**10.9**	**73.7**	**15.2**	**0.3**	**12.5**	**59.4**	**0.2**	**3.3**	**23.8**	**0.1**	**0.1**	**2.8**	**4.5**	**0.02**	**85.9**	**6.8**

Figure 8.6. Percentage mean values of the kerogen categories for **Unit A-17**. Relative abundances and abbreviations as in Figure 8.5.

Ratios and parameters. The average values of the O:TR ratio are higher than the general mean (Figure 8.7). The ratio curve shows a constant trendline (Figure 8.23). The O-Eq:O-La shows a strong fluctuation; however, the trendline shows a slight decreasing trend indicating an increase of O-La upwards. The tetrad abundances show the highest values found in this well (23.5%), with a marked increasing trend upwards. The unit is characterized by moderate to high PMI values. The PMI curve also increases upwards; however, in the uppermost sample no marine palynomorphs were observed (Figure 8.23).

Ratios and Parameters	Max.	Min.	*Unit Mean*	**General mean**	Trendline	Remarks
O:TR ratio (log10)	0.92	0.25	*0.64*	**0.47**	constant	
O-Eq:O-La ratio (log10)	0	-1.85	*-0.77*	**-0.79**	slightly decrease upwards	
Tetrad abundance (%)	23.50	-	*5.90*	**3.80**	increase upwards	highest value
PMI	150.00	100.00	*119.4*	**122.9**	increase upwards	

Figure 8.7. Summary of palynofacies ratios and parameters of Unit A-17. For abbreviations see Table 8.1.

Unit B-17 (393-374 m) - Palynofacies association Phy-o/Pal-s

Unit B-17 is strongly dominated by opaque phytoclasts, which are associated with moderate to high contents of terrestrial palynomorphs (Figure 8.8). The phytoclast group is composed mainly of opaque-lath particles. Translucent particles are mainly composed of Ww particles. The palynomorph group in this unit contains mainly terrestrial palynomorphs, particularly pollen grains. The marine palynomorphs are represented by only two forms (FTL and dinocysts). The AOM occur in low to moderate abundances increasing gradually within the uppermost part of the unit.

		Kerogen groups				**Phytoclast Group**							**Palynomorph Group**				
						Opaque		Translucent					Marine		Terrestrial		
		AOM %	Ph%	Pa %	Zoocl %	O-Eq	O-La	Fh	Wp	Cu	Ww	Mb	Ftl	Df	Fwp	Pl	Sp
Unit B-17 **(Phy-o/ Pal-mp)**	Max.	38.0	87.2	23.0	0.2	20.7	87.8	1.0	1.3	5.3	34.9	0.5	0.5	0.5	-	99.0	5.0
	Min.	1.0	44.2	10.0	-	2.1	57.3	-	-	-	9.0	-	-	-	-	95.0	1.0
	Mean	15.3	67.9	16.9	0.1	7.7	66.6	0.3	0.5	1.9	22.8	0.1	0.1	0.1	-	97.3	2.5
General mean		**10.9**	**73.7**	**15.2**	**0.3**	**12.5**	**59.4**	**0.2**	**0.7**	**3.3**	**23.8**	**0.1**	**2.8**	**4.5**	**0.02**	**85.9**	**6.8**

Figure 8.8. Percentage mean values of the kerogen categories for **Unit B-17**. Relative abundances and abbreviations as in Figure 8.5.

Ratios and parameters. The ratio curve of O:TR shows a decreasing trend upwards. The mean value is higher than the general average (Figure 8.9). The O-Eq:O-La ratio clearly shows an increasing trend, due to the progressive increase of equidimensional particles. The tetrad abundances show low to moderate values, with a slight increasing trend upwards (Figure 8.23). The unit is characterized by low PMI values; marine palynomorphs are present only in two samples.

Ratios and Parameters	Max.	Min.	*Unit Mean*	**General mean**	Trendline
O:TR ratio (log10)	0.98	0.23	*0.49*	**0.47**	decrease upwards
O-Eq:O-La ratio (log10)	-0.70	-1.50	*-1.10*	**-0.79**	increase upwards
Tetrad abundance (%)	4.00	0.50	*2.60*	**3.80**	constant
PMI	150.00	100.00	*119.40*	**122.90**	constant

Figure 8.9. Summary of palynofacies ratios and parameters of Unit B-17. For abbreviations see Table 8.1.

Unit C-17 (374-325 m) - Palynofacies association AOM/Pal-s

Unit C-17 shows the same characteristics as Unit A-17, in which a high relative abundance of the AOM group (Figure 8.10) is observed. The palynomorphs are composed mainly of terrestrial palynomorphs; however at 328.67 the marine palynomorphs show a major peak in abundance due to the high relative abundances of FTL and the genus *Spiniferites*. The phytoclast group is also present in moderate to high abundances (Figure 8.10). This group is composed mainly of O-La particles. The translucent particles are predominately composed of Ww particles, which show moderate to high values (Figure 8.10).

		Kerogen groups				**Phytoclast Group**							**Palynomorph Group**				
						Opaque		Translucent					Marine		Terrestrial		
		AOM %	Ph%	Pa %	Zoocl %	O-Eq	O-La	Fh	Wp	Cu	Ww	Mb	Ftl	Df	Fwp	Pl	Sp
Unit C-17 **(AOM/ Pal-s)**	Max.	67.2	73.4	30.2	1.2	8.6	86.5	1.1	4.4	5.7	59.8	1.2	13.5	9.5	-	100	8.5
	Min.	13.6	14.0	10.0	-	2.7	34.6	-	-	-	9.9	-	-	-	-	75.5	-
	Mean	35.0	50.4	14.3	0.3	4.7	64.9	0.3	0.8	1.9	27.3	0.2	2.4	1.1	-	94.1	2.4
General mean		**10.9**	**73.7**	**15.2**	**0.3**	**12.5**	**59.4**	**0.2**	**0.7**	**3.3**	**23.8**	**0.1**	**2.8**	**4.5**	**0.02**	**85.9**	**6.8**

Figure 8.10. Percentage mean values of the kerogen categories for **Unit C-17**. Relative abundances and abbreviations as in Figure 8.5.

Ratios and parameters. The O:TR ratio in Unit C-17 is characterized by strong fluctuations; however, the ratio curve shows a clear decrease upward reflecting an increase in translucent particles (Figure 8.11). The average value (0.39) is lower than the general mean (Figure 8.11). The O-Eq:O-La ratio also shows strong fluctuations, but the ratio curve increases slightly upward due to an increase in equidimensional particles. Tetrad abundances range from 0 to 10%, and its trendline is constant. Unit C-17 is characterized by the highest PMI value (200.00) of the entire succession. The PMI values increase markedly in the upper part of the unit (Figure 8.23).

Ratios and Parameters	Max.	Min.	*Unit Mean*	**General mean**	Trendline
O:TR ratio (log10)	0.92	-0.21	*0.39*	**0.47**	decrease upwards
O-Eq:O-La ratio (log10)	-0.83	-1.50	*-1.14*	**-0.79**	increase upwards
Tetrad abundance (%)	10.00	-	*4.50*	**3.80**	slightly decrease upwards
PMI	200.00	100.00	*116.20*	**122.90**	increase upwards

Figure 8.11. Summary of palynofacies ratios and parameters of Unit C-17. For abbreviations see Table 8.1.

Unit D-17 (325-300 m) - Palynofacies association Phy-o-t

Unit D-17 is strongly dominated by the phytoclast group. The abundance difference between the subgroups (opaque and translucent) is very small; therefore, this unit was named ***Phy-o-t***. The O-La (opaque) and Ww (translucent) are the most abundant particles; however, the cuticle fragments show a marked increase. The AOM group shows very low to high abundances, though, the average abundance is low. The palynomorphs are dominated by pollen grains. The spores show low to moderate abundances. The marine palynomorphs are mainly represented by rare dinocysts (Figure 8.12).

		Kerogen groups				**Phytoclast Group**							**Palynomorph Group**				
						Opaque		Translucent					Marine		Terrestrial		
		AOM %	Ph%	Pa %	Zoocl %	O-Eq	O-La	Fh	Wp	Cu	Ww	Mb	Ftl	Df	Fwp	Pl	Sp
Unit D-17 **(Phy-o-t)**	Max.	43.8	88.6	20.6	0.8	16.6	64.2	0.7	1.7	7.2	45.8	0.9	3.5	5.5	0.6	98.5	4.5
	Min.	0.4	35.2	9.6	0.4	5	41.2	-	0.2	0.6	22.4	-	-	-	-	91.0	1.0
	Mean	6.1	79.1	14.2	0.6	9.6	52.6	0.4	0.9	3.7	32.6	0.2	1.4	1.8	0.1	94.4	2.2
General mean		**10.9**	**73.7**	**15.2**	**0.3**	**12.5**	**59.4**	**0.2**	**0.7**	**3.3**	**23.8**	**0.1**	**2.8**	**4.5**	**0.02**	**85.9**	**6.8**

Figure 8.12. Percentage mean values of the kerogen categories for **Unit D-17**. Relative abundances and abbreviations as in Figure 8.5.

Ratios and parameters. All O:TR values are lower than the general average (0.47) (Figure 8.13). The trendline is constant reflecting the stable amount of translucent particles in this unit (Figure 8.23). The O-Eq:O-La curve shows a gradual increase upward. Like the other ratio, the average value (-0.77) is lower than the general mean. The abundances of tetrads show a slightly increase towards the top. In this unit the PMI values are moderate to high and the trendline shows an increase upwards (Figure 8.23).

Ratios and Parameters	Max.	Min.	*Unit Mean*	**General mean**	Trendline
O:TR ratio (log10)	0.46	0.03	*0.22*	**0.47**	constant
O-Eq:O-La ratio (log10)	-0.51	-1.00	*-0.77*	**-0.79**	slightly decrease upwards
Tetrad abundance (%)	9.50	-	*3.10*	**3.80**	decrease upwards
PMI	160.00	100.00	*130.70*	**122.90**	slightly increase upwards

Figure 8.13. Summary of palynofacies ratios and parameters of Unit D-17. For abbreviations see Table 8.1.

Unit E-17 (300-277 m) - Palynofacies association Pal-mp/Phy-o-t

This unit is characterized by the relatively high abundances of marine palynomorphs, in particular dinocysts (Figure 8.14). This is combined with nearly equal amounts of opaque and translucent particles (phytoclast group), in which O-La and O-Eq of the opaque subgroup and Ww (translucent) are the most abundant. The AOM group reaches moderate values, and its abundance curve increases towards the top.

		Kerogen groups				Phytoclast Group							Palynomorph Group				
						Opaque		Translucent					Marine		Terrestrial		
		AOM %	Ph%	Pa %	Zoocl %	O-Eq	O-La	Fh	Wp	Cu	Ww	Mb	Ftl	Df	Fwp	Pl	Sp
Unit E-17 **(Pal-mp/ Phy-o-t)**	Max.	25.8	86.2	28.8	0.8	26.2	59.4	0.3	1.2	3.5	51.4	0.3	3.5	28.5	-	95	6.0
	Min.	0.4	54.8	12.0	-	4.1	40.7	-	0.3	0.9	19.9	-	0.5	0.5	-	69.5	1.5
	Mean	7.2	69.2	22.7	0.4	12.9	50.1	0.1	0.7	2.7	33.5	0.1	1.8	11.5	-	83.8	3.0
General mean		**10.9**	**73.7**	**15.2**	**0.3**	**12.5**	**59.4**	**0.2**	**0.7**	**3.3**	**23.8**	**0.1**	**2.8**	**4.5**	**0.02**	**85.9**	**6.8**

Figure 8.14. Percentage mean values of the kerogen categories for **Unit E-17**. Relative abundances Relative abundances and abbreviations as in Figure 8.5.

Ratios and parameters. The average values of the O:TR ratio are lower than the general mean (0.47) due to the relatively large amounts of translucent particles. The ratio curve is characterized by a progressive decrease upwards (Figure 8.15). The abundance curve for the O-Eq:O-La ratio reflects the moderate to high abundance of the O-Eq particles; however, the abundance curve decreases upwards. The tetrad abundances show low to moderate values with a slight increasing trend upward. All values obtained for the tetrad abundance are lower than the general mean (Figure 8.15). Unit E-17 is characterized by moderate to high PMI values. The PMI curve shows a clear increase upwards.

Ratios and Parameters	Max.	Min.	*Unit Mean*	**General mean**	Trendline
O:TR ratio (log10)	0.50	-0.10	*0.24*	**0.47**	decrease upwards
O-Eq:O-La ratio (log10)	-0.21	-1.00	*-0.69*	**-0.79**	decrease upwards
Tetrad abundance (%)	3.00	-	*0.90*	**3.80**	slightly increase upwards
PMI	150.00	120.00	*136.30*	**122.90**	increase upwards

Figure 8.15. Summary of palynofacies ratios and parameters of Unit E-17. For abbreviations see Table 8.1.

Unit F-17 (277-143 m) - Palynofacies association Phy-o/Pal-s

Unit F-17 is strongly dominated by opaque phytoclasts combined with a moderate to high content of terrestrial palynomorphs (Figure 8.16) which characterize this unit. The phytoclast group is composed mainly of opaque-lath particles (O-La); however O-Eq shows the highest peak in abundance of this well. Translucent particles are mainly composed of Ww particles and cuticles that are common in this unit. The palynomorph group contains mainly terrestrial palynomorphs, in particular pollen grains. The marine palynomorphs are mainly represented by dinocysts. Generally, ‘AOM’ occurs in low abundances and decreases towards the top (Figure 8.22).

		Kerogen groups				Phytoclast Group							Palynomorph Group				
						Opaque		Translucent					Marine		Terrestrial		
		AOM %	Ph%	Pa %	Zoocl %	O-Eq	O-La	Fh	Wp	Cu	Ww	Mb	Ftl	Df	Fwp	Pl	Sp
Unit F-17 **(Phy-o/ Pal-s)**	Max.	17.4	99.3	35.6	1.8	53.5	74.7	2.6	2.4	19.1	51.4	1.4	6.5	13.0	-	97.5	31.0
	Min.	-	64.2	0.7	-	2.0	36.3	-	0.3	0.3	0.5	-	-	-	-	69	2.5
	Mean	1.9	82.4	15.5	-	12.6	54.5	0.3	0.8	4.3	27.5	0.2	0.9	2.0	-	88.4	8.7
General mean		**10.9**	**73.7**	**15.2**	**0.2**	**12.5**	**59.4**	**0.2**	**0.7**	**3.3**	**23.8**	**0.1**	**2.8**	**4.5**	**0.02**	**85.9**	**6.8**

Figure 8.16. Percentage mean values of the kerogen categories for **Unit F-17**. Relative abundances Relative abundances and abbreviations as in Figure 8.5.

Ratios and parameters. The O:TR ratio shows a progressive increasing upwards indicated by a rise in opaque particles. In this unit the highest value of this ratio (1.9) is found; however, the average (0.39) is lower than the general mean value (0.47). The curve for the O-Eq:O-La ratio shows the same pattern as the O:TR. The curve for tetrad abundances shows strong fluctuations and a slight decrease upwards. The PMI curve also shows a strong fluctuations. In the upper part of the unit, two major peaks are recorded; however, the trendline shows a slight decrease towards the top (Figure 8.23).

Ratios and Parameters	Max.	Min.	*Unit Mean*	**General mean**	Trendline
O:TR ratio (log10)	1.90	-0.20	*0.39*	**0.47**	decrease upwards
O-Eq:O-La ratio (log10)	0.07	-1.50	*-0.78*	**-0.79**	decrease upwards
Tetrad abundance (%)	15.00	0.50	*4.30*	**3.80**	slightly increase upwards
PMI	162.50	100.00	*120.50*	**122.90**	increase upwards

Figure 8.17. Summary of palynofacies ratios and parameters of Unit F-17. For abbreviations see Table 8.1.

Unit G-17 (143-85 m) - Palynofacies association Pal-mp/Phy-o

This unit is characterized by the highest abundance of the palynomorph group, which is dominated by terrestrial elements. However, the percentages of these palynomorphs decrease upwards, whereas a clear increase in abundance of marine palynomorphs is observed. The high abundance of marine palynomorphs, in particular dinocysts (Figure 8.18), is characterized of this unit, as are high amounts of phytoclast particles. This group is composed mainly of opaque particles, in which O-La and O-Eq are the most abundant. The translucent particles are made up of moderate amounts of Ww and cuticle particles. The AOM group is rare, but increase in abundances upwards (Figure 8.22).

		Kerogen groups				**Phytoclast Group**							**Palynomorph Group**				
						Opaque		Translucent					Marine		Terrestrial		
		AOM %	Ph%	Pa %	Zoocl %	O-Eq	O-La	Fh	Wp	Cu	Ww	Mb	Ftl	Df	Fwp	Pl	Sp
Unit G-17 **(Pal-mp/ Phy-o)**	Max.	6.0	98.3	49.2	2.0	34.3	78.0	0.3	0.9	10.6	34.6		25.5	42.0	0.5	94.5	36.0
	Min.	0.3	44.0	-	-	11.4	47.0	-	-	0.3	4.9		-	-	-	36.8	5.0
	Mean	2.7	75.5	21.2	0.6	20.2	57.5	0.1	0.5	2.8	19.1		12.5	5.6	0.1	66.6	15.3
General mean		**10.9**	**73.7**	**15.2**	**0.3**	**12.5**	**59.4**	**0.2**	**0.7**	**3.3**	**23.8**	**0.1**	**2.8**	**4.5**	**0.02**	**85.9**	**6.8**

Figure 8.18. Percentage mean values of the kerogen categories for **Unit G-17**. Relative abundances Relative abundances and abbreviations as in Figure 8.5.

Ratios and parameters. The average value (0.59) of the O:TR ratio is higher than the general mean value (Figure 8.19). The ratio curve shows a constant trendline (Figure 8.23). The O-Eq:O-La ratio is characterized by moderate to high values, in which the mean is lower than the general mean. The ratio curve shows a progressive decrease upwards. The tetrad abundances show a clear increase upward. The average abundance of the tetrads in this unit (4.6%) is higher than the general value (3.8%). The PMI values are moderate to high and the trendline indicates a slight increase upwards (Figure 8.23). The average (133.90) is higher than the general mean (Figure 8.45).

Ratios and Parameters	Max.	Min.	*Unit Mean*	**General mean**	Trendline
O:TR ratio (log10)	1.13	0.21	*0.59*	**0.47**	constant
O-Eq:O-La ratio (log10)	-0.16	-0.75	*-0.48*	**-0.79**	decrease upwards
Tetrad abundance (%)	11.00	0.50	*4.60*	**3.80**	increase upwards
PMI	160.00	100.00	*133.90*	**122.90**	slightly increase upwards

Figure 8.19. Summary of palynofacies ratios and parameters of Unit G-17. For abbreviations see Table 8.1.

Unit H-17 (85-18 m) - Palynofacies association Phy-o

Unit H-17 is strongly dominated by opaque phytoclasts reaching up to 100.0% of all kerogen categories. This group is composed mainly of O-La (Figure 8.20), but O-Eq particles are also present in large amounts. Translucent particles show moderate to high abundances and are mainly composed of Ww particles. The cuticle fragments show the highest value recorded in the well (see Figure 8.20). The unit is also characterized by extremely low abundances of the AOM group. The palynomorph group occurs in small to moderate amounts; however, despite of very high amounts of phytoclasts, the marine palynomorphs, in particular dinocysts, show the highest abundances in the whole section (Figure 8.20). The terrestrial palynomorphs show relatively low abundances. These elements are composed mainly of pollen grains; however, the spores show moderate to high abundances.

		Kerogen groups				Phytoclast Group							Palynomorph Group				
						Opaque		Translucent					Marine		Terrestrial		
		AOM %	Ph%	Pa %	Zoocl %	O-Eq	O-La	Fh	Wp	Cu	Ww	Mb	Ftl	Df	Fwp	Pl	Sp
Unit H-17 **(Phy-o)**	Max.	3.2	100	15.3	1	38.1	79.8	0.2	1.2	24.7	40.1	0.2	12.5	71.1	-	89	29.5
	Min.	-	81.4	-	-	2.8	32.4	-	-	-	2.2	-	-	-	-	24.6	2.6
	Mean	1.5	91.3	7	0.2	19.6	61.5	0.03	0.4	4.4	14.1	0.02	3.1	20.7	-	66.5	9.7
General mean		**10.9**	**73.7**	**15.2**	**0.3**	**12.5**	**59.4**	**0.2**	**0.7**	**3.3**	**23.8**	**0.1**	**2.8**	**4.5**	**0.02**	**85.9**	**6.8**

Figure 8.20. Percentage mean values of the kerogen categories for **Unit H-17**. Relative abundances and abbreviations as in Figure 8.5.

Ratios and parameters. The curve for the O:TR ratio reflects the very large amounts of opaque particles. In spite of a strong fluctuations, the ratio curve shows a clear increasing trend. In the lower part of the curve there is an abrupt decrease (increase in translucent particles), where the lowest value of this ratio (-0.26) (Figure 8.21) is observed. The abundance curve for the O-Eq:O-La ratio reflects the moderate to high abundances of O-Eq particles. The tetrad abundance show very low to moderate values. The abundance curve shows a slight decreasing trend upwards (Figure 8.23). The PMI is characterized by a decrease in abundance upwards. In the abundance curve two parts can be distinguished: a lower part characterized by high PMI values, and an upper part marked by an abrupt decrease in PMI values (Figure 8.23).

Ratios and Parameters	Max.	Min.	*Unit Mean*	**General mean**	Trendline	Remarks
O:TR ratio (log10)	1.47	-0.26	*0.70*	**0.47**	increase upwards	lowest value
O-Eq:O-La ratio (log10)	-0.17	-1.06	*-0.61*	**-0.79**	increase upwards	
Tetrad abundance (%)	8.00	-	*1.00*	**3.80**	slightly increase upwards	
PMI	175.00	100.00	*140.60*	**122.90**	decrease upwards	

Figure 8.21. Summary of palynofacies ratios and parameters of Unit H-17. For abbreviations see Table 8.1.

8.2.2 Palynofacies units of GTP-24-SE

The succession of well GTP-24-SE is characterized by a long-term transgressive trend indicated by an increase of the AOM and palynomorph groups. This trend is best indicated by a progressive upward increase in marine palynomorph abundance, especially of dinocysts. The maximum, minimum and general means of kerogen categories for well GTP-24-SE are summarized in Figure 8.24. The sedimentary succession of GTP-24-SE was subdivided into ten units (Unit A-24-J-24) described below and illustrated in Figure 8.45.

GTP-24-SE

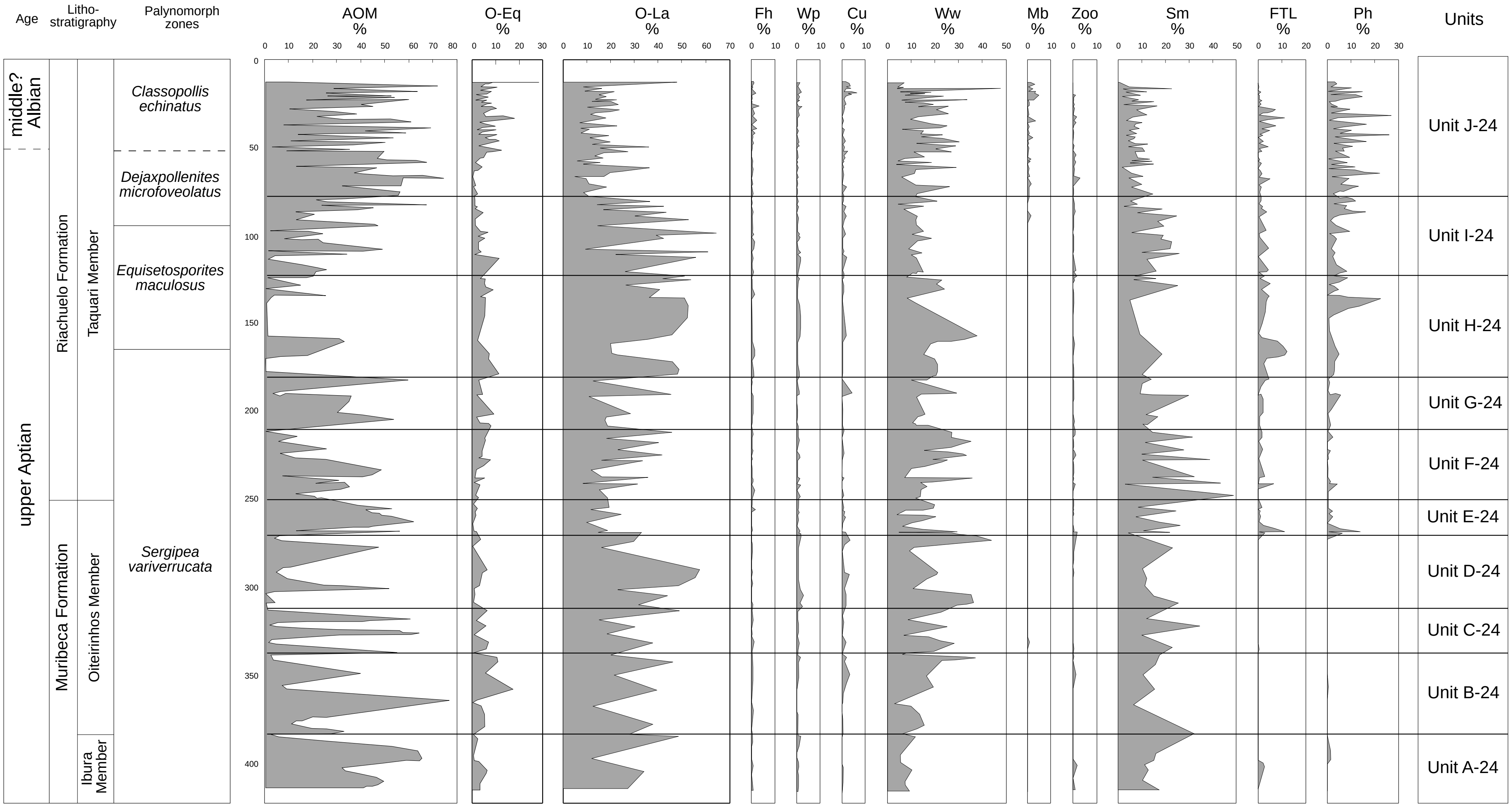

Figure 8.45. Stratigraphic distribution of kerogen categories in well GTP-24-SE. ‘AOM‘= amophous organic matter; Re= resin; O-Eq= opaque equidimensional; O-La= opaque lath; Fh= fungal hyphae; Wp= wood tracheid with pits; Ww=wood tracheid without pits; Cu= cuticle; Mb= membrane; Zoo= zooclast; Sm= sporomorphs; FTL= foraminiferal test linings; Ph= phytoplankton.

	Kerogen groups				Phytoclast Group							Palynomorph Group				
					Opaque		Translucent					Marine		Terrestrial		
	AOM %	Ph%	Pa %	Zoocl %	O-Eq	O-La	Fh	Wp	Cu	Ww	Mb	Ftl	Df	Fwp	Pl	Sp
Max.	75.3	87.4	49	3.0	39.0	79.7	11.5	8.5	14.7	72.3	14.8	53.7	89.0	1.5	100	32.5
Min.	0.6	12.8	1.2	-	0.6	14.2	-	-	-	8.0	-	-	-	-	4.0	-
General mean	**32.7**	**47.9**	**19.0**	**0.3**	**9.0**	**52.2**	**1.1**	**1.3**	**1.8**	**33.5**	**1.1**	**7.8**	**24.9**	**0.1**	**61.0**	**6.3**

Figure 8.24. Palynofacies summary for well GTP-24-SE. Relative abundances (%) of the kerogen groups from total kerogen. Relative abundances (%) of the phytoclast group from total phytoclasts. Relative abundances (%) of the palynomorph group from total palynomorphs. For abbreviations see Figure 8.5.

The highest and lowest values and means of entire succession of this well (general means) of the ratios and parameters of well GTP-24-SE are displayed in Table 8.2 and illustrate in Figure 46. The *O:TR* ratio curve is characterized by a slight long-term decreasing upward and the O-Eq:O-La ratio shows a clear increase towards the top. The curve of tetrad abundances is characterized by a slight long-term decrease upwards. The PMI curve is marked by a increase upwards reflecting the increase of marine palynomorphs.

Table 8.2. Summary of palynofacies parameters of well GTP-24-SE. For abbreviations see Table 8.1.

	O:TR ratio (log10)	O-Eq:O-La ratio (log10)	Tetrad frequency (%)	PMI
Max.	0.83	0.01	73.40	250.00
Min.	-0.53	-2.15	-	100.00
General mean	**0.21**	**-0.84**	**5.90**	**138.90**

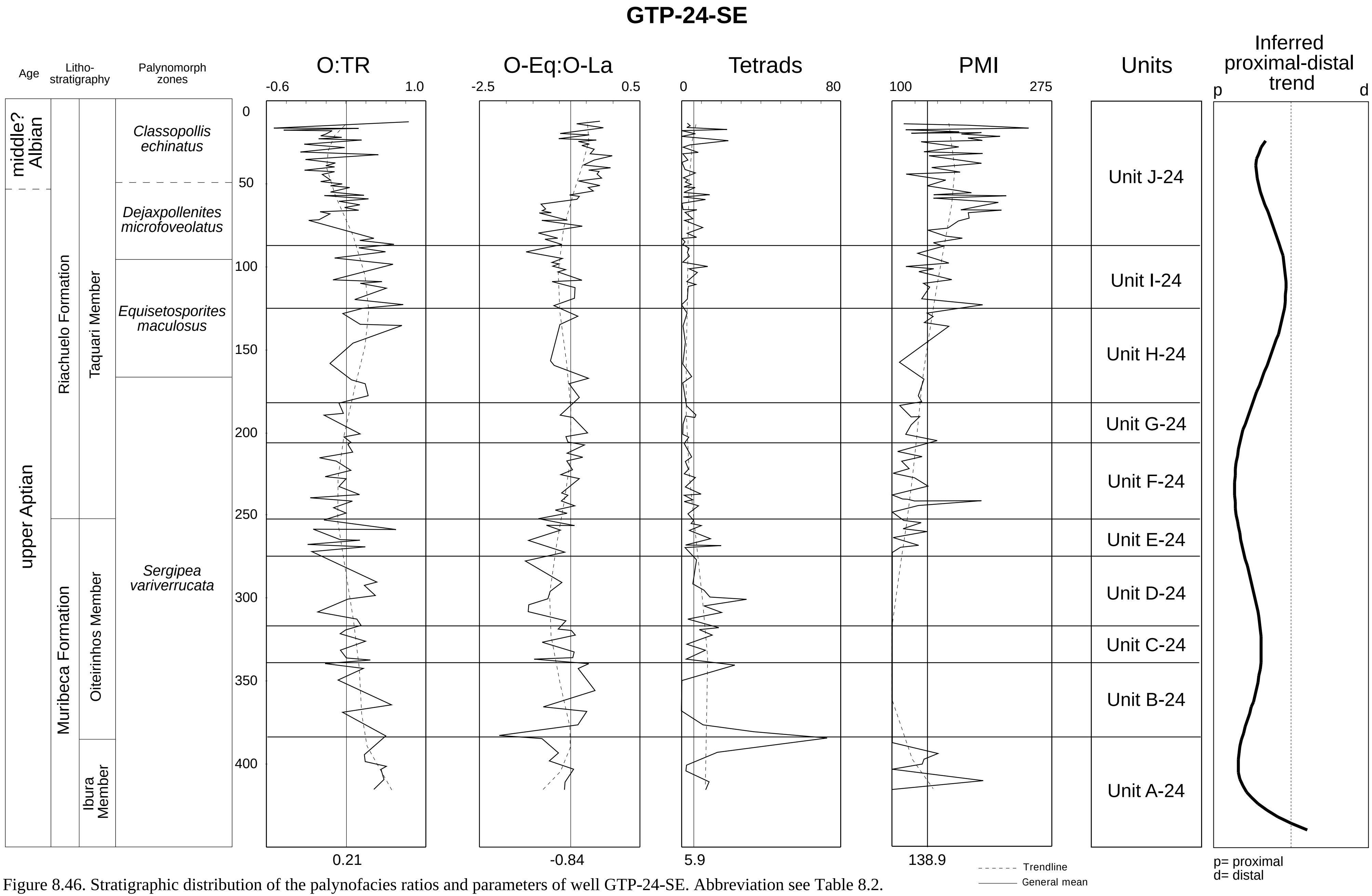

Figure 8.46. Stratigraphic distribution of the palynofacies ratios and parameters of well GTP-24-SE. Abbreviation see Table 8.2.

Unit A-24 (415-383 m) - Palynofacies association AOM/Pal-s

This unit is characterized by a high abundance of the AOM group combined with the palynomorph group that mainly consist of terrestrial elements, especially pollen grains (95.8% of sporomorph subgroup). Marine palynomorphs are relatively few and represented mainly by FTL.

The phytoclast group is composed mainly of O-La particles, which show high abundances. Translucent particles are present but in moderate numbers. They are composed basically of Ww particles (Figure 8.25).

		Kerogen groups				**Phytoclast Group**							**Palynomorph Group**				
						Opaque		Translucent					Marine		Terrestrial		
		AOM %	Ph%	Pa %	Zoocl %	O-Eq	O-La	Fh	Wp	Cu	Ww	Mb	Ftl	Df	Fwp	Pl	Sp
Unit A-24 **(AOM/ Pal-s)**	Max.	65.0	51.7	17.8	1.6	12.3	70.4	1.6	2.0	0.6	28.3	-	17.7	11.3	-	100	8.0
	Min.	32.3	18.8	11.4	-	4.3	65.7	-	-	-	17.1	-	-	-	-	79.7	1.0
	Mean	49.0	35.1	15.2	0.6	8.2	67.6	0.6	0.2	0.2	22.3	-	7.5	4.8	-	87.7	3.7
General mean		**32.7**	**47.9**	**19.0**	**0.3**	**9.0**	**52.2**	**11.1**	**0.7**	**1.8**	**33.5**	**11.1**	**7.8**	**24.9**	**0.1**	**61.0**	**6.3**

Figure 8.25. Percentage mean values of the kerogen categories for **Unit A-24**. Relative abundances and abbreviations as in Figure 8.5.

Ratios and parameters. The O:TR ratio reflects the high content of opaque particles. However, the ratio curve shows a progressive decrease upwards (Figure 8.46). The values of the O-Eq:O-La ratio also reflect the high content of O-La particles. The ratio curve decreases towards to the top. The abundances of tetrads in Unit A-24 are moderate to high, ranging from 2.1 to 14.2% (Figure 8.26). The abundance curve shows a progressive decrease upwards. The PMI values are moderate (from 100.00 to 150.00), in which the mean value is 136.10. The trendline increases slightly upwards (Figure 8.46).

Ratios and Parameters	Max.	Min.	*Unit Mean*	**General mean**	Trendline
O:TR ratio (log10)	0.6	0.39	*0.50*	**0.21**	decrease upwards
O-Eq:O-La ratio (log10)	-0.73	-1.20	*-0.94*	**-0.84**	decrease upwards
Tetrad abundance (%)	14.20	2.10	*8.20*	**5.90**	decrease upwards
PMI	150.00	100.00	*136.10*	**138.90**	slightly increase upwards

Figure 8.26. Summary of palynofacies ratios and parameters of Unit A-24. For abbreviations see Table 8.1.

Unit B-24 (385-339 m) - Palynofacies association Phy-o/Pal-s

Unit B-24 is characterized by a high opaque particle content. It is composed mainly of O-La particles. The O-Eq particles show moderate values. The Ww particles are the principal content of the translucent particles (Figure 8.27), present in moderate to large amounts. The phytoclast particles occur combined with moderate to high abundances of the palynomorph group, composed only of terrestrial elements, especially pollen grains. The AOM group shows low to moderate abundances. It decreases towards the top of the unit (Figure 8.45).

		Kerogen groups				**Phytoclast Group**							**Palynomorph Group**				
						Opaque		Translucent					Marine		Terrestrial		
		AOM %	Ph%	Pa %	Zoocl %	O-Eq	O-La	Fh	Wp	Cu	Ww	Mb	Ftl	Df	Fwp	Pl	Sp
Unit B-24 **(Phy-o/ Pal-s)**	Max.	75.3	80.8	32.0	1.4	22.1	79.5	1.8	2.8	6.2	47.2	-	-	-	-	100	7.9
	Min.	3.0	18.0	6.5	-	0.6	35.6	-	-	-	16.7	-	-	-	-	92.1	-
	Mean	27.2	54.3	18.1	0.2	10.0	59.0	0.6	1.0	1.5	28.0	-	-	-	-	96.7	3.3
General mean		**32.7**	**47.9**	**19.0**	**0.3**	**9.0**	**52.2**	**11.1**	**0.7**	**1.8**	**33.5**	**11.1**	**7.8**	**24.9**	**0.1**	**61.0**	**6.3**

Figure 8.27. Percentage mean values of the kerogen categories for **Unit B-24**. Relative abundances and abbreviations as in Figure 8.5.

Ratios and parameters. The O:TR ratio is characterized by high contents of opaque particles. The ratio curve shows a progressive decrease upwards (Figure 8.46). The O-Eq:O-La shows a clear increase trend indicated by the increase of O-Eq particles upwards. In this unit the lowest value of this ratio (-2.15) is recorded (Figure 8.28). The tetrad abundances in the Unit B-24 show a great variation ranging from very low to very high abundance. The abundance curve shows a clear decrease upwards. The highest abundance of tetrads in well GTP-24-SE (73.4%) is recognized in this unit (Figure 8.28). Owing to the absence of marine palynomorphs the PMI values are constant (100.00).

Ratios and Parameters	Max.	Min.	*Unit Mean*	**General mean**	Trendline	Remarks
O:TR ratio (log10)	0.64	-0.03	*0.37*	**0.21**	decrease upwards	
O-Eq:O-La ratio (log10)	-0.37	-2.15	*-0.90*	**-0.84**	increase upwards	lowest value
Tetrad abundance (%)	73.40	-	*17.50*	**5.90**	decrease upwards	highest value
PMI	100.00	100.00	*100.00*	**138.90**	-	no marine palynomorphs

Figure 8.28. Summary of palynofacies ratios and parameters of Unit B-24. For abbreviations see Table 8.1.

Unit C-24 (338-318 m) - Palynofacies association AOM/Phy-o

Unit C-24 is characterized by relatively high abundances of the AOM group that decreases upwards combined with moderate to high abundances of the phytoclast group. This group is predominately composed of O-La particles, occurring in moderate to high abundances. Translucent particles are present in moderate to high amounts and are mainly composed of Ww particles (Figure 8.29).

As in Unit B-24, here the palynomorphs are also only composed of continental elements, in which pollen grains are the most frequent. However, the spores show a major peak in abundance at 331.30 m.

		Kerogen groups				**Phytoclast Group**							**Palynomorph Group**				
						Opaque		Translucent					Marine		Terrestrial		
		AOM %	Ph%	Pa %	Zoocl %	O-Eq	O-La	Fh	Wp	Cu	Ww	Mb	Ftl	Df	Fwp	Pl	Sp
Unit C-24 **(AOM/ Phy-o)**	Max.	62.8	77.2	34.6	0.2	9.6	71.4	2.1	1.4	2.3	40.1	0.8	-	-	-	100	8.3
	Min.	1.0	26.8	10.0	-	2.4	49.0	-	0.7	-	23.8	-	-	-	-	91.7	-
	Mean	37.2	44.3	18.5	0.01	6.3	59.0	0.9	1.0	1.2	32.0	0.1	-	-	-	97.0	3.0
General mean		**32.7**	**47.9**	**19.0**	**0.3**	**9.0**	**52.2**	**11.1**	**0.7**	**1.8**	**33.5**	**11.1**	**7.8**	**24.9**	**0.1**	**61.0**	**6.3**

Figure 8.29. Percentage mean values of the kerogen categories for **Unit C-24**. Relative abundances and abbreviations as in Figure 8.5.

Ratios and parameters. As with Unit B-24, the O:TR ratio also is characterized by a slight decreasing trend upwards. The pattern of the O-Eq:O-La curve is inversely synchronous with the O:TR ratio (Figure 8.46). The ratio curve shows a progressive increase upwards. The tetrad abundances in Unit C-24 are moderate to high and increase progressively upwards. Like the previous unit, no marine palynomorphs were recorded in this unit; thus the values of PMI are constant (100.00) (Figure 8.30).

Ratios and Parameters	Max.	Min.	*Unit Mean*	**General mean**	Trendline	Remarks
O:TR ratio (log10)	0.45	0.14	*0.27*	**0.21**	slightly decrease upwards	
O-Eq:O-La ratio (log10)	-0.71	-1.48	*-1.01*	**-0.84**	slightly increase upwards	
Tetrad abundance (%)	18.90	1.90	*8.70*	**5.90**	increase upwards	
PMI	100.00	100.00	*100.00*	**138.90**	-	no marine palynomorphs

Figure 8.30. Summary of palynofacies ratios and parameters of Unit C-24. For abbreviations see Table 8.1.

Unit D-24 (318-265) - Palynofacies association Phy-o

This unit is strongly dominated by opaque phytoclast. The opaque particles are composed mainly of O-La particles (Figure 8.45). Translucent particles are present in moderate to high abundances, in which the Ww particles are the most abundant. The abundance of the AOM group in this unit is very low to moderate (Figure 8.31). The abundance curve shows a strong fluctuation; however, it increases towards the top of the unit reaching 51.4% at 300.60 m. The palynomorph group is represented only by continental elements, in particular pollen grains. The abundance of spores is moderate to high.

		Kerogen groups				**Phytoclast Group**							**Palynomorph Group**				
						Opaque		Translucent					Marine		Terrestrial		
		AOM %	Ph%	Pa %	Zoocl %	O-Eq	O-La	Fh	Wp	Cu	Ww	Mb	Ftl	Df	Fwp	Pl	Sp
Unit D-24 **(Phy-o)**	Max.	51.4	85.4	25.2	0.2	7.8	71.0	0.8	3.3	3.3	51.3	-	-	-	-	97.9	15.0
	Min.	0.6	36.4	10.2	-	1.1	43.6	-	0.5	0.8	20.2	-	-	-	-	85.0	2.0
	Mean	11.5	73.1	15.4	0.01	4.2	60.6	0.2	1.8	2.2	31.1	-	-	-	-	92.8	7.2
General mean		**32.7**	**47.9**	**19.0**	**0.3**	**9.0**	**52.2**	**11.1**	**0.7**	**1.8**	**33.5**	**11.1**	**7.8**	**24.9**	**0.1**	**61.0**	**6.3**

Figure 8.31. Percentage mean values of the kerogen categories for **Unit D-24**. Relative abundances and abbreviations as in Figure 8.5.

Ratios and parameters. The O:TR ratio is characterized by a higher content of opaque particles, in which the average value is higher than the general mean (Figure 8.32). The ratio curve is characterized by a clearly increasing trend that reflects a decrease of translucent particles upwards (Figure 8.46). The O-Eq:O-La ratio is characterized by high O-La contents. The ratio curve shows an increasing trend upwards. The abundance of tetrads in this unit range from moderate to high (Figure 8.32). The curve shows strong fluctuations, with a slight decrease upwards. Marine palynomorphs are recorded only in one sample and in very low abundances; therefore the PMI values are very low.

Ratios and Parameters	Max.	Min.	*Unit Mean*	**General mean**	Trendline	Remarks
O:TR ratio (log10)	0.49	-0.09	*0.28*	**0.21**	increase upwards	
O-Eq:O-La ratio (log10)	-0.89	-1.59	*-1.24*	**-0.84**	increase upwards	
Tetrad abundance (%)	33.30	3.70	*12.90*	**5.90**	slightly decrease upwards	
PMI	107.10	100.00	*100.80*	**138.90**	-	rare marine palynomorphs

Figure 8.32. Summary of palynofacies ratios and parameters of Unit D-24. For abbreviations see Table 8.1.

Unit E-24 (265-253 m) - Palynofacies association AOM/Pal-s

Like Unit A-24, this unit is characterized by high abundances of the AOM group combined with frequent terrestrial palynomorphs. However, despite the high abundance of terrestrial palynomorphs (pollen grains), the moderate abundance of marine palynomorphs, in particular dinocysts (figure 8.33), differentiates this unit from Unit A-24. The unit is also characterized by two major peaks in abundance of dinocysts. The phytoclast group is moderately abundant and composed predominately of O-La particles. Translucent particles are present in moderate to large numbers with the Ww particles being the most abundant.

		Kerogen groups				Phytoclast Group							Palynomorph Group				
						Opaque		Translucent					Marine		Terrestrial		
		AOM %	Ph%	Pa %	Zoocl %	O-Eq	O-La	Fh	Wp	Cu	Ww	Mb	Ftl	Df	Fwp	Pl	Sp
Unit E-24 **(AOM/ Pal-s)**	Max.	62.0	82.6	34.4	1.6	8.6	77.4	6.3	3.3	3.9	57.7	-	34.5	54.5	-	96.5	7.0
	Min.	4.6	20.8	10.2	-	1.4	36.9	-	-	-	13.4	-	-	-	-	16.0	-
	Mean	50.1	30.4	19.4	0.1	4.8	56.3	1.0	1.6	1.8	34.6	-	10.1	6.0	-	81.8	2.1
General mean		**32.7**	**47.9**	**19.0**	**0.3**	**9.0**	**52.2**	**11.1**	**0.7**	**1.8**	**33.5**	**11.1**	**7.8**	**24.9**	**0.1**	**61.0**	**6.3**

Figure 8.33. Percentage mean values of the kerogen categories for **Unit E-24**. Relative abundances and abbreviations as in Figure 8.5.

Ratios and parameters. The values of the O:TR ratio are characterized by higher content of opaque particles. The ratio shows a strong fluctuation, but in general it shows a progressive increase upwards. The high amounts of O-La particles is also reflected in the O-Eq:O-La ratio. The ratio curve shows a marked increasing trend towards the top (Figure 8.46). In this unit the tetrad abundances show low to high values (Figure 8.34). The trendline for the tetrad abundance curve is constant. Unit E-24 is characterized by low to moderate PMI values, in which the mean is 121.20. The PMI curve shows a slight increase upwards.

Ratios and Parameters	Max.	Min.	*Unit Mean*	**General mean**	Trendline
O:TR ratio (log10)	0.69	-0.20	*0.21*	**0.21**	increase upwards
O-Eq:O-La ratio (log10)	-0.70	-1.60	*-1.11*	**-0.84**	increase upwards
Tetrad abundance (%)	20.20	0.50	*8.60*	**5.90**	constant
PMI	140.00	100.00	*121.20*	**138.90**	increase upwards

Figure 8.34. Summary of palynofacies ratios and parameters of Unit E-24. For abbreviations see Table 8.1.

Unit F-24 - Palynofacies association Pal-s/Phy-t (253-209 m)

This unit is characterized by the abundance of the palynomorph group combined with moderate to high numbers of translucent phytoclasts. The palynomorphs here show a marked increase in abundance, when compared with the other units. This group is composed mainly of pollen grains that show the highest abundance value of the whole succession (Figure 8.35). The marine palynomorphs show moderate to high abundances, with the FTL more abundant than the dinocysts. The average abundance of the AOM group is moderate, decreasing towards the top. The phytoclast group is composed mainly of O-La particles. Here the major average abundance of translucent particles which are attributed to the great numbers of Ww particles.

		Kerogen groups				Phytoclast Group							Palynomorph Group				
						Opaque		Translucent					Marine		Terrestrial		
		AOM %	Ph%	Pa %	Zoocl %	O-Eq	O-La	Fh	Wp	Cu	Ww	Mb	Ftl	Df	Fwp	Pl	Sp
Unit F-24 **(Pal-s/ Phyt)**	Max.	48	82.2	45.2	1.2	11.4	62.1	4.1	3.7	1.6	57.4	-	53.7	22.0	-	96.4	10.5
	Min.	0.8	24.4	10.8	-	1.9	35.4	-	-	-	28.8	-	-	-	-	22	1.0
	Mean	22.3	49.0	28.4	0.3	7.2	49.5	1.0	1.2	0.4	40.7	-	6.0	4.7	-	85.1	4.3
General mean		**32.7**	**47.9**	**19.0**	**0.3**	**9.0**	**52.2**	**11.1**	**0.7**	**1.8**	**33.5**	**11.1**	**7.8**	**24.9**	**0.1**	**61.0**	**6.3**

Figure 8.35. Percentage mean values of the kerogen categories for **Unit F-24**. Relative abundances and abbreviations as in Figure 8.5.

Ratios and parameters. The O:TR ratio is characterized by moderate content of opaque particles. The ratio curve shows strong fluctuations; and a progressive increase. The O-Eq-O-La ratio shows clearly a progressive increasing trend upwards. The mean value of this ratio is higher than the general mean (Figure 8.36). Generally, the tetrad abundances are low and the average abundance is lower than the general value (Figure 8.36). The abundance curve shows a decreasing trend upwards. In this unit the PMI values are moderate; but show a high peak in abundance at 241.25. The PMI values range from 100.00 to 200.00, in which the mean value is 120.60. The PMI curve increases slightly upwards.

Ratios and Parameters	Max.	Min.	*Unit Mean*	**General mean**	Trendline
O:TR ratio (log10)	0.35	-0.17	*0.12*	**0.21**	increase upwards
O-Eq:O-La ratio (log10)	-0.50	-1.40	*-0.86*	**-0.84**	increase upwards
Tetrad abundance (%)	10.00	-	*4.30*	**5.90**	constant
PMI	200.00	100.00	*120.60*	**138.90**	increase upwards

Figure 8.36. Summary of palynofacies ratios and parameters of Unit F-24. For abbreviations see Table 8.1.

Unit G-24 (209-183 m)- Palynofacies association AOM/Pal-s

This unit shows similar kerogen characteristics as in Unit E-24, in which high abundances of the AOM group combined with terrestrial palynomorphs are observed. The marine palynomorphs show moderate abundances (Figure 8.37), as well as the phytoclast group. This group is consists mainly of O-La. The translucent particles are composed mainly of Ww; however, the cuticle fragments reach 4.0% of %TK.

		Kerogen groups				Phytoclast Group							Palynomorph Group				
						Opaque		Translucent					Marine		Terrestrial		
		AOM %	Ph%	Pa %	Zoocl %	O-Eq	O-La	Fh	Wp	Cu	Ww	Mb	Ftl	Df	Fwp	Pl	Sp
Unit G-24 **(AOM/ Pal-s)**	Max.	58.6	84.4	37.6	0.6	17.1	56.0	3.0	1.5	4.7	47.4	-	30.0	42.0	-	83.4	17.2
	Min.	5.2	26.6	10.2	-	5.7	41.5	-	-	-	29.1	-	2.6	0.5	-	47.5	3.0
	Mean	38.5	43.7	17.5	0.3	10.0	50.5	1.0	0.6	1.0	37.0	-	12	13.4	-	66.8	7.8
General mean		**32.7**	**47.9**	**19.0**	**0.3**	**9.0**	**52.2**	**11.1**	**0.7**	**1.8**	**33.5**	**11.1**	**7.8**	**24.9**	**0.1**	**61.0**	**6.3**

Figure 8.37. Percentage mean values of the kerogen categories for **Unit G-24**. Relative abundances and abbreviations as in Figure 8.5.

Ratios and parameters. The O:TR is characterized by a decreasing trend upwards (Figure 8.46). The average values are lower than the general mean (Figure 8.38). The O-Eq-O-La shows a greater amount of the O-La than O-Eq indicated by a slightly decreasing of the ratio. In spite of the decreasing trend, at the uppermost part of unit, the ratio curve shows a smooth increase upwards (Figure 8.46). The tetrad abundances are low in abundance, but increase slightly towards the top. In Unit G there are low to moderate values of PMI, decreasing upwards (Figure 8.46).

Ratios and Parameters	Max.	Min.	*Unit Mean*	**General mean**	Trendline
O:TR ratio (log10)	0.34	-0.02	*0.19*	**0.21**	increase upwards
O-Eq:O-La ratio (log10)	-0.48	-0.98	*-0.73*	**-0.84**	increase upwards
Tetrad abundance (%)	10.00	-	*4.30*	**5.90**	constant
PMI	200.00	100.00	*120.60*	**138.90**	increase upwards

Figure 8.38. Summary of palynofacies ratios and parameters of Unit G-24. For abbreviations see Table 8.1.

Unit H-24 (183-88 m)- Palynofacies association Phy-o/Pal-mp

This unit is characterized by a relatively high abundances of opaque phytoclasts, in which the O-La particles are the most abundant. The translucent particles are present in low to moderate abundances (Figure 8.39). The percentages of the AOM group show very low to moderate values. The percentage curve shows abrupt fluctuations. However, this group increases gradually upwards. The occurrence of the phytoclast group is combined with relatively high abundances of marine palynomorphs. Despite the domain of terrestrial palynomorphs, in particular pollen grains, this unit was characterized as **Pal-mp** because its average abundance in this unit (26.4%) is higher than its general mean (24.9%) (Figure 8.39). The marine palynomorphs are mainly composed of dinocysts; however, the FTL are also present in moderate abundance (Figure 8.39). Fresh-water palynomorphs (only *Botryococcus*) are also present in this unit.

		Kerogen groups				**Phytoclast Group**							**Palynomorph Group**				
						Opaque		Translucent					Marine		Terrestrial		
		AOM %	Ph%	Pa %	Zoocl %	O-Eq	O-La	Fh	Wp	Cu	Ww	Mb	Ftl	Df	Fwp	Pl	Sp
Unit H-24 **(Phy-o/ Pal-mp)**	Max.	32.8	86.8	35.2	0.6	16.0	76.9	3.1	2.1	1.8	45.0	-	33.5	79	1.5	73.5	24.5
	Min.	1.6	43.6	11.6	-	3.5	46.2	-	0.3	0.2	13.2	-	2.0	10.5	-	8.1	2.5
	Mean	10.6	67.1	22.1	0.2	9.1	56.6	0.9	0.9	0.8	31.7	-	16.2	26.4	0.2	45.7	11.5
General mean		**32.7**	**47.9**	**19.0**	**0.3**	**9.0**	**52.2**	**11.1**	**0.7**	**1.8**	**33.5**	**11.1**	**7.8**	**24.9**	**0.1**	**61.0**	**6.3**

Figure 8.39. Percentage mean values of the kerogen categories for **Unit H-24**. Relative abundances and abbreviations as in Figure 8.5.

Ratios and parameters. The O:TR ratio shows a clear increasing trend upwards (Figure 8.40). The average value is higher than the general mean (Figure 8.40) indicating the high opaque particle content. The O-Eq:O-La shows a slight decreasing upwards, indicated by the marked increase of O-La particles. The tetrad abundance in this unit shows low to moderate abundances. The abundance curve shows an increase towards the top of the unit. The PMI values in this unit are characterized by low to moderate values, with decreasing trend upwards (Figure 8.46).

Ratios and Parameters	Max.	Min.	*Unit Mean*	**General mean**	Trendline
O:TR ratio (log10)	0.76	0.04	*0.30*	**0.21**	slightly increase upwards
O-Eq:O-La ratio (log10)	-0.46	-1.15	*-0.83*	**-0.84**	slightly decrease upwards
Tetrad abundance (%)	5.00	0.50	*1.70*	**5.90**	constant
PMI	162.50	109.50	*134.20*	**138.90**	increase upwards

Figure 8.40. Summary of palynofacies ratios and parameters of Unit H-24. For abbreviations see Table 8.1.

Unit I-24 (183-88 m) - Palynofacies association Phy-o/Pal-s

Unit I-24 is characterized by a high content of phytoclast combined with moderate to high terrestrial palynomorphs. The phytoclast group reaches very high abundances and is predominantly made up of O-La particles (Figure 8.41). The translucent particles are present in moderate to high abundances and mainly composed of Ww. The palynomorph group that also characterizes this unit, is dominated by pollen grains. The marine palynomorphs are constituted mainly of dinocysts. These palynomorphs are present in moderate to high abundances. The presence the marine palynomorphs is the main difference between this and Unit B-24. As in the previous unit, the AOM group shows very low to moderate abundances.

		Kerogen groups				Phytoclast Group							Palynomorph Group				
						Opaque		Translucent					Marine		Terrestrial		
		AOM %	Ph%	Pa %	Zoocl %	O-Eq	O-La	Fh	Wp	Cu	Ww	Mb	Ftl	Df	Fwp	Pl	Sp
Unit I-24 (Phy-o/ Pal-s)	Max.	48.8	85.8	30.0	1.8	13.4	79.7	4.3	2.6	2.4	42.2	0.3	17	56.1	0.5	73.5	22.7
	Min.	1.2	23.2	11.0	-	1.8	42.2	-	-	-	12.3	-	1.7	9.5	-	24.4	0.8
	Mean	18.2	60.5	20.9	0.4	7.1	65.7	1.1	1.3	1.0	23.8	0.02	9.2	29.3	0.1	52.4	8.9
General mean		**32.7**	**47.9**	**19.0**	**0.3**	**9.0**	**52.2**	**11.1**	**0.7**	**1.8**	**33.5**	**11.1**	**7.8**	**24.9**	**0.1**	**61.0**	**6.3**

Figure 8.41. Percentage mean values of the kerogen categories for **Unit I-24**. . Relative abundances and abbreviations as in Figure 8.5.

Ratios and parameters. The O:TR ratio shows strong fluctuations, with a decreasing trend upwards. The average value is higher than the general mean (Figure 8.42). The O-Eq-O-La shows a progressive decrease upwards, which is indicated by a marked increase of O-La particles. The tetrad abundance in this unit shows low to moderate abundances with a clear increase towards the top. In contrast with the previous unit, the PMI values in this unit clearly show a decrease upwards (Figure 8.46).

Ratios and Parameters	Max.	Min.	*Unit Mean*	**General mean**	Trendline
O:TR ratio (log10)	0.78	0.06	*0.45*	**0.21**	slightly decrease upwards
O-Eq:O-La ratio (log10)	-0.58	-1.64	*-1.00*	**-0.84**	decrease upwards
Tetrad abundance (%)	13.50	-	*3.60*	**5.90**	constant
PMI	200.00	115.80	*149.50*	**138.90**	increase upwards

Figure 8.42. Summary of palynofacies ratios and parameters of Unit I-24. For abbreviations see Table 8.1.

Unit J-24 (88-10 m) - Palynofacies association AOM/Pal-mp

Unit J-24 is characterized by a high abundance values of the AOM group; however this decreases upwards. This unit is also characterized by moderate to high amounts marine palynomorphs. In contrast with all other units, it is marked by a conspicuous dominance of marine palynomorphs. However, their abundance decreases slightly upwards. The marine palynomorphs are composed mainly of dinocysts, whereas the continental palynomorphs are mainly composed of pollen grains (Figure 8.43). This unit is also marked by the highest peak in abundance of spores (32.5% of %TPa at 22.88 m).

The abundances of the phytoclast group range from low to very high. The O-La particles are the most frequent; however, the O-Eq shows the highest abundance peak of this well. Translucent particles are represented mainly by Ww.

		Kerogen groups				**Phytoclast Group**							**Palynomorph Group**				
						Opaque		Translucent					Marine		Terrestrial		
		AOM %	Ph%	Pa %	Zoocl %	O-Eq	O-La	Fh	Wp	Cu	Ww	Mb	Ftl	Df	Fwp	Pl	Sp
Unit J-24 **(AOM/ Pal-mp)**	Max.	74.2	87.4	35.8	3.0	39.0	74.5	11.5	8.5	14.7	72.3	14.8	35.7	89.0	1.4	92.3	32.5
	Min.	3.0	12.8	1.2	-	1.7	14.2	-	-	-	8.0	-	-	1.6	-	4.0	-
	Mean	42.3	40.8	16.5	0.4	11.7	44.2	1.6	1.4	2.9	35.5	2.8	8.7	46.7	0.1	37.8	6.7
General mean		**32.7**	**47.9**	**19.0**	**0.3**	**9.0**	**52.2**	**11.1**	**0.7**	**1.8**	**33.5**	**11.1**	**7.8**	**24.9**	**0.1**	**61.0**	**6.3**

Figure 8.43. Percentage mean values of the kerogen categories for **Unit J-24**. Relative abundances and abbreviations as in Figure 8.5.

Ratios and parameters. The O:TR curve shows a decreasing trend indicated by an increase of translucent particles, and displays strong fluctuation. In this unit the lowest abundance values of the O:TR (Figure 8.44) is recognized. The O-Eq:O-La curve shows a marked increasing trend upwards, through an increase in numbers of equidimensional particles (Figure 8.46). The tetrad abundance in this unit is marked by strong fluctuations; with a slight increasing trend upwards. This unit is characterized by the highest PMI value (250.00 at 16.65 m). In spite of that, the PMI curve shows a slight decrease upwards.

Ratios and Parameters	Max.	Min.	*Unit Mean*	**General mean**	Trendline	Remarks
O:TR ratio (log10)	0.69	-0.53	*0.08*	**0.21**	decrease upwards	
O-Eq:O-La ratio (log10)	0.01	-1.41	*-1.00*	**-0.84**	increase upwards	highest value
Tetrad abundance (%)	24.20	-	*3.60*	**5.90**	slightly increase upwards	
PMI	250.00	112.50	*166.40*	**138.90**	constant	highest value

Figure 8.44. Summary of palynofacies ratios and parameters of Unit J-24. For abbreviations see Table 8.1.

8.3 Effects of lithology on the kerogen distribution

As previously mentioned in Chapter 4, Mendes (1994) indicated through lithological maps (see Figures 4.6-4.7) that during the Aptian–Albian, the study area was dominated by siliciclastic lithologies. This is confirmed in the two studied wells. The succession is dominated by shales (Figure 8.47) reflecting the terrestrial influx in the area. However, carbonates, in particular calcilutites of the Taquari Member (27.4%), predominate at some intervals in well GTP-24-SE.

Lithology		**%**	**AOM**	**Phytoclasts**	**Palynomorphs**
	anhydrites	7.0	43.9	35.5	20.6
carbonates	calcarenites	1.3	18.6	62.4	18.9
	calcilutites	27.4	31.1	52.2	16.2
mean			**26.7**	**53.2**	**19.7**
siliciclastics	sandstones	15.2	2.1	84.3	13.4
	siltstones	3.7.	15.5	68.3	16.0
	shales	37.8	25.1	56.1	18.6
mean			**14.2**	**69.3**	**16.0**

Figure 8.47. Lithological composition of the two well studied and the average abundances of kerogen groups (excluding zooclast group) for each lithology. Thin intercalations of shales and calcilutites (6.8%) are not presented.

The distribution of the three main kerogen groups (AOM, phytoclasts and palynomorphs) is moderately influenced by the different lithologies. The AOM group occurs mainly in carbonate rocks such as calcilutites. However, the shale samples also show moderate abundances of the AOM group. The AOM group is further present in high abundances in anhydrite layers. The phytoclast group is markedly more abundant in coarse siliciclastic lithologies, especially in sandstones. The zooclast group is rare in the studied succession; although it is locally more abundant in carbonate lithologies. The difference in abundance of the palynomorph group between the various lithologies is relatively low.

Well GTP-17-SE is dominated by siliciclastic rocks of the Angico Member (Figure 8.48). Sandstones are slightly more common, followed by shales. The high abundances of the phytoclast group in well GTP-17-SE are strongly related to siliciclastic sedimentation (Figure 8.48). The units, which are characterized by phytoclast predominance show a direct relationship with siliciclastic rocks, especially sandstones and shales (Figure 8.49). In the lower part of the succession (units A-17 and C-17), in the Muribeca Formation, moderate to high abundances of the AOM group are observed (Figure 49). The abundance of this group seems to be more influenced by lithology. The difference in abundance between the carbonates and siliciclastics is the highest observed. The dominant lithology apparently did not influence the distribution of palynomorph group. The difference in palynomorph abundances between carbonates and siliciclastic rocks is very low. However, in well GTP-17-SE, the units that are characterized by a relative high abundance of palynomorph are directly related to the siliciclastic deposition, especially of shales. In fact, this is reflected in the higher abundances of terrestrial palynomorphs rather than marine (Figure 49).

Lithology		**%**	**AOM**	**Phytoclasts**	**Palynomorphs**
	anhydrites	13.3	56.0	29.0	15.0
carbonates	calcarenites	1.0	7.4	68.7	23.1
	calcilutites	12.5	24.6	62.2	13.0
mean			**16.0**	**65.4**	**18.1**
siliciclastics	sandstones	32.1	2.0	85.0	12.8
	siltstones	8.9	15.5	68.3	15.9
	shales	29.2	9.8	74.1	15.9
	claystones	1.4	10.3	81.3	8.2
mean			**9.4**	**77.2**	**13.2**

Figure 8.48. Lithological composition of well GTP-17-SE and the average abundances of kerogen groups (excluding zooclast group) for each lithology. Thin intercalations of shales and calcilutites (1.6%) are not presented.

Units	**Palynofacies associations**	**Lithology**							**Kerogen groups**		
		anhydrites	calcarenites	calcilutites	claystones	sandstones	shales	siltstones	AOM	Phytoclast	Palynomorph
Unit A-17	AOM/Pal-s	42.7	0.5	40.7	-	9.3	5.0	1.8	32.3	51.1	16.5
Unit B-17	Phy-o/ Pal-s	-	-	6.9	-	45.4	33.3	11.9	15.3	67.9	16.9
Unit C-17	AOM/Pal-s	8.9	9.1	-	-	24.8	21.9	24.9	35.0	50.4	14.3
Unit D-17	Phy-o-t	-	-	-	-	-	100	-	6.1	79.1	14.2
Unit E-17	Pal-mp/ Phy-o-t	-	-	-	-	-	80.8	19.2	7.2	69.2	22.7
Unit F-17	Phy-o/ Pal-s	-	-	-	5.3	68.6	18.1	8.0	3.3	80.4	16.1
Unit G-17	Pal-mp/ Phy-o	-	-	-	3.0	37.5	40.8	18.7	2.7	75.5	21.2
Unit H-17	Phy-o	-	-	0.7	3.6	77.0	14.6	2.7	1.5	91.3	7.0
mean		**13.3**	**1.0**	**12.5**	**1.4**	**32.1**	**29.2**	**8.9**	**10.9**	**73.7**	**15.2**

Figure 8.49. Lithological composition (%) and kerogen groups (average abundances) for each palynofacies unit in well GTP-17-SE. Thin intercalations of shales and calcilutites are not presented.

Well GTP-24-SE is dominated by shales (Figure 8.50); however, in contrast to well GTP-17-SE, carbonate deposits also occur in moderate to high amounts, especially calcilutites. The distribution of kerogen groups in this well shows the same pattern as in well GTP-17-SE. The AOM group is more abundant in carbonate rocks; however this group is also abundant in shales. In coarse deposits such as sandstones, the AOM group shows low to very low abundance. This group characterizes units A-24, C-24, E-24 and G-24, where the calcilutite layers are thicker. In Unit J-24, which is also characterized by the AOM group, the shale package is thicker. The phytoclast group, as in well GTP-17-SE, shows high abundances in siliciclastic rocks, especially in sandstones. This group is also common in carbonates (e.g., Unit F-24) (Figure 8.51). As in well GTP-17-SE, the distribution of palynomorphs shows only minor differences in abundance between carbonate and siliciclastic rocks. However, In this well the effect of lithology on two main groups of palynomorphs (marine and terrestrial) is observed more clearly. The units that are characterized by relatively high abundance of marine palynomorphs (unit H-24 and J-24) are common in carbonate deposits, and in the units (e.g., units B-24, F-24 and I-24) (Figure 8.51) that are characteristic of siliciclastic deposits, terrestrial palynomorphs are more abundant (discussed in more detail in Chapter 5).

Lithology		**%**	**AOM**	**Phytoclasts**	**Palynomorphs**
	anhydrites	2.6	39.9	37.6	22.5
carbonate	calcarenites	1.5	34.6	53.0	16.6
	calcilutites	37.7	31.8	51.1	16.2
mean			**32.3**	**49.6**	**17.7**
siliciclasts	sandstones	3.4	4.2	70.6	25.2
	shales	43.8	34.3	45.2	20.3
mean			**19.3**	**57.9**	**22.7**

Figure 8.50. Lithological composition of well GTP-24-SE and the average abundances of kerogen groups (excluding zooclast group) for each lithology. A succession of thin intercalations of shales and calcilutites (10.6%) is not presented.

Units	Palynofacies associations	Lithology						Kerogen groups		
		anhydrites	calcarenites	calcilutites	calcirudites	sandstones	shales	AOM	Phytoclast	Palynomorph
Unit A-24	AOM/Pal-s	27.8	-	53.3	-	-	18.9	49	35.1	15.2
Unit B-24	Phy-o/Pal-s	3.2	7.9	14.3	-	13.2	46.3	27.2	54.3	18.1
Unit C-24	AOM/Pal-s	8.9	-	-	-	2.4	-	37.2	44.3	18.5
Unit D-24	Phy-o	-	-	-	-	17.7	44.3	11.5	73.1	15.4
Unit E-24	AOM/Pal-s	-	-	62.4	7.7	-	29.8	50.1	30.4	19.4
Unit F-24	Pal-s/Phy-o	-	-	30.9	-	-	69.1	22.3	49.0	28.4
Unit G-24	AOM/Pal-s	-	-	71.9	-	-	28.1	38.5	43.7	17.5
Unit H-24	Phy-o/Pal-mp	-	-	83.5	-	-	16.5	10.6	67.1	22.1
Unit I-24	Phy-o/Pal-s	-	-	16.2	-	-	77.8	18.2	60.5	20.9
Unit J-24	AOM/Pal-mp	-	-	37.2	-	-	62.8	42.3	40.8	16.5
mean		**0.4**	**1.7**	**36.4**	**0.4**	**3.7**	**46**	**32.7**	**47.9**	**19.0**

Figure 8.51. Lithological composition (%) and kerogen groups (average abundances) for each palynofacies unit in well GTP-24-SE. Thin intercalations of shales and calcilutites are not presented.

CHAPTER 9
GEOCHEMICAL ANALYSIS

The results for each sample are shown in Appendix 4 and are illustrated graphically in geochemical logs (Figure 9.4).

9.1 Total Organic Carbon (TOC)

TOC ranges from 0.07% at the top of Unit A-24 in the Ibura Member to 9.59% in Unit B-24 of the Oiteirinhos Member (Figure 9.4). The highest TOC values are recorded in the Muribeca Formation, where the highest average TOC value (Unit E-24) is also recorded (Figure 9.1). The lowest average TOC (0.7%) is recorded in Unit H-24. The general mean is 1.4%. This mean shows that the succession has a moderate organic matter accumulation. The TOC values tend to decrease slightly upward.

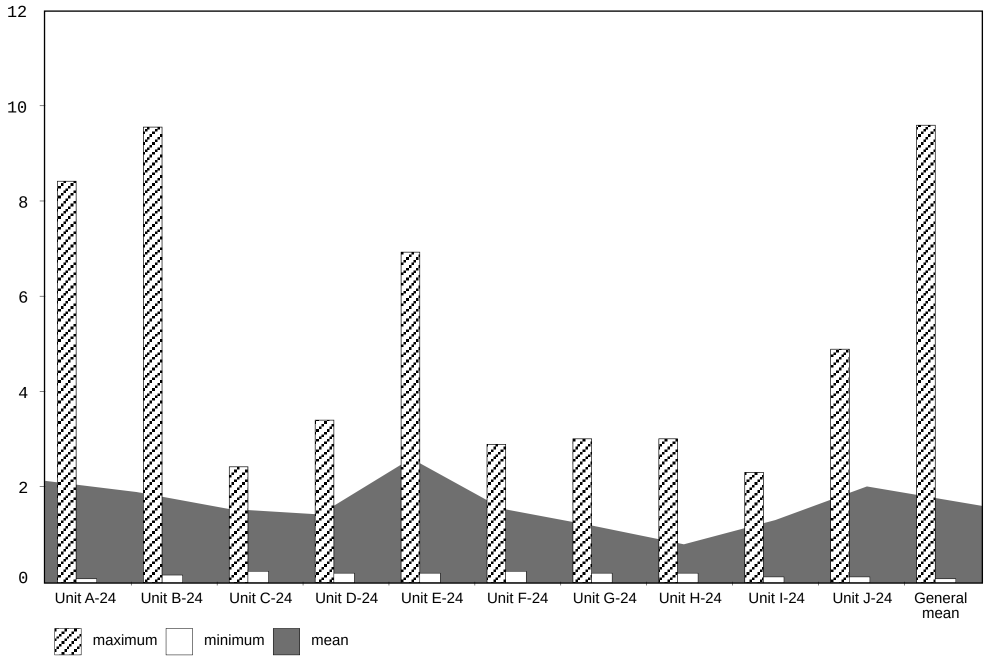

Figure 9.1. TOC values for each palynofacies units in well GTP-24-SE.

The higher average values of TOC show a direct relationship with the units characterized by a high abundance of AOM. In Unit E-24, where the highest TOC is observed, AOM surpasses 50.0% of the total kerogen, in contrast with the units that are dominated by the phytoclast group (Figure 9.1). The palynomorph group does not show any relationship with high or low values of TOC (Table 9.1).

Table 9.1. Comparison between the average of TOC and the palynofacies associations.

Palynofacies associations	AOM group	Phytoclast group	Palynomorph group	Zooclast group	TOC% (average)
Phy-o	11.5	73.1	15.4	-	**1.1**
Phy-o/Pal-s	22..7	57.5	19.5	0.3	**1.4**
Pal-s/Phy-t	22.3	49.0	28.4	0.3	**1.3**
Phy-o/Pal-mp	10.6	64.1	22.1	0.2	**0.7**
AOM/Phy-o	37.6	44.3	18.5	-	**1.3**
AOM/Pal-s	45.9	36.4	17.4	0.3	**1.7**
AOM/Pal-mp	42.3	40.8	16.5	0.4	**1.7**

9.1.2 TOC and lithology

The TOC values show a positive correlation with siliciclastic deposits. The highest average of TOC is recorded in shales (Figure 9.2) and in fine intercalations between shales and calcilutites, but are clearly dominated by the first situation. In the carbonates the average is lower than in siliciclastics. In fact, the succession is dominated by only two lithologies: shales (43.8%), with an average TOC of 1.9%, and calcilutites (37.6%) with 1.0%; thus, data on the minor lithologies are not included as they are unlikely to influence the interpretations.

Lithology		%	AOM	Phytoclasts	Palynomorphs	TOC%
	anhydrites	2.6	39.9	37.6	22.5	0.9
carbonates	calcarenites	1.5	34.6	53.0	16.6	1.6
	calcilutites	37.7	31.8	51.1	16.2	1.0
	calcirudites	0.4	30.4	44.9	23.9	0.6
mean			**32.3**	**49.6**	**17.7**	**1.1**
siliciclasts	sandstones	3.4	4.2	70.6	25.2	0.84
	shales	43.8	34.3	45.2	20.3	1.9
mean			**19.3**	**57.9**	**22.7**	**1.4**

Figure 9.2. Comparison between the lithological composition and kerogen group with the mean of TOC for well GTP-24-SE. Fine intercalations (not presented) between shales and calcilutites (dominated by shales) show an average TOC of 1.7%.

9.2 Hydrogen and Oxygen indices (Rock-Eval pyrolysis)

The Hydrogen Index (HI) can be used to characterize the kerogen type and the level of thermal maturity, whereas the oxygen index (OI) becomes useful for this purpose only in conjunction with the HI (Miles 1989). HI values range from 1 to 1345 mgHC/g TOC, while OI values range from 14 to 740 mgCO_2/g TOC (Appendix 4). The HI values generally lie within a typical range of kerogen type III organic matter, i.e. 0-300 (Miles, 1989). The general average is 303 mgHC/g TOC, which lies between gas and oil prone organic matter. The highest value of HI is recorded in Unit I-24 (1345 mgHC/g TOC) (Figure 9.4); whereas the highest average value is recorded in Unit A-24 (587 mgHC/g TOC), characterized by an oil prone organic matter (Table 9.2). The values of Unit A-24 are contained in a mixed Type II/III organic matter. The HI values show a marked decrease upwards. The general mean of the OI is 94 $mgCO_2$/g TOC, and the highest average of OI is recorded in Unit-B-24 (162 $mgCO_2$/g TOC). However, the highest value of OI (740 $mgCO_2$/g TOC) is recorded in Unit I-24.

Table 9.2. Comparison between the averages of HI and OI and the palynofacies associations.

Palynofacies association	AOM group	Phytoclast group	Palynomorph group	Zooclast group	HI (HC/g TOC)	OI (CO_2/g TOC)
Phy-o	11.5	73.1	15.4	-	**268**	**71**
Phy-o/Pal-s	22.7	57.5	19.5	0.3	**348**	**187**
Pal-s/Phy-t	22.3	49.0	28.4	0.3	**224**	**64**
Phy-o/Pal-mp	10.6	64.1	22.1	0.2	**94**	**112**
AOM/Phy-o	37.6	44.3	18.5	-	**287**	**79**
AOM/Pal-s	45.9	36.4	17.4	0.3	**354**	**143**
AOM/Pal-mp	42.3	40.8	16.5	0.4	**186**	**68**

9.3 Organic facies characterization

The organic facies characterization was carried out using the HI versus OI diagram (Figure 9.3). The diagrams are shown for each type of palynofacies association of GTP-24-SE. The organic matter type in well GTP-24-SE belongs predominantly to kerogen Type III derived from higher land plants (Figure 9.3). However, in samples, where the AOM is dominant (AOM/Phy-o, AOM/Pal-s and AOM/Pal-mp) kerogen type II is recorded, especially in palynofacies association AOM/Pal-s.

9.4 Kerogen fluorescence

The results of the fluorescence investigations confirm that kerogen types III and II predominated throughout the succession studied. The kerogen intensities range from 1 to 4 or 5 (scale of Tyson, 1995, p. 347), and the average is 3.1. Points 4 and 5 on the scale are recorded only in the palynofacies association where the AOM group is dominant (Figure 9.4).

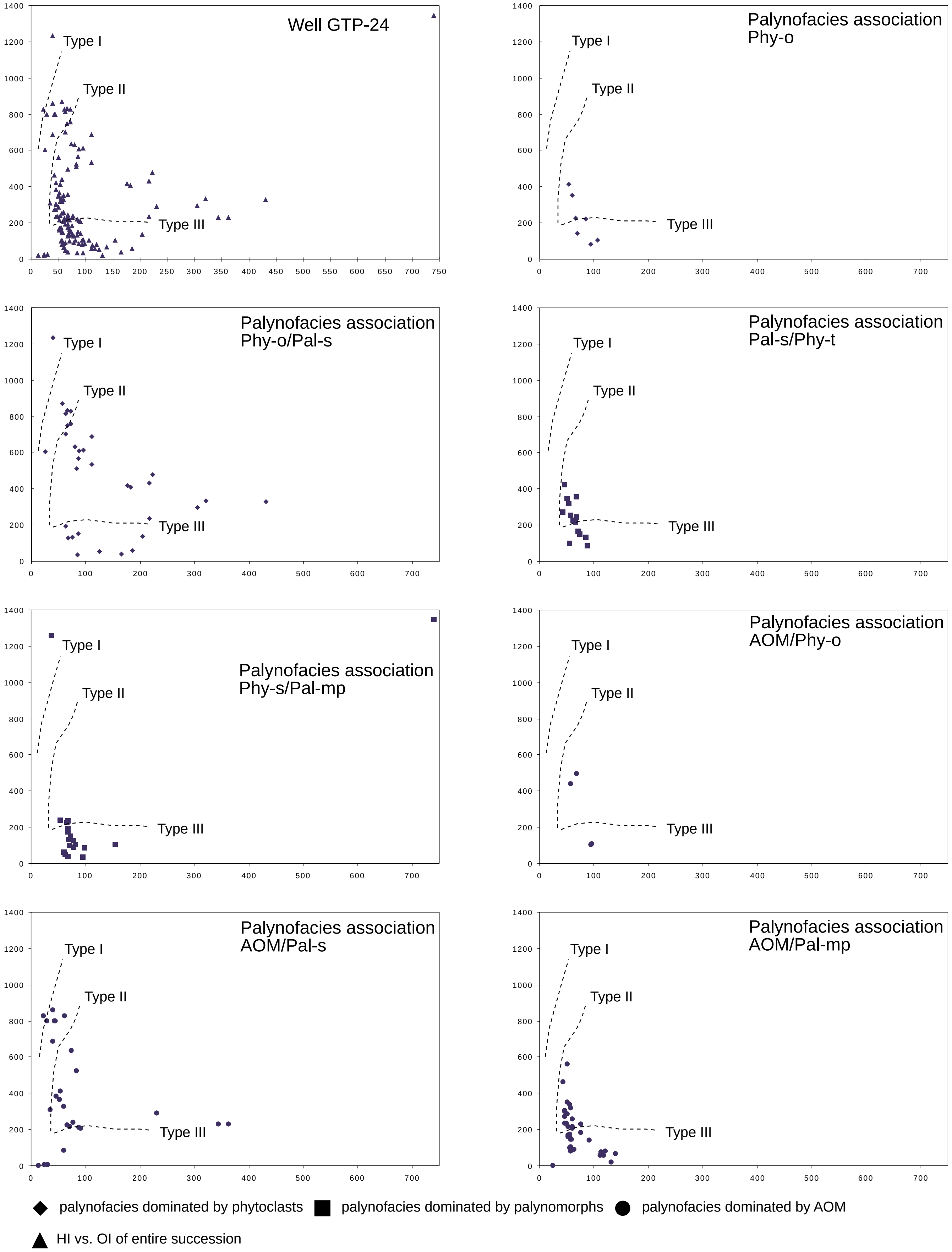

Figure 9.3. Hydrogen index (y axis) vs. oxygen index (X axis) diagram of each palynofacies association and general succession of well GTP-24-SE.

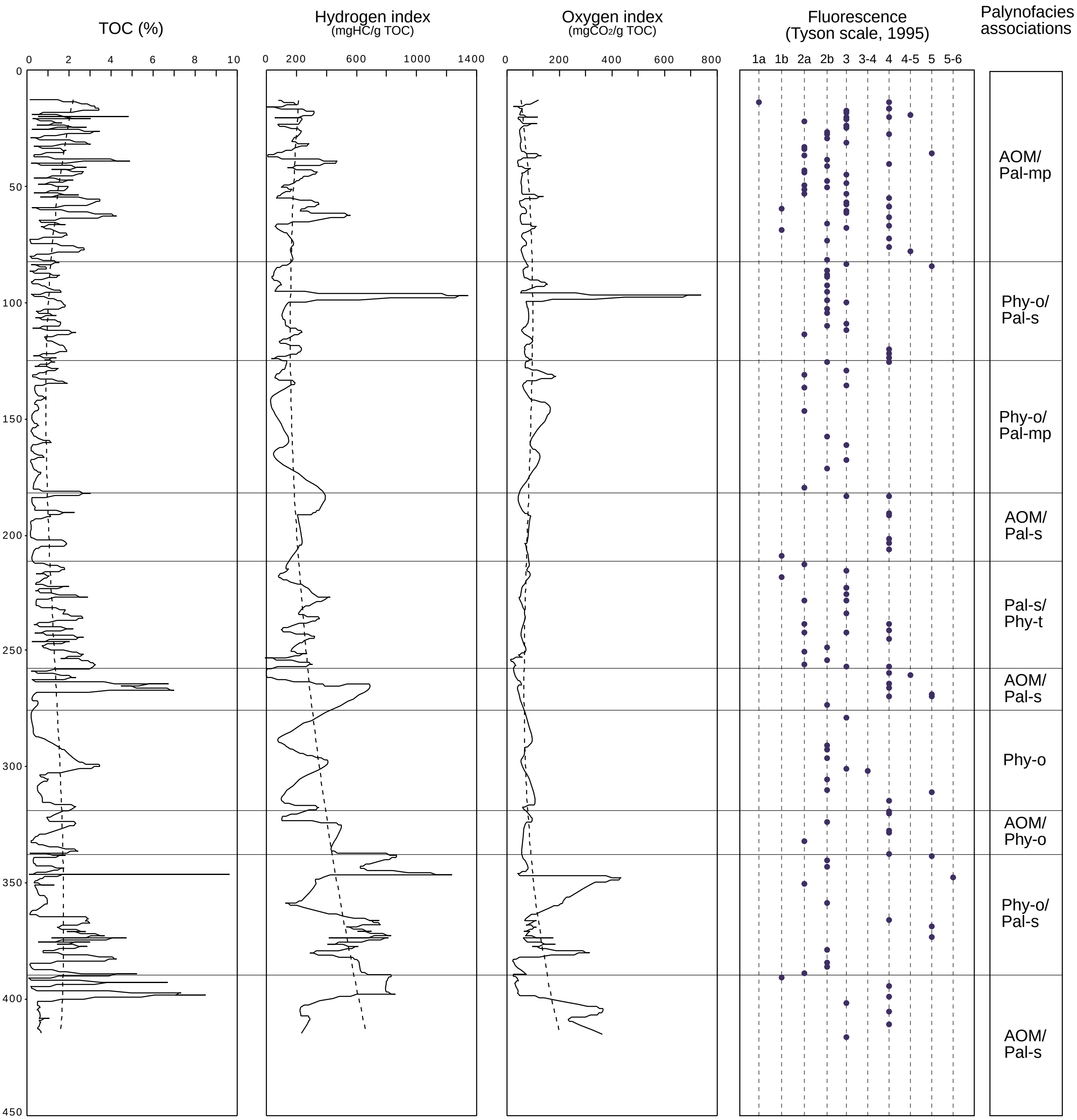

Figure 9.4. Stratigraphic distribution of selected geochemical data (TOC, HI, OI and fluorescence) and the palynofacies associations of well GTP-24-SE.

CHAPTER 10
PALYNOFACIES AND SEQUENCE STRATIGRAPHY

In order to place the information from the palynofacies variations in a sequence stratigraphic context, the palynofacies units for wells GTP-17-SE and GTP-24-SE were integrated with the sequence stratigraphy framework of Pereira (1994), Feijó (1995) and Hamsi Junior *et al*. (1999) (Figure 10.1). Feijó (1995) assigned the large-scale sequence stratigraphic framework of the succession to two second-order sequences, K50 and K60. Sequence K50 corresponds to the SBL–ALs sequence of Pereira (1994). Sequence K60 was subdivided into systems tracts KM1 and KM2 by Hamsi Junior *et al*. (1999) (Figure 10.1).

By combining lithofacies data and gamma-ray logs from the studied wells with palynofacies and paleoecological data (especially the PMI), the succession was subdivided into third-order sequences and correlated with the integrated sequence stratigraphic framework. The sequences and boundaries (SB) are described within the “classical” sequence stratigraphic context (e.g., van Wagoner *et al.*, 1988; Posamentier *et al.*, 1988; Posamentier & Vail, 1988; Sarg, 1988; García-Mondéjar & Fernández-Mendiola, 1993).

Stages	Lithostratigraphy	Major sequences	2nd-order sequences	Systems tracts
Albian	Taquari Member Angico Member (lower part)	Passive margin	K60	**KM2** Highstand Systems Tract
Aptian (upper part)				**KM1** Transgressive Systems Tract
	Oiteirinhos Mb. Ibura Mb. (upper part)	Transitional	K50	Highstand Systems Tract

Figure 10.1. Integrated sequence stratigraphic framework based on Pereira (1994), Feijó (1995) and Hamsi Junior *et al*. (1999).

10.1 Palynofacies and sequence stratigraphy

The composition and quantity of kerogen deposited in marine paleoenvironments is directly related to sea-level as shown by many authors (e.g., Habib & Miller, 1989; Gorin & Steffen, 1991; Steffen & Gorin, 1993a,b; Blondel *et al.* 1993; Tyson, 1993, 1995, 1996; Bombardiere & Gorin, 2000) who placed them in a sequence stratigraphic context.

The background models for palynofacies in sequence stratigraphic context that were integrated herein for the distribution of kerogen in the different systems tracts, were taken from Steffen & Gorin (1993b), Tyson (1995), and Hart *et al*. (1994). The general trends of the palynofacies parameters are shown in Figure 10.2

Lowstand Systems Tract (LST)

This LST is the lowermost tract in a sequence (van Wagoner *et al.*, 1988). The LST is characterized by a progradational parasequence set. Owing to this progradational nature, the deposits are mainly characterized by proximal facies, formed during periods of rapid but decelerating sea-level fall (Tyson, 1995). Many authors agree that terrestrial particles (phytoclasts) increase in abundance during deposition of the lowstand tract (Steffen & Gorin, 1993b; Tyson, 1995). According to Tyson (1995) in the lowest parts of the LST the highest amounts of phytoclasts are recorded (Figure 10.2). As a result of terrestrial input, the abundance of marine palynomorphs, especially dinocysts, decreases in lowstand deposits. The geochemical parameters are characterized by the lowest values of TOC and HI in comparison with others tracts (Hart *et al*. 1994).

Transgressive Systems Tract (TST)

The TST is the middle tract distinguished by the retrogradational parasequence sets (van Wagoner *et al.*, 1988). This tract is bounded at the base by a transgressive surface (ts) and at the top by the “maximum flooding surface” (mfs) that is the most important condensed section (CS). These surfaces are also recognized though the kerogen distribution. According to Tyson (1995) the TST is related to increasing acceleration in sea-level rise, and marked by a progressive decrease in abundance of phytoclast particles, with the particles becoming more rounded (Steffen & Gorin, 1993b) (Figure 10.2). The phytoclasts reach the lowest values at the CS; however, the percentage of opaque particles (of % phytoclasts) increases up to the mfs.

The abundance and diversity of marine palynomorphs increase during deposition of the TST. Normally, at the mfs the highest diversity of marine palynomorphs (especially dinocysts) is recorded (Tyson, 1995) the abundance of AOM depends on the nature of the CS. In oxic CS the AOM is at a minimum, whereas in anoxic CS this group reaches high abundances. According to Hart *et al.* (1994) the TST may contain the highest values of TOC and HI. However, the highest peaks of TOC and HI do not necessarily occur at the mfs.

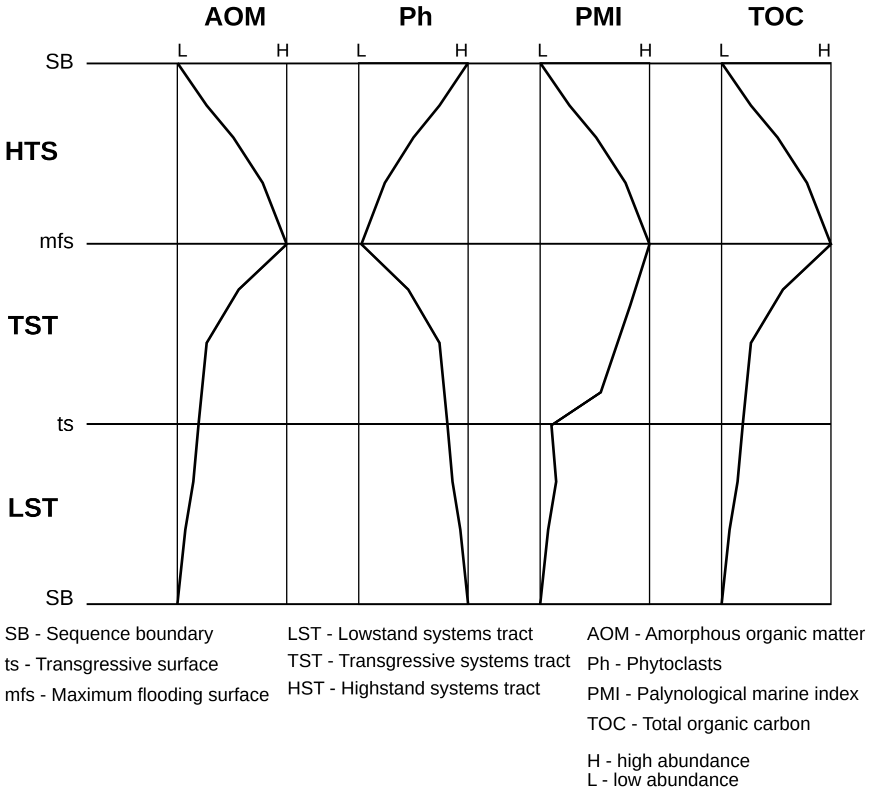
AOM
Ph
PMI
TOC
L
H
L
H
L
H
L
H
SB
HTS
mfs
TST
ts
LST
SB
SB - Sequence boundary
ts - Transgressive surface
mfs - Maximum flooding surface
LST - Lowstand systems tract
TST - Transgressive systems tract
HST - Highstand systems tract
AOM - Amorphous organic matter
Ph - Phytoclasts
PMI - Palynological marine index
TOC - Total organic carbon
H - high abundance
L - low abundance

Figure 10.2. Schematic relationship between organic matter abundance throughout a stratigraphic sequence (modified from Tyson, 1995).

Highstand Systems Tract (HST)

The HTS is the upper systems tract distinguished by one or more aggradational parasequence sets followed by progradational parasequence sets (Van Wagoner *et al.,* 1988). This tract is related to a decreasing rate of sea-level rise and initial sea-level fall (Tyson, 1995). According to Steffen & Gorin (1993b) it is characterized by inverted trends with respect to the LST, in which the major difference is that the shelf is not exposed. This was based on the observation that the terrigenous fragments (phytoclasts) were not degraded. The HST can be subdivided into two parts: early and late. The early HST still shows almost the same characteristics as the TST. The abundance of marine palynomorphs and the geochemical parameters TOC and HI are still high; however, the abundance curve decreases progressively upwards (late HST) (Figure 10.2), whereas the amount of phytoclasts increases.

10.2 Results

10.2.1 Sequence stratigraphic subdivision based on palynofacies

The sequence stratigraphic interpretation is based on the integrated framework shown in Figure 10.1. The KM1 sequence (Hamsi Junior *et al.*, 1999) is here subdivided in three sequences on basis of palynofacies associations: am1, am2 and am3 (Angico Member) for GTP-17-SE, and tm1, tm2, tm3 (Taquari Member) for GTP-24-SE.

K50 Sequence

According to Gilvan Hamsi Jr. (written comm., 2000) the K50 sequence is difficult to interpret because the upper part of the Muribeca Formation was deposited on a break-up unconformity, which is interpreted as the transition from rift phase to drift phase (e.g., Maerten & Séranne, 1995). Thus, subdivision of the sequence based on palynofacies analysis is poorly defined. However, this sequence shows a slightly transgressive trend upwards.

Pereira (1994) interpreted the Ibura evaporites and part of the Oiteirinhos Member as a HTS. This is confirmed here through the marked increase in phytoclast particles towards the top of the sequence (Figures 10.3-10.4). However, in the lower part of the sequence relatively high amounts of AOM and phytoplankton are recorded, which decrease upwards. In some intervals in the two wells no phytoplankton was recorded. The sequence boundaries of K50 are marked by a major peak in abundance of phytoplankton, which is observed in both wells. At the boundaries a peak in AOM and in the gamma-ray profile are also observed.

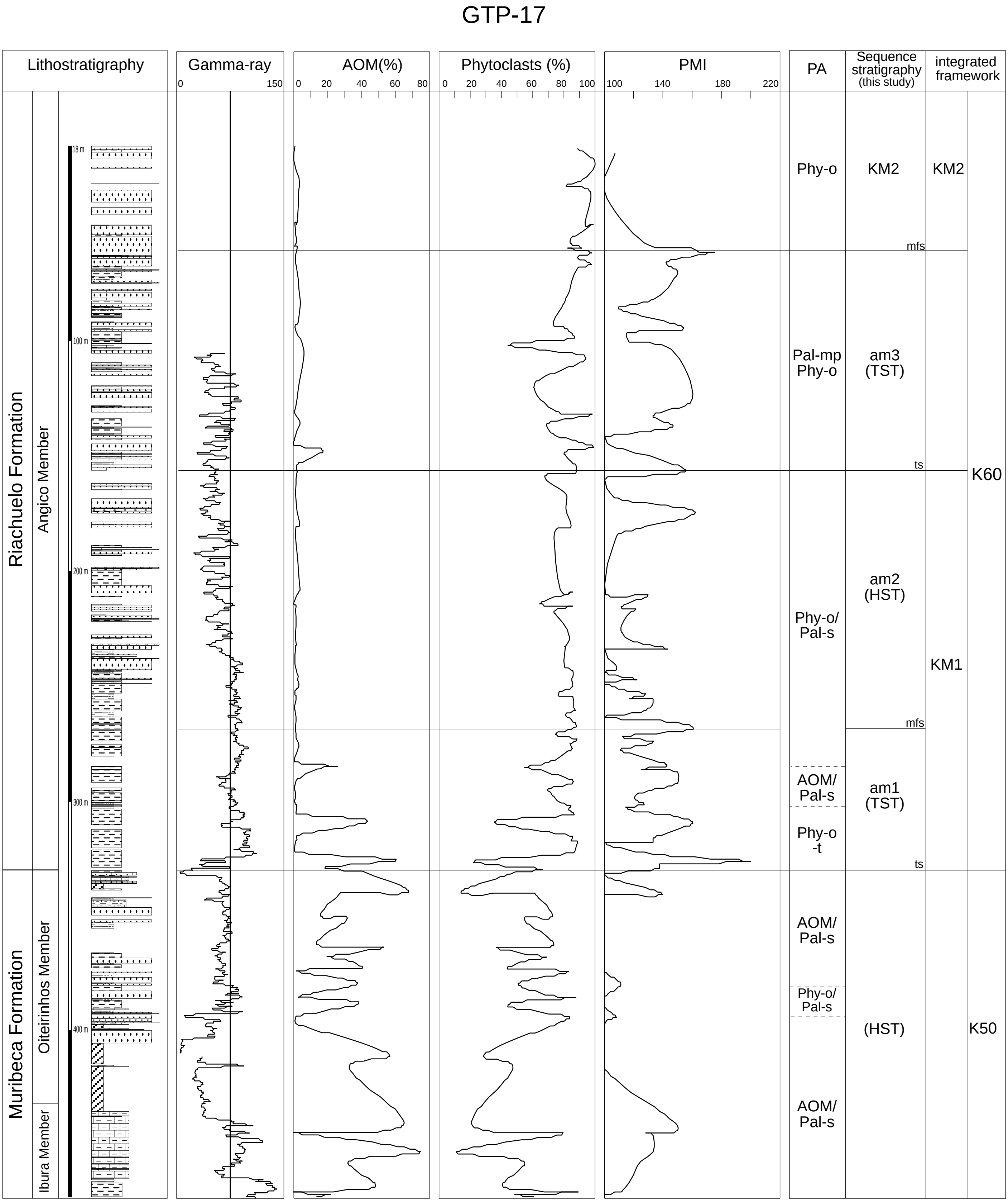

Figure 10.3. Stratigraphic distribution of gamma-ray and selected palynofacies data correlated with the sequence straigraphic interpretation for well GTP-17-SE. PA= palynofacies associations.

GTP-24

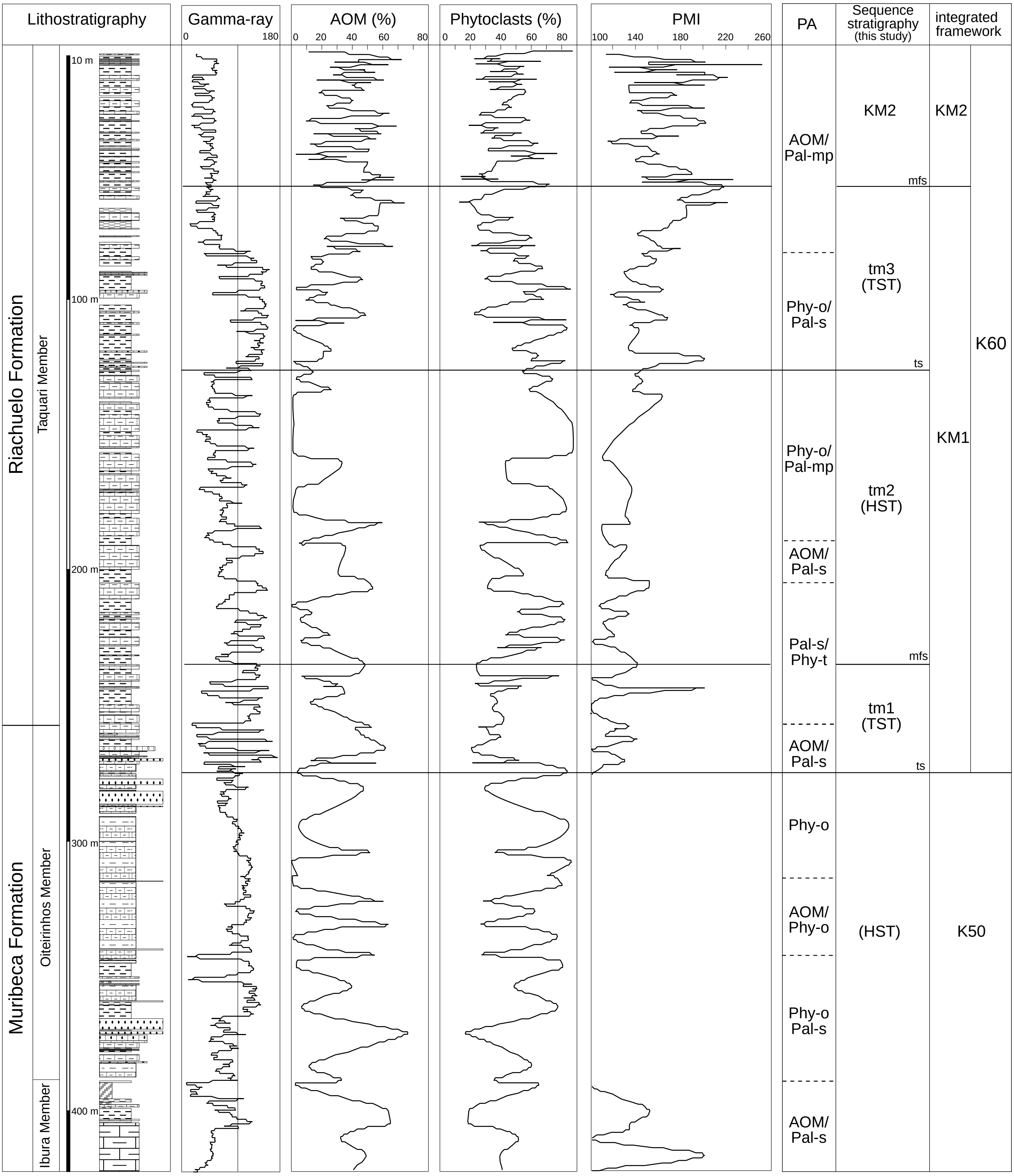

Figure 10.4. Stratigraphic distribution of gamma-ray and selected palynofacies data correlated with the sequence straigraphic interpretation for well GTP-24-SE. PA= palynofacies associations.

K60 Sequence

The Sequence K60 was subdivided by Hamsi Jr. *et al.* (1999) in two sequences: KM1 and KM2. The KM1 is here further subdivided into three parasequences (Figure 10.5); KM2 is maintained according to the definition of Hamsi Jr. *et al.* (1999).

The KM1 sequence was previously interpreted as a transgressive sequence. However, in spite of the transgressive trend upwards, which observed more clearly in well GTP-24-SE, especially based on the PMI, one interval (tm2 and am2) shows features of an HST. The KM1 starts below of the boundary between Muribeca and Riachuelo formations. This led to interpret that the systems tracts and palynofacies data are more related with the depositional sequence independent of the lithologies.

The interpretation that **tm1** and **am1** are a TST is supported by a marked increase in the PMI and AOM values. The phytoclast particles show a progressive decrease (Figure 10.3-10.4). The upper boundaries are marked by a maximum flooding surface (mfs) characterized by high abundances of dinoflagellates, particularly of the genus *Spiniferites*. The boundaries are also marked by an abrupt decrease of phytoclasts, which is best observed in well GTP-24-SE

The **tm2** and **am2** parasequences are characterized by an increase in abundance of phytoclast particles and a clear decrease in AOM and are interpreted as HTS. In well GTP-17-SE (**am2 parasequence**) the phytoclast particles show very low values. The PMI is characterized by moderate values that tend to increase upwards. The upper boundary of these sequences is marked by a peak of dinoflagellates indicating the transgressive surface. In well GTP-24-SE the boundary is placed at the base of an abrupt lithological change, from calcilutites to dark shales

Sequence		GTP-17-SE	GTP-24-SE
K60	KM2		
	KM1	am3	tm3
		am2	tm2
		am1	tm1

Figure 10.5. Sequence stratigraphic subdivision proposed for the K60 sequence.

The **tm3** and **am3** parasequences are interpreted as TST based on the marked increase in PMI and AOM, together with the clear decrease in phytoclast particles (Figure 10.3-10.4). These are observed clearly in well GTP-24-SE, especially the decrease of phytoclasts. The top of these parasequences is distinguished on the basis of the peaks of PMI indicating the mfs. At the mfs of well GTP-24-SE the lowest abundances of the phytoclast group are recorded.

KM2 sequence

This sequence is identified in both wells. It was interpreted by Hamsi Jr. *et al.* (1999) as a HTS, which is confirmed herein, on the basis of palynofacies.

From the base of the sequence, which was marked by the mfs, a clear decrease in dinoflagellate abundance is observed. However, the highest peak in abundance of dinoflagellates is observed in this sequence (Figures 10.3-10.4). Tyson (1995) mentioned that the highest peak of phytoplankton diversity occurs in the TST as well as in the early HST. The abundance curve of phytoclasts shows a slight increase upwards indicating the HST. In well GTP-24-SE the AOM group is abundant.

CHAPTER 11

PALEOENVIRONMENTAL INTERPRETATION

The paleoenvironmental reconstruction is based on an integration of ecophases and the palynofacies units with the lithological, sequence stratigraphic and biostratigraphic data. The Aptian-Albian of the Sergipe Basin is characterized by a transgressional trend related to the African-South American separation. The transition from a brackish lagoon to an open marine environment is recognizable in the ecophases and palynofacies data, and form the basis for the subdivision of the succession into these major paleoenvironments. These two paleoenvironments are subdivided into six events (depositional environments 1-6) that were mainly controlled by sea-level changes. The boundary between the two major paleoenvironments is marked by the first major transgression in the area. The paleoenvironmental interpretations were supported using ternary diagrams (cf. Tyson, 1993, 1995) (Figure 11.1).

Palynofacies fields distinguished on ternary diagrams and the inferred environment		Comments
I	Highly proximal shelf or basin	High phytoclast supply dilutes all other components.
II	Marginal dysoxic-anoxic basin	AOM diluted by high phytoclast input, but AOM preservation moderated to good. Amount of marine TOC depending on basin redox state.
III	Heterolithic oxic shelf ("proximal shelf")	Generally low AOM preservation rate; absolute phytoclast abundance dependent on actual proximity to fluvial-deltaic source. Oxidation and reworking common.
IV	Shelf to basin transition	Transition from shelf to basin in time (e.g., increased subsidence/water depth) or space (e.g., basin slope). Absolute phytoclast abundance depends on proximity to source and degree of deposition. Amount of marine TOC depends on basin redox state. IVa dysoxic, IVb suboxic-anoxic.
V	Mud- dominated oxic shelf ("distal shelf")	Low to moderate AOM (usually degradated). Palynomorphs abundant. Light coloured bioturbated calcareous mudstones are typical.
VI	Proximal suboxic-anoxic shelf	Good AOM preservation rate due to reducing basin conditions. Absolute phytoclast content may be moderate to high due to turbiditic input and/or general proximity to source.
VII	Distal dysoxic-anoxic "shelf"	Moderate to good AOM preservation, low to moderate abundance of palynomorphs. Dark-coloured slightly bioturbated mudstones are typical.
VIII	Distal dysoxic-oxic shelf	AOM-dominated assemblages, excellent AOM preservation. Low to moderate palynomorphs (partly due to masking). Typical of organic-rich shales deposited under stratified shelf sea conditions.
IX	Proximal suboxic-anoxic basin	AOM-dominated assemblages. Low abundance of palynomorphs partly due to masking. Frenquently alginite-rich. Deep basin or stratified shelf sea deposits, especially sediment-starved basins.

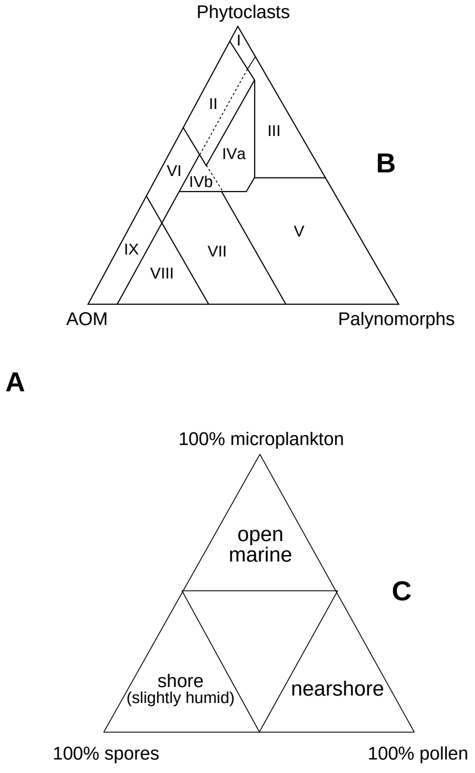

Figure 11.1. Schematic illustration of palynofacies and palynomorph groups used for paleoenvironmental interpretations. A- Key to marine palynofacies fields defined using a ternary diagram (B). C- Ternary diagram for total palynomorphs groups (modified from Tyson, 1993).

11.1 Interpretation of the depositional history

The lowest part of the sedimentary succession is interpreted as a brackish lagoonal to shallow-marine environment with a semi-arid to arid hinterland. During a relative highstand the lagoon was influenced by shallow-marine waters, which is confirmed by the presence of marine palynomorphs (PA1) (Figures 101 and 10.2). In the upper part of these beds, the marine connection seems to have been closed as a result of a relative sea-level fall. This regressive trend is mainly indicated by a maximum abundance of tetrads and high abundances of phytoclast particles deposited, together with an abrupt disappearance of marine palynomorphs. The sea-level fall is also indicated by the presence of anhydrite at the top of the sequence. According to Koutsoukos (1991) the presence of anhydrite suggest subaerial (sabkha) settings and marginal subaqueous (saline) environments along tidal-type feeding channels, marginal lagoons and interlagoonal salt flats. The ternary diagrams in Figure 11.2 show that the environment was relatively suboxic-anoxic (IVb), reflecting a restricted lagoon with normal salinity indicated by a dominance of gonyaulacoid over peridinoids. This restriction is probably reflected in the increase in AOM abundance.

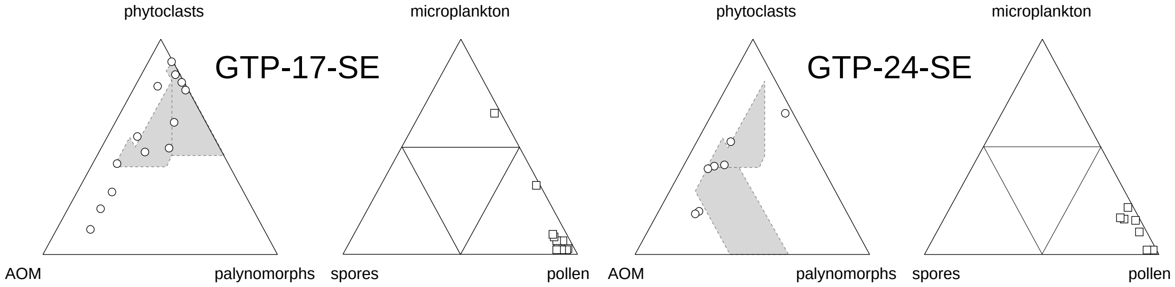

Figure 11.2. Ternary diagrams of palynofacies and palynomorph groups (see also Figure 11.1).

Evidence of subaerial exposure or, at least, extremely shallow conditions with rare marine palynomorphs (foraminifera and *Subtilisphaera*) and conspicuous high abundances of phytoclast particles represented by palynofacies units B-17, C-17 and C-24 is observed in this sequence. This suggests a nonmarine/lagoonal coastal plain with an arid hinterland environment. Terrestrial palynomorphs reach nearly 100.0% of the total palynomorphs. During a relative lowstands and drier conditions (Ecophase 2) it is possible that a restriction of the lagoon occurred. This led to water evaporation reflected in an increase of AOM and TOC values and intense growth of anhydrite (lithofacies association 2). However, the climate changed slightly from arid (PA3 dominance) to semi-arid. This change is indicated by the increase of PA4 elements, in particular by *Araucariacites*, which probably inhabited areas more inland. The moderate abundance of AOM seems to be related to the anhydrite deposition (see Figures 80-81). However, a high input of phytoclast continued. This is shown in the ternary diagrams of the palynofacies, which reflect the transition from an environment where AOM was preserved to one with a strong phytoclast input. The palynomorph ternary diagrams clearly show the strong dominance of terrestrial palynomorphs (Figure 11.3).

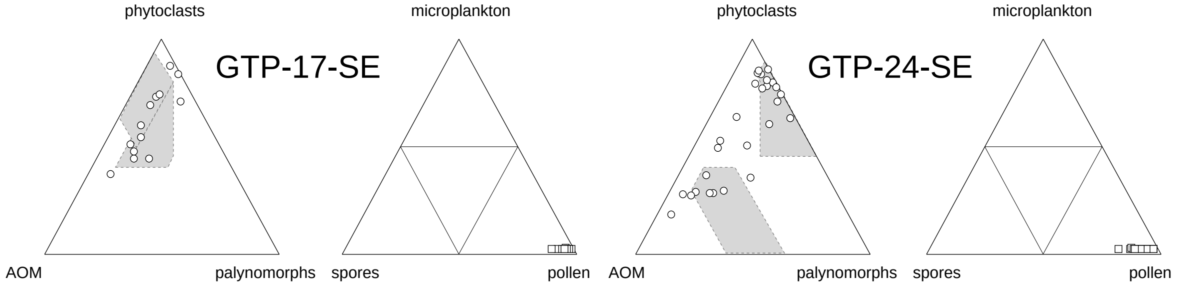

Figure 11.3. Ternary diagrams of palynofacies and palynomorphs groups for depositional environment 2 (see also Figure 11.1).

After the first major transgression, fully marine conditions were established in the area. This transgression is placed at the base of sequences am1 (GTP-17-SE) and tm1 (GTP-24-SE). The depositional environment of this sequence coincides with that suggested by Koutsoukos (1989), i.e., extensive tidal flats in an intertidal to shallow, subaqueous, hypersaline marginal sea with influence by nearby open-marine conditions. Until then the depositional history corresponding to the Muribeca Formation seems to have been the same for GTP-17-SE as GTP-24-SE. However, in comparison with the area of GTP-17-SE, there is evidence that the area of GTP-24-SE became slightly deeper. This event may be attributed to the last tectonic pulse that affected the basement (Hamsi Junior, written comm., 2000) and led to the recognition of a more proximal (facies) depositional environments in the area of well GTP-17-SE, and a more distal one in the area of GTP-24-SE.

The open-marine succession starts with a terrigenous interval with high abundances of terrestrial palynomorphs of PA3, in particular *Classopollis*, and phytoclasts. This interval is recognizable in both areas. The high abundances of *Classopollis* indicate an arid climate. The proximal facies (GTP-17-SE) is characterized by siliciclastic deposition in an intertidal to nearshore environment of LA3, and consequently, large amounts of phytoclast particles were deposited (see Figure 8.45). Moreover, this strong influx reduced the salinity causing an increase in abundance of *Subtilisphaera*. The ternary diagrams (Figure 11.4) show that, despite the high terrestrial influx, the transgression also affected the palynofacies and the palynomorph distribution.

This first major transgression is more clearly manifested in the GTP-24-SE area. The relatively high PMI values, TOC and AOM (units E-24 and G-24) are the main indicators of this transgression. This is also recognizable in the palynomorph ternary diagram (Figure 11.4), where the three points near the microplankton apex indicate the first transgression. A sea-level rise is also suggested by the dominance of gonyaulacoids over peridinoids, which indicates normal salinity. The highest abundance of palynomorphs in the succession is related to the fine lithology of Lithofacies 4a, which is typical of deposition in a more distal environment. From this point in time a more extensive carbonate deposition began as the coarse siliciclastic sediments no longer reached this area. This leads to an interpretation of this paleoenvironment as shallow-marine. This environment is also reflected in the ternary diagram of the palynomorphs, where some points are plotted in palynofacies field V, in which according to Tyson (1993) (Figure 11.1) palynomorphs are abundant and calcareous mudstones are typical.

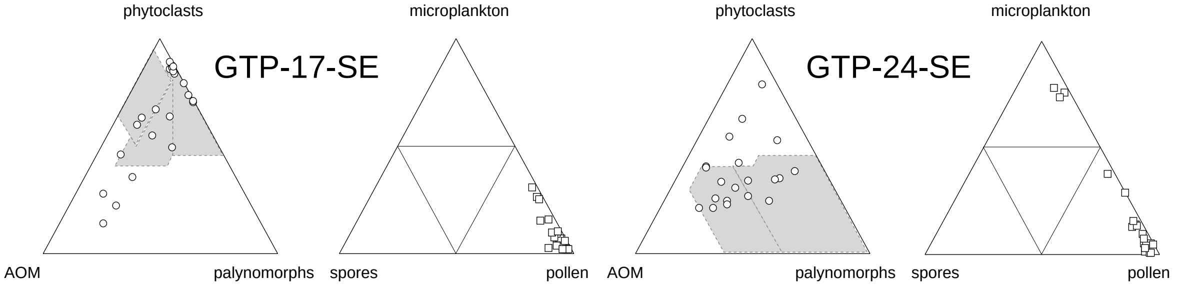

Figure 11.4. Ternary diagrams of palynofacies and palynomorph groups for depositional environment 3 (see also Figure 11.1).

Despite of the first major is transgression recorded in the lower part of the sequence, there is a slightly regressive general trend. This minor regression is suggested by the slight decrease of PMI values (both wells) and the increase of phytoclast deposition (unit E-17 and unit H-24) in the upper part of the sequence.

After the minor regression recognized in both wells, the PMI (only in GTP-24-SE) shows a clear increase upwards. However, the depositional environment is also characterized as intertidal to shallow subaqueous (GTP-17-SE) and shallow neritic (GTP-24-SE), although the increase of PMI values observed in the area of well GTP-24-SE indicates a more open-marine environment in comparison to the previous sequence. According to Koutsoukos *et al.* (1991) the local sea-level changes demonstrate the clear cyclic nature of this early open-marine episode.

The sequence is also characterized by signs of increasing humidity (Ecophase 5). Carbonate productivity was moderate as indicated by the deposition of rhythmic shales and calcilutite in GTP-24-SE. This may be directly related to the development of patch reefs, as mentioned by Koutsoukos *et al.* (1991). In nearshore environment (GTP-17-SE) a extensive siliciclastic deposition is indicated by lithofacies 3a and 3b and high abundance of phytoclasts and spores (Figure 11.5). The P/G ratio also suggests low salinity (high abundance of peridinoids) which is typical of nearshore environments with strong terrestrial input. On the other hand, the P/G ratio of well GTP-24-SE demonstrates an increase in dinoflagellates of the gonyaulacoid group indicating normal salinity.

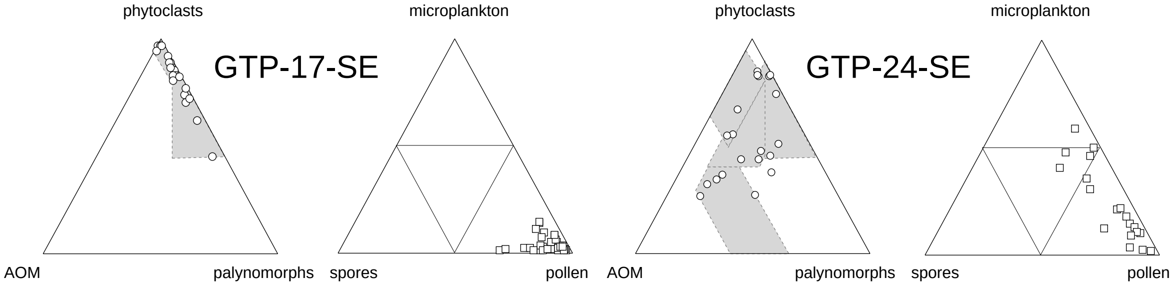

Figure 11.5. Ternary diagrams of palynofacies and palynomorph assemblages for depositional environment 4 (see also Figure 11.1).

In the entire area the sequence starts with fine siliciclastic sediments dominated by relatively dark shales (lithofacies 3c and 4c). The siliciclastic influx also brought a high concentration of phytoclasts; however this is manifested by small particles deposited mainly in the area of well GTP-24-SE. A strong increase in PMI values reflects the occurrence of the deepest marine environment in the studied succession. Therefore, the sequence is interpreted representing as shallow-neritic (GTP-17-SE) and middle-neritic environments (GTP-24-SE). This interpretation is also supported by the palynomorph ternary diagrams (Figure 11.6), in which (at least of GTP-24-SE) the points are not concentrated to the pollen apices as in the other diagrams.

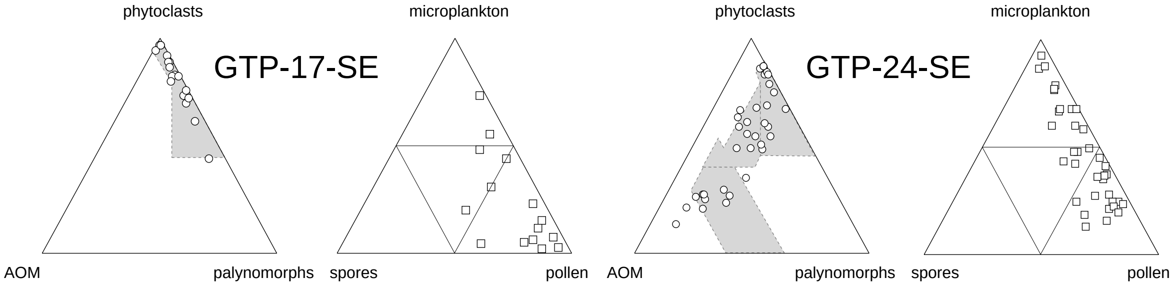

Figure 11.6. Ternary diagrams of palynofacies and palynomorph groups for depositional environment 5 (see also Figure 11.1).

The slight decrease in PMI and the increase of phytoclast input and terrestrial palynomorphs reflect a change to shallow-neritic to intertidal in GTP-17-SE and middle-neritic to shallow-neritic environments in GTP-24-SE. The Palynomorph assemblage 1 is still very abundant, although a bloom of *Subtilisphaera* is recorded, suggesting that the increase in terrestrial input affected the distribution of palynomorphs. The increase in TOC, AOM and the high abundance of *Cyclonephelium* suggest that the environment was dysoxic-anoxic. The palynofacies ternary diagrams of the GTP-24-SE also reflect this tendency. The majority of the points concentrate in palynofacies fields VII, VI and IV. In nearshore settings the situation is different, because in this area a strong influx of siliciclastic sediments possibly related to proximal turbidites is recognizable. The climate was subtropical to warm tropical as indicated by the strong increase in spores and decrease of *Classopollis* abundance.

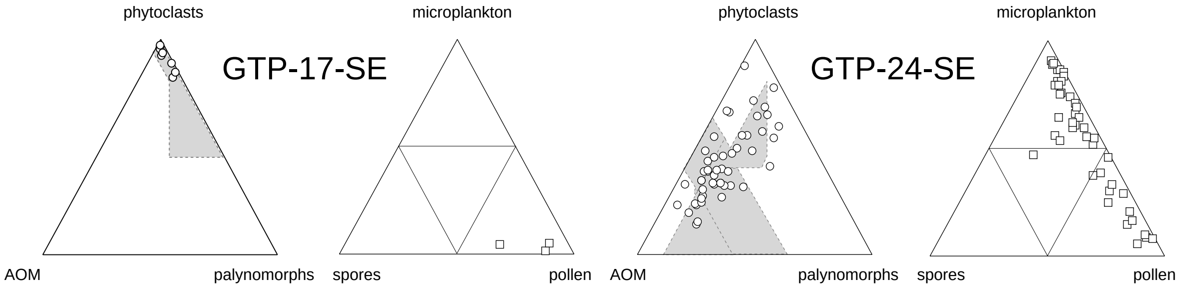

Figure 11.7. Ternary diagrams of palynofacies and palynomorph groups for depositional environment 6 (see Figure 11.1).

The integration of the results for the two wells studied is summarized in Figures 11.8 and 11.9, and the distribution of the depositional environments are shown in Figure 11.10.

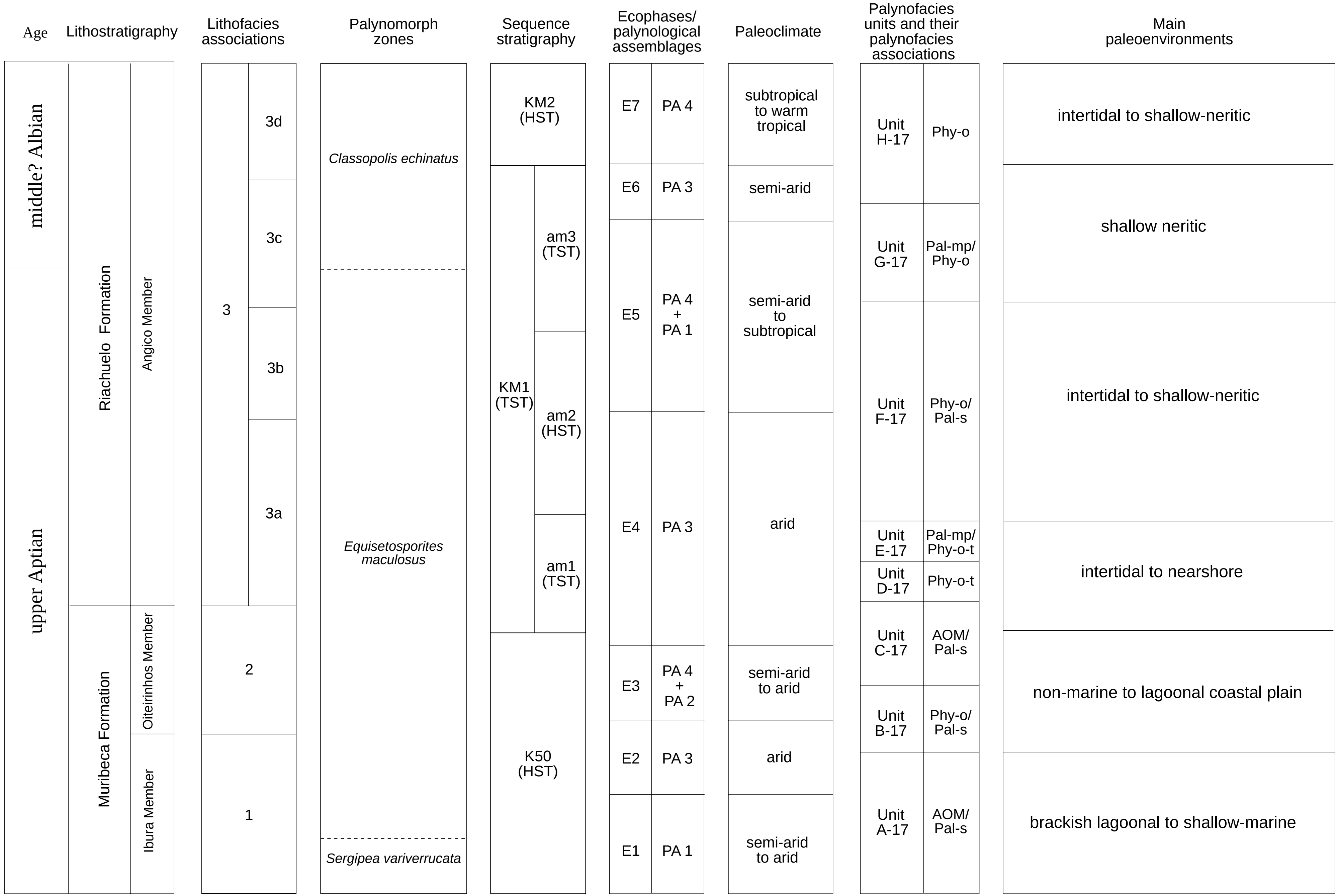
Age
Lithostratigraphy
Lithofacies associations
Palynomorph zones
Sequence stratigraphy
Ecophases/ palynological assemblages
Paleoclimate
Palynofacies units and their palynofacies associations
Main paleoenvironments
middle? Albian
upper Aptian
Riachuelo Formation
Angico Member
Muribeca Formation
Oiteirinhos Member
Ibura Member
3
3d
3c
3b
3a
2
1
Classopolis echinatus
Equisetosporites maculosus
Sergipea variverrucata
KM2 (HST)
KM1 (TST)
am3 (TST)
am2 (HST)
am1 (TST)
K50 (HST)
E7
PA 4
E6
PA 3
E5
PA 4 + PA 1
E4
PA 3
E3
PA 4 + PA 2
E2
PA 3
E1
PA 1
subtropical to warm tropical
semi-arid
semi-arid to subtropical
arid
semi-arid to arid
arid
semi-arid to arid
Unit H-17
Phy-o
Unit G-17
Pal-mp/ Phy-o
Unit F-17
Phy-o/ Pal-s
Unit E-17
Pal-mp/ Phy-o-t
Unit D-17
Phy-o-t
Unit C-17
AOM/ Pal-s
Unit B-17
Phy-o/ Pal-s
Unit A-17
AOM/ Pal-s
intertidal to shallow-neritic
shallow neritic
intertidal to shallow-neritic
intertidal to nearshore
non-marine to lagoonal coastal plain
brackish lagoonal to shallow-marine

Figure 11.8. Paleoenvironmental interpretartion derived from correlation of the results of well GTP-17-SE.

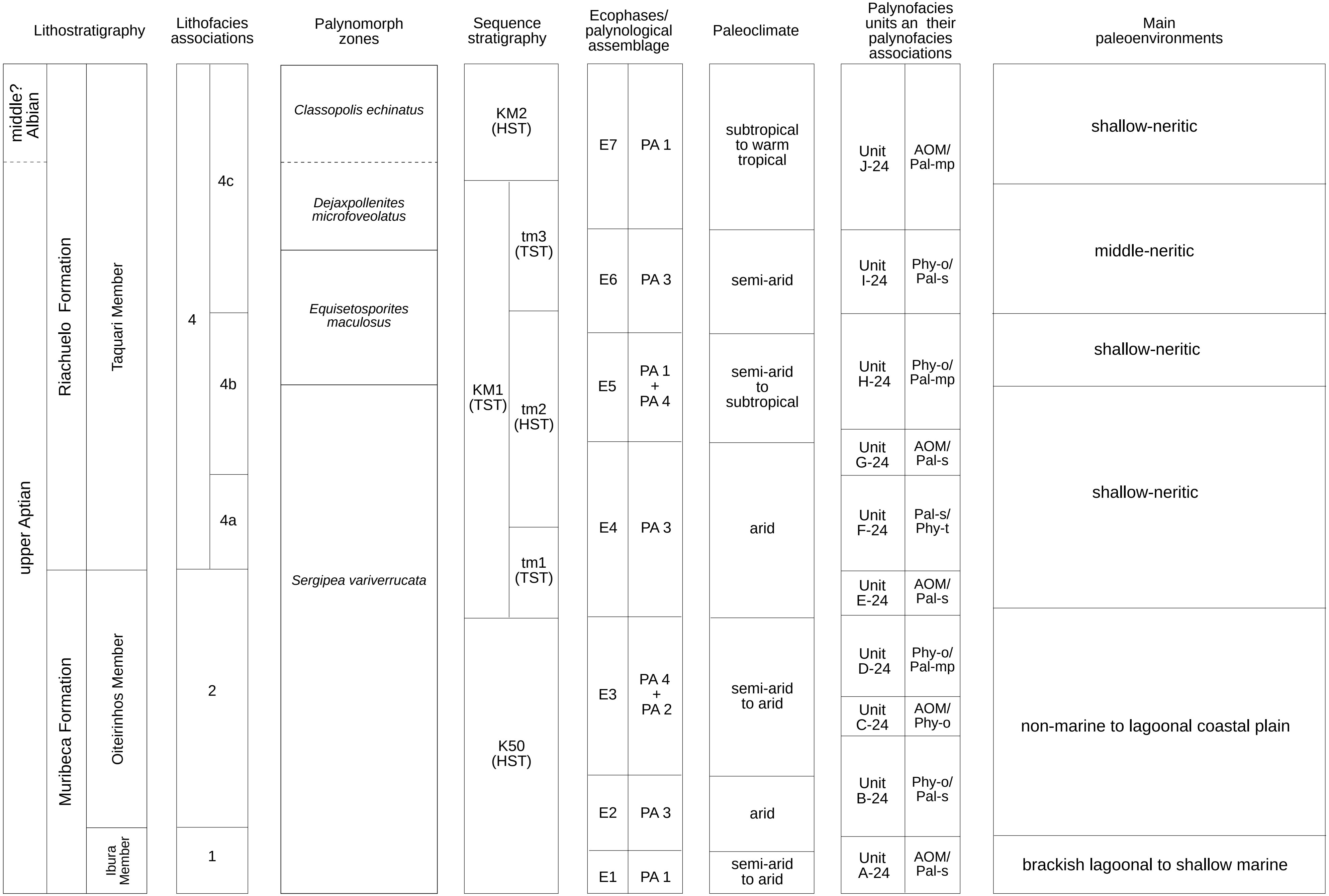
Lithostratigraphy
middle? Albian
upper Aptian
Riachuelo Formation
Muribeca Formation
Taquari Member
Oiteirinhos Member
Ibura Member
Lithofacies associations
4
4c
4b
4a
2
1
Palynomorph zones
Classopolis echinatus
Dejaxpollenites microfoveolatus
Equisetosporites maculosus
Sergipea variverrucata
Sequence stratigraphy
KM2 (HST)
KM1 (TST)
tm3 (TST)
tm2 (HST)
tm1 (TST)
K50 (HST)
Ecophases/ palynological assemblage
E7
PA 1
E6
PA 3
E5
PA 1 + PA 4
E4
PA 3
E3
PA 4 + PA 2
E2
PA 3
E1
PA 1
Paleoclimate
subtropical to warm tropical
semi-arid
semi-arid to subtropical
arid
semi-arid to arid
arid
semi-arid to arid
Palynofacies units an their palynofacies associations
Unit J-24
AOM/ Pal-mp
Unit I-24
Phy-o/ Pal-s
Unit H-24
Phy-o/ Pal-mp
Unit G-24
AOM/ Pal-s
Unit F-24
Pal-s/ Phy-t
Unit E-24
AOM/ Pal-s
Unit D-24
Phy-o/ Pal-mp
Unit C-24
AOM/ Phy-o
Unit B-24
Phy-o/ Pal-s
Unit A-24
AOM/ Pal-s
Main paleoenvironments
shallow-neritic
middle-neritic
shallow-neritic
shallow-neritic
non-marine to lagoonal coastal plain
brackish lagoonal to shallow marine

Figure 11.9. Paleoenvironmental interpretartion derived from correlation of the results of well GTP-24-SE.

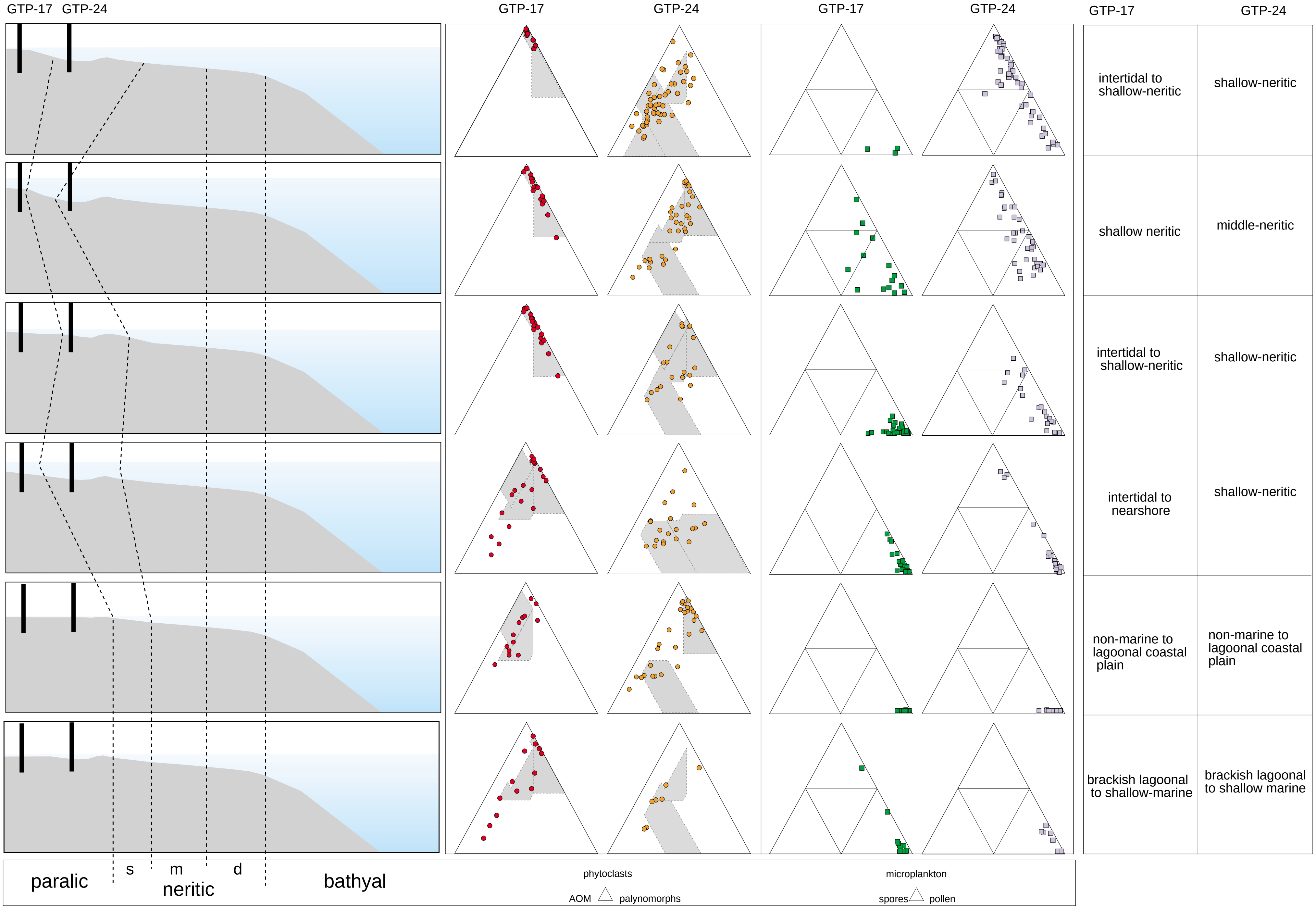
GTP-17
GTP-24
GTP-17
GTP-24
GTP-17
GTP-24
GTP-17
GTP-24
intertidal to shallow-neritic
shallow-neritic
shallow neritic
middle-neritic
intertidal to shallow-neritic
shallow-neritic
intertidal to nearshore
shallow-neritic
non-marine to lagoonal coastal plain
non-marine to lagoonal coastal plain
brackish lagoonal to shallow-marine
brackish lagoonal to shallow marine
paralic
s
m
d
neritic
bathyal
phytoclasts
AOM
palynomorphs
microplankton
spores
pollen

Figure 11.10. Schematic distribution of the paleoenvironments for the studied succession. S= shallow; m= middle; d= deep.

CHAPTER 12
CONCLUSIONS

- The succession studied in wells GTP-17-SE and GTP-24-SE yielded a rich palynomorph assemblage, mainly represented by terrestrial components. Altogether 17 genera and 19 species of spores, 24 genera and 31 species of pollen grains, and 17 genera and 20 species of dinocysts were identified. In addition, one genus of Acritarcha (*Leiosphaeridia*) and one genus of fresh-water algae (*Botryococcus*) were recorded. The marine palynomorphs show high abundances in the upper part of well GTP-24-SE. Preservation of the palynomorphs is variable, ranging from moderate to well-preserved for the miospores and from poorly to moderately well-preserved for the dinocysts.

- The gymnosperms are the most abundant group, as a consequence of the high abundances of the genus *Classopollis* in well GTP-17-SE. In well GTP-24-SE a relatively high abundance of marine palynomorphs is observed. Fresh-water palynomorphs are rare.

- The lithology influenced the occurrence and distribution of palynomorphs. The highest occurrence of terrestrial palynomorphs is recorded in siliciclastic rocks, whereas the marine groups occur mainly in carbonate deposits.

- The palynomorph zonation is based on the distribution of selected taxa, mainly from well GTP-24-SE. The establishment of a zonation for well GTP-17-SE is difficult due to the low diversity of palynomorphs and the proximal facies nature. The *Sergipea variverrucata* Zone and the *Equisetosporites maculosus* and *Dejaxpollenites microfoveolatus* sub-zones of the upper Aptian and the *Classopollis echinatus* Zone of the middle Albian (Regali & Santos, 1999) were identified the biostratigraphic framework introduced by. The absence of forms indicating the *Cardiongulina elongata*, *Brenneripollis reticulatus* and *Retiquadricolpites reticulatus* sub-zones and *Steevesipollenites alatiformis* Zone of the uppermost Aptian–lower middle Albian of the biostratigraphic framework of Regali & Santos (1999) indicates a possible hiatus comprising the stage boundary.

- The cluster analysis based on the abundance and composition of all 68 palynomorph genera revealed four superclusters, which represent different palynological assemblages

(PA). The stratigraphic distribution of these assemblages allowed the definition of seven ecophases.

- The relative abundance of spores and the genus *Classopollis* are evidence of a predominantly arid paleoclimate during the deposition of the succession. However, these conditions tend to change upwards to tropical and humid climates.

- The Palynological Marine Index (PMI) and peridinoid to gonyaulacoid ratio (P/G) curves confirm the progressively increasing marine influence in the region. However, the strong fluctuations of the curve reflect a continuous terrestrial influx to the area.

- Based on the distribution of palynofacies associations that define eight palynofacies units in well GTP-17-SE and ten in well GTP-24-SE, a continuous terrestrial influx is indicated throughout the succession by moderate to very high abundances of phytoclasts. The AOM and palynomorph groups, especially in well GTP-24-SE, show moderate to high abundances. The increase in abundance of these groups indicates a transgression or a decrease in terrestrial influx in the area.

- The lithology also influenced the distribution of palynofacies. The AOM group occurs mainly in carbonate rocks such as calcilutites, but also shows moderate abundances in shales. The phytoclast group is conspicuously the most abundant in coarse siliciclastic lithologies, particularly in sandstones. The abundance differences of the palynomorph group among the lithologies are relatively small.

- The average of TOC shows that the succession has a moderate organic matter accumulation. The higher average TOC values show a direct correlation with the units characterized by high abundances of AOM

- The organic matter in well GTP-24-SE belongs predominantly to Kerogen type III. However, in samples where the AOM is dominant (AOM/Phy-o, AOM/Pal-mp) Kerogen type II is also recorded. This is confirmed by the fluorescence investigations.

- The sequence stratigraphic interpretation based on the palynofacies data enabled the recognition of system tracts and their boundaries within a pre-established framework

(Feijó, 1995; Hamsi Junior *et al*., 1999; Pereira, 1994) as well as the subdivision of the KM1 sequence (Hamsi Junior *et al*., 1999) in three parasequences: am1, am2 and am3 (Angico Member) for GTP-17-SE, and tm1, tm2, tm3 (Taquari Member) for GTP-24-SE.

- By using the PMI, based on the diversity of marine palynomorphs, it was possible to recognize the maximum flooding surfaces (mfs) in the successions.

- The palynological and palynofacies analyses allowed detailed environmental reconstruction of the successions studied. A long-term transgressive trend is recognizable in the ecophases and palynofacies units. The depositional environments changed from a brackish lagoonal/nonmarine-lagoonal coastal plain environment, intertidal-nearshore (GTP-17-SE) and shallow-neritic (GTP-24-SE), intertidal to shallow-marine (GTP-17-SE) and shallow-neritic (GTP-24-SE), shallow-marine (GTP-17-SE) and middle-neritic (GTP-24-SE), to intertidal to shallow-marine (GTP-17-SE) and shallow-neritic (GTP-24-SE).

- The paleoenvironmental history is strongly marked by the progressive late Aptian–middle Albian transgression into the area. The data confirm that the change from a brackish lagoon to open marine environment was controlled by sea-level during the deposition of the Muribeca Formation, and dominantly by a progressive sea-level rise during the beginning of the Riachuelo Formation deposition.

CHAPTER 13
REFERENCES

Alberti, G., 1959. Zur Kenntnis der Gattung Deflandrea Eisenack (Dinoflagellaten) in der Kreide und im Alttertiär Nord- und Mitteldeutschlands. *Mitteilungen des Geologischen Staatsinstitut Hamburg* **28**, 93-105, pls. 8-9.

Alpern, B., 1970. Classification petrographique des constituants organiques fossiles des roches sedimentaires. *Revue de l'Institut Français du Petrole* **25**, 1233-1267.

Arai, M., Lana, C. C. & Pedrão, E., 1994. Ecozona *Subtilisphaera*. Registro Eocretáceo de um importante episódio ecológico do Oceano Atlântico primitivo: *Acta Geologica Leopoldinensia* **17**, 521–538.

Arai, M., Botelho Neto, J., Lana, C. C. & Pedrão, E., 2000. Cretaceous dinoflagellate provincialism in Brazilian marginal basins. *Cretaceous Research* **21**, 351-366.

Arai, M. & Coelho, P. S. M. (*in press*). Aferição do valor paleoecológico dos palinomorfos fósseis por meio de análise estatística: exemplo a partir da microflórula Albo-Aptiana da Bacia do Araripe. *Boletim de Geociencias da PETROBRAS*, 36 pp.

Araujo, C. V., Condé, V. C., Botelho-Neto, J., Pedrão, E., Conceição, J. C. J., 1998. Palynofacies in a sequence stratigraphy context, an example of an upper Aptian section from Almada Basin, Brazil. *The American Association of Petroleum Geologists, International Conference and Exhibition, abstracts* **82**, 1886-1887.

Archangelsky, S. & Gamerro, J. C., 1966. Estudio Palinológico de la Formación Baqueró (Cretácico), Provincia de Santa Cruz II. *Ameghiniana* **4**, 201-209.

Balme, B. E., 1957. Spores and pollen grains from the Mesozoic of Western Australia. *Commonwealth Scientific and Industrial Research Organization Minerals Research Laboratories, Coal Research Sector* **25**, 1-58, pls.1-11.

Batten, D. J. & Lister, J. K., 1988. Evidence of freshwater dinoflagellates and other algae in the English Wealden (Early Cretaceous). *Cretaceous Research* **9**, 171-179.

Below, R., 1981. Dinoflagellaten-Zysten aus dem oberen Hauterive bis unteren Cenoman Süd-West-Marokkos. *Palaeontographica, Abteilung B* **176**, 1-145, pls. 1-15.

Below, R., 1982. Dinoflagellate cysts from Valanginian to Lower Hauterivian sections near Ait Hamouch, Morocco. *Revista Española de Micropaleontología* **14**, 23-52, Plate1-4.

Below, R., 1982. Scolochorate Zysten der Gonyaulacaceae (Dinophyceae) aus der Unterkreide Marokkos. *Palaeontographica, Abteilung B*, **182**, 1-51, Plate 1-9.

Below, R., 1984. Aptian to Cenomanian dinoflagellate cysts from the Mazagan Plateau, northwest Africa (Sites 545 and 547, Deep Sea Drilling Project Leg 79). *Initial Reports, Deep Sea Drilling Project* **79**, 621-649.

Bengtson, P., 1983. The Cenomanian-Coniacian of the Sergipe Basin, Brazil. *Fossils and Strata* **12**, 1-78, one fold-out map.

Bint, A.N., 1986. Fossil Ceratiaceae: a restudy and new taxa from the mid-Cretaceous of the Western Interior, U.S.A. *Palynology* **10**, 135-180, Plate1-9.

Blondel, T. J. A., Gorin, G. E. & Jan du Chene, R., 1993. Sequence stratigraphy in coastal environments: sedimentology and palynofacies of the Miocene in central Tunisia. *In*: Posamentier, H. W., Summerhayes, C. P., Haq, B. U. & Allen, G. P. (eds.): *Sequence stratigraphy and facies associations*. *Special Publication of the International Association of Sedimentologists* **18**, 161-179. Blackwell Oxford, International.

Bombardiere, L. & Gorin, G. E., 2000. Stratigraphical and lateral distribution of sedimentary organic matter in Upper Jurassic carbonates of SE France. *Sedimentary Geology* **132**, 177-203.

Borchert, H., 1977. On the formation of Lower Cretaceous potassium salts and tachhydrite in the Sergipe Basin (Brazil) with some remarks on similar occurrences in West Africa (Gabon, Angola etc.). *In:* Klemm, D. D. & Schneider, H. J. (eds.): *Time- and Strata-bound Ore Deposits,* 94-111. Springer-Verlag, Berlin.

Bordenave, M. L., 1993. The vitrinite reflectance as a geological interpretation tool. *In*: Bordenave, M. L. (ed.): *Applied Petroleum Geochemistry,* 290-314. Editions Technip, Paris.

Boulter, M. C. & Riddick, A., 1986. Classification and analysis of palynodebris from the Palaeocene sediments of the Forties Field. *Sedimentology* **33**, 871-886.

Boulter, M. C., 1994. An approach to a standard terminology for palynodebris. *In*: Traverse, A. (ed.): *Sedimentation of organic particles*, 199-216. Cambridge University Press.

Brenner, G. J., 1963. The spores and pollen of the Potomac Group of Maryland. *Bulletin of Mines and Water Resources, Maryland* **27**, 215 pp.

Brenner, G. J., 1968. Middle Cretaceous spores and pollen from northeastern Peru. *Pollen et Spores* **10**, 341-383, 10 pls. 1 table.

Brideaux, W. W., 1971. Palynology of the Lower Colorado Group, central Alberta, Canada. I. Introductory remarks. Geology and microplankton studies. P*alaeontographica, Abteilung B* **135**, 53-114, pls. 21-30.

Brinkhuis, H., 1994. Late Eocene to early Oligocene dinoflagellate cysts from the Priabonian type-area (Northeast Italy); biostratigraphy and paleoenvironmental interpretation. *Palaeogeography, Palaeoclimatology, Palaeoecology* **107**, 121-163.

Brugman, W. A., Van Bergen, P. F. & Kerp, J. H. F., 1994. A quantitative approach to Triassic palynology: the Lettenkeuper of the Germanic Basin as an example. *In*: Traverse, A. (ed.): *Sedimentation of organic particles*, 409-429. Cambridge University Press.

Bujak, J. P., 1984. Cenozoic dinoflagellate cysts and acritarchs from the Bering Sea and northern North Pacific, D.S.D.P. Leg 19. *Micropaleontology* **30**, 180-212.

Cainelli, C., Babinski, N. A., dos Santos, R. C. R. & Uesugui, N., 1987. Sedimentos Albo-Santonianos da Bacia de Sergipe-Alagoas: ambientes de sedimentação e perspectivas petrolíferas. *Revista Brasileira de Geociências* **17**, 135-138.

Carvalho, M. A., 1999. Preliminary results of palynofacies analysis of the upper Aptian succession of the Sergipe Basin, Brazil. *Boletim do 5º Simpósio sobre o Cretáceo do Brasil*, Serra Negra-SP, 545-549.

Chang, Y., 1967. Accuracy of fossil percentage estimation. *Journal of Paleontology* **41**, 500-502.

Chang, H. K., Kowsmann, R. O. & Figueiredo, A. M. F., 1988. New concepts on the development of the east Brazilian marginal basins. *Episodes* **11**, 194-202.

Clarke, R.F.A. and Verdier, J.-P., 1967. An investigation of microplankton assemblages from the Chalk of the Isle of Wight, England. *Verhandelingen der Koninklijke Nederlandse Akademie van Wetenschappen, Afdeeling Natuurkunde, Eerste Reeks* **24**, 1-96, pls.1-17.

Combaz, A., 1964. Les palynofacies. *Revue de Micropaléontologie* **7**, 205-218.

Cookson, I. C., 1947. Plant microfossils from the lignites of Kerguelen archipelago. *Proceedings of the Linnean Society of New South Wales* **72**, 127-142.

Cookson, I.C., & Eisenack, A., 1970. Cretaceous microplankton from the Eucla Basin, Western Australia. *Proceedings of the Royal Society of Victoria* **83**, 137-157, pls.10-14.

Cookson, I.C. & Eisenack, A., 1974. Mikroplankton aus australischen mesozoischen und tertiären Sedimenten. *Palaeontographica, Abteilung B* **148**, 44-93, Plate20-29.

Couper, R. A., 1958. British Mesozoic microspores and pollen grains; a systematic and stratigraphic study. *Palaeontographica, Abteilung B* **103**, 75-174.

Cross, A. T., Thompson, G. G. & Zaitzeff, J. B., 1966. Source and distribution of palynomorphs in bottom sediments, southern part of Gulf of California. *Marine Geology* **4**, 467-524.

Davey, R. J., 1969. Non-calcareous microplankton from the Cenomanian of England, northern France and North America, part I. *British Museum (Natural History) Geology Bulletin* **17**, 103-180, pls.1-11.

Davey, R. J., 1970. Non-calcareous microplankton from the Cenomanian of England, northern France and North America, part II. *British Museum (Natural History) Geology Bulletin* **18**, 333-397, pls.1-10.

Davey, R. J., 1978. Marine Cretaceous palynology of Site 361, DSDP Leg 40, off southwestern Africa. *Initial Reports of the Deep Sea Drilling Project* **40**, 883-913.

Davey, R. J., 1979. Marine Apto-Albian palynomorphs from Holes 400A and 402A, IPOD Leg 48, northern Bay of Biscay. *Initial Reports Deep Sea Drilling Project* **48**, 547-577.

Davey, R. J. & Williams, G. L., 1966. The genus *Hystrichosphaeridium* and its allies. In: Davey, R. J., Downie, C., Sarjeant, W. A. S. & Williams, G. L., Studies on Mesozoic and Cenozoic dinoflagellate cysts; *British Museum (Natural History) Geology, Bulletin,* **Supplement 3**, p.53-106.

Davey, R. J. & Williams, G. L., 1969. Generic reallocations. In: Davey, R.J., Downie, C., Sarjeant, W.A.S. & Williams, G. L., Appendix to "Studies on Mesozoic and Cenozoic dinoflagellate cysts"; *British Museum (Natural History) Geology, Bulletin,* **Appendix to Supplement 3**, p.4-7.

Davey, R. J., Downie, C., Sarjeant, W. A. S. & Williams, G. L., 1969. Generic reallocations. In: Davey, R. J., Downie, C., Sarjeant, W.A.S. & Williams, G. L., Appendix to "Studies on Mesozoic and Cenozoic dinoflagellate cysts"; *Bulletin of the British Museum (Natural History), Geology,* **Supplement 3**, 15-17.

Davey, R.J. & Verdier, J. -P., 1971. An investigation of microplankton assemblages from the Albian of the Paris Basin. *Verhandelingen der Koninklijke Nederlandse Akademie van Wetenschappen, Afdeeling Natuurkunde, Eerste Reeks* **26**, 1-58, pls.1-7.

Davey, R.J. & Verdier, J. -P., 1973. An investigation of microplankton assemblages from latest Albian (Vraconian) sediments. *Revista Española de Micropaleontologia* **5**, 173-212, pls.1-5.

Davey, R.J. & Verdier, J. -P., 1974. Dinoflagellate cysts from the Aptian type sections at Gargas and La Bédoule, France. *Palaeontology* **17**, 623-653, pls.91-93.

De Jersey, N. J., 1963. Jurassic spores and pollen grains from the Margburg Sandstone. *Geological Survey of Queensland* **313**, 1-15, pls. 1-3.

Deák, M. H., 1964. Contribution l'etude palynologique de Groupe d'argiles Munieria de l'etage Aptien. *Acta Botanicae Acad.Sci.Hungar* **10**, 95-126.

Deflandre, G. & Cookson, I.C., 1955. Fossil microplankton from Australian Late Mesozoic and Tertiary sediments. *Australian Journal of Marine and Freshwater Research* **6**, 242-313, pls. 1-9.

Deflandre, G., 1935. Considérations biologiques sur les microorganisms d'origine planctonique conservés dans les silex de la craie. *Bulletin biologique de la France et de la Belgique*, **69**, 213-244, pls.5-9.

Deflandre, G., 1937. Microfossiles des silex crétacés. Deuxième partie. Flagellés incertae sedis. Hystrichosphaeridés. Sarcodinés. Organismes divers. *Annales de paléontologie* **26**, 51-103, pls.11-18 (al. pls.8-15).

Deflandre, G., 1946. Fichier micropaléontologique - série 6. Hystrichosphaeridés II. Espèces du Secondaire et du Tertiaire. Archives originales, Centre de documentation; *Centre national de la recherche scientifique, France* **235**, 1-4, fiches 860-1019.

Delcourt, A. & Sprumont, G., 1955. *Les spores et grains de pollen du wealdien du Hainaut. A systematic study of spores and pollen (including new genera and species) from Wealden (Cretaceous) localities of Hainaut, Belgium.* 73pp

Della Fávera, J. C., 1990. Simetria estratigráfico-faciológica das sequências eocretáceas e neopaleozóicas do Brasil. *Boletim do 1° Simpósio sobre as Bacias Cretácicas Brasileiras,* Rio Claro-SP, 15-16.

Dettmann, M., 1973. Angiospermous pollen from Albian to Turonian sediments of eastern Australia. *Geological Society of Australia, Special Publications* **4**, 34 pp.

Dev, S., 1961. The fossil flora of the Japalpur Series-3. Spores and pollen grains. *The Palaeobotanist* **8**, 43-56, pls. 1-8.

Dino, R., 1992. *Palinologia, bioestratigrafia e paleoecologia da Formação Alagamar, Cretáceo da Bacia Potiguar, nordeste do Brasil*. PhD Thesis, Universidade de São Paulo, 300 pp. [Unpublished].

Dino, R., 1996. Algumas espécies novas de grãos de pólen do Cretáceo Inferior do nordeste do Brasil *Boletim de Geociências da Petro*brás **8**, 257-273. [for 1994].

Downie, C., Hussain, M. A. & Williams, G. L., 1971. Dinoflagellate cysts and acritarch associations in the Paleogene of southeast England. *Geoscience and Man* **3**, 29-35.

Doyle, J. A., Biens, P., Doerenkamp, A. & Jardiné, S., 1977. Angiosperm pollen from the pre-Albian Lower Cretaceous of Equatorial Africa. *Bulletin des Centres de Recherches Exploration-Production Elf-Aquitaine* **1**, 451-473.

Doyle. J. A., Jardine, S. & Dorenkamp, A., 1982. *Afropollis*, a new genus of early angiosperm pollen, with notes on the Cretaceous palynostratigraphy and paleoenvironments of northern Gondwana. *Bulletin des Centres de Recherches Exploration-Production Elf-Aquitaine* **6**, 39-117.

Durand, B., Espitalie, J. & Oudin, J. L., 1970. Analyse géochemique de la matière organique extraite desroches sédimentaires: III. Accroissement de la rapidité du protocole opératoire par l´amelioration de l´appareillages. *Revue de l'Institut Français du Petrole* **25**, 1268-1279.

Eisenack, A., 1958. Mikroplankton aus dem norddeutschen Apt, nebst einigen Bemerkungen über fossile Dinoflagellaten. *Neues Jahrbuch für Geologie und Paläontologie, Abhandlungen* **106**, 383-422, Plate21-27.

Erdtman, G., 1969. *Handbook of palynology*. 486 pp. Copenhagen, Munksgaard (Scandinavian University Books).

Erdtman, G., 1943. *An introduction to pollen analysis*. 239 pp. New York, Ronald Press.

Eshet, Y., Moshkovitz, S., Habib, D., Benjamini, C. & Magaritz, M., 1992. Calcareous nannofossil and dinoflagellate stratigraphy across the Cretaceous–Tertiary boundary at Hor Harar, Israel. *Marine Geology* **18**, 199-228.

Faegri, K. & Iversen, J., 1966. *Textbook of pollen analysis*. 169 pp. Copenhagen, Munksgaard (Scandinavian university books).

Farr, K. M., 1989. Palynomorph and palynodebris distributions in modern British and Irish estuarine sediments. *In*: Batten, D. J. & Keen, M. C. (eds.): *Northwest European micropalaeontology and palynology. British Micropalaeontology Society Series,* 265-285. Chichester, Ellis Horwood.

Feijó, F. J., 1980. Estudo dos carbonatos Muribeca e Riachuelo no Alto de Aracaju-Bacia de Sergipe/Alagoas nordeste do Brasil. *Anais do XXXI Congresso Brasileiro de Geologia*, Camburiú-SC, 320-332.

Feijó, F. J., 1995. Bacias de Sergipe e Alagoas. *Boletim de Geociências da Petrobrás* **8**, 149-161. [for 1994].

Fensome, R. A., MacRae, R. A. & Williams, G. L., 1998. DINOFLAJ. Geological Survey of Canada Open File, no.3653.

García-Mondéjar, J. & Fernández-Mendiola, P. A., 1993. Sequence stratigraphy and system tracts of a mixed carbonate and siliciclastic platform-basin setting: the Albian of Lunada and Soba, northern Spain. *The American Association of Petroleum Geologists Bulletin* **77**, 245-275.

Gehmann Jr., H. M., 1962. Organic matter in limestones. *Geochimica et Cosmochimica Acta* **26,** 885-897.

Gocht, H., 1959. Mikroplankton aus dem nordwestdeutschen Neokom (Teil II). *Paläontologische Zeitschrift*, 50-89, Plate3-8.

Gorin, G. & Sttefen, D., 1991. Organic facies as a tool for recording eustatic variations in marine fine-grained carbonates–examples of the Berriasian stratotype at Berrias (Ardèche, SE France). *Palaeogeography, Palaeoclimatology, Palaeoecology* **85**, 303-320.

Groot, J. J. & Groot, C. R., 1966. Marine palynology: possibilities, limitations, problems. *Marine Geology* **4**, 387-395.

Habib, D. & Miller, J. A., 1989. Dinoflagellate species and organic facies evidence of marine transgression and regression in the Atlantic Coastal Plain. *Palaeogeography, Palaeoclimatology, Palaeoecology* **74**, 23-42.

Habib, D., 1975. Neocomian dinoflagellate zonation in the western North Atlantic. *Micropaleontology* **21**, 373-392.

Habib, D., 1977. Comparison of Lower and Middle Cretaceous palynostratigraphic zonations in the western North Atlantic. *In*: Swain, F.W. (ed.): *Stratigraphic Micropaleontology of Atlantic Basin and Borderlands*, 341-367. Elsevier Scientific Publishing Company, Amsterdam.

Habib, D., 1978. Palynostratigraphy of the Lower Cretaceous section at Deep Sea Drilling Project Site 391, Blake-Bahamas Basin, and its correlation in the North Atlantic. *Initial Reports of Deep Sea Drilling Project* **44**, 887-897.

Hamsi Junior, G. P., Campos Neto, O. P. de A., Araújo, C. V. & Frota, E. S. T., 1999. Intervalos potencialmente geradores das sequências mesocretaceas da Bacia Sergipe-Alagoas, NE Brasil. *Boletim do 5º Simpósio sobre o Cretáceo do Brasil*. Serra Negra-SP, 97-102.

Harding, I. C., 1990. *Palaeoperidinium cretaceum*: a brackish-water peridiniinean dinoflagellate from the Early Cretaceous. *Palaeontology* **33**, 35-48, pls.1-3.

Harland, R., 1973. Dinoflagellates cysts and acritarchs from the Bearpaw Formation (upper Campanian) of southern Alberta, Canada. *Palaeontology* **16**, 665-706.

Hart, G. F., Pasley, M. A. & Gregory, W. A., 1994. Particulate organic matter, maceral facies models, and applications to sequence stratigraphy. *In*: Traverse, A. (ed.): *Sedimentation of Organic Particles*, 337-390. Cambridge University Press.

Hart, M., 1996 (compiler). The Albian stage and substage boundaries. *Bulletin de l'Institut Royal des Sciences Naturelles de Belgique, Sciences de la Terre* **66, Supplement**, 45-56.

Hashimoto, A. T., 1995. *Contribuição ao estudo do relacionamento da palinologia e a estratigrafia de sequências. Análise da seção do Cretáceo Médio/Superior da Bacia de Santos*. MSc Thesis, Universidade Federal do Rio Grande do Sul, Porto Alegre, RS, Brazil, 130 pp., 12 Appendices [Unpublished].

Helenes, J., de-Guerra, C. & Vásquez, J., 1998. Palynology and chronostratigraphy of the Upper Cretaceous in the subsurface of the Barinas area, western Venezuela. *The American Association of Petroleum Geologists Bulletin* **82**, 1308-1328.

Herngreen, G. F. W., 1973. Palynology of Albian-Cenomanian strata of borehole 1-QS-1-MA, State of Maranhao, Brazil. *Pollen et Spores* **15**, 515-555.

Herngreen, G. F. W., Van Hoeken-Klinkenberg, P. M. J. & De Boer, K. F., 1980. Some remarks on selected palynomorphs near the Jurassic-Cretaceous boundary in the Netherlands. *Proceedings of the 4th International Conference*, Lucknow, 1976-1977, 357-367.

Herngreen; G. F. W. & Duenas-Jimenez, H., 1990. Dating of the Cretaceous Une Formation, Colombia and the relationship with the Albian-Cenomanian African-South American microfloral province. *Review of Palaeobotany and Palynology* **66**, 345-359.

Heusser, L. M. & Balsam, W. L., 1977. Pollen sedimentation in the northwest Atlantic: effects of the Western Boundary Undercurrent. *Marine Geology* **69**, 149-153.

Hochuli, P., 1981. North Gondwana floral elements in Lower to middle Cretaceous sediments of the southern Alps (souothern Switzerland, northern Italy). *Review of Palaeobotany and Palynology* **35**, 337-358.

Horowitz, A., 1970. Juraassic microflora from the northern Negev, Israel. *Israel Journal of Earth-Sciences* **19**, 153-185, 5 pls., 3 tabs.

Hughes, N. F. & Moody-Stuart, J. C., 1967. Palynological facies and correlation in the English Wealden. *Review of Palaeobotany and Palynology* **1**, 259-268.

Jain, K. P., 1977. Additional dinoflagellates and acritarchs from Grey Shale Member of Dalmiapuram Formation, south India. *The Palaeobotanist* **24**, 170-194, Plate1-6.

Jain, K. P. & Millepied, P., 1973. Cretaceous microplankton from Senegal Basin, NW Africa. 1. Some new genera, species and combinations of dinoflagellates. *The Palaeobotanist* **20**, 22-32, pls.1-3.

Jaminski, J., 1995. The mid-Cretaceous palaeoenvironmental conditions in the Polish Carpathians–a palynological approach. *Review of Palaeobotany and Palynology* **87**, 43-50.

Jardiné, S. & Magloire, L., 1965. Palynologie et stratigraphie du cretace des bassins du Senegal et de Cote d'Ivoire. *Bureau de Recherches Geologiques et Minieres* **32**; 187-245.

Juhász, M. & Góczán, F., 1985. Comparative study of Albian monosulcate angiosperm pollen grains. *Acta Biologica Szeged* **31**, 147-172.

Kar, R. K. & Singh R. S., 1986. Palynology of the Cretaceous sediments of Meghalaya, India. *Palaeontographica, Abteilung B* **202**, 83-153.

Kar, R. K. & Singh R. S., 1986. Palynology of the Cretaceous sediments of Meghalaya, India. *Palaeontographica, Abteilung A* **195**; 1-3, Pages 83-153.

Kennedy, W. J., Gale, A.S., Bown, P. R., Caron, M., Davey, R. J., Gröcke, D. & Wray, D. S., 2000. Integrated stratigraphy across the Aptian–Albian boundary in the Marnes Bleus, at the Col de Pré-Guittard, Arnayon (Drôme), and at Tartonne (Alpes-de-Haute-Provence), France: a candidate Global Boundary Stratotype Section and Boundary Point for the base of the Albian Stage. *Cretaceous Research* **21**, 591-720.

Koutsoukos, E. A. M., 1989. *Mid- to Late Cretaceous microbiostratigraphy, palaeo-ecology and palaeogeography of the Sergipe Basin, northeastern Brazil*. PhD Thesis, Council for National Academic Awards, Polytechnic South West, Plymouth, UK, 2 vols., 886 pp. [Unpublished].

Koutsoukos, E. A. M., Mello, M. R., Azambuja Filho, N. C., Hart, M. B. & Maxwell, J. R., 1991. The upper Aptian–Albian succession of the Sergipe Basin, Brazil- an integrated palaeoenvironmental assessment. *The American Association of Petroleum Geologists Bulletin* **75**, 479-498.

Koutsoukos, E. A. M. & Bengtson, P., 1993. Towards an integrated biostratigraphy of the upper Aptian-Maastrichtian of the Sergipe Basin, Brazil. *Documents des Laboratoires de Geologie de Lyon* **125**, 241-262.

Koutsoukos, E. A. M., Destro, N., Azambuja Filho, N. C. de & Spadini, A. R., 1993. Upper Aptian-lower Coniacian carbonate sequences in the Sergipe Basin, northeastern Brazil. *The American Association of Petroleum Geologists Memoir* **56**, 127-144.

Lana, C. C., 1997. *Palinologia e estratigrafia integrada da seção Cenomaniano médio-Turoniano inferior da porção centro-leste da Bacia Potiguar, NE do Brasil*. MSc Thesis, Universidade Federal do Rio Grande do Sul, Porto Alegre, RS, Brazil, 2 vols., 341pp. [Unpublished].

Lana, M. C., 1990. Bacia de Sergipe-Alagoas- uma hipótese de evolução tectono-sedimentar. *In*: Gabaglia, G.P.R. & Milani, E. J. (eds.): *Origen e Evolução de Bacias Sedimentares,* 311-332. Ed. Gávea, R. Redisch Prog. Visual Prod. Gráf. e Editoração, Petrobrás, Rio de Janeiro.

Lejeune-Carpentier, M., 1940. L'étude microscopique des silex. Systématique et morphologie des "tubifères". (Huitième note.). *Annales de la Société géologique de Belgique* **63**, B216-B236.

Lentin, J. K. and Williams, G. L., 1976. A monograph of fossil peridinioid dinoflagellate cysts. *Bedford Institute of Oceanography, Report Series* **BI-R-75-16**, 237 pp.

Lentin, J. K. & Williams, G. L., 1993. Fossil dinoflagellates: index to genera and species. *American Association of Stratigraphic Palynologists, Contributions Series* **28**, 856 pp.

Lewis, J., Dodge, J. D. & Powell, A. J., 1990. Quaternary dinoflagellate cysts from the upwelling system offshore Peru, hole 686B, ODP leg 112. *Proceedings of Ocean Drilling Project, Scientific Results* **112**, 323-327.

Lima, M. R., 1976. *Crotnonipollis,* a new pollen genus from Santana Formation, Cretaceous of Northeastern Brazil. *Boletim de la Association.Latinoamericana de Paleobotânica e Palinologia* **3**, 14-20.

Lima, M. R., 1978. *Palinologia da Formação Santana (Cretáceo do Nordeste do Brasil*). São Paulo. Universidade de São Paulo 1978. PhD Thesis, Universidade de São Paulo, 338 pp. [Unpublished].

Lima, M. R. 1980. Palinologia da Formacao Santana (Cretáceo do Nordeste do Brasil); III, Descrição sistemática dos polens da Turma Plicates (Subturma Costates) *Ameghiniana* **17**; 15-47.

Lima, M. R., 1983. Paleoclimatic reconstruction of the Brazilian Cretaceous based on palynological data. *Revista Brasileira de Geociências* **13**, 223-228.

Lorente, M. A. & Ran, E. T. H., 1991 (eds.). *Open workshop on Organic Matter Classification, Amsterdam,* 73 pp. Hugo de Vries-Laboratory.

Lorente, M. A., 1990. Textural characteristics of organic matter in several subenvironments of Orinoco Upper delta. *Geologie en Mijnbouw* **69**, 263-278.

Lucas-Clark, J., 1987. *Wigginsiella* n. gen., *Spongodinium*, and *Apteodinium* as members of the Aptiana-Ventriosum complex (fossil Dinophyceae). *Palynology* **11**, 155-184, pls.1-5.

Maerten, L. & Séranne, M., 1995. Extensional Tectonics of the Oligo-Miocene Hérault Basin (S. France), Gulf of Lion margin. *Bulletin de la Sociéte Geologique de France* **6**, 739-749.

Marshall, K. L. & Batten, D. J., 1988. Dinoflagellate cyst associations in Cenomanian-Turonian "black shale" sequences of northern Europe. *Review of Palaeobotany and Palynology* **54**, 85-103.

Masure, E., 1984. L'indice de diversite et les dominances des "communautes" de kystes de dinoflagelles; marqueurs bathymetriques; forage 398 D, croisiere 47 B. *Bulletin de la Societe Geologique de France* **26**, 93-111.

Masure; E. Rauscher, R., Dejax, J., Schuler, M. & Ferre, B., 1998. Cretaceous-Paleocene palynology from the Cote d'Ivoire-Ghana transform margin, sites 959, 960, 961, and 962. *Proceedings of the Ocean Drilling Program, Scientific Results* **159**, 253-276.

Melia, M. B., 1984. The distribution and relationship between palynomorphs in aerosols and deep-sea sediments off the coast of Northwest Africa. *Marine Geology* **58**, 345-371.

Mendes, J. M. C., 1994. *Análise estratigráfica da seção neo-Aptiana/Eocenomaniana (Fm. Riachuelo) na área do Alto de Aracaju e adjacências - Bacia de Sergipe/Alagoas*. MSc Thesis, Universidade Federal do Rio Grande do Sul, Porto Alegre, RS, Brazil, 166 pp. 7 Appendices. [Unpublished]

Mendonça Filho, J. G., 1999. *Aplicação de estudos de palinofácies e fácies orgânicas em rochas do Paleozóico Superior da Bacia do Paraná, sul do Brasil*. PhD Thesis, Universidade Federal do Rio Grande do Sul, Porto Alegre, RS, Brazil, 2 vols., 254 pp., 5 plates. [Unpublished].

Miles, J. A., 1989. *Illustrated glossary of petroleum geochemistry*. 137 pp. Clarendon Press, Oxford.

Mudie, P. J., 1982. Pollen distribution in recent marine sediments, eastern Canada. *Canadian Journal of Earth Sciences* **19**, 729-747.

Muller, J., 1959. Palynology of Recent Orinoco Delta and shelf sediments: reports of the Orinoco Shelf Expedition; volume 5. *Micropaleontology* **5**, 1-32.

Muller, J., 1968. Palynology of the Pedawann and Plateau sandstone formations (Cretaceous–Eocene) in Sarawak, Malasia. *Micropaleontology* **14**, 1-37.

Muller, J., di Giacomo, E. & van Erve, A., 1985. A palynological zonation for the Cretaceous, Tertiary and Quaternary of northern South America. *VI Congresso Geológico Venezolano*, Caracas, 1985, 1041-1079.

Norris, G., 1966. Miospores from the Purbeck beds and marine Upper Jurassic of southern England. *Palaeontology* **12**, 586.

Norris, G., 1967. Spores and pollen from the lower Colorado Group (Albian-?Cenomanian) of central Alberta. *Palaeontographica, Abteilung B* **120**, 72-115.

Ojeda, H. A. O., 1982. Structural framework, stratigraphy and evolution of Brazilian marginal basins. *The American Association of Petroleum Geologists Bulletin* **66**, 732-749.

Ojeda, H. A. O. & Fugita, A. M., 1976. Bacia Sergipe/Alagoas: geologia regional e perspectivas petrolíferas. *Anais do XXVIII Congresso Brasileiro de Geologia*, Porto Alegre-RS, 137-158.

Penny, J. H. J., 1986 An Early Cretaceous angiosperm pollen assemblage from Egypt. *Special Papers in Palaeontology*, **35**, 121-134.

Pereira, M. J., 1994. *Sequências deposicionais de segunda e terceira ordem (50 a 2,0 Ma) e tectono-estratigrafia no Cretáceo de cinco bacias marginais brasileiras: comparação com outras áreas do Globo e implicações geodinâmicas*. PhD Thesis, Universidade Federal do Rio Grande do Sul, Porto Alegre, RS, Brazil, 2 vols., 280 pp. [Unpublished].

Petrobras 1978a. Relatório geológico semanal. Descrição de testemunho. Poço 9-GTP-17-SE. RPNE-DIREX 69 pages unnumbered. Unpublished internal report.

Petrobras 1978b. Relatório geológico semanal. Descrição de testemunho. Poço 9-GTP-24-SE. RPNE-DIREX 53 pages unnumbered. Unpublished internal report.

Pflug, H. D., 1953. Zur Entstehung und Entwicklung des angiospermiden Pollens in der Erdgeschichte. *Palaeontographica, Abteilung B* **95**, 60-171.

Pierce, R. L., 1961. Lower Upper Cretaceous plant microfossils from Minnesota. *Minnesota Geological Survey Bulletin* **42**, 1-86.

Piper, A., 1996. *Evaluation of palynofacies analysis in the interpretation of depositional environments in the Middle Jurassic of Yorkshire*. PhD Thesis, University of Newcastle upon Tyne, 278 pp. [Unpublished].

Pocock, S.A.J., 1962. Microfloral analysis and age determination of strata at the Jurassic-Cretaceous boundary in the western Canada plains. *Palaeontographica, Abteilung B* **111**, p.1-95, pls.1-15.

Pocock, S. A. J., 1964. Pollen and spores of the Chlamydospermidae and Schiziaceae from Upper Mannville strata of the Saskatoon are of Saskatchewan. *Grana Palynologica* **5**, 129-209.

Pocock, S. A. J., 1972. Palynology of the Jurassic sediments of western Canada. Part 2: Marine species. *Palaeontographica Abteilung B* **137**, 85-153.

Pocock, S. J. & Jansonius. J., 1961. The pollen genus *Classopollis* Pflug 1953. *Micropaleontology* **7**, 439-449.

Posamentier, H. W & Vail, P. R., 1988. Eustatic controls on clastic deposition; II, Sequence and systems tract models. *In*: Wilgus, C. K., Hastings, B. S., Ross, C. A., Posamentier, H. W., Van Wagoner, J., Kendall, B. S. & Christopher, G. St. C. (eds.)*: Sea-level changes; an integrated approach*. *Society of Economic Paleontologists and Mineralogists, Special Publication* **42**, 125-154.

Posamentier, H. W., Jervey, M. T. & Vail, P. R., 1988. Eustatic controls on clastic deposition; I, Conceptual framework. *In*: Wilgus, C. K., Hastings, B. S., Ross, C. A., Posamentier, H. W., Van Wagoner, J., Kendall, B. S. & Christopher, G. St. C. (eds.): *Sea-level changes; an integrated approach*. *Society of Economic Paleontologists and Mineralogists, Special Publication* **42**, 109-124.

Powell, A. J., Dodge, J. D. & Lewis, J., 1990. Late Neogene to Pleistocene palynological facies of the Peruvian continental margin upwelling, Leg 112. *Proceedings of the Ocean Drilling Project, Scientific Results* **112**, 297-321.

Ravn, R. L., 1995. Miospores from the study the muddy sandstones (upper Albian), Wind River Basin, Wyoming, USA. *Palaeontographica, Abteilung B* **234**, p. 41-91, pls.1-18. 1962

Regali, M. S. J., 1987a. Palinomorfos do Barremiano/Albiano Brasileiros Parte I. *Anais do X Congresso Brasileiro de Paleontologia*, Rio de Janeiro-RJ, 615-623.

Regali, M. S. J., 1987b. Palinomorfos do Barremiano/Albiano Brasileiros Parte II. *Anais do X Congresso Brasileiro de Paleontologia*, Rio de Janeiro-RJ, 647-655.

Regali, M. S. P, Uesugui, N. & Santos, A. da S., 1974a. Palinologia dos sedimentos meso-cenozoicos do Brasil II. *Boletim Técnico da PETROBRAS* **17**, 177-191.

Regali, M. S. P, Uesugui, N. & Santos, A. da S., 1974b. Palinologia dos sedimentos meso-cenozoicos do Brasil II. *Boletim Técnico da PETROBRAS* **17**, 263-30, 25 plates.

Regali, M. S. P. & Viana, C. F., 1989. Sedimentos do neojurássico-eocretácico do Brasil: idade e correlação com a escala internacional. *PETROBRAS/SEDES*, 15 pp. [Pre-print].

Regali, M. S. P. & Santos, P. R. S., 1995. Palinoestratigrafia do Neoaptiano da Bacia de Sergipe. *Anais do XIV Congresso Brasileiro de Paleontologia*, Uberaba-MG, 105.106.

Regali, M. S. P. & Santos, P. R. S., 1996. Palinoestratigrafia e geocronologia dos sedimentos albo-aptianos das bacias de Sergipe e Alagoas. Petrobras-Serec/Cen-Sud, Rio de Janeiro, 71pp. Unpublished internal report.

Regali, M. S. P. & Santos, P. R. S., 1999. Palinoestratigrafia e geocronologia dos sedimentos Albo-Aptianos das bacias de Sergipe e de Alagoas. *Boletim do 5° Simpósio sobre o Cretáceo do Brasil*, Serra Negra-SP, 411-420.

Sarg, J. F., 1988. Carbonate sequence stratigraphy. *In*: Wilgus, C. K., Hastings, B. S., Ross, C. A., Posamentier, H. W., Van Wagoner, J., Kendall, B. S. & Christopher, G. St. C. (eds.): *Sea-level changes; an integrated approach. Society of Economic Paleontologists and Mineralogists, Special Publication* **42**, 155-181. 1988.

Scarparo, A. A. C. & Koutsoukos, E. A. M., 1998. Calcareous nannofossils and planktic foraminifers in the upper Aptian of the Sergipe Basin, northeastern Brazil; palaeoecological inferences. *Palaeogeography, Palaeoclimatology, Palaeoecology* **142**, 175-184.

Schaller, H., 1970. Revisão estratigráfica da Bacia Sergipe-Alagoas. *Boletim Técnico da PETROBRAS* **12**, 21-86.

Schrank, E. & Ibrahim, M. I. A., 1995. Cretaceous (Aptian–Maastrichtian) palynology of foraminifera-dated wells (KRM-1, AG-18) in northwestern Egypt. *Berliner Geowissenschaftliche Abhandlungen* **177**, 44pp.

Schuurman, W. M. L., 1977. Aspects of Late Triassic palynology. 2. Palynology of the ‘Grès et Schiste à *Avicula contorta*’ and ‘Argiles de Levallois’ (Rhaetian) of northeastern France and southern Luxembourg. *Review of Palaeobotany and Palynology* **23**, 159-253.

Seeling, J., 1999. *Palaeontology and biostratigraphy of the macroinvertebrate fauna of the Cenomanian–Turonian transition of the Sergipe Basin, northeastern Brazil-with systematic description of bivalves and echnoids*. PhD Thesis, University of Heidelberg, 163 pp. [Unpublished].

Singh, C., 1964. Microflora of the Lower Cretaceous Mannville Group, east-central Alberta. *Research Council of Alberta, Bulletin*. 1964, 238 pp.

Singh, C., 1971. Lower Cretaceous microfloras of the Peace River area, northwestern Alberta. *Research Council of Alberta Bulletin* **28**, 301-542, pls.39-80.

Singh, C., 1983. Cenomanian microfloras of the Peace River area, northwestern Alberta. *Alberta Research Council Bulletin* **44**, 1-322.

Skarby, A., 1964. Revision of *Gleicheniidites senonicus* Ross. *Stockholm Contribution in Geology* **11**, 59-77.

Speelman, J. D. & Hills, L. V., 1980. Megaspore paleoecology: Pakowki, Foremost and Oldman formations (Upper Cretaceous), southeastern Alberta. *Bulletin of Canadian Petroleum Geologists* **28**, 522-541.

Srivastava, S. K., 1977. Microspsores from the Fredericksburg Group (Albian) of the southern United States. Paleobiologie Continentale **6**, 1-119.

Srivastava, S. K., 1976. The fossil pollen genus *Classopollis*. *Lethaia* **9**, 437-457.

Srivastava, S. K., 1968. Ephedralean pollen from the Upper Cretaceous Edmonton Formation of Alberta (Canada) and their paleoecological significance. *Canadian Journal of Earth-Sciences* **5**, 211-221.

Steffen, D. & Gorin, G., 1993a. Palynofacies of the upper Tithonian–Berriasian deep-sea carbonates in the Vocotian Trough (SE France). *Bulletin Centres Recheches Exploration-Prodution Elf Aquitaine* **17**, 235-247.

Steffen, D. & Gorin, G., 1993b. Sedimentology of organic matter in upper Tithonian–Berriasian deep-sea carbonates of southeast France: evidence of eustatic control. *In*: Katz, B. & Prott, L. (eds.) *Source Rocks in Sequence Stratigraphic Framework. American Association of Petroleum Geologists, Studies in Geology* **37**, 49-65.

Stover, L. E., 1963. Some Middle Cretaceous palynomorphs from West Africa. *Micropaleontology* **9**, 85-94.

Stover, L. E., 1964. Cretaceous ephedroid pollen from West Africa. *Micropaleontology* **10**, 145-156.

Thiergart, F., 1949. Der stratigraphische Wert mesozoischer Pollen und Sporen. *Palaeontographica, Abteilung* **89**, 1-29.

Torricelli, S., 2000. Lower Cretaceous dinoflagellate cyst and acritarch stratigraphy of the Cismon APTICORE (southern Alps, Italy). *Review of Palaeobotany and Palynology* **108**, 213-266.

Traverse, A., 1955. Occurrence of the oil-forming alga Botryococcus in lignites and other Tertiary sediments. *Micropaleontology* **1**, 343-350.

Traverse, A & Ginsburg, R. N., 1966. Palynology of the surface sediments of Great Bahama Banks, as related to water movements and sedimentation. *Marine Geology* **4**, 417-459.

Tschudy, R. H., 1969. Relationship of palynomorphs to sedimentation. *In*: Tschudy, R. H. & Scott, R. A. (eds.), *Aspects of Palynology*, 79-96. Wiley, New York.

Tyson, R. V., 1993. Palynofacies analysis. *In*: Jenkins, D.J. (ed.): *Applied Micropalaeontology*, 153-191. Kluwer Academic Publishers, Dordrecht.

Tyson, R. V., 1995. *Sedimentary Organic Matter: organic facies and palynofacies*. 615 pp. Chapman & Hall, London.

Tyson, R. V. 1996. Sequence-stratigraphical interpretation of organic facies variations in marine siliciclastic systems; general principles and application to the onshore Kimmeridge Clay Formation, UK. *In*: Hesselbo, S. P. & Parkinson, D. N. (eds.), *Sequence stratigraphy in British geology, Geological Society Special Publications* **103**, 75-96. 1996.

Uesugui, N., 1979. Palinologia; técnicas de tratamento de amostras. *Boletim Técnico da PETROBRAS* **22**, 229-240.

Vakhrameev, V. A., 1970. Range and paleoecology of Mesozoic conifers. The Cheirolepidiaceae. *Paleontology Journal* **41**, 11-25.

Vakhrameev, V. A., 1981. Pollen *Classopollis*: indicator of Jurassic and Cretaceous climates. *The Paleobotanist* **28/29**, 301-307.

Van der Zwan, C. J., 1990. Palynostratigraphy and palynofacies reconstruction of the upper Jurassic to lowermost Cretaceous of the Draugen Field, offshore mid Norway. *Review of Palaeobotany and Palynology* **62**, 157-186.

Van Wagoner, J. C., Posamentier, H. W. Mitchum, R. M., Vail, P. R Sarg, J. F. Loutit, T. S. & Hardenbol, J., 1988. An overview of the fundamentals of sequence stratigraphy and key definitions. *In*: Wilgus, C. K. Hastings, B. S., Kendall, C. G. St .C., Posamentier, H. W., Ross, C. A. & Van Wagoner, J. C. (eds.): *Sea-level changes: an integrated approach. Society of Economic Paleontologists and Mineralogists Special Publication* **42**, 39-45.

Viviers, M. C., Koutsoukos, E. A. M., Silva-Teles Junior, A. C. & Bengtson, P., 2000. Stratigraphy and biostratigraphic affinities of the late Aptian–Campanian ostracods of the Potiguar and Sergipe basins in northeastern Brazil. *Cretaceous Research* **21**, 407-455.

Wall, D., Dale, B., Lohmann, G. P. & Smith, W. K., 1977. The environmental and climatic distribution of dinoflagellate cysts in modern marine sediments from regions in the North and South Atlantic Oceans and adjacent areas. *Marine Micropaleontology* **2**, 121-200.

Wetzel, O., 1933. Die in organischer Substanz erhaltenen Mikrofossilien des baltischen Kreide-Feuersteins mit einem sediment-petrographischen und stratigraphischen Anhang. *Palaeontographica*, *Abteilung A* **77**, 141-186.

White, H. H. 1842. On fossil *Xanthidia*; *Microscopical Journal* **11**, 35-40, Plate 4.

Williams, G. L., 1977. Dinocysts. Their classification, biostratigraphy and palaeoecology. *Oceanic Micropalaeontology* **2**, 1231-1325.

Williams, G. L., 1992. Palynology as a paleoenvironmental indicator in the Brent Group, northern North Sea. In: Morton, A. C., Haszeldine, R. S., Giles, M. R. & Brown, S. (eds.*)*, *Geological Society of London Special Publication* **61**, 203-212.

Williams, G. L. & Bujak, J. P., 1985. Mesozoic and Cenozoic dinoflagellates. *In:* Bolli, H. M., Saunders, J. B & Perch, N. K. (eds.): *Plankton stratigraphy.* 847-964*. Cambridge earth science series,* Cambridge University Press.

Wingate, F. H., 1980. Plant microfossils from the Denton Shale Member of the Bokchito Formation (Lower Cretaceous, Albian) in southern Oklahoma. *Oklahoma Geological Survey Bulletin* **130**, 1-93.

PLATES

PLATE 1

Figure 1. *Antulsporites baculatus*. EFR Z39/3, sample 9700156 (101.7 m), GTP-24-SE.

Figure 2. *Cyathidites* sp. EFR W16/3, sample 9700174 (170.43 m), GTP-24-SE.

Figure 3. *Microfoveolatosporis daukiensis*. EFR F14/2, sample 9700156 (101.7 m), GTP-24-SE.

Figure 4. *Klukisporites pseudoreticulatus*. EFR V9, sample 9700188 (222.25 m), GTP-24-SE.

Figure 5. *Echinatisporites varispinosus*. EFR K33, sample 9700160 (110.6 m), GTP-24-SE.

Figure 6. *Cicatricosisporites avnimelechi.* EFR G17, sample 9704614 (242.05 m), GTP-17-SE.

Figure 7. *Klukisporites foveolatus*. EFR W34, sample 9700224 (318 m), GTP-24-SE.

Figure 8. *Foveosporites canalis*. EFR C8/4, sample 9700226 (322.25 m), GTP-24-SE.

Figure 9. *Reticulosporis foveolatus*. EFR Q30, sample 9704583 (93.9 m), GTP-17-SE.

Figure 10. *Crybelosporites pannuceus*. EFR H25, sample 9704637 (298.3 m), GTP-17-SE.

Figure 11. *Cicatricosisporites microstriatus*. EFR Q32, sample 9700219 (300.6 m), GTP-24-SE.

Figure 12. *Clavatriletes* sp. EFR R11/3, sample 9700225 (318.65 m), GTP-24-SE.

Figure 13. *Verrucosisporites* sp. EFR L10/2, sample 9700174 (170.43 m), GTP-24-SE.

Figure 14. *Matonisporites silvai*. EFR J30/2, sample 9700183 (207.8 m), GTP-24-SE.

Figure 15. *Retitriletes* sp. 3. (Regali, 1989) EFR S13/2, sample 9700150 (88.4 m), GTP-24-SE.

Figure 16. *Perotriletes* sp. EFR N17/1, sample 9700121 (46.35 m), GTP-24-SE.

Figure 17. *Collarisporites fuscus*. EFR H28, sample 9704585 (100.9 m), GTP-17-SE.

Figure 18. *Leptolepidites psarosus.* EFR V34, sample 9700126 (51.8 m), GTP-24-SE.

Figure 19. *Pilosisporites trichopapillosus*. EFR M31, sample 9704632 (283.83 m), GTP-24-SE.

EFR- England Finder Reference

PLATE 1

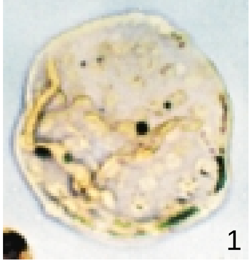
1

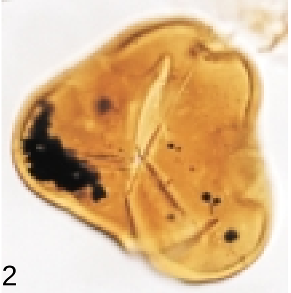
2

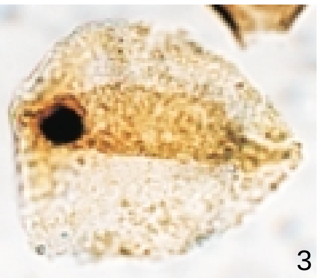
3

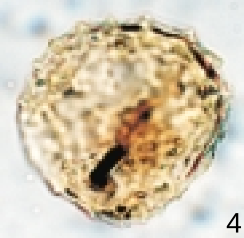
4

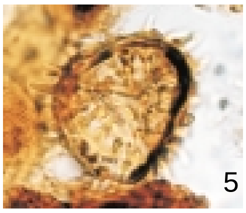
5

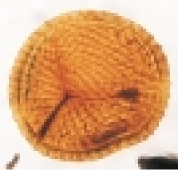
6

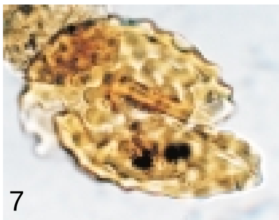
7

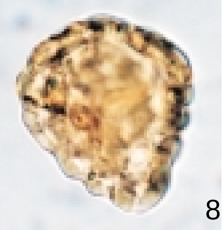
8

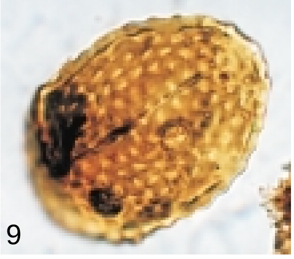
9

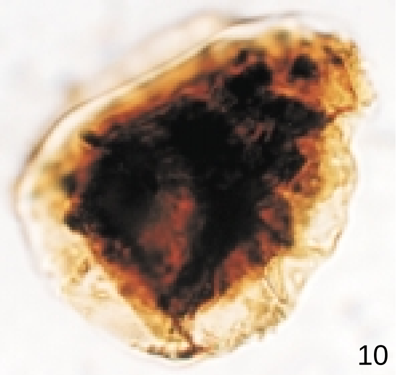
10

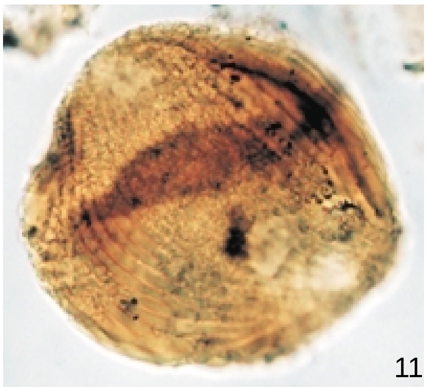
11

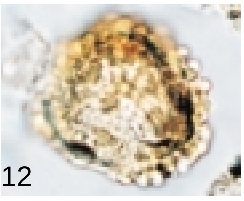
12

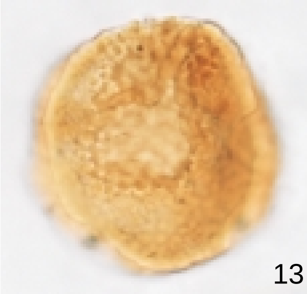
13

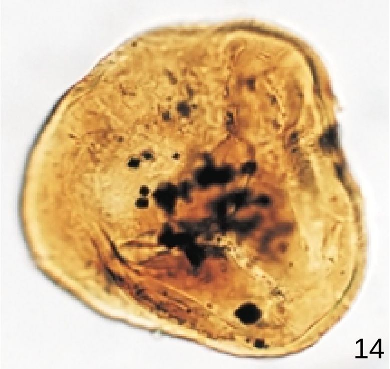
14

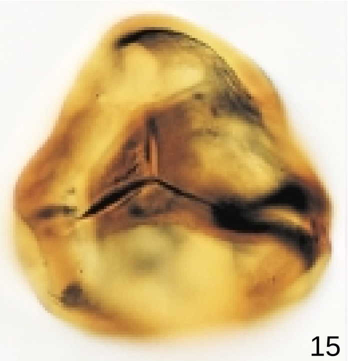
15

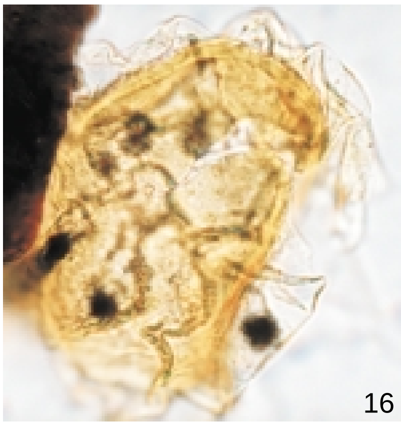
16

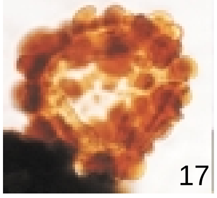
17

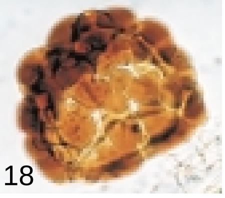
18

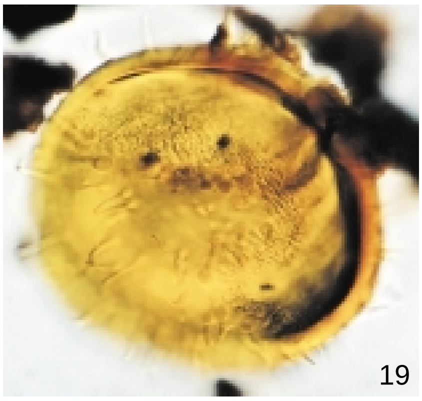
19

30µm

PLATE 2

Figure 1. Megaspore. EFR X37/1, , sample 9700185 (214.75 m), GTP-24-SE.

Figure 2. *Araucariacites australis.* EFR J24/4, sample 9704606 (210.55 m), GTP-17-SE.

Figures 3-4. *Sergipea variverrucata.* EFR M42/1-3, sample 9700172 (160.35 m), GTP-17-SE.

Figure 5. *Sergipea naviformis***.** EFR U12/1, sample 9700121 (46.35 m), GTP-24-SE.

Figures 6-7. *Uesuguipollenites callosus.* EFR S10, sample 9700185 (214.75 m), GTP-24-SE.

Figure 8. *Sergipea simplex*. EFR P19/4, sample 9700117 (40.1 m), GTP-24-SE.

Figure 9. *Classopollis classoides.* EFR H25, sample 9704637 (298.3 m), GTP-17-SE.

Figure 10. *Callialasporites segmentatus*. EFR N15, sample 9700124 (49.7 m), GTP-24-SE.

Figure 11. *Vitreisporites pustulosus.* EFR S6/2, sample 9700102 (22.8 m), GTP-24-SE.

Figure 12. *Complicatisaccus cearensis*? EFR Y12, sample 9700188 (222.25 m), GTP-24-SE.

Figure 13-14. *Equisetosporites maculosus*. EFR ER17/4, sample 9700226 (322.25 m), GTP-24-SE.

Figure 15. *Equisetosporites albertensis*. EFR H17, sample 9700155 (99.2 m), GTP-24-SE.

Figure 16. *Bennettitaepollenites regaliae*. EFR B30/2, sample 9704634 (287.02 m), GTP-17-SE.

Figure 17. *Cycadopites* sp. EFR X32, sample 9700121 (46.35 m), GTP-24-SE.

Figure 18. *Steevesipollenites binodosus*? EFR G27/3, sample 9700092 (16 m), GTP-24-SE.

Figure 19. *Equisetosporites ovatus.* EFR L39/4, sample 9700157 (103.15 m), GTP-24-SE.

Figure 20. *Gnetaceaepollenites chlatratus*. EFR E25/2, sample 9700171 (157.15 m), GTP-24-SE.

Figure 21. *Gnetaceaepollenites uesuguii*. EFR G23/3, sample 9700127 (52.35 m), GTP-24-SE

Figure 22. *Gnetaceaepollenites diversus* EFR U14, sample 9700174 (170.43 m), GTP-24-SE**.**

Figure 23. *Equisetosporites concinnus*. EFR V11/2, sample 9700219 (300.6 m), GTP-24-SE**.**

EFR- England Finder Reference

PLATE 2

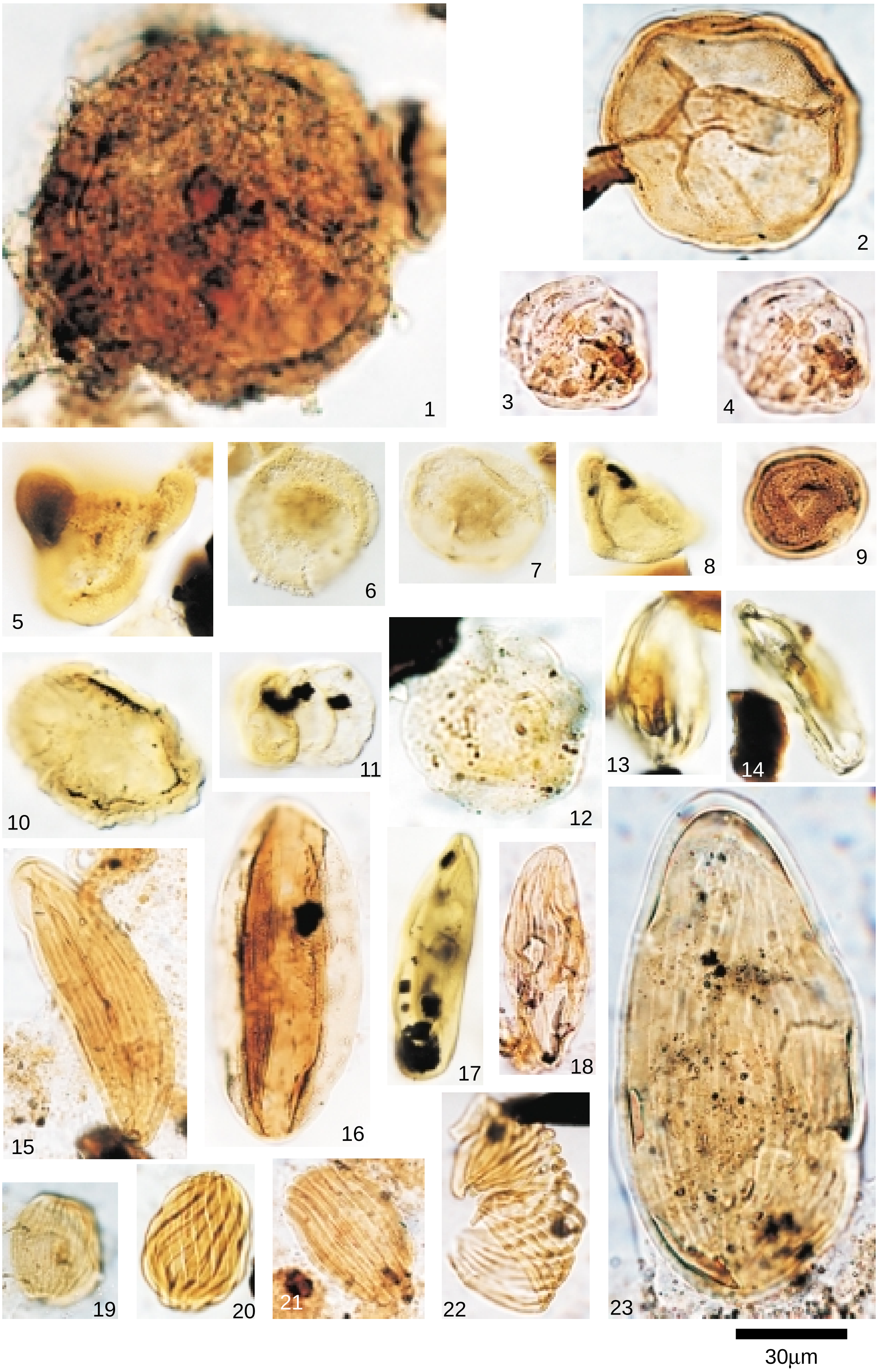
1
2
3
4
5
6
7
8
9
10
11
12
13
14
15
16
17
18
19
20
21
22
23
30µm

PLATE 3

Figure 1. *Gnetaceaepollenites jansonii*. EFR C11/2-4, sample 9700214 (277.7 m), GTP-24-SE**.**

Figures 2-3. *Elaterosporites klaszi.* EFR H13, sample 9704593 (137.7 m), GTP-17-SE**.**

Figure 4. *Elaterosporites klaszi.* EFR K20/2, sample 9700125 (50.6 m), GTP-24-SE**.**

Figure 5. *Afropollis* aff. *jardinus.* EFR W16/3, sample 9700123 (48.6 m), GTP-24-SE**.**

Figure 6. *Retimonocolpites textus*?. EFR V29/4, sample 9700231 (337.45 m), GTP-24-SE**.**

Figure 7. *Afropollis operculatus.* EFR M31/2, sample 9700117 (50.6 m), GTP-24-SE**.**

Figure 8. *Rousea georgensis.* EFR G38/1, sample 9700171 (157.15 m), GTP-24-SE**.**

Figure 9. *Retitricolpites* sp. EFR C11, sample 9700155 (99.2 m), GTP-24-SE**.**

Figure 10. *Retimonocolpites textus*?. EFR V29/4, sample 9700231 (337.45 m), GTP-24-SE**.**

Figures 11-12. *Brenneripollis reticulatus*. EFR T10, sample 9700165 (124.4 m), GTP-24-SE**.**

Figure 13. *Tricolpites* sp. EFR K29, sample 9704573 (57.3 m), GTP-17-SE**.**

Figure 14. *Dejaxpollenites foveoreticulatus*. EFR H18/3, sample 9700175 (178.56 m), GTP-24-SE**.**

Figures 15-16. *Dejaxpollenites foveoreticulatus*. EFR Y13, sample 9700156 (101.7 m), GTP-24-SE**.**

Figure 17. *Dejaxpollenites microfoveolatus*. EFR M24/3, sample 9700126 (51.8 m), GTP-24-SE**.**

Figure 18. *Schrankpollis reticulatus*? EFR H179, sample 9700126 (51.8 m), GTP-24-SE.

Figures 19-20. *Quadricolpites reticulatus*? EFR X19/2, sample 9700154 (98.2 m), GTP-24-SE**.**

Figure 21. *Striatopollis reticulatus.* EFR P13, sample 9700171 (157.15 m), GTP-24-SE**.**

Figure 22. *Stellatopollis barghoornii*. EFR K25/2, sample 9700135 (60.7 m), GTP-24-SE.

Figure 23. *Stellatopollis dubius.* EFR K12/2, sample 9700166 (124.67 m), GTP-24-SE**.**

Figure 24. *Stellatopollis* sp. 1 (Doyle *et al*., 1977). EFR P39/1, sample 9700168 (130.55 m), GTP-24-SE**.**

EFR- England Finder Reference

PLATE 3

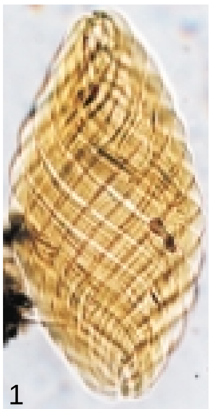
1

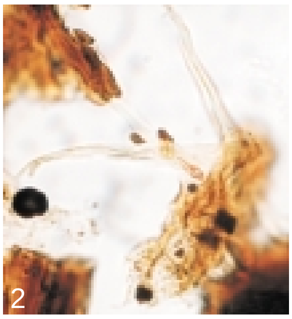
2

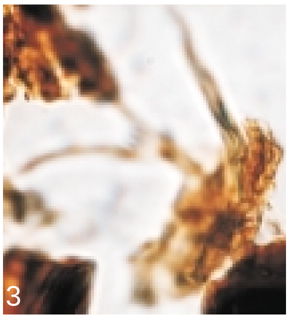
3

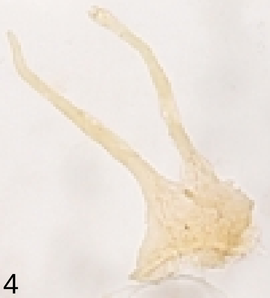
4

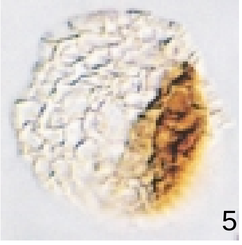
5

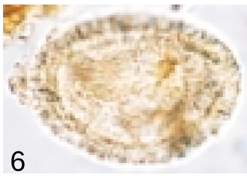
6

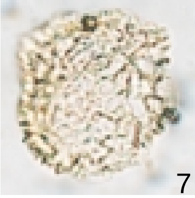
7

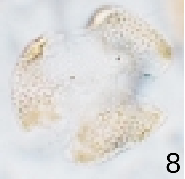
8

9

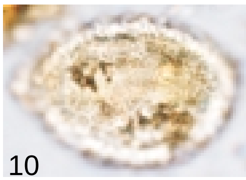
10

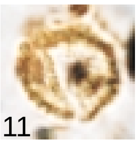
11

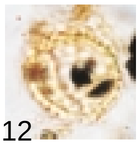
12

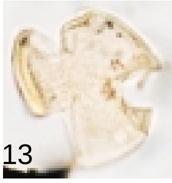
13

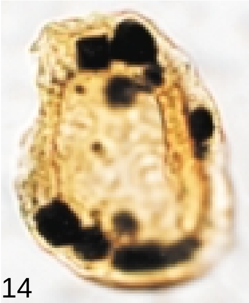
14

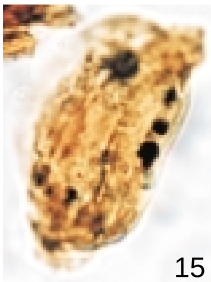
15

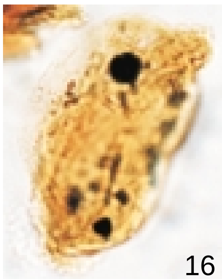
16

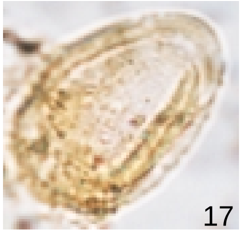
17

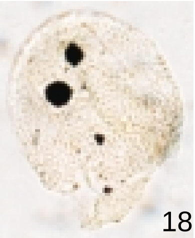
18

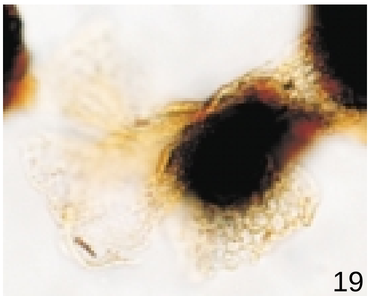
19

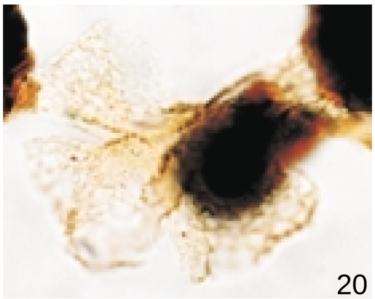
20

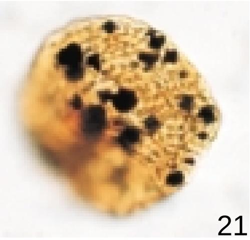
21

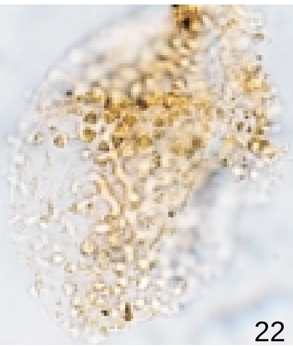
22

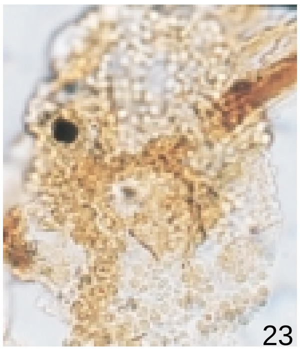
23

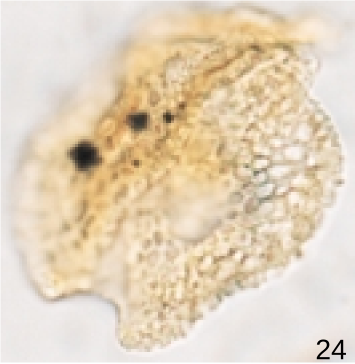
24

30µm

PLATE 4

Figure 1. *Circulodinium* sp. EFR U33/3-4, sample 9700150 (88.4 m), GTP-24-SE**.**

Figure 2. *Cyclonephelium* sp. EFR Q31/2, sample 9700150 (88.4 m), GTP-24-SE**.**

Figure 3. *Cyclonephelium* sp. EFR L6, sample 9700101 (20.85 m), GTP-24-SE**.**

Figure 4. *Cyclonephelium* sp. EFR X33/1, sample 9700119 (42.65 m), GTP-24-SE**.**

Figure 5. *Cyclonephelium* sp. EFR Q17/4, sample 9700150 (88.4 m), GTP-24-SE**.**

Figure 6. *Odontochitina operculata*. EFR L4/4, sample 9700139 (67 m), GTP-24-SE**.**

Figure 7. *Odontochitina operculata*. EFR Z7/3, sample 9700139 (67 m), GTP-24-SE**.**

Figure 8. *Palaeoperidinium cretaceum.* EFR Q25, sample 9700165 (124.4 m), GTP-24-SE**.**

Figure 9. *Pseudoceratium securigerum*? EFR M33/1, sample 9700141 (71.6 m), GTP-24-SE**.**

Figure 10. *Subtilisphaera trendallii*? EFR R9/2, sample 9700160 (110.6 m), GTP-24-SE**.**

Figure 11. *Subtilisphaera senegalensis*. EFR E20/1-3, sample 9700150 (88.4 m), GTP-24-SE**.**

Figure 12. *Tanyosphaeridium* sp. EFR M9/2, sample 9700126 (110.6 m), GTP-24-SE**.**

Figure 13. *Florentina mantellii*. EFR M20/2, sample 9700175 (178.56 m), GTP-24-SE**.**

Figure 14. *Prolixosphaeridium parvispinum*. EFR V25/2, sample 9700129 (56.1 m), GTP-24-SE**.**

EFR- England Finder Reference

PLATE 4

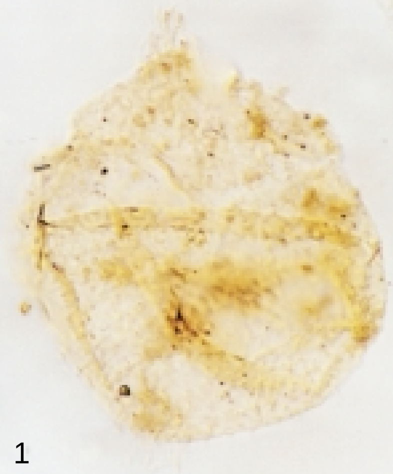
1

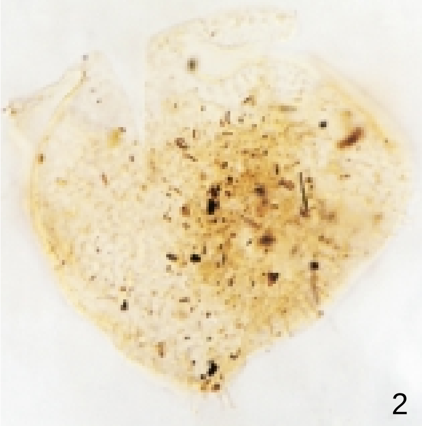
2

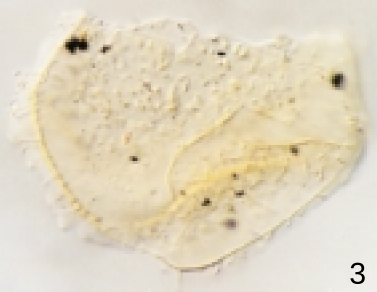
3

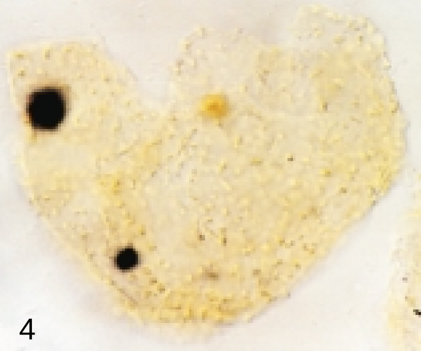
4

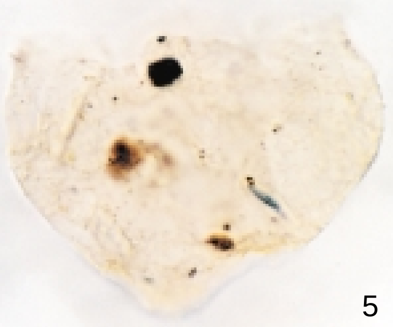
5

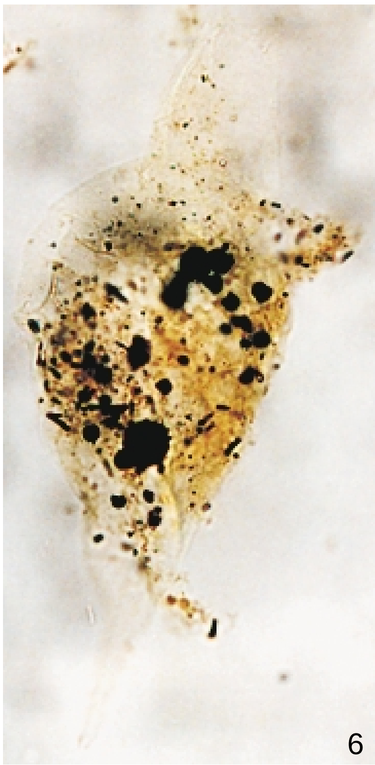
6

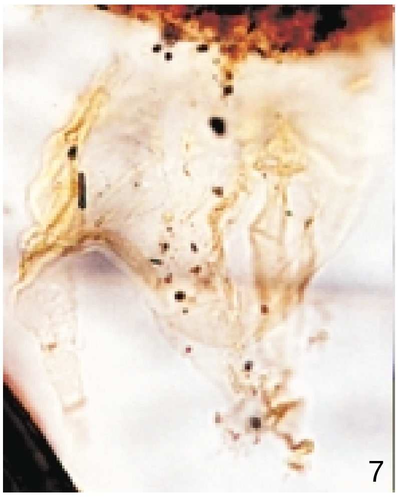
7

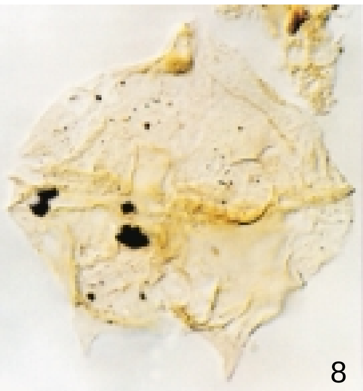
8

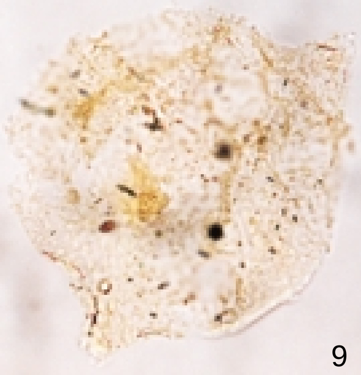
9

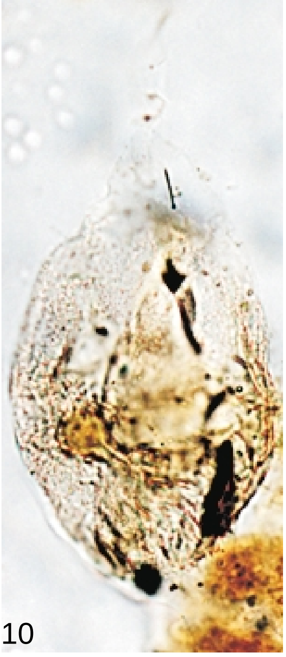
10

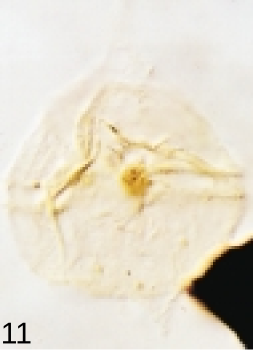
11

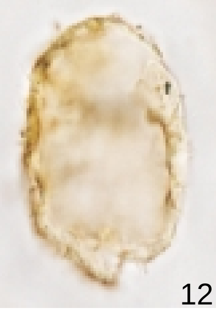
12

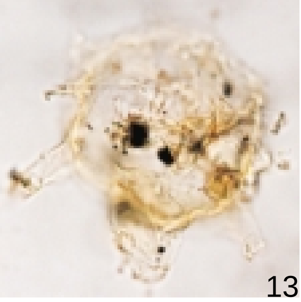
13

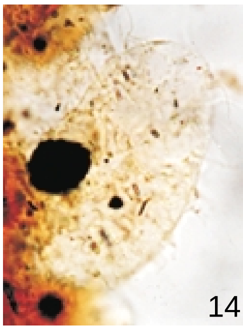
14

30µm

PLATE 5

Figure 1. *Cribroperidinium* sp. EFR M6/3, sample 9700103 (22.88 m), GTP-24-SE**.**

Figures 2-3. *Apteodinium granulatum*. EFR S9, sample 9700103 (22.88 m), GTP-24-SE**.**

Figure 4. *Systematophora cretacea*? EFR Z36/2, sample 9700119 (42.65 m), GTP-24-SE**.**

Figure 5. *Dinopterygium*? sp. EFR Y27/1, sample 9700111 (32.25 m), GTP-24-SE**.**

Figure 6. *Spiniferites lenzi*. EFR G31/1, sample 9700103 (22.88 m), GTP-24-SE**.**

Figure 7-8. *Spiniferites chebca*. EFR V18/3, sample 9700111 (32.25 m), GTP-24-SE**.**

Figure 9. *Spiniferites ancoriferus*. EFR Q28/4, sample 9700161 (112.7 m), GTP-24-SE**.**

Figure 10. *Spiniferites* sp. EFR L7/2, sample 9700109 (28 m), GTP-24-SE**.**

Figure 11. *Spiniferites* sp. EFR F8/1, sample 9700103 (22.88 m), GTP-24-SE**.**

Figure 12. *Spiniferites bejuii*. EFR M25/2, sample 9700109 (28 m), GTP-24-SE**.**

Figure 13 *Oligosphaeridium irregulare*. EFR J10/1, sample 9700109 (28 m), GTP-24-SE**.**

Figure 14. *Oligosphaeridium pulcherrimum*. EFR P28, sample 9700138 (65.9 m), GTP-24-SE**.**

Figure 15. *Oligosphaeridium totum*. EFR U5, sample 9700137 (65.45 m), GTP-24-SE**.**

Figure 16. *Oligosphaeridium poculum*. EFR J25/4, sample 9700127 (52.35 m), GTP-24-SE**.**

Figure 17. *Oligosphaeridium complex*. EFR P21, GTP-24-SE, sample 9700129 (56.1 m)**.**

Figure 18. *Oligosphaeridium albertense*. EFR T18/2, sample 9700138 (65.9 m), GTP-24-SE**.**

EFR- England Finder Reference

PLATE 5

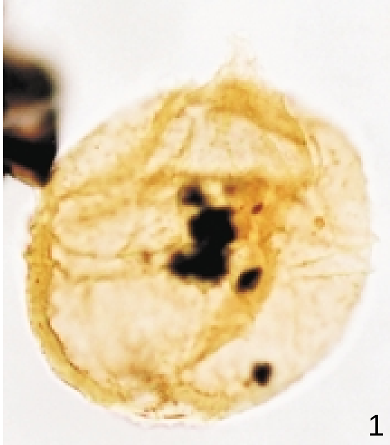
1

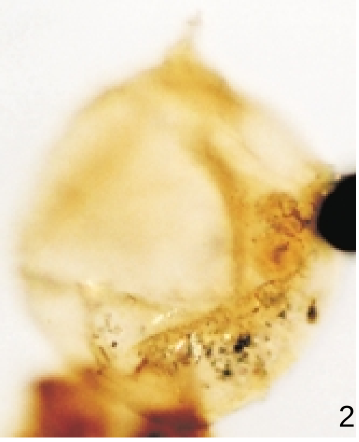
2

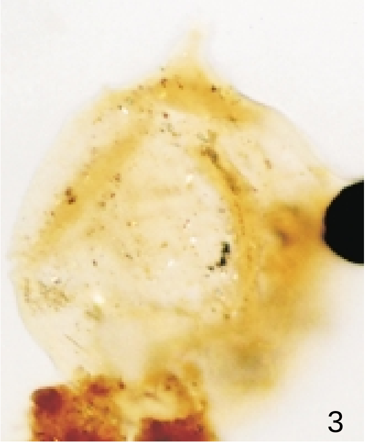
3

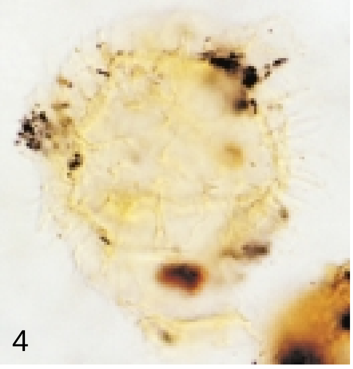
4

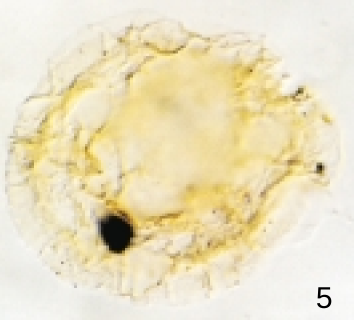
5

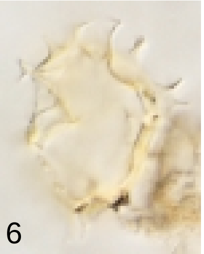
6

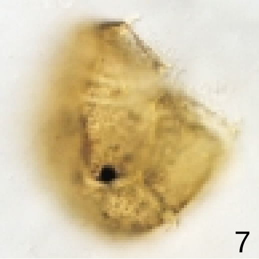
7

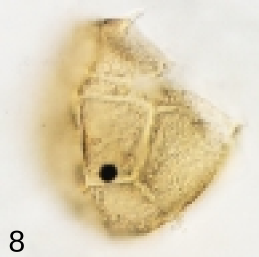
8

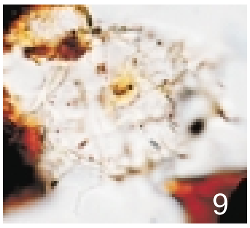
9

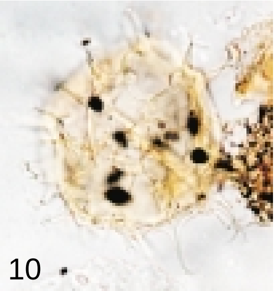
10

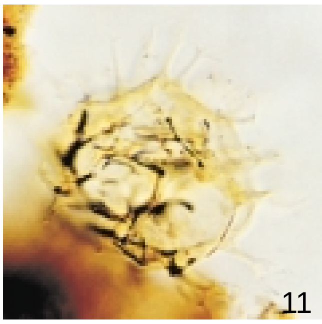
11

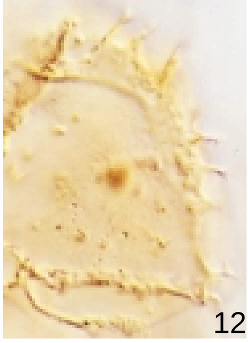
12

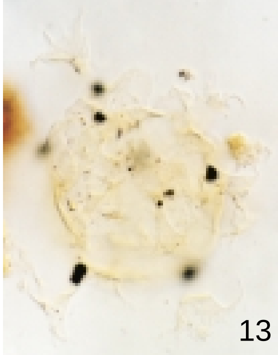
13

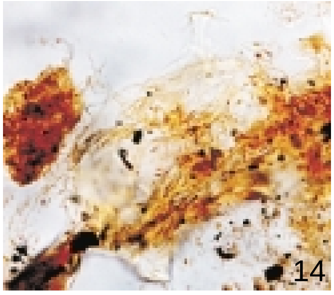
14

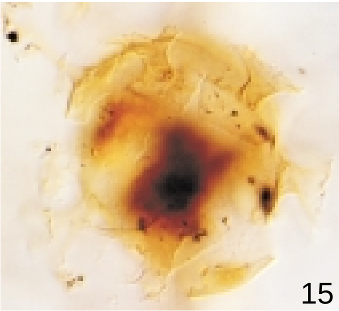
15

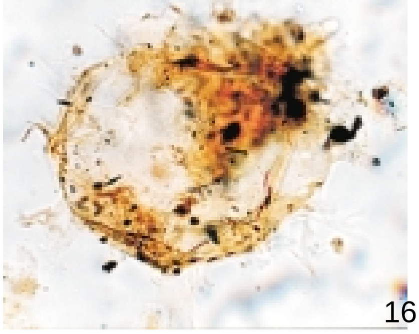
16

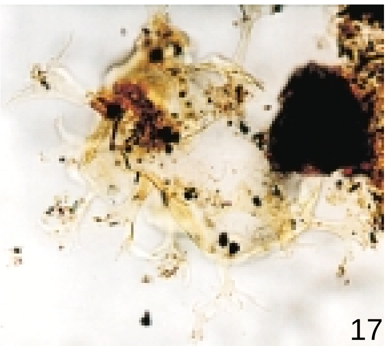
17

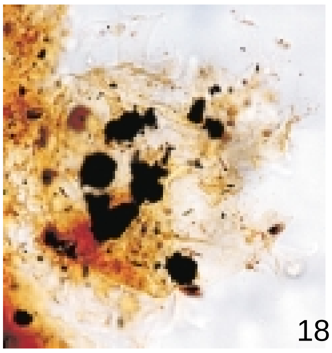
18

30µm

PLATE 6

Figure 1. *Exochosphaeridium* sp. EFR L20/1, sample 9700111 (32.25 m), GTP-24-SE**.**

Figures 2-3. *Trichodinium castanea*. EFR K12, sample 9700124 (49.7 m), GTP-24-SE**.**

Figure 4. Scolecodont. EFR L28/4, sample 9700115 (37.55 m), GTP-24-SE**.**

Figure 5. Scolecodont. EFR B18/2-4, sample 9700168 (130.55 m), GTP-24-SE**.**

Figure 6. Foraminiferal test lining. EFR W14/4, sample 9700141 (71.6 m), GTP-24-SE**.**

Figure 7. Foraminiferal test lining. EFR S19/2-4, sample 9700173 (167.25 m), GTP-24-SE**.**

Figure 8. *Botryococcus* sp. EFR K13/2, sample 9700150 (88.4 m), GTP-24-SE**.**

Figure 9. *Leiosphaeridia* sp. EFR W11, sample 9700185 (214.75 m), GTP-24-SE**.**

EFR- England Finder Reference

PLATE 6

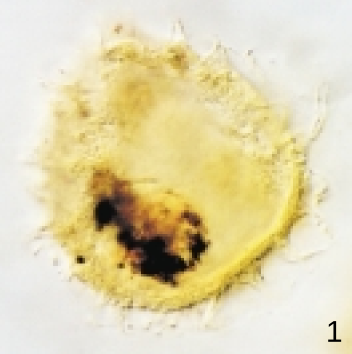
1

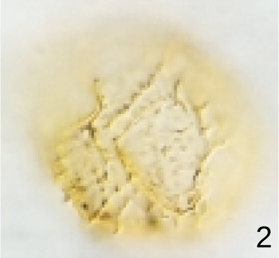
2

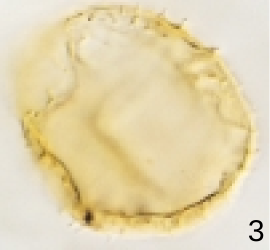
3

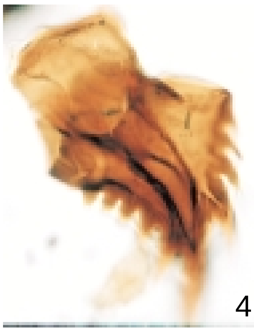
4

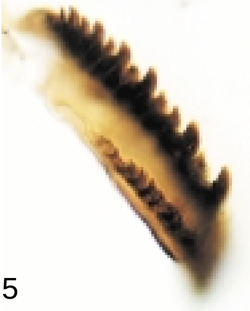
5

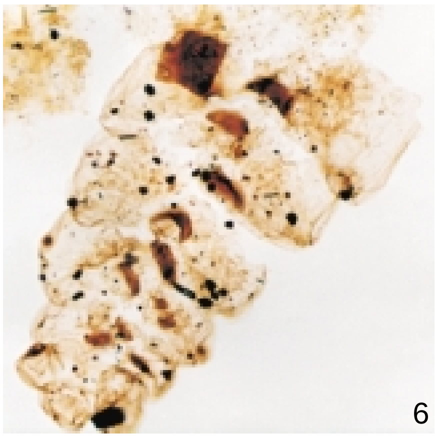
6

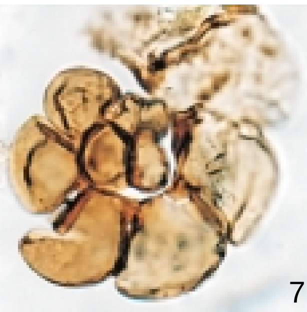
7

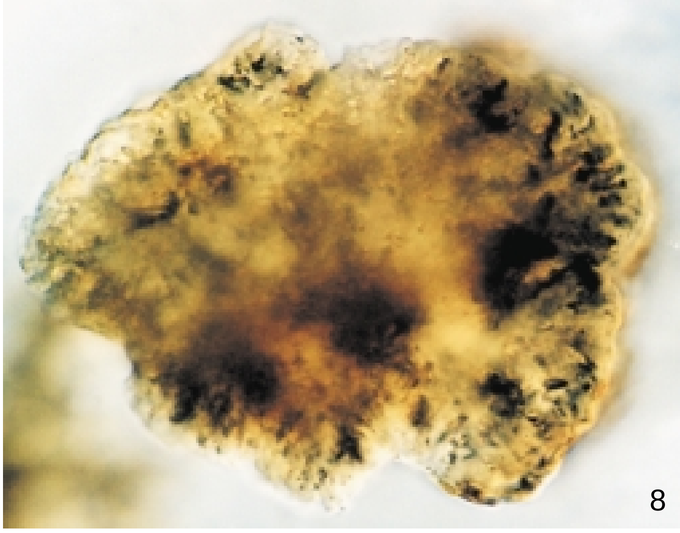
8

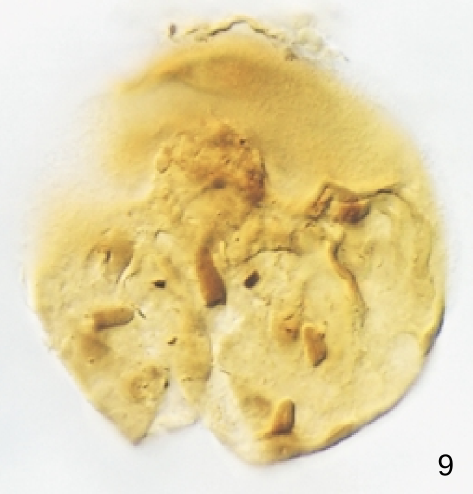
9

30µm

APPENDICES

Sample no.	Depth (m)	Core	Box	Lithology
9704565	18.00	2	4.6	shale
9704566	25.10	3	1.1	sandstone
9704567	31.85	5	1.1	sandstone
9704568	34.75	7	1.6	sandstone
9704569	36.80	7	3.6	sandstone
9704571	51.15	9	1.7	sandstone
9704572	51.70	9	4.7	sandstone
9704573	57.30	10	2.5	sandstone
9704574	58.95	10	4.5	sandstone
9704575	61.05	10	1.5	sandstone
9704576	61.70	11	2.5	sandstone
9704577	63.50	11	4.5	shale
9704578	65.80	12	1.5	sandstone
9704579	68.95	12	4.5	shale
9704580	70.60	13	3.6	shale
9704581	82.15	14	5.5	claystone
9704582	85.70	15	4.8	siltstone
9704583	93.90	16	4.8	sandstone
9704584	96.00	16	7.8	sandstone
9704585	100.90	17	2.7	shale
9704586	103.30	17	5.7	siltstone
9704587	109.00	18	1.4	shale
9704589	125.50	21	1.3	sandstone
9704590	131.70	22	3.4	shale
9704591	133.55	23	1.4	siltstone
9704592	135.55	23	3.4	shale
9704593	137.70	24	1.1	shale
9704594	141.60	25	3.3	sandstone
9704595	143.97	26	2.3	shale
9704596	147.06	27	1.4	siltstone
9704597	149.90	27	4.4	claystone
9704598	155.70	27	1.5	shale
9704599	158.30	28	4.5	sandstone
9704600	159.43	28	5.5	shale
9704601	167.70	29	4.6	shale
9704602	174.06	30	2.3	siltstone
9704603	182.10	31	1.5	shale
9704604	184.00	31	4.5	shale
9704605	209.50	35	3.7	sandstone
9704606	210.55	35	4.7	sandstone
9704607	215.05	35	1.4	shale
9704608	216.60	36	2.4	siltstone
9704609	218.10	36	3.4	shale
9704610	225.15	37	2.2	siltstone
9704611	230.50	37	3.9	siltstone
9704612	233.27	38	6.9	shale
9704613	233.70	38	7.9	calcarenite
9704614	242.05	39	6.9	shale
9704615	244.35	39	8.9	shale
9704616	246.75	39	1.10	shale
9704617	248.40	39	3.10	shale
9704618	250.73	40	5.10	shale
9704619	252.75	40	7.10	siltstone

Appendix 1a. List of samples of well GTP-17-SE.

Identification	Depth (m)	Core	Box	Lithology
9704620	254.83	40	9.10	shale
9704621	255.57	40	1.9	shale
9704622	257.65	40	3.9	shale
9704623	259.87	41	5.9	siltstone
9704624	261.70	41	7.9	shale
9704625	263.32	41	9.9	shale
9704626	265.78	41	2.8	shale
9704627	268.40	42	5.8	shale
9704628	271.42	42	8.8	shale
9704629	273.20	42	1.5	shale
9704630	275.72	43	3.5	shale
9704631	277.75	43	5.5	siltstone
9704632	283.83	43	2.7	shale
9704633	285.83	44	4.7	siltstone
9704634	287.02	44	6.7	shale
9704635	292.25	45	2.6	siltstone
9704636	294.75	45	4.6	shale
9704637	298.30	46	2.4	shale
9704638	300.93	46	1.8	shale
9704639	302.25	46	3.8	shale
9704640	304.18	47	5.8	shale
9704641	306.00	47	7.8	shale
9704642	309.05	47	1.9	shale
9704643	315.23	48	7.9	shale
9704644	317.12	48	9.9	shale
9704645	318.00	48	1.9	shale
9704646	322.95	49	5.9	shale
9704647	325.80	49	9.9	shale
9704648	327.31	49	1.3	shale
9704649	328.67	50	2.3	calcarenite
9704650	329.50	50	3.3	shale
9704651	331.50	51	2.7	calcilutite
9704652	333.20	51	4.7	anhydrite
9704653	339.80	51	1.8	siltstone
9704654	340.40	52	2.8	shale/siltstone
9704655	341.30	52	3.8	shale/siltstone
9704656	350.50	53	3.5	siltstone
9704657	351.50	53	4.5	siltstone
9704658	362.72	53	1.8	siltstone
9704659	363.83	53	2.8	shale
9704660	368.30	55	6.8	shale
9704661	369.13	55	7.8	calcilutite
9704662	372.95	55	3.10	siltstone
9704663	374.15	56	4.10	sandstone
9704664	378.77	56	9.10	shale
9704665	384.15	56	5.10	shale
9704666	385.27	57	6.10	shale
9704667	386.86	57	8.10	calcilutite
9704668	389.35	57	1.10	siltstone
9704669	393.25	58	5.10	shale
9704670	396.62	58	10.10	calcarenite
9704671	409.50	60	7.10	anhydrite
9704672	415.88	61	1.10	siltstone

Appendix 1a. List of samples of well GTP-17-SE.

Identification	Depth (m)	Core	Box	Lithology
9704673	440.65	63	9.9	shale
9704674	443.20	64	3.10	calcilutite
9704675	444.17	64	7.10	calcilutite
9704676	451.40	65	2.6	shale
9704677	456.25	66	1.4	shale
9704678	467.40	68	6.6	siltstone
9704679	469.25	68	1.7	shale
9704680	470.10	69	2.7	shale
9704681	470.95	69	3.7	shale

Appendix 1a. List of samples of well GTP-17-SE.

Sample no.	Depth (m)	Core	Box	Lithology
9700088	12.64	1	2.1	calcilutite
9700089	13.25	1	2.1	calcilutite
9700090	15.55	2	1.5	shale
9700091	15.78	2	1.5	shale
9700092	16.00	2	1.5	shale
9700093	16.45	2	2.5	shale
9700094	16.65	2	2.5	shale
9700095	17.30	2	3.5	shale
9700096	18.63	2	4.5	calcilutite
9700097	19.24	2	5.5	shale
9700098	19.35	2	5.5	shale
9700099	19.85	2	5.5	shale
9700100	20.53	3	1.4	calcilutite
9700101	20.85	3	2.4	calcilutite
9700102	22.80	3	4.4	calcilutite
9700103	22.88	3	4.4	calcilutite
9700104	23.55	4	1.7	shale
9700105	24.05	4	2.7	shale
9700106	25.30	4	3.7	calcilutite
9700107	26.23	4	4.7	shale
9700108	26.83	4	5.7	shale
9700109	28.00	4	6.7	shale
9700110	30.60	5	2.6	shale
9700111	32.25	5	4.6	shale
9700112	33.20	5	5.6	calcilutite
9700113	34.87	5	6.6	shale
9700114	35.95	6	1.8	shale
9700115	37.55	6	3.8	calcilutite
9700116	39.45	6	4.8	shale
9700117	40.10	6	5.8	calcilutite
9700118	42.25	6	7.8	shale
9700119	42.65	7	1.10	calcilutite
9700120	44.15	7	2.10	shale
9700121	46.35	7	5.10	calcilutite
9700122	47.90	7	6.10	shale
9700123	48.60	7	7.10	shale
9700124	49.70	7	8.10	shale
9700125	50.60	7	9.10	shale
9700126	51.80	8	1.16	shale
9700127	52.35	8	3.16	calcilutite
9700128	54.50	8	4.16	calcilutite
9700129	56.10	8	6.16	calcilutite
9700130	56.95	8	7.16	shale
9700131	57.60	8	8.16	shale
9700132	57.80	8	8.16	calcilutite
9700133	58.70	8	9.16	shale
9700134	59.30	8	10.16	calcilutite
9700135	60.70	8	11.16	shale
9700136	62.25	8	13.16	calcilutite
9700137	65.45	8	15.16	calcilutite
9700138	65.90	8	16.16	shale
9700139	67.00	9	1.2	calcilutite
9700140	67.40	9	1.2	calcilutite

Appendix 1b. List of samples of well GTP-24-SE (continued).

Identification	Depth (m)	Core	Box	Lithology
9700141	71.60	10	1.7	shale
9700142	72.25	10	2.7	shale
9700143	75.40	10	5.7	shale
9700144	77.20	10	7.7	calcilutite
9700145	80.40	11	1.1	shale
9700146	82.55	12	1.9	shale
9700147	83.00	12	2.9	calcilutite
9700148	84.90	12	4.9	shale
9700149	86.70	12	6.9	calcilutite
9700150	88.40	12	8.9	shale
9700151	91.25	13	1.8	shale
9700152	94.35	13	4.8	shale
9700153	97.65	13	7.8	calcarenite
9700154	98.20	14	1.10	calcilutite
9700155	99.20	14	2.10	calcilutite
9700156	101.70	14	6.10	shale
9700157	103.15	14	8.10	shale
9700158	108.10	15	1.8	shale
9700159	109.40	15	5.8	shale
9700160	110.60	15	6.8	shale
9700161	112.70	15	8.8	shale
9700162	119.50	16	5.10	shale
9700163	120.60	16	6.10	shale
9700164	122.85	16	9.10	shale
9700165	124.40	16	10.10	shale
9700166	124.67	17	1.10	shale
9700167	128.10	17	5.10	shale
9700168	130.55	17	7.10	calcilutite
9700169	134.45	18	2.9	shale
9700253	135.75	18	4.9	calcilutite
9700170	146.10	19	5.10	shale
9700171	157.15	20	3.9	calcilutite
9700172	160.35	21	1.10	shale
9700173	167.25	21	9.10	shale
9700174	170.43	22	2.11	calcilutite
9700175	178.56	23	1.10	calcilutite
9700176	182.06	23	5.10	shale
9700177	182.60	23	6.10	shale
9700178	189.80	24	4.10	shale
9700179	190.75	24	5.10	shale
9700180	200.68	25	5.10	calcilutite
9700181	202.37	25	7.10	shale
9700182	205.35	26	1.70	shale
9700183	207.80	26	4.70	shale
9700184	211.85	27	1.10	shale
9700185	214.75	27	4.10	shale
9700186	217.00	27	7.10	shale
9700187	222.00	28	2.10	shale
9700188	222.25	28	3.10	shale
9700189	224.60	28	5.10	calcilutite
9700190	227.10	28	8.10	shale
9700191	227.70	28	9.10	shale
9700192	232.90	29	3.10	shale

Appendix 1b. List of samples of well GTP-24-SE (continued).

Identification	Depth (m)	Core	Box	Lithology
9700194	237.60	29	9.10	shale
9700195	237.70	29	10.10	shale
9700196	239.75	30	2.11	shale
9700197	240.65	30	3.11	shale
9700198	241.25	30	4.11	calcilutite
9700199	243.95	30	7.11	shale
9700200	247.00	30	11.11	shale
9700201	249.10	31	2.10	shale
9700202	252.60	31	8.10	shale
9700203	254.60	31	10.10	calcilutite
9700204	255.65	32	1.10	shale
9700205	256.10	32	2.10	shale
9700206	258.50	32	4.10	calcilutite
9700207	259.05	32	5.10	shale
9700208	262.95	32	9.10	shale
9700209	265.10	33	2.10	shale
9700210	268.05	33	5.10	calcirudite
9700211	268.30	33	5.10	calcirudite
9700212	268.50	33	6.10	calcirudite
9700213	272.55	33	10.10	calcilutite
9700214	277.70	34	6.10	shale/calcilutite
9700215	289.60	35	9.90	shale/calcilutite
9700216	291.50	36	1.10	shale/calcilutite
9700217	295.10	36	5.10	shale/calcilutite
9700218	299.30	36	10.10	shale/calcilutite
9700219	300.60	37	1.10	shale
9700220	304.05	37	5.10	shale
9700221	308.95	37	10.10	sandstone
9700222	309.53	38	1.10	shale
9700223	313.25	38	5.10	siltstone
9700224	318.00	38	10.10	calcilutite
9700225	318.65	39	1.10	shale
9700226	322.25	39	5.10	shale
9700227	326.45	39	10.10	shale
9700228	327.43	40	1.10	calcilutite
9700229	331.30	40	5.10	calcilutite
9700230	336.20	41	2.10	shale
9700231	337.45	41	2.90	anhydrite
9700232	339.30	41	4.90	shale
9700233	342.05	41	7.9	shale
9700234	346.20	42	2.10	calcilutite
9700235	349.18	42	5.10	shale
9700236	357.50	43	4.10	shale
9700237	364.90	44	3.9	shale
9700238	367.65	44	6.9	calcarenite
9700239	372.50	45	1.3	calcilutite
9700240	377.65	46	3.7	shale
9700241	382.75	47	1.10	shale
9700242	384.60	47	3.10	anhydrite
9700243	387.35	47	6.10	anhydrite
9700244	389.75	47	9.10	shale
9700245	393.05	48	3.9	anhydrite
9700246	398.05	48	8.9	shale

Appendix 1b. List of samples of well GTP-24-SE (continued).

Identification	Depth (m)	Core	Box	Lithology
9700247	400.53	50	1.6	calcilutite
9700248	403.75	50	4.6	calcilutite
9700250	409.90	51	5.1	calcilutite
9700249	414.95	51	10.10	calcilutite

Appendix 1b. List of samples of well GTP-24-SE (continued).

Depth (m)	Acritarcha	*Afropollis* spp.	*Araucariacites autralis*	*Bennettitaepollenites regaliae*	Bisaccate forms	*Botryococcus* spp.	*Brenneripollis peroreticulatus*	*Callialasporites segmentatus*	*Cicatricosisporites avnimelechi*	*Cicatricosisporites microstriatus*	*Cicatricosisporites* spp.	*Circulodinium* spp.	*Classopollis classoides*	*Collarisporites fuscus*	*Crybelosporites pannuceus*	*Cyathidites* spp.	*Cycadopites* spp.	*Cyclonephelium* spp.	*Dejaxpollenites microfoveolatus*	*Dejaxpollenites* spp.	*Echinatisporis varispinosus*	*Elaterosporites klaszi* ?	*Equisetosporites consinnus*	*Equisetosporites maculosus*	*Equisetosporites* spp.	*Exochosphaeridium* spp.	Foramiferal linings	*Foveosporites* spp.	*Gnetaceaepollenites cahlatratus*	*Gnetaceaepollenites jansonii*	*Gnetaceaepollenites* spp.	*Gnetaceaepollenites uesugui*	*Klukisporites foveolatus*	*Klukisporites pseudoreticulatus*	*Klukisporites* spp.	*Leptolepidites psarosus*	*Matonisporites silvai*	Megaspores	*Perotriletes* spp.	*Pilosisporites trichopapillosus*	*Pseudoceratium* spp.	*Reticulosporis foveolatus*	*Retitriletes* sp. 3 (Regali, 1989)	*Retitriletes* spp.	*Schrankipollis reticulatus* ?	*Sergipea naviformis*	*Sergipea simplex*	*Sergipea* spp.	*Spiniferites chebca*	*Spiniferites* spp.	*Steevesipollenites* spp.	*Stellatopollis barghoornii*	*Stellatopollis dubius*	*Stellatopollis* sp.1 (Doyle et al., 1977)	*Stellatopollis* spp.	*Striatipollis reticulatus*	*Subtilisphaera senegalensis*	*Trichodinium castanea*	*Tricolpites* spp.	*Uesuguipollenites callosus*	*Verrucosisporites* spp.	TOTAL
18.00	0.0	0.5	17.6	0.0	0.0	0.0	0.0	0.0	0.0	1.0	8.5	0.0	46.2	0.0	0.0	12.6	1.0	0.0	0.0	0.0	0.0	0.0	0.0	0.0	0.5	0.0	4.0	0.0	0.5	0.0	0.0	0.0	0.0	0.0	0.0	1.0	2.0	0.0	0.0	2.0	0.0	0.0	0.0	0.0	0.0	0.0	0.0	0.0	0.0	0.0	0.0	0.0	0.0	0.0	0.0	0.0	0.0	0.0	0.0	0.5	2.0	199
34.75	0.0	0.0	71.0	0.0	0.0	0.0	0.0	0.0	0.0	0.0	4.7	0.0	15.5	0.0	0.0	3.1	0.5	0.0	0.0	0.0	0.0	0.0	0.0	0.0	0.5	0.0	0.0	0.0	0.0	0.0	0.0	0.0	0.0	0.0	0.0	0.0	0.0	0.5	0.0	1.0	0.0	0.0	0.5	0.0	0.0	0.0	0.0	0.0	0.0	0.0	0.0	0.0	0.0	0.0	0.5	0.0	0.0	0.0	0.0	0.0	2.1	193
57.30	0.0	0.0	68.5	0.0	0.0	0.0	0.0	0.5	0.0	0.0	2.5	0.0	16.5	0.0	0.0	3.0	0.0	0.0	0.0	0.0	0.0	0.0	0.0	0.0	0.5	0.5	0.0	0.0	0.0	0.0	1.0	0.0	0.0	0.0	0.0	0.5	0.0	0.0	0.0	1.0	0.0	0.0	1.0	0.0	0.0	0.0	0.0	0.0	1.0	2.0	0.0	0.0	0.0	0.0	0.0	0.0	0.0	1.0	0.5	0.0	0.0	200
58.95	0.0	1.0	43.0	0.0	0.0	0.0	0.0	0.5	0.0	0.5	3.0	0.0	24.5	0.0	0.0	0.5	0.0	1.0	0.0	0.0	0.0	0.0	0.0	0.0	0.5	2.0	12.5	0.0	0.0	0.0	3.0	0.0	0.0	0.0	0.0	0.0	0.0	0.0	0.0	0.0	0.5	0.0	0.5	0.0	0.0	0.0	0.0	0.0	1.0	6.0	0.0	0.0	0.0	0.0	0.0	0.0	0.0	0.0	0.0	0.0	0.0	200
61.05	0.0	0.0	12.5	0.0	0.0	0.0	0.0	0.0	0.0	0.0	5.2	0.0	22.9	0.0	0.0	1.0	0.0	1.0	0.0	0.0	0.0	0.0	0.0	0.0	2.1	0.0	3.1	0.0	0.0	0.0	0.0	0.0	0.0	0.0	0.0	0.0	0.0	0.0	0.0	0.0	0.0	0.0	1.0	0.0	0.0	0.0	0.0	0.0	1.0	0.0	0.0	0.0	0.0	0.0	0.0	0.0	50.0	0.0	0.0	0.0	0.0	96
61.70	0.0	0.0	9.6	0.0	0.0	0.0	0.0	0.0	0.0	0.0	2.6	0.0	14.0	0.0	0.0	0.0	0.0	0.0	0.0	0.0	0.0	0.0	0.0	0.0	0.9	0.0	1.8	0.0	0.0	0.0	0.0	0.0	0.0	0.0	0.0	0.0	0.0	0.0	0.0	0.0	0.0	0.0	0.0	0.0	0.0	0.0	0.0	0.0	0.0	0.9	0.0	0.0	0.0	0.0	0.0	0.0	70.2	0.0	0.0	0.0	0.0	114
65.80	0.0	0.0	24.5	0.0	0.0	0.0	0.0	0.0	0.0	0.5	1.0	0.0	63.5	0.0	0.0	2.0	0.0	0.0	0.0	0.0	0.0	0.0	0.0	0.0	0.5	0.0	0.5	0.0	0.0	0.0	0.5	0.0	0.0	0.0	0.0	0.0	0.5	0.0	0.0	0.0	0.0	0.0	0.0	0.0	0.0	0.0	0.0	0.0	0.5	2.5	0.0	0.0	0.0	0.0	0.0	0.0	3.5	0.0	0.0	0.0	0.0	200
70.60	0.0	1.0	32.0	0.0	0.5	0.0	0.0	1.0	0.0	1.0	7.0	0.0	46.0	0.0	0.0	4.5	0.0	0.0	0.0	0.0	0.0	0.0	0.0	0.0	0.0	0.5	0.5	0.0	0.0	0.0	0.0	0.0	0.0	0.0	0.0	0.0	0.0	0.0	0.0	0.0	0.0	0.0	1.0	0.0	0.0	0.0	0.0	0.0	0.0	0.5	0.0	0.0	0.0	0.0	0.0	0.0	4.5	0.0	0.0	0.0	0.0	200
82.15	0.0	0.5	42.9	0.0	0.0	0.0	0.0	1.0	0.0	0.0	7.6	0.0	5.1	0.0	0.0	6.1	0.0	0.0	0.0	0.0	0.0	0.0	0.0	0.0	1.5	1.5	2.0	0.0	0.0	0.0	0.0	0.0	0.0	0.0	0.0	1.5	0.5	0.0	0.0	0.0	0.0	0.0	1.0	0.0	0.0	0.0	0.0	0.0	1.0	1.0	0.0	0.0	0.0	0.0	0.0	0.0	25.3	0.0	0.0	0.0	1.5	198
85.70	0.0	0.0	67.0	0.0	0.0	0.0	0.0	1.0	0.0	0.0	5.5	0.0	7.0	0.0	0.0	8.5	0.5	0.0	0.0	0.0	0.0	0.0	0.0	0.0	1.0	0.0	4.5	0.0	0.0	0.0	1.0	0.0	0.0	0.0	0.0	0.0	0.5	0.0	0.0	0.0	0.0	0.0	3.5	0.0	0.0	0.0	0.0	0.0	0.0	0.0	0.0	0.0	0.0	0.0	0.0	0.0	0.0	0.0	0.0	0.0	0.0	200
93.90	0.0	0.5	32.5	0.0	0.0	0.0	0.0	0.0	0.0	0.0	7.0	0.0	10.5	0.0	0.0	21.0	0.0	3.5	0.0	0.0	0.0	0.0	0.0	0.0	0.5	1.5	8.0	0.0	0.0	0.0	0.0	0.0	0.0	0.0	0.0	0.5	3.5	0.0	0.0	0.0	0.0	0.5	0.0	0.0	0.0	0.0	0.0	0.0	0.0	3.5	0.0	0.0	0.5	0.0	0.0	0.0	1.5	2.0	0.0	0.0	3.0	200
96.00	0.0	0.5	39.0	0.0	0.0	0.0	0.0	0.5	0.0	0.0	3.5	0.0	42.5	0.0	0.0	5.5	0.0	0.0	0.0	0.0	0.0	0.0	0.0	0.0	1.0	0.0	0.0	0.0	0.0	0.0	1.5	0.0	0.0	0.0	0.0	0.5	0.5	0.0	0.0	1.0	0.0	0.0	0.0	0.0	0.0	0.0	0.0	0.0	0.0	0.5	0.0	0.0	0.0	0.0	0.0	0.0	1.5	0.0	0.0	1.5	0.5	200
100.90	0.0	0.5	8.0	0.0	0.0	0.5	0.0	0.5	0.0	0.5	11.0	0.0	49.0	0.5	1.5	18.5	0.0	0.5	0.0	0.0	0.5	0.0	0.0	0.0	0.5	0.0	0.0	0.0	0.0	0.0	0.5	0.0	0.0	0.0	1.5	0.5	0.5	0.0	0.0	0.0	0.0	0.0	0.5	0.0	0.0	0.0	0.0	0.0	0.5	0.0	0.0	0.0	0.0	0.0	0.0	0.0	3.0	0.0	0.0	0.5	0.5	200
103.30	0.0	0.0	34.0	0.0	0.0	0.0	0.0	0.5	0.0	0.0	0.5	0.0	14.0	0.0	0.5	3.5	0.0	1.0	0.0	0.0	0.0	0.0	0.0	0.0	0.5	0.0	25.5	0.0	0.0	0.0	0.5	0.0	0.0	0.0	0.0	0.0	1.0	0.0	0.0	0.0	0.0	0.0	0.0	0.0	0.0	0.0	0.0	0.0	0.5	0.0	0.0	0.0	0.0	0.0	0.5	0.0	8.0	9.0	0.0	0.5	0.0	200
125.50	0.0	0.5	22.3	0.0	0.0	0.0	0.0	0.0	0.0	0.0	4.1	0.0	10.9	0.0	0.0	4.1	0.0	2.6	0.0	0.0	0.0	0.0	0.0	0.0	1.6	0.0	6.2	0.0	0.0	0.0	1.6	0.0	0.0	0.0	0.0	3.6	0.5	0.0	0.0	0.0	0.5	0.0	0.0	0.0	0.0	0.0	0.0	0.0	1.6	2.6	0.0	0.0	0.0	0.0	0.0	0.0	24.9	9.8	0.0	0.0	2.6	193
131.70	0.0	0.0	13.0	0.0	0.0	0.0	0.0	0.5	0.0	0.0	0.5	0.0	63.5	0.0	0.0	2.5	0.5	1.0	0.0	0.0	0.0	0.0	0.0	0.5	0.5	0.0	2.0	0.0	0.0	0.0	0.5	0.0	0.0	0.0	0.5	0.0	0.0	0.0	0.0	0.5	0.0	0.0	0.0	0.0	0.0	0.0	0.0	0.0	0.0	0.0	0.0	0.0	0.0	0.0	0.0	0.0	0.5	11.5	0.0	1.0	1.0	200
137.70	0.5	0.0	13.0	0.0	0.0	0.0	0.0	0.0	0.0	0.0	2.0	1.0	63.5	0.0	0.0	4.0	0.5	3.5	0.0	0.0	0.0	0.5	0.0	0.5	0.0	0.0	3.0	0.0	0.0	0.0	0.5	0.0	0.0	0.0	0.0	0.0	1.5	0.0	0.5	0.0	0.0	0.0	0.5	0.0	0.0	0.0	0.0	0.0	0.0	0.0	0.5	0.0	0.0	0.5	0.0	0.5	1.5	2.0	0.0	0.0	0.0	200
141.60	0.0	0.0	27.5	0.0	0.0	0.0	0.0	0.0	0.0	0.0	3.0	0.0	67.0	0.0	0.0	1.0	0.0	0.0	0.0	0.0	0.0	0.0	0.0	0.0	0.0	0.0	0.0	0.0	0.0	0.0	0.0	0.0	0.0	0.0	0.5	0.0	0.0	0.0	0.0	0.5	0.0	0.0	0.5	0.0	0.0	0.0	0.0	0.0	0.0	0.0	0.0	0.0	0.0	0.0	0.0	0.0	0.0	0.0	0.0	0.0	0.0	200
143.97	0.0	0.0	25.5	0.0	0.0	0.0	0.0	0.5	0.0	1.5	10.5	0.0	40.0	0.0	0.0	3.5	0.0	0.0	0.0	0.0	0.0	0.0	0.0	0.0	0.5	0.0	0.0	0.0	0.0	0.0	1.0	0.0	0.0	0.0	1.0	0.5	3.0	0.5	0.0	6.5	0.0	0.0	4.0	0.0	0.0	0.0	0.0	0.5	0.0	0.0	0.5	0.5	0.0	0.0	0.0	0.0	0.0	0.0	0.0	0.0	0.0	200
155.70	0.0	0.8	9.0	0.0	0.0	0.0	0.0	0.0	0.0	0.0	3.8	0.0	68.4	0.0	0.0	1.5	0.0	1.5	0.0	0.0	0.0	0.0	0.0	0.0	0.0	0.8	0.8	0.0	0.0	0.0	1.5	0.0	0.0	0.0	0.8	0.0	0.8	0.0	0.0	0.0	0.0	0.0	0.0	0.0	0.0	0.0	0.0	0.0	0.8	1.5	0.0	0.0	0.0	0.0	0.0	0.0	7.5	0.0	0.0	0.0	0.8	133
158.30	0.0	0.0	33.0	0.0	0.0	0.0	0.0	0.0	0.0	0.0	8.5	0.0	46.0	0.0	0.0	9.1	0.0	0.0	0.0	0.0	0.0	0.0	0.0	0.0	0.0	0.0	1.1	0.6	0.0	0.0	0.0	0.0	0.0	0.0	0.0	0.0	0.0	0.0	0.0	0.0	0.0	0.0	0.0	0.0	0.0	0.0	0.0	0.0	0.0	0.0	0.0	0.0	0.0	0.0	0.0	0.0	0.0	0.0	0.0	0.0	1.7	176
159.43	0.0	0.0	3.5	0.0	0.0	0.0	0.0	0.0	0.0	0.5	0.5	0.0	82.0	0.0	0.0	7.5	0.0	0.0	0.0	0.0	0.0	0.0	0.0	0.0	0.5	0.0	0.0	0.0	0.0	0.0	0.5	0.0	0.0	0.0	0.5	0.5	0.0	0.0	0.0	1.0	0.0	0.0	0.0	0.0	0.0	0.0	0.0	0.0	0.0	0.0	0.0	0.0	0.0	0.0	0.0	0.0	0.0	0.0	0.0	0.0	3.0	200
167.70	0.0	0.0	9.5	0.0	1.5	0.0	0.0	0.5	0.0	1.5	8.5	0.0	58.0	0.0	0.0	8.5	0.0	0.0	0.0	0.0	0.0	0.0	0.0	0.0	0.0	0.0	0.0	0.5	0.0	0.0	0.5	0.0	0.0	0.0	0.0	2.5	0.5	0.0	0.0	2.5	0.0	0.0	1.0	0.0	0.0	0.0	0.0	0.0	0.0	0.0	0.0	0.0	0.0	0.0	1.0	0.5	0.5	0.0	0.0	0.0	2.5	200
174.06	0.5	0.0	7.5	0.0	0.0	0.0	0.0	0.0	0.0	1.0	3.5	0.0	75.0	0.0	0.0	2.5	0.0	0.0	0.0	0.0	0.0	0.0	0.0	0.0	0.5	0.0	0.5	0.0	0.0	0.0	0.5	0.0	0.0	0.0	0.0	0.0	0.0	0.0	0.0	0.0	0.0	0.0	0.0	0.0	0.0	0.0	0.0	0.0	0.5	0.5	0.0	0.0	0.0	0.0	0.0	0.5	5.5	1.0	0.0	0.0	0.5	200
182.10	0.0	0.0	56.7	0.0	0.0	0.0	0.0	0.5	0.0	0.5	6.4	0.0	24.6	0.0	0.0	2.7	0.0	0.5	0.0	0.0	0.0	0.0	0.0	0.0	1.1	0.0	1.1	0.5	0.0	0.0	0.5	0.0	0.0	0.0	0.0	0.5	0.0	0.0	0.0	0.0	0.0	0.0	0.0	0.0	0.0	0.0	0.5	0.0	0.0	0.0	0.0	0.0	0.0	0.0	0.0	0.0	0.0	0.0	0.0	2.7	1.1	187
184.00	0.0	0.5	4.0	0.0	0.0	0.0	0.5	1.0	0.0	0.5	1.0	0.0	87.0	0.0	0.0	2.0	0.0	0.0	0.0	0.0	0.0	0.0	0.0	0.0	1.0	0.0	0.5	0.5	0.0	0.0	0.5	0.0	0.0	0.0	0.0	0.0	0.0	0.0	0.0	0.5	0.0	0.0	0.0	0.0	0.0	0.0	0.0	0.0	0.0	0.0	0.0	0.0	0.0	0.0	0.0	0.0	0.0	0.0	0.0	0.0	0.5	200
209.50	0.0	0.0	15.0	0.0	0.0	0.0	0.0	1.0	0.0	0.0	0.0	0.0	81.0	0.0	0.0	0.5	0.0	0.0	0.0	0.0	0.0	0.0	0.0	0.0	0.0	0.0	0.0	1.0	0.0	0.0	0.0	0.0	0.0	0.0	0.0	0.0	0.0	0.0	0.0	0.5	0.0	0.0	0.0	0.0	0.0	0.0	0.0	0.0	0.0	0.0	0.0	0.0	0.0	0.0	0.0	0.0	0.0	0.0	0.0	0.5	0.5	200
210.55	0.0	0.0	20.0	0.0	0.5	0.0	0.0	1.1	0.0	0.0	7.0	0.0	63.2	0.0	0.0	2.7	0.0	0.5	0.0	0.0	0.0	0.0	0.0	0.0	0.0	0.0	1.1	0.0	0.0	0.0	0.0	0.0	0.0	0.0	0.0	0.0	0.0	1.1	0.0	0.0	0.0	0.0	0.5	0.0	0.0	0.0	0.0	0.0	0.0	0.0	0.0	0.0	0.0	0.0	0.0	0.0	0.5	0.0	0.0	0.5	1.1	185
215.05	0.0	0.0	0.5	0.0	2.5	0.0	0.0	0.0	0.0	0.0	1.5	0.0	88.5	0.0	0.0	3.0	0.0	0.0	0.0	0.0	0.0	0.0	0.0	0.0	1.0	0.0	1.0	0.0	0.0	0.0	0.0	0.0	0.0	0.0	0.0	0.0	0.0	0.0	0.0	0.0	0.0	0.0	0.0	0.0	0.0	0.0	0.0	0.0	0.0	0.0	0.0	0.5	0.0	0.0	0.0	0.0	0.0	0.0	0.0	0.5	1.0	200
216.60	0.0	0.0	13.1	0.0	0.0	0.0	0.0	0.5	0.0	0.0	0.5	0.0	74.4	0.0	0.0	2.0	0.0	1.0	0.0	0.0	0.0	0.0	0.0	0.0	0.5	0.0	1.0	0.5	0.0	0.0	0.0	0.0	0.0	0.0	0.0	0.0	0.0	0.0	0.0	0.5	0.0	0.0	0.0	0.0	0.0	0.0	0.0	0.5	0.0	2.0	0.0	0.0	1.0	0.0	0.0	0.5	0.0	0.0	0.0	1.5	0.5	199
218.10	0.0	0.0	5.1	0.0	0.0	0.0	0.0	0.5	0.0	0.0	2.6	0.0	88.7	0.0	0.0	1.0	0.0	0.0	0.0	0.0	0.0	0.0	0.0	0.0	0.0	0.0	1.0	0.0	0.0	0.0	0.0	0.0	0.0	0.0	0.0	0.0	0.0	0.0	0.0	0.0	0.0	0.0	1.0	0.0	0.0	0.0	0.0	0.0	0.0	0.0	0.0	0.0	0.0	0.0	0.0	0.0	0.0	0.0	0.0	0.0	0.0	195
225.15	0.0	0.0	5.5	0.0	1.5	0.0	0.0	0.0	0.0	0.5	5.0	0.0	84.5	0.0	0.0	0.5	0.0	0.0	0.0	0.0	0.0	0.0	0.0	0.0	0.0	0.0	0.5	0.5	0.0	0.0	0.0	0.0	0.0	0.5	0.0	0.0	0.0	0.0	0.0	0.5	0.0	0.0	0.0	0.0	0.0	0.0	0.0	0.0	0.0	0.0	0.0	0.0	0.0	0.0	0.0	0.0	0.0	0.0	0.0	0.0	0.5	200
230.50	0.0	0.0	7.8	0.0	0.0	0.0	0.0	0.0	0.0	0.0	2.1	0.0	74.5	0.0	0.0	5.7	0.7	0.7	0.0	0.0	0.0	0.0	0.0	0.0	0.7	0.0	0.0	0.0	0.0	0.0	0.7	0.0	0.0	0.0	0.0	0.0	0.0	0.0	0.0	0.0	0.0	0.0	0.7	0.0	0.0	0.0	0.0	0.0	2.8	2.8	0.0	0.0	0.0	0.0	0.7	0.0	0.0	0.0	0.0	0.0	0.0	141
233.27	0.0	0.0	10.5	0.0	0.0	0.0	0.0	0.0	0.0	0.0	4.5	0.0	68.5	0.0	0.0	4.0	0.5	0.0	0.0	0.0	0.0	0.0	0.0	0.0	0.0	0.0	3.0	0.0	0.0	0.0	0.0	0.0	0.0	0.0	0.0	0.0	0.0	0.0	0.0	0.5	0.0	0.0	1.5	0.0	0.0	0.0	0.0	0.0	3.0	3.0	0.0	0.0	0.0	0.0	0.0	0.0	1.0	0.0	0.0	0.0	0.0	200
233.70	0.0	0.0	13.6	0.0	0.0	0.0	0.0	0.0	0.0	0.0	2.5	0.0	78.9	0.0	0.0	1.5	0.5	0.0	0.0	0.0	0.0	0.0	0.0	0.0	0.5	0.0	0.0	0.0	0.0	0.0	0.0	0.5	0.0	0.0	0.0	0.0	0.0	0.0	0.0	0.0	0.0	0.5	1.5	0.0	0.0	0.0	0.0	0.0	0.0	0.0	0.0	0.0	0.0	0.0	0.0	0.0	0.0	0.0	0.0	0.0	0.0	199
242.05	0.0	0.5	10.0	0.0	0.0	0.0	0.0	1.5	0.5	0.0	0.5	0.0	81.0	0.0	0.0	0.5	0.5	0.0	0.0	1.0	0.0	0.0	0.0	0.0	1.0	0.0	0.5	0.0	0.0	0.0	0.5	0.5	0.0	0.0	0.5	0.0	0.0	0.0	0.0	0.5	0.0	0.0	0.0	0.0	0.0	0.0	0.0	0.0	0.0	0.0	0.0	0.0	0.0	0.0	0.0	0.0	0.0	0.0	0.0	0.5	0.0	200
244.35	0.0	0.0	38.7	0.0	0.0	0.0	0.0	1.0	2.5	0.5	6.5	0.0	48.2	0.0	0.0	2.0	0.0	0.0	0.0	0.0	0.0	0.0	0.0	0.0	0.0	0.0	0.0	0.0	0.0	0.0	0.0	0.0	0.0	0.0	0.0	0.0	0.0	0.0	0.0	0.5	0.0	0.0	0.0	0.0	0.0	0.0	0.0	0.0	0.0	0.0	0.0	0.0	0.0	0.0	0.0	0.0	0.0	0.0	0.0	0.0	0.0	199
246.75	0.0	0.0	20.5	0.0	0.0	0.0	0.0	0.5	2.5	1.0	10.0	0.0	60.0	0.0	0.0	1.5	0.0	0.5	0.0	0.0	0.0	0.0	0.0	0.0	0.0	0.0	0.5	0.5	0.0	0.0	0.0	0.0	0.0	0.0	0.0	0.0	0.0	0.0	0.0	0.0	0.0	0.0	1.5	0.0	0.0	0.0	0.0	0.0	0.0	0.0	0.0	0.0	0.0	0.0	0.5	0.0	0.0	0.0	0.0	0.0	0.5	200
248.40	0.0	0.0	10.7	0.0	0.0	0.0	0.0	1.0	0.5	0.5	9.2	0.0	71.4	0.0	0.0	2.0	0.0	0.0	0.0	0.0	0.0	0.0	0.0	0.0	0.0	0.0	0.0	1.0	0.0	0.0	0.0	0.0	0.0	0.0	1.0	0.0	0.0	0.0	0.0	1.5	0.0	0.0	0.5	0.0	0.0	0.0	0.0	0.0	0.0	0.0	0.0	0.0	0.0	0.0	0.0	0.0	0.0	0.0	0.0	0.0	0.0	196
250.73	0.0	0.0	9.0	0.0	0.0	0.0	0.0	2.0	0.5	0.0	6.0	0.0	76.5	0.0	0.0	1.0	0.0	0.0	0.0	0.0	0.0	0.0	0.0	0.0	0.0	0.0	0.0	0.0	0.0	0.0	0.0	0.0	0.0	0.0	1.5	0.0	0.5	0.0	0.0	0.5	0.0	0.0	0.0	0.0	0.0	0.0	0.0	0.0	0.0	0.5	0.0	0.0	0.0	0.0	0.0	0.0	0.0	0.0	0.0	2.0	0.0	200
252.75	0.0	0.0	9.0	0.0	0.0	0.0	0.0	0.0	0.0	0.0	3.0	0.0	70.5	0.0	0.0	3.0	0.0	0.0	0.0	0.0	0.0	0.0	0.0	0.0	0.0	0.0	0.0	0.0	0.0	0.0	0.0	0.0	0.0	0.0	0.5	0.0	0.0	0.0	0.0	0.5	0.0	0.0	0.5	0.0	0.0	0.0	0.0	0.0	2.0	6.0	0.0	0.0	0.0	0.0	0.0	0.0	5.0	0.0	0.0	0.0	0.0	200
254.83	0.0	0.0	11.5	0.0	0.0	0.0	0.0	0.0	0.0	0.0	1.0	0.0	84.0	0.0	0.0	0.0	0.0	0.0	0.0	0.0	0.0	0.0	0.0	0.0	0.0	0.0	0.0	0.0	0.0	0.0	0.5	0.0	0.0	0.0	0.0	0.0	0.0	0.0	0.0	0.0	0.0	0.0	2.0	0.0	0.0	0.0	0.0	0.0	0.5	0.0	0.0	0.0	0.0	0.0	0.0	0.0	0.0	0.0	0.0	0.5	0.0	200
255.57	0.0	0.0	13.0	0.0	0.0	0.0	0.0	0.0	0.0	0.0	0.5	0.0	82.0	0.0	0.0	0.5	0.0	0.0	0.0	0.0	0.0	0.0	0.0	0.0	0.0	0.0	0.5	0.5	0.0	0.0	0.0	0.0	0.0	0.0	0.0	0.0	0.0	0.0	0.0	0.0	0.0	0.0	1.5	0.0	0.0	0.0	0.0	0.0	0.5	1.0	0.0	0.0	0.0	0.0	0.0	0.0	0.0	0.0	0.0	0.0	0.0	200
257.65	0.0	0.0	15.0	0.0	0.0	0.0	0.0	0.0	1.0	0.0	2.5	0.0	73.0	0.0	0.0	1.0	0.0	0.0	0.5	0.0	0.0	0.0	0.0	0.0	0.0	0.0	1.5	0.5	0.0	0.0	0.0	0.5	0.0	0.0	0.0	0.0	0.0	0.0	0.0	0.0	0.0	0.0	1.5	0.0	0.0	0.0	0.0	0.0	0.5	1.5	0.0	0.0	0.0	0.0	0.5	0.0	0.0	0.5	0.0	0.0	0.0	200
259.87	0.0	0.0	14.5	0.0	0.0	0.0	0.0	0.0	0.0	0.0	1.5	0.0	77.5	0.0	0.0	1.5	0.0	0.0	0.0	0.0	0.0	0.0	0.0	0.0	0.5	0.0	0.5	0.0	0.0	0.0	1.0	0.0	0.0	0.0	0.0	0.0	0.0	0.0	0.0	0.0	0.0	0.0	2.5	0.0	0.0	0.0	0.0	0.0	0.5	0.0	0.0	0.0	0.0	0.0	0.0	0.0	0.0	0.0	0.0	0.0	0.0	200
261.70	0.0	0.0	6.0	0.0	0.0	0.0	0.0	0.0	0.0	0.0	1.0	0.0	82.5	0.0	0.0	1.5	0.0	0.0	0.0	0.0	0.0	0.0	0.0	0.0	0.5	0.0	4.5	0.0	0.0	0.0	0.5	0.0	0.0	0.0	0.0	0.0	0.0	0.0	0.0	0.5	0.0	0.0	1.0	0.0	0.0	0.0	0.0	0.0	0.0	2.0	0.0	0.0	0.0	0.0	0.0	0.0	0.0	0.0	0.0	0.0	0.0	200
263.32	0.0	0.0	12.8	0.0	0.0	0.0	0.0	0.5	0.0	0.0	1.5	0.0	82.1	0.0	0.0	1.0	0.5	0.0	0.0	0.0	0.0	0.0	0.0	0.0	0.5	0.0	0.0	0.0	0.0	0.0	0.0	0.0	0.0	0.0	0.0	0.0	0.0	0.0	0.0	0.0	0.0	0.0	1.0	0.0	0.0	0.0	0.0	0.0	0.0	0.0	0.0	0.0	0.0	0.0	0.0	0.0	0.0	0.0	0.0	0.0	0.0	195
265.78	1.5	0.0	20.5	0.0	0.0	0.0	0.0	0.0	0.5	0.0	1.5	0.0	67.5	0.0	0.0	3.0	0.0	0.0	0.0	0.0	0.0	0.0	0.0	0.0	0.5	0.0	1.0	0.0	0.0	0.0	0.0	0.0	0.0	0.0	0.5	0.0	0.0	0.0	0.0	0.0	0.0	0.0	1.5	0.0	0.0	0.0	0.0	0.0	0.5	0.5	0.0	0.0	0.0	0.0	0.0	0.0	0.5	0.0	0.0	0.5	0.0	200
268.40	0.0	0.0	17.6	0.0	0.0	0.0	0.0	0.0	0.0	0.0	0.0	0.0	73.1	0.0	0.0	1.7	0.0	0.0	0.0	0.0	0.0	0.0	0.0	0.0	0.0	0.8	0.8	0.0	0.0	0.0	0.0	0.0	0.0	0.0	0.0	0.0	0.0	0.0	0.0	0.0	0.0	0.0	2.5	0.0	0.0	0.0	0.0	0.0	1.7	1.7	0.0	0.0	0.0	0.0	0.0	0.0	0.0	0.0	0.0	0.0	0.0	119
271.42	0.0	0.0	3.5	0.0	0.0	0.0	0.0	0.0	0.0	0.0	0.0	0.0	90.5	0.0	0.0	2.5	0.0	0.0	0.0	0.0	0.0	0.0	0.0	0.0	0.0	0.0	1.5	0.0	0.0	0.0	0.5	0.0	0.0	0.0	0.5	0.0	0.0	0.5	0.0	0.0	0.0	0.0	0.5	0.0	0.0	0.0	0.0	0.0	0.0	0.0	0.0	0.0	0.0	0.0	0.0	0.0	0.0	0.0	0.0	0.0	0.0	200
273.20	0.0	0.0	8.3	0.0	0.0	0.0	0.0	0.0	0.0	0.0	1.9	0.0	85.9	0.0	0.0	0.6	0.0	0.0	0.0	0.0	0.0	0.0	0.0	0.0	0.0	0.6	1.3	0.6	0.0	0.0	0.6	0.0	0.0	0.0	0.0	0.0	0.0	0.0	0.0	0.0	0.0	0.0	0.0	0.0	0.0	0.0	0.0	0.0	0.0	0.0	0.0	0.0	0.0	0.0	0.0	0.0	0.0	0.0	0.0	0.0	0.0	156
275.72	0.0	0.0	9.0	0.0	0.0	0.0	0.5	0.0	0.0	0.0	2.0	0.0	78.5	0.0	0.0	1.0	0.0	0.0	0.0	0.0	0.0	0.0	0.0	0.0	1.0	0.0	6.5	0.5	0.0	0.0	0.0	0.0	0.0	0.0	0.0	0.0	0.0	0.0	0.0	0.0	0.0	0.0	0.0	0.0	0.0	0.0	0.0	0.0	0.0	0.5	0.0	0.0	0.0	0.0	0.0	0.0	0.0	0.0	0.0	0.0	0.5	200
277.75	0.0	0.0	7.3	0.0	0.0	0.0	0.0	0.0	0.0	0.0	4.4	0.0	81.8	0.0	0.0	2.2	0.0	0.0	0.0	0.0	0.0	0.0	0.7	0.0	0.0	0.0	0.7	0.0	0.0	0.0	0.7	0.0	0.0	0.0	0.7	0.0	0.0	0.0	0.0	0.7	0.0	0.0	0.7	0.0	0.0	0.0	0.0	0.0	0.0	0.0	0.0	0.0	0.0	0.0	0.0	0.0	0.0	0.0	0.0	0.0	0.0	137
283.83	0.0	0.0	11.0	0.0	0.0	0.0	0.0	1.0	0.0	0.0	1.0	0.0	78.0	0.0	0.0	1.0	0.0	0.0	0.0	0.0	0.0	0.0	0.0	0.0	0.0	1.0	2.5	0.0	0.0	0.0	0.0	0.0	0.0	0.0	0.0	0.0	0.0	0.0	0.0	0.5	0.0	0.0	0.0	0.0	0.0	0.0	0.0	0.0	0.5	2.5	0.0	0.0	0.0	0.0	0.0	0.0	0.0	0.0	0.0	1.0	0.0	200
285.83	0.0	0.0	3.0	0.0	0.0	0.0	0.0	0.5	0.5	0.0	0.5	0.0	64.5	0.0	0.0	0.5	0.5	0.0	0.0	0.0	0.0	0.0	0.0	0.0	0.0	0.0	0.5	0.0	0.0	0.0	0.5	0.0	0.0	0.0	0.0	0.0	0.0	0.0	0.0	0.0	0.0	0.0	0.0	0.0	0.0	0.0	0.0	0.0	0.0	0.0	0.0	0.0	0.0	0.0	0.0	0.0	28.5	0.0	0.0	0.5	0.0	200
287.02	0.0	0.0	5.0	1.0	0.0	0.0	0.0	0.0	0.0	0.0	0.5	0.0	68.0	0.0	0.0	0.5	0.0	0.0	0.0	0.0	0.0	0.0	0.0	0.0	0.0	0.0	2.0	0.0	0.0	0.0	0.0	0.0	0.0	0.0	0.0	0.0	0.0	0.0	0.0	0.0	0.0	0.0	0.0	0.5	0.0	0.0	0.0	0.0	2.0	0.0	0.0	0.0	0.0	0.0	0.0	0.0	20.5	0.0	0.0	0.0	0.0	200
292.25	0.0	0.5	11.0	0.0	0.0	0.0	0.0	0.0	0.0	0.5	1.0	0.0	69.0	0.0	0.0	2.0	0.0	1.0	0.0	0.0	0.0	0.0	0.0	0.0	0.0	3.0	3.5	0.0	0.0	0.0	0.5	0.0	0.0	0.0	0.0	0.0	1.0	0.0	0.0	0.0	0.0	0.0	1.5	0.0	0.0	0.0	0.0	0.0	3.5	2.0	0.0	0.0	0.0	0.0	0.0	0.0	0.0	0.0	0.0	0.0	0.0	200
294.75	0.0	0.0	7.0	0.0	0.0	0.0	0.0	0.0	0.0	0.0	1.0	0.0	83.0	0.0	0.0	0.5	1.0	0.0	0.0	0.0	0.0	0.0	0.0	0.0	0.5	0.5	1.0	0.5	0.0	0.5	0.0	0.0	0.0	0.0	0.0	0.0	0.5	0.0	0.0	0.0	0.0	0.0	0.5	0.0	0.0	0.0	0.0	0.0	1.5	2.0	0.0	0.0	0.0	0.0	0.0	0.0	0.0	0.0	0.0	0.0	0.0	200
298.30	0.0	0.0	5.0	0.0	0.0	0.0	0.0	0.0	0.0	0.0	0.5	0.0	89.0	0.0	0.5	1.0	0.0	0.0	0.0	0.0	0.0	0.0	0.0	0.0	0.5	0.0	1.0	0.5	0.0	0.0	0.5	0.0	0.0	0.0	0.0	0.0	0.5	0.0	0.0	0.0	0.0	0.0	0.5	0.0	0.0	0.0	0.0	0.0	0.5	0.0	0.0	0.0	0.0	0.0	0.0	0.0	0.0	0.0	0.0	0.0	0.0	200
300.93	0.0	0.0	7.5	0.0	0.0	0.5	0.0	0.0	0.0	0.0	0.5	0.0	84.0	0.0	0.0	0.0	0.0	0.0	0.0	0.0	0.0	0.0	0.0	0.0	0.5	1.0	0.5	0.5	0.0	0.0	0.0	0.5	0.0	0.0	0.0	0.0	0.5	0.0	0.0	0.0	0.0	0.0	0.5	0.0	0.0	0.0	0.0	0.0	0.5	1.5	0.0	0.0	0.0	0.0	0.0	0.0	0.0	0.0	0.0	1.0	0.5	200
302.25	0.0	0.0	11.0	0.0	0.0	0.0	0.0	0.0	0.0	0.0	0.0	0.0	86.5	0.0	0.0	0.5	0.5	0.0	0.0	0.0	0.0	0.0	0.0	0.0	0.5	0.0	0.5	0.0	0.0	0.0	0.0	0.0	0.0	0.0	0.0	0.0	0.5	0.0	0.0	0.0	0.0	0.0	0.0	0.0	0.0	0.0	0.0	0.0	0.0	0.0	0.0	0.0	0.0	0.0	0.0	0.0	0.0	0.0	0.0	0.0	0.0	200
304.18	0.0	0.0	12.5	0.0	0.0	0.0	0.0	0.0	0.0	0.0	0.0	0.0	78.5	0.0	0.0	0.0	0.5	0.0	0.0	0.0	0.0	0.0	0.0	0.0	0.5	1.5	3.5	0.5	0.0	0.0	0.5	0.0	0.0	0.0	0.0	0.0	0.0	0.0	0.0	0.0	0.0	0.0	0.5	0.0	0.0	0.0	0.0	0.0	0.0	0.0	0.0	0.0	0.0	0.0	0.0	0.0	0.0	0.0	0.0	1.5	0.0	200
306.00	0.0	0.0	6.5	0.0	0.0	0.0	0.0	0.0	0.0	0.0	0.5	0.0	86.5	0.0	0.0	0.0	0.0	0.0	0.0	0.0	0.0	0.0	0.0	0.0	0.5	0.5	3.5	0.5	0.0	0.0	0.0	0.0	0.0	0.0	0.0	0.0	0.0	0.0	0.0	0.0	0.0	0.0	0.0	0.0	0.0	0.0	0.0	0.0	0.0	1.0	0.0	0.0	0.0	0.0	0.0	0.0	0.0	0.0	0.0	0.0	0.5	200
309.05	0.0	0.0	3.0	0.0	0.0	0.0	0.0	0.0	0.0	0.0	1.0	0.0	88.0	0.0	0.0	0.5	0.0	0.0	0.0	0.0	0.0	0.0	0.0	0.0	0.0	0.0	1.5	0.5	0.0	0.0	0.0	0.0	0.0	0.0	0.0	0.0	0.0	0.0	0.0	0.0	0.0	0.0	0.0	0.0	0.0	0.0	0.0	0.0	0.0	1.5	0.0	0.0	0.0	0.0	0.0	0.0	4.0	0.0	0.0	0.0	0.0	200
315.23	0.0	0.0	2.5	0.0	0.0	0.0	0.0	0.0	0.0	0.0	1.5	0.0	93.5	0.0	0.0	0.5	0.0	0.5	0.0	0.0	0.0	0.0	0.0	0.0	0.5	0.0	0.0	0.0	0.0	0.0	0.0	0.0	0.0	0.0	0.0	0.0	0.0	0.0	0.0	0.0	0.0	0.0	0.0	0.5	0.0	0.0	0.0	0.0	0.0	0.5	0.0	0.0	0.0	0.0	0.0	0.0	0.0	0.0	0.0	0.0	0.0	200
317.12	0.0	0.0	3.0	0.0	0.0	0.0	0.0	0.0	0.0	0.5	2.0	0.0	87.5	0.0	0.0	0.0	0.0	0.0	0.0	0.0	0.0	0.0	0.0	0.0	0.5	0.0	2.5	0.0	0.0	0.0	0.0	0.0	0.0	0.0	0.0	0.0	0.5	0.0	0.0	0.0	0.0	0.0	0.5	0.0	0.0	0.0	0.0	0.0	0.0	3.0	0.0	0.0	0.0	0.0	0.0	0.0	0.0	0.0	0.0	0.0	0.0	200
318.00	0.0	0.0	3.9	0.0	0.0	0.6	0.0	0.6	0.0	0.0	1.1	0.0	93.3	0.0	0.0	0.0	0.0	0.0	0.0	0.0	0.0	0.0	0.0	0.0	0.0	0.0	0.0	0.0	0.0	0.0	0.0	0.0	0.0	0.0	0.0	0.0	0.0	0.0	0.0	0.6	0.0	0.0	0.0	0.0	0.0	0.0	0.0	0.0	0.0	0.0	0.0	0.0	0.0	0.0	0.0	0.0	0.0	0.0	0.0	0.0	0.0	180
322.95	0.0	0.0	6.5	0.5	0.0	0.0	0.0	0.0	0.0	0.0	2.0	0.0	87.0	0.0	0.0	0.0	0.0	0.0	0.0	0.0	0.0	0.0	0.0	0.0	0.0	0.0	1.0	0.0	0.0	0.0	0.0	0.0	0.0	0.0	0.0	0.0	0.0	0.0	0.0	2.0	0.0	0.0	0.5	0.0	0.0	0.0	0.0	0.0	0.0	0.5	0.0	0.0	0.0	0.0	0.0	0.0	0.0	0.0	0.0	0.0	0.0	200
325.80	0.0	0.0	0.6	0.0	0.0	0.0	0.0	0.0	0.0	0.0	0.0	0.0	95.7	0.0	0.0	0.0	0.0	0.0	0.0	0.0	0.0	0.0	0.0	0.0	0.0	0.0	3.1	0.0	0.0	0.0	0.0	0.0	0.0	0.0	0.0	0.0	0.0	0.0	0.0	0.0	0.0	0.0	0.0	0.0	0.0	0.0	0.0	0.0	0.6	0.0	0.0	0.0	0.0	0.0	0.0	0.0	0.0	0.0	0.0	0.0	0.0	161
327.31	0.0	0.0	1.5	0.0	0.0	0.0	0.0	0.0	0.0	0.0	0.5	0.0	81.5	0.0	0.0	0.5	0.5	0.0	0.0	0.0	0.0	0.0	0.0	0.0	0.5	0.5	10.0	0.0	0.0	0.0	0.0	0.0	0.0	0.0	0.0	0.0	0.5	0.0	0.0	0.0	0.0	0.0	0.0	0.0	0.0	0.0	0.0	0.0	2.0	1.5	0.0	0.0	0.0	0.0	0.0	0.0	0.0	0.0	0.0	0.0	0.5	200
328.67	0.0	1.0	1.0	0.0	0.0	0.0	0.0	0.5	0.0	0.0	1.0	0.0	71.5	0.0	0.0	0.5	0.0	0.0	0.0	0.0	0.0	0.0	0.0	0.0	0.5	0.5	13.5	0.0	0.0	0.0	1.0	0.0	0.0	0.0	0.0	0.0	0.0	0.0	0.0	0.0	0.0	0.0	0.0	0.0	0.0	0.0	0.0	0.0	3.0	6.0	0.0	0.0	0.0	0.0	0.0	0.0	0.0	0.0	0.0	0.0	0.0	200
329.50	0.0	0.0	1.0	0.0	0.0	0.0	0.0	0.0	0.0	0.0	1.0	0.0	87.0	0.0	0.0	0.0	0.5	0.0	0.0	0.0	0.0	0.0	0.0	0.0	0.0	0.0	5.0	0.5	0.0	0.0	0.0	0.0	0.0	0.0	0.0	0.0	1.0	0.0	0.0	0.0	0.0	0.0	1.0	0.0	0.0	0.0	0.0	0.0	3.0	0.0	0.0	0.0	0.0	0.0	0.0	0.0	0.0	0.0	0.0	0.0	0.0	200
331.50	0.0	0.0	23.6	0.9	0.0	0.0	0.0	0.0	0.0	0.0	0.0	0.0	69.1	0.0	0.0	0.9	0.0	0.0	0.0	0.0	0.0	0.0	0.0	1.8	2.7	0.0	0.0	0.0	0.0	0.0	0.0	0.9	0.0	0.0	0.0	0.0	0.0	0.0	0.0	0.0	0.0	0.0	0.0	0.0	0.0	0.0	0.0	0.0	0.0	0.0	0.0	0.0	0.0	0.0	0.0	0.0	0.0	0.0	0.0	0.0	0.0	110
339.80	0.0	0.0	7.5	0.0	0.0	0.0	0.0	0.0	0.0	0.0	0.5	0.0	81.5	0.0	0.0	0.0	0.0	0.0	0.0	0.0	0.0	0.0	0.0	0.0	0.5	0.0	7.5	0.0	0.0	0.0	1.5	0.0	0.0	0.0	0.0	0.0	0.0	0.0	0.0	0.0	0.0	0.0	0.0	0.0	0.0	0.0	0.0	0.0	1.0	0.0	0.0	0.0	0.0	0.0	0.0	0.0	0.0	0.0	0.0	0.0	0.0	200
340.40	0.0	0.0	27.5	0.0	0.0	0.0	0.0	0.0	0.0	0.0	0.0	0.0	70.0	0.0	0.0	0.5	0.5	0.0	0.0	0.0	0.0	0.0	0.0	0.0	0.5	0.0	0.0	0.0	0.0	0.0	1.0	0.0	0.0	0.0	0.0	0.0	0.0	0.0	0.0	0.0	0.0	0.0	0.0	0.0	0.0	0.0	0.0	0.0	0.0	0.0	0.0	0.0	0.0	0.0	0.0	0.0	0.0	0.0	0.0	0.0	0.0	200
341.30	0.0	0.0	24.0	0.0	0.0	0.0	0.0	0.0	0.0	0.5	2.5	0.0	70.5	0.0	0.0	0.0	0.0	0.0	0.0	0.0	0.0	0.0	0.0	1.0	0.5	0.0	0.0	0.0	0.0	0.0	1.0	0.0	0.0	0.0	0.0	0.0	0.0	0.0	0.0	0.0	0.0	0.0	0.0	0.0	0.0	0.0	0.0	0.0	0.0	0.0	0.0	0.0	0.0	0.0	0.0	0.0	0.0	0.0	0.0	0.0	0.0	200
350.50	0.0	0.0	9.0	0.0	0.0	0.0	0.0	0.0	0.0	0.0	3.5	0.0	84.0	0.0	0.0	0.5	0.0	0.0	0.0	0.0	0.0	0.0	0.0	0.0	0.5	0.0	0.0	0.0	0.0	0.5	0.0	0.0	0.0	0.0	0.0	0.0	0.0	0.0	0.0	0.0	0.0	0.0	1.0	0.0	0.0	0.0	0.0	0.0	0.0	0.0	0.0	0.0	0.0	0.0	0.0	0.0	0.0	0.0	0.0	0.0	1.0	200
351.50	0.0	0.0	18.5	0.5	0.0	0.0	0.0	0.0	0.5	1.0	1.0	0.0	68.5	0.0	0.0	3.0	0.0	0.0	0.0	0.0	0.0	0.0	0.0	0.0	2.5	0.0	0.0	0.0	0.0	0.0	1.0	0.0	0.0	1.0	0.0	0.0	0.0	0.5	0.0	0.0	0.0	0.0	1.0	0.0	0.0	0.0	0.0	0.0	0.0	0.0	0.0	0.0	0.5	0.0	0.0	0.0	0.0	0.0	0.0	0.0	0.5	200
362.72	0.0	0.7	15.8	0.0	0.0	0.0	0.0	0.0	0.0	0.0	0.0	0.0	82.9	0.0	0.0	0.0	0.0	0.0	0.0	0.0	0.0	0.0	0.0	0.0	0.0	0.0	0.0	0.0	0.0	0.0	0.7	0.0	0.0	0.0	0.0	0.0	0.0	0.0	0.0	0.0	0.0	0.0	0.0	0.0	0.0	0.0	0.0	0.0	0.0	0.0	0.0	0.0	0.0	0.0	0.0	0.0	0.0	0.0	0.0	0.0	0.0	152
363.83	0.0	0.0	27.0	0.0	0.0	0.0	0.0	0.0	0.0	0.0	0.0	0.0	67.6	0.0	0.0	0.0	0.0	0.0	0.0	0.0	1.4	0.0	0.0	0.0	1.4	0.0	0.0	1.4	0.0	0.0	1.4	0.0	0.0	0.0	0.0	0.0	0.0	0.0	0.0	0.0	0.0	0.0	0.0	0.0	0.0	0.0	0.0	0.0	0.0	0.0	0.0	0.0	0.0	0.0	0.0	0.0	0.0	0.0	0.0	0.0	0.0	74
368.30	0.0	0.5	25.5	0.0	0.0	0.0	0.0	0.0	0.0	0.0	0.5	0.0	71.0	0.0	0.0	0.0	0.0	0.0	0.0	0.0	0.0	0.0	0.0	0.0	1.5	0.0	0.0	0.5	0.0	0.0	0.0	0.0	0.0	0.0	0.0	0.0	0.0	0.0	0.0	0.0	0.0	0.0	0.0	0.0	0.5	0.0	0.0	0.0	0.0	0.0	0.0	0.0	0.0	0.0	0.0	0.0	0.0	0.0	0.0	0.0	0.0	200
369.13	0.0	0.0	27.5	0.0	0.0	0.0	0.0	0.0	0.0	0.0	0.0	0.0	71.0	0.0	0.0	0.5	0.0	0.0	0.0	0.0	0.0	0.0	0.0	0.0	0.0	0.0	0.0	0.0	0.0	0.0	0.0	0.0	0.0	1.0	0.0	0.0	0.0	0.0	0.0	0.0	0.0	0.0	0.0	0.0	0.0	0.0	0.0	0.0	0.0	0.0	0.0	0.0	0.0	0.0	0.0	0.0	0.0	0.0	0.0	0.0	0.0	200
372.95	0.0	0.0	26.0	0.0	0.0	0.0	0.0	0.0	0.0	0.0	0.5	0.0	73.0	0.0	0.0	0.0	0.0	0.0	0.0	0.0	0.0	0.0	0.0	0.0	0.0	0.0	0.0	0.0	0.0	0.0	0.0	0.0	0.0	0.0	0.0	0.0	0.5	0.0	0.0	0.0	0.0	0.0	0.0	0.0	0.0	0.0	0.0	0.0	0.0	0.0	0.0	0.0	0.0	0.0	0.0	0.0	0.0	0.0	0.0	0.0	0.0	200
374.15	0.0	1.0	18.5	0.0	0.0	0.0	0.0	0.5	0.0	0.0	1.5	0.0	74.0	0.0	0.0	1.0	0.0	0.0	0.0	0.0	0.0	0.0	0.0	0.0	1.0	0.0	0.0	0.0	0.0	0.0	0.5	0.5	0.0	0.0	0.0	0.0	0.5	0.0	0.0	0.0	0.0	0.0	0.5	0.0	0.0	0.0	0.0	0.0	0.0	0.0	0.0	0.0	0.0	0.0	0.0	0.0	0.0	0.0	0.0	0.0	0.5	200
378.77	0.0	0.0	23.5	0.0	0.5	0.0	0.0	0.0	0.0	0.0	1.0	0.0	71.5	0.0	0.0	0.0	1.0	0.0	0.0	0.0	0.0	0.0	0.0	0.0	0.0	0.0	0.5	0.0	0.0	0.0	0.5	0.0	0.0	0.0	0.0	0.0	0.0	0.0	0.0	0.0	0.0	0.0	0.5	0.0	0.0	0.0	0.0	0.0	0.0	0.0	0.0	0.0	0.5	0.0	0.0	0.0	0.0	0.0	0.0	0.0	0.5	200
384.15	0.0	0.5	21.5	0.0	0.0	0.0	0.0	0.5	0.0	0.0	1.0	0.0	73.5	0.0	0.0	0.0	0.0	0.0	0.0	0.0	0.0	0.0	0.0	0.5	1.5	0.0	0.0	0.5	0.0	0.0	0.5	0.0	0.0	0.0	0.0	0.0	0.0	0.0	0.0	0.0	0.0	0.0	0.0	0.0	0.0	0.0	0.0	0.0	0.0	0.0	0.0	0.0	0.0	0.0	0.0	0.0	0.0	0.0	0.0	0.0	0.0	200
385.27	0.0	0.0	32.0	0.5	0.0	0.0	0.0	0.5	0.0	0.0	0.5	0.0	64.0	0.0	0.0	0.0	0.5	0.0	0.0	0.0	0.0	0.0	0.0	0.0	1.0	0.0	0.0	0.0	0.0	0.0	0.0	0.5	0.0	0.0	0.0	0.0	0.0	0.0	0.0	0.0	0.0	0.0	0.0	0.5	0.0	0.0	0.0	0.0	0.0	0.0	0.0	0.0	0.0	0.0	0.0	0.0	0.0	0.0	0.0	0.0	0.0	200
386.86	0.0	0.0	16.5	0.0	0.0	0.0	0.0	0.0	0.0	0.0	1.5	0.0	79.5	0.0	0.0	0.0	0.0	0.0	0.5	0.0	0.0	0.0	0.0	0.0	1.0	0.0	0.0	0.0	0.0	0.0	0.5	0.0	0.0	0.0	0.5	0.0	0.0	0.0	0.0	0.0	0.0	0.0	0.0	0.0	0.0	0.0	0.0	0.0	0.0	0.0	0.0	0.0	0.0	0.0	0.0	0.0	0.0	0.0	0.0	0.0	0.0	200
389.35	0.0	0.0	8.3	0.0	0.0	0.0	0.0	0.0	0.0	0.0	1.8	0.0	88.1	0.0	0.0	0.9	0.0	0.0	0.9	0.0	0.0	0.0	0.0	0.0	0.0	0.0	0.0	0.0	0.0	0.0	0.0	0.0	0.0	0.0	0.0	0.0	0.0	0.0	0.0	0.0	0.0	0.0	0.0	0.0	0.0	0.0	0.0	0.0	0.0	0.0	0.0	0.0	0.0	0.0	0.0	0.0	0.0	0.0	0.0	0.0	0.0	109
393.25	0.0	0.0	25.5	0.5	0.0	0.0	0.0	0.0	0.0	0.0	0.5	0.0	68.0	0.0	0.0	0.5	0.5	0.0	0.0	0.0	0.0	0.0	0.0	0.0	1.5	0.0	0.0	0.0	0.0	0.0	0.5	0.0	0.0	0.0	0.0	0.0	0.0	0.0	0.5	0.0	0.0	0.0	0.0	0.0	0.0	0.0	0.0	0.0	0.0	0.0	0.0	0.0	0.0	0.0	0.5	0.5	0.5	0.0	0.0	0.0	0.5	200
396.62	0.0	0.0	3.0	0.5	0.0	0.0	0.0	0.0	0.5	0.0	2.0	0.0	88.5	0.0	0.5	0.0	0.0	0.0	0.0	0.0	0.0	0.0	0.0	0.0	1.5	0.0	0.0	0.0	0.0	0.0	1.5	0.0	0.0	0.0	0.0	0.0	1.0	0.0	0.0	0.0	0.0	0.0	1.0	0.0	0.0	0.0	0.0	0.0	0.0	0.0	0.0	0.0	0.0	0.0	0.0	0.0	0.0	0.0	0.0	0.0	0.0	200
415.88	0.0	0.0	3.0	0.0	0.0	0.0	0.0	0.0	0.0	0.0	1.0	0.0	94.0	0.0	0.0	0.5	0.0	0.0	0.0	0.0	0.0	0.0	0.0	0.0	0.5	0.0	0.0	0.0	0.0	0.0	0.0	0.0	0.0	0.0	0.0	0.0	0.0	0.0	0.0	0.0	0.0	0.0	0.5	0.0	0.0	0.0	0.0	0.0	0.0	0.0	0.0	0.0	0.0	0.0	0.0	0.0	0.0	0.0	0.0	0.0	0.5	200
440.65	0.0	0.0	1.2	0.0	0.0	0.0	0.0	0.0	0.0	0.0	1.2	0.0	92.4	0.0	0.0	1.2	0.0	0.0	0.0	0.0	0.0	0.0	0.0	0.0	0.0	0.0	3.5	0.0	0.0	0.0	0.0	0.0	0.0	0.0	0.0	0.0	0.0	0.0	0.0	0.0	0.0	0.0	0.0	0.0	0.0	0.0	0.0	0.0	0.0	0.0	0.0	0.0	0.0	0.0	0.0	0.0	0.6	0.0	0.0	0.0	0.0	172
443.20	0.0	0.0	4.5	0.0	0.0	0.0	0.0	0.0	0.0	0.0	0.5	0.0	61.5	0.0	0.0	0.5	0.5	0.0	0.0	0.0	0.0	0.0	0.0	0.0	0.0	0.0	30.5	0.0	0.0	0.0	0.5	0.0	0.0	0.0	0.0	0.0	0.0	0.0	0.0	0.0	0.0	0.0	0.5	0.0	0.0	0.0	0.0	0.0	0.0	1.0	0.0	0.0	0.0	0.0	0.0	0.0	0.0	0.0	0.0	0.0	0.0	200
444.17	0.0	0.0	7.0	0.0	0.0	0.5	0.0	2.5	0.5	1.0	2.5	0.0	81.0	0.0	0.0	0.0	0.0	0.0	0.0	0.0	0.0	0.0	0.0	0.0	0.0	0.5	3.5	0.0	0.0	0.0	0.0	0.0	0.0	0.0	0.0	0.0	0.0	0.0	0.0	0.0	0.0	0.0	0.0	0.0	0.0	0.0	0.0	0.0	0.0	0.0	0.0	0.0	0.0	0.0	0.0	0.0	0.0	0.0	0.0	0.0	1.0	200
451.40	0.0	0.0	0.0	0.0	0.0	0.0	0.0	0.0	0.0	0.0	1.2	0.0	32.5	0.0	0.0	0.0	0.0	0.0	0.0	0.0	0.0	0.0	0.0	0.0	0.0	0.0	65.1	0.0	0.0	0.0	0.0	0.0	0.0	0.0	0.0	0.0	1.2	0.0	0.0	0.0	0.0	0.0	0.0	0.0	0.0	0.0	0.0	0.0	0.0	0.0	0.0	0.0	0.0	0.0	0.0	0.0	0.0	0.0	0.0	0.0	0.0	83
456.25	0.0	0.0	2.0	0.0	0.0	0.0	0.0	0.0	0.0	0.5	2.0	0.0	85.5	0.0	0.0	1.5	0.5	0.0	0.0	0.0	0.0	0.0	0.0	0.0	0.5	0.0	5.5	0.0	0.0	0.0	0.0	0.0	0.0	0.0	0.0	0.0	1.0	0.0	0.0	0.0	0.0	0.0	0.0	0.0	0.0	0.5	0.0	0.0	0.0	0.5	0.0	0.0	0.0	0.0	0.0	0.0	0.0	0.0	0.0	0.0	0.0	200
467.40	0.0	1.0	18.2	0.0	0.0	0.0	0.0	0.0	0.0	0.0	4.0	0.0	66.7	0.0	0.0	0.0	0.0	0.0	0.0	0.0	0.0	0.0	0.0	0.0	0.0	0.0	7.1	0.0	0.0	0.0	1.0	0.0	1.0	0.0	0.0	0.0	0.0	0.0	0.0	0.0	0.0	0.0	0.0	0.0	0.0	0.0	0.0	1.0	0.0	0.0	0.0	0.0	0.0	0.0	0.0	0.0	0.0	0.0	0.0	0.0	0.0	99
469.25	0.0	0.5	22.0	0.0	0.0	0.0	0.0	0.0	0.0	0.0	4.0	0.0	65.0	0.0	0.0	1.0	1.5	0.0	0.0	0.0	0.0	0.0	0.0	0.0	2.0	0.0	0.5	0.0	0.0	0.0	1.5	0.0	0.0	0.0	0.0	0.0	0.0	0.0	0.0	0.0	0.0	0.0	0.0	0.0	0.0	0.0	0.5	0.0	0.0	0.0	0.0	0.0	0.0	0.0	0.0	0.5	0.0	0.0	0.0	0.0	1.0	200
470.10	0.0	0.0	10.5	0.0	0.0	0.0	0.0	0.0	0.0	0.5	3.5	0.0	83.5	0.0	0.0	0.0	0.0	0.0	0.0	0.0	0.0	0.0	0.0	0.0	1.0	0.0	0.0	0.0	0.0	0.0	0.0	0.0	0.0	0.0	0.0	0.0	0.5	0.0	0.0	0.0	0.0	0.0	0.0	0.0	0.0	0.0	0.0	0.0	0.0	0.0	0.0	0.0	0.0	0.0	0.0	0.0	0.0	0.0	0.0	0.0	0.5	200
470.95	0.0	0.0	17.5	0.0	0.0	0.0	0.0	0.5	0.5	0.0	4.0	0.0	74.5	0.0	0.0	1.5	0.0	0.0	0.0	0.0	0.0	0.0	0.0	0.0	0.0	0.0	0.0	0.0	0.0	0.0	0.0	0.0	0.0	0.0	0.0	0.5	0.0	0.5	0.0	0.0	0.0	0.0	0.0	0.0	0.0	0.0	0.0	0.0	0.0	0.0	0.0	0.0	0.0	0.0	0.0	0.5	0.0	0.0	0.0	0.0	0.0	200

DEPH (m)	*Acritarca*	*Afropollis operculatus*	*Afropollis* spp.	*Antulsporites baculatus*	*Apteodinium granulatum*	*Araucariacites australis*	*Bennettitaepollenites regaliae*	Bisaccate forms	*Botryococcus* spp.	*Brenneripollis peroreticulatus*	*Callialasporites segmentatus*	*Cicatricosisporites microstriatus*	*Cicatricosisporites microstriatus*	*Cicatricosisporites* spp.	*Circulodinium* spp.	*Classopollis classoides*	*Clavatriletes* spp.	*Collarisporites fuscus*	*Complicatisaccus cearensis* ?	*Cribroperidinium edwardsii*	*Crybelosporites pannuceus*	*Cyathidites* spp.	*Cycadopites* spp.	*Cyclonephelium* spp.	*Dejaxpollenites foveoreticulatus*	*Dejaxpollenites microfoveolatus* ?	*Dejaxpollenites* spp.	*Dinopterigium* ? spp.	*Echinatisporis varispinosus*	*Elaterosporites klaszi* ?	*Equisetosporites albertenses*	*Equisetosporites concinnus*	*Equisetosporites maculosus*	*Equisetosporites ovatus*	*Equisetosporites* spp.	*Equisetosporites* spp.	*Exochosphaeridium* spp.	*Florentina mantelli*	Foraminiferal linings	*Foveosporites canalis*	*Gnetaceaepollenites chlatratus*	*Gnetaceaepollenites diversus*	*Gnetaceaepollenites jansonii*	*Gnetaceaepollenites* spp.	*Gnetaceaepollenites uesugui*
13.25	0.0	0.0	0.0	0.0	0.0	16.9	0.0	0.0	1.4	0.0	0.0	0.0	0.0	1.4	0.0	7.0	0.0	0.0	0.0	0.0	0.0	5.6	0.0	0.0	0.0	0.0	0.0	0.0	0.0	0.0	0.0	0.0	0.0	0.0	0.0	0.0	0.0	0.0	0.0	0.0	0.0	0.0	0.0	1.4	0.0
15.78	0.0	0.0	0.0	0.0	0.0	0.0	0.0	0.0	0.0	0.0	0.0	0.0	0.0	2.1	0.0	29.2	0.0	0.0	0.0	0.0	0.0	1.0	0.0	13.5	0.0	0.0	0.0	0.0	0.0	0.0	0.0	0.0	0.0	0.0	0.0	0.0	0.0	0.0	5.2	0.0	0.0	0.0	0.0	0.0	0.0
16.00	0.0	0.0	0.0	0.0	0.0	1.1	0.0	0.0	0.0	0.0	0.0	0.0	0.0	1.1	0.0	27.3	0.0	0.0	0.0	0.0	0.0	2.3	0.0	20.5	0.0	0.0	0.0	0.0	0.0	0.0	0.0	0.0	0.0	0.0	1.1	0.0	0.0	0.0	3.4	0.0	0.0	0.0	0.0	1.1	0.0
16.45	0.0	0.0	0.0	0.0	0.0	9.4	0.0	0.0	0.0	0.0	0.0	0.0	0.0	0.8	0.0	76.6	0.0	0.0	0.0	0.0	0.0	0.8	0.0	0.8	0.0	0.0	0.0	0.0	0.0	0.0	0.0	0.0	0.0	0.0	0.0	0.0	0.0	0.0	3.1	0.0	0.0	0.0	0.0	0.0	0.0
16.65	0.0	0.0	0.0	0.0	4.1	10.2	0.0	0.0	0.0	0.0	0.0	0.0	0.0	2.0	0.0	8.2	0.0	0.0	0.0	0.0	0.0	0.0	0.0	36.7	0.0	0.0	0.0	0.0	0.0	0.0	0.0	0.0	0.0	0.0	0.0	0.0	2.0	0.0	0.0	0.0	0.0	0.0	0.0	0.0	0.0
17.30	0.0	0.0	0.0	0.0	0.0	15.8	0.0	0.0	0.0	0.0	0.0	0.0	0.0	1.8	0.0	68.4	0.0	0.0	0.0	0.0	0.0	3.5	0.0	0.0	0.0	0.0	0.0	0.0	0.0	0.0	0.0	0.0	0.0	0.0	0.0	0.0	0.0	0.0	3.5	0.0	0.0	0.0	0.0	1.8	0.0
18.63	0.0	0.0	0.0	0.0	3.5	7.0	0.0	0.0	0.0	0.0	0.0	0.0	0.0	0.7	0.0	3.5	0.0	0.0	0.0	0.0	0.0	3.5	0.7	20.4	0.0	0.0	0.0	0.0	0.0	0.0	0.0	0.0	0.0	0.0	0.7	0.0	0.0	0.0	7.0	0.0	0.0	0.0	0.0	2.1	0.0
19.24	0.0	0.0	0.0	0.0	0.0	5.7	0.0	0.0	0.0	0.0	0.0	0.0	0.0	2.9	0.0	71.4	0.0	0.0	0.0	0.0	0.0	2.9	0.0	0.0	0.0	0.0	0.0	0.0	0.0	0.0	0.0	0.0	0.0	0.0	0.0	0.0	0.0	0.0	5.7	0.0	0.0	0.0	0.0	0.0	0.0
19.35	0.0	0.0	0.0	0.0	7.3	17.1	0.0	0.0	0.0	0.0	0.0	0.0	0.0	2.4	0.0	24.4	0.0	0.0	0.0	0.0	0.0	2.4	0.0	7.3	0.0	0.0	0.0	0.0	0.0	0.0	0.0	0.0	0.0	0.0	2.4	0.0	0.0	0.0	7.3	0.0	0.0	0.0	0.0	0.0	0.0
19.85	0.0	0.0	0.0	0.0	1.6	14.3	0.0	0.0	0.0	0.0	0.0	0.0	0.0	4.8	0.0	47.6	0.0	0.0	0.0	0.0	0.0	1.6	0.0	11.1	0.0	0.0	0.0	0.0	0.0	0.0	0.0	0.0	0.0	0.0	0.0	0.0	0.0	0.0	3.2	0.0	0.0	0.0	0.0	0.0	0.0
20.53	0.0	0.0	0.0	0.0	0.0	17.4	0.0	0.0	0.0	0.0	0.0	0.0	0.0	0.0	0.0	28.3	0.0	0.0	0.0	0.0	0.0	0.0	0.0	2.2	0.0	0.0	0.0	0.0	0.0	0.0	0.0	0.0	0.0	0.0	6.5	0.0	0.0	0.0	2.2	0.0	0.0	0.0	0.0	2.2	0.0
20.85	0.0	0.0	0.0	0.0	17.5	0.0	0.0	0.0	0.0	0.0	0.0	0.0	0.0	1.6	0.0	3.2	0.0	0.0	0.0	0.0	0.0	1.6	0.0	41.3	0.0	0.0	0.0	0.0	0.0	0.0	0.0	0.0	0.0	0.0	1.6	0.0	1.6	0.0	14.3	0.0	0.0	0.0	0.0	1.6	0.0
22.80	0.0	0.0	0.0	0.0	6.5	7.6	0.0	0.0	0.0	0.0	0.0	0.0	0.0	1.1	0.0	10.9	0.0	0.0	0.0	0.0	0.0	1.1	0.0	0.0	0.0	0.0	0.0	0.0	0.0	0.0	0.0	0.0	0.0	0.0	5.4	0.0	0.0	0.0	1.1	0.0	0.0	0.0	0.0	0.0	0.0
22.88	0.0	0.0	0.0	0.0	23.5	12.5	0.0	0.0	0.0	0.0	0.0	0.0	0.0	4.5	0.0	2.5	0.0	0.0	0.0	0.0	0.5	10.0	0.0	3.0	0.0	0.0	0.0	0.0	0.0	0.0	0.0	0.0	0.0	0.0	3.0	0.0	0.0	0.0	2.5	0.0	0.0	0.0	0.0	1.5	0.0
23.55	0.0	0.0	0.0	0.0	12.5	21.9	0.0	0.0	0.0	0.0	0.0	0.0	0.0	6.3	0.0	6.3	0.0	0.0	0.0	0.0	0.0	3.1	0.0	6.3	0.0	0.0	0.0	0.0	0.0	0.0	0.0	0.0	0.0	0.0	0.0	0.0	0.0	0.0	25.0	0.0	0.0	0.0	0.0	3.1	0.0
24.05	0.0	0.0	0.0	0.0	1.6	14.5	0.0	0.0	0.0	0.0	0.0	0.0	0.0	0.0	0.0	72.6	0.0	0.0	0.0	0.0	0.0	3.2	0.0	0.0	0.0	0.0	0.0	0.0	0.0	0.0	0.0	0.0	0.0	0.0	0.0	0.0	0.0	0.0	8.1	0.0	0.0	0.0	0.0	0.0	0.0
26.23	0.0	0.0	2.0	0.0	0.0	23.0	0.0	0.0	0.0	0.0	0.0	0.0	0.0	0.7	0.0	42.1	0.0	0.0	0.0	0.0	0.0	0.7	2.0	0.0	0.0	0.0	0.0	0.0	0.0	0.0	0.0	0.0	0.0	0.0	3.3	0.0	0.0	0.0	3.9	0.0	0.0	0.0	0.0	2.0	0.0
26.83	0.0	0.0	1.5	0.0	0.0	10.9	0.0	0.0	0.0	0.0	0.0	0.0	0.0	3.5	0.0	46.0	0.0	0.0	0.0	0.0	0.0	0.5	0.0	1.0	0.0	0.0	0.0	0.0	0.0	0.0	0.0	0.0	0.0	0.0	0.5	0.0	1.0	0.0	1.5	0.0	0.0	0.0	0.0	2.5	0.0
28.00	0.0	0.0	0.5	0.0	0.5	5.0	0.0	0.0	0.0	0.0	0.0	0.0	0.0	0.5	0.0	3.0	0.0	0.0	0.0	0.0	0.0	1.0	0.0	12.0	0.0	0.0	0.0	0.0	0.0	0.0	0.0	0.0	0.0	0.0	1.0	0.0	0.0	0.0	32.0	0.0	0.0	0.0	0.0	2.0	0.0
30.60	0.0	0.0	1.2	0.0	0.0	35.0	0.0	0.0	0.0	0.0	0.6	0.0	0.0	0.0	0.0	31.3	0.0	0.0	0.0	0.0	0.0	1.8	0.0	0.0	0.0	0.0	0.0	0.0	0.0	0.0	0.0	0.0	0.0	0.0	2.5	0.0	0.0	0.0	3.1	0.0	0.0	0.0	0.0	8.0	0.0
32.25	0.0	0.0	2.2	0.0	0.0	6.7	0.0	0.0	0.0	0.0	0.0	0.0	0.0	0.6	0.0	2.2	0.0	0.0	0.0	0.0	0.0	0.0	0.0	3.4	0.0	0.0	0.0	0.6	0.0	0.0	0.0	0.0	0.0	0.0	1.1	0.0	14.5	0.6	7.3	0.0	0.0	0.0	0.0	0.6	0.0
33.20	0.0	0.0	3.4	0.0	0.0	6.3	0.0	0.0	0.0	0.0	0.5	0.0	0.0	0.0	0.0	6.3	0.0	0.0	0.0	0.0	0.0	0.5	0.0	1.9	0.0	0.0	0.5	0.0	0.0	0.0	0.0	0.0	0.0	0.0	3.4	0.0	0.0	0.0	33.3	0.0	0.0	0.0	0.0	5.3	0.0
35.95	0.0	0.0	0.0	0.0	0.0	13.0	0.0	0.0	1.1	0.0	0.0	0.0	0.0	0.0	0.0	15.2	0.0	0.0	0.0	0.0	0.0	1.1	0.0	14.1	0.0	0.0	0.0	0.0	0.0	0.0	0.0	0.0	0.0	0.0	4.3	0.0	23.9	0.0	6.5	0.0	0.0	0.0	0.0	3.3	0.0
37.55	0.0	0.0	1.5	0.0	0.0	1.0	0.0	0.0	0.0	0.0	0.0	0.0	0.0	0.0	0.0	11.4	0.0	0.0	0.0	0.0	0.0	0.0	0.0	5.0	0.0	0.0	0.0	0.0	0.0	0.0	0.0	0.0	0.0	0.0	0.0	0.0	0.0	0.5	27.4	0.0	0.0	0.0	0.0	0.5	0.0
40.10	0.0	0.5	1.0	0.0	0.0	5.4	0.0	0.0	0.0	0.0	0.0	0.0	0.0	0.0	0.0	5.4	0.0	0.0	0.0	0.0	0.5	0.0	0.0	24.0	0.0	0.0	0.0	0.0	0.0	0.0	0.0	0.0	0.0	0.0	0.0	0.0	0.0	0.0	18.1	0.0	0.0	0.0	0.0	2.0	0.0
42.25	0.0	0.0	0.6	0.0	0.0	9.4	0.0	0.0	0.0	0.0	0.0	0.0	0.0	0.6	0.0	20.0	0.0	0.0	0.0	0.0	0.0	1.2	0.6	2.4	0.0	0.0	0.0	0.0	0.0	0.0	0.0	0.0	0.0	0.0	0.0	0.0	1.2	0.0	4.1	0.0	0.0	0.0	0.0	1.2	0.0
42.65	0.0	0.0	0.5	0.0	0.0	2.5	0.0	0.0	0.0	0.0	0.0	0.0	0.0	1.5	0.0	4.5	0.0	0.0	0.0	0.0	0.0	0.5	0.0	11.0	0.0	0.0	0.0	0.0	0.0	0.0	0.0	0.0	0.0	0.0	0.5	0.0	49.5	0.0	11.0	0.0	0.0	0.0	0.0	0.0	0.0
44.15	0.0	0.0	7.7	0.0	0.0	23.1	0.0	0.0	0.0	0.0	2.6	0.0	0.0	0.0	0.0	38.5	0.0	0.0	0.0	0.0	0.0	0.0	0.0	0.0	0.0	0.0	0.0	0.0	0.0	0.0	0.0	0.0	0.0	0.0	0.0	15.4	7.7	0.0	0.0	0.0	0.0	0.0	0.0	2.6	0.0
46.35	0.0	0.0	1.0	0.0	0.5	2.0	0.0	0.0	0.0	0.0	0.0	0.0	0.0	0.5	0.0	7.0	0.0	0.0	0.0	0.0	0.0	0.0	0.5	14.9	0.0	0.0	0.0	0.0	0.0	0.0	0.0	0.0	0.0	0.0	2.0	0.0	32.8	0.0	6.5	0.0	0.0	0.0	0.0	1.5	0.0
47.90	0.0	0.0	0.5	0.0	0.0	16.2	0.0	0.0	0.0	0.0	0.5	0.0	0.0	2.5	0.0	30.9	0.0	0.0	0.0	0.0	0.0	2.0	1.5	5.4	0.0	0.0	0.0	0.0	0.0	0.0	0.0	0.0	0.0	0.0	3.4	0.0	15.2	0.5	2.9	0.0	0.0	0.0	0.0	1.0	0.0
48.60	0.0	0.0	1.5	0.0	0.0	3.9	0.0	0.5	0.0	0.0	0.0	0.0	0.0	0.5	0.0	36.3	0.0	0.0	0.0	0.0	0.0	0.5	0.5	10.3	0.0	0.0	0.0	0.0	0.0	0.0	0.0	0.0	0.0	0.0	0.0	1.0	2.5	0.0	8.8	0.0	0.0	0.0	0.0	0.5	0.0
49.70	0.0	0.0	1.5	0.0	0.0	4.5	0.0	0.0	0.0	0.0	0.5	0.0	0.0	1.0	0.0	7.5	0.0	0.0	0.0	0.0	0.0	2.0	0.0	17.6	0.0	0.0	0.0	0.0	0.0	0.0	0.0	0.0	0.0	0.0	0.0	3.0	13.6	0.0	21.1	0.0	0.0	0.0	0.0	0.5	0.0
50.60	0.0	0.0	1.0	0.0	0.0	17.3	0.0	0.0	0.0	0.0	0.5	0.0	0.0	4.2	0.0	28.3	0.0	0.5	0.0	0.0	0.0	4.2	0.0	5.2	0.0	0.0	0.0	0.0	0.0	0.5	0.0	0.0	0.0	0.0	1.6	0.5	21.5	0.0	1.0	0.0	0.0	0.0	0.0	0.5	0.0
51.80	0.0	0.0	1.0	0.0	0.0	12.6	0.0	0.0	0.5	0.0	0.5	0.0	0.0	3.7	0.0	5.8	0.0	0.0	0.0	0.0	0.0	3.1	1.6	12.6	0.0	0.5	0.5	0.0	0.0	0.0	0.0	0.0	0.5	0.0	0.5	2.1	11.0	0.0	7.3	0.0	0.0	0.0	0.5	1.0	0.0
52.35	0.0	0.0	0.0	0.0	0.0	24.0	0.0	0.0	0.0	0.0	0.5	0.0	0.0	1.5	0.0	14.7	0.0	0.0	0.0	0.0	0.0	0.5	0.0	1.0	0.0	0.0	0.0	0.0	0.0	0.0	0.0	0.0	0.0	0.0	0.0	0.5	7.8	0.0	6.9	0.0	0.0	0.0	0.0	0.0	0.5
54.50	0.0	0.0	0.0	0.0	0.0	27.7	0.0	0.0	0.0	0.0	0.0	0.0	0.0	3.8	0.0	2.3	0.0	0.0	0.0	0.0	0.0	3.8	0.0	33.8	0.0	0.0	0.0	0.0	0.0	0.0	0.0	0.0	0.0	0.0	0.0	0.0	6.2	0.0	1.5	0.0	0.0	0.0	0.0	0.0	0.0
56.10	0.0	0.0	0.0	0.0	0.0	10.0	0.0	0.0	0.6	0.0	0.6	0.0	0.0	1.2	0.0	2.9	0.0	0.0	0.0	0.0	0.0	4.7	0.0	22.9	0.0	0.0	0.0	0.0	0.0	0.0	0.0	0.0	0.0	0.0	0.0	0.0	24.1	0.0	8.2	0.0	0.0	0.0	0.6	0.0	0.0
56.95	0.0	0.0	0.0	0.0	0.0	13.1	0.0	0.0	0.0	0.0	0.0	0.0	0.0	4.9	0.0	47.5	0.0	0.0	0.0	0.0	0.0	1.6	1.6	1.6	0.0	0.0	0.0	0.0	0.0	0.0	0.0	0.0	0.0	0.0	0.0	0.0	0.0	0.0	16.4	0.0	0.0	0.0	0.0	1.6	0.0
57.60	0.0	0.0	0.0	0.0	0.0	12.1	0.0	0.0	0.0	0.0	0.0	0.0	0.0	0.9	0.0	2.6	0.0	0.0	0.0	0.0	0.0	2.6	0.0	41.4	0.0	0.0	0.0	0.0	0.0	0.0	0.0	0.0	0.0	0.0	0.9	0.0	18.1	0.0	1.7	0.0	0.0	0.0	0.0	0.0	0.0
57.80	0.0	0.0	0.0	0.0	0.0	14.0	0.0	0.0	0.0	0.0	0.0	0.0	0.0	0.0	0.0	12.1	0.0	0.0	0.0	0.0	0.0	2.8	0.0	2.8	0.0	0.0	0.0	0.0	0.0	0.0	0.0	0.0	0.0	0.0	0.0	1.9	23.4	0.0	6.5	0.0	0.0	0.0	0.0	0.0	0.0
58.70	0.0	0.0	0.0	0.0	0.0	13.3	0.0	0.0	0.0	0.0	0.0	0.0	0.0	3.5	0.0	7.0	0.0	0.0	0.0	0.0	0.0	2.8	0.0	35.0	0.0	0.0	0.0	0.0	0.0	0.0	0.0	0.0	0.0	0.0	0.7	0.0	2.1	0.0	3.5	0.0	0.0	0.0	0.0	1.4	0.0
59.30	0.0	0.0	0.0	0.0	0.0	22.6	0.0	0.0	0.0	0.0	0.0	0.0	0.0	0.8	0.0	43.6	0.0	0.0	0.0	0.0	0.0	2.3	0.0	4.5	0.0	0.0	0.0	0.0	0.0	0.0	0.0	0.0	0.0	0.0	0.0	2.3	2.3	0.0	9.0	0.0	0.0	0.0	0.0	0.0	0.0
60.70	0.0	0.0	0.0	0.0	0.0	3.2	0.0	0.0	0.0	0.0	0.0	0.0	0.0	0.5	0.0	3.2	0.0	0.0	0.0	0.0	0.0	2.1	0.0	49.2	0.0	0.0	0.0	0.0	0.0	0.0	0.0	0.0	0.0	0.0	0.0	0.0	13.8	0.0	2.6	0.0	0.0	0.0	0.0	1.1	0.0
65.45	0.0	0.0	0.0	0.0	0.0	2.0	0.0	0.0	0.0	0.0	0.0	0.0	0.0	1.5	0.0	1.5	0.0	0.0	0.0	0.0	0.0	0.5	0.0	19.4	0.0	0.0	0.0	0.0	0.0	0.0	0.0	0.0	0.0	0.0	0.0	0.0	37.8	0.0	3.5	0.0	0.0	0.0	0.0	0.5	0.0
65.90	0.0	0.0	0.0	1.4	0.0	29.0	0.0	0.0	0.0	0.0	0.0	0.0	0.0	0.0	0.0	26.1	0.0	0.0	0.0	0.0	0.0	5.8	0.0	1.4	0.0	0.0	0.0	0.0	0.0	0.0	0.0	0.0	0.0	0.0	0.0	2.9	1.4	0.0	11.6	0.0	0.0	0.0	0.0	0.0	0.0
67.00	0.0	0.0	0.0	0.0	0.0	33.3	0.0	0.0	0.0	0.0	0.0	0.0	0.0	10.7	0.0	3.6	0.0	0.0	0.0	0.0	0.0	6.0	0.0	0.0	0.0	0.0	0.0	0.0	0.0	0.0	0.0	0.0	0.0	0.0	0.0	1.2	6.0	0.0	1.2	0.0	0.0	0.0	0.0	0.0	0.0
67.40	0.0	0.0	0.0	0.0	0.0	12.9	0.0	0.0	0.0	0.0	0.0	0.0	0.0	2.9	0.0	1.4	0.0	0.0	0.0	0.0	0.0	0.0	0.0	1.4	0.0	0.0	0.0	0.0	0.0	0.0	0.0	0.0	0.0	0.0	1.4	0.0	15.7	0.0	35.7	0.0	0.0	0.0	0.0	1.4	0.0
71.60	0.0	0.0	0.0	0.0	0.0	17.9	0.0	0.0	0.0	0.0	0.0	0.0	0.0	1.2	0.0	7.1	0.0	0.0	0.0	0.0	0.0	6.0	0.0	13.1	0.0	0.0	0.0	0.0	0.0	0.0	0.0	0.0	0.0	0.0	0.0	0.0	26.2	0.0	9.5	0.0	0.0	0.0	0.0	0.0	0.0
72.25	0.0	0.0	0.0	0.0	0.0	0.8	0.0	0.0	0.0	0.0	0.0	0.0	0.0	1.5	0.0	4.6	0.0	0.0	0.0	0.0	0.0	1.5	0.0	38.5	0.0	0.0	0.0	0.0	0.0	0.0	0.0	0.0	0.0	0.0	0.0	0.0	9.2	0.0	13.1	0.0	0.0	0.0	0.0	0.8	0.0
75.40	0.0	0.0	0.0	0.0	0.0	37.2	0.0	0.0	0.0	0.0	0.0	0.0	0.0	1.9	0.0	19.9	0.0	0.0	0.0	0.0	0.0	0.0	0.0	7.7	0.0	0.0	0.0	0.0	0.0	0.0	0.0	0.0	0.0	0.0	1.3	0.0	1.3	0.0	2.6	0.0	0.0	0.0	0.0	1.3	0.0
77.20	0.0	0.0	0.0	0.0	0.0	9.3	0.0	0.0	0.0	0.0	0.0	0.0	0.0	2.3	0.0	37.2	0.0	0.0	0.0	0.0	0.0	1.2	0.0	0.0	0.0	0.0	0.0	0.0	0.0	0.0	0.0	0.0	0.0	0.0	0.0	0.0	2.3	0.0	22.1	0.0	0.0	0.0	0.0	0.0	0.0
80.40	0.0	0.0	0.0	0.0	0.0	8.8	0.0	0.0	0.0	0.0	0.0	0.0	0.0	3.9	0.0	13.3	0.0	0.0	0.0	0.0	0.0	1.7	0.0	6.1	0.0	0.0	0.0	0.0	0.0	0.0	0.0	0.0	0.0	0.0	0.0	0.0	12.2	0.0	15.5	0.0	0.0	0.0	0.0	2.8	0.0
82.55	0.0	0.0	0.0	0.0	0.6	14.0	0.0	0.0	0.0	0.0	0.0	0.0	0.0	4.5	0.0	23.6	0.0	0.0	0.0	0.0	0.0	4.5	0.0	1.3	0.0	0.0	0.0	0.0	0.0	0.0	0.0	0.0	0.0	0.0	2.5	0.0	15.9	0.0	1.9	0.0	0.0	0.0	0.6	0.6	0.0
83.00	0.0	0.0	0.0	0.0	0.0	1.0	0.0	0.0	0.0	0.0	0.0	0.0	0.0	1.0	0.0	14.9	0.0	0.0	0.0	0.0	0.0	2.0	0.0	3.0	0.0	0.0	0.0	6.9	0.0	0.0	0.0	0.0	0.0	0.0	1.0	0.0	6.9	0.0	14.9	0.0	0.0	0.0	0.0	1.0	0.0
84.90	0.5	0.0	0.0	0.0	0.0	17.5	0.0	0.5	0.5	0.0	0.0	0.0	0.0	0.5	0.0	41.3	0.0	0.0	0.0	0.0	0.0	3.2	0.0	0.0	0.0	0.0	0.0	0.0	0.0	0.0	0.0	0.0	0.0	0.0	5.8	0.0	7.9	0.0	5.3	0.0	0.0	0.0	0.0	0.0	0.0
86.70	0.0	0.0	0.0	0.0	0.0	3.8	0.0	0.0	0.0	0.0	0.0	0.0	0.0	2.3	0.8	12.0	0.0	0.0	0.0	0.0	0.0	3.0	0.0	3.8	0.0	0.0	0.0	0.0	0.0	0.0	0.0	0.0	0.0	0.0	0.8	0.0	45.9	0.0	12.0	0.0	0.0	0.0	0.0	0.8	0.0
88.40	0.0	0.0	0.5	0.0	0.0	4.5	0.0	0.0	0.5	0.0	0.0	0.0	0.0	1.5	2.0	64.5	0.0	0.0	0.0	0.0	0.0	0.5	0.0	1.0	0.0	0.0	0.0	0.0	0.0	0.0	0.0	0.0	0.0	0.0	0.0	1.0	0.5	0.0	4.0	0.0	0.0	0.0	0.0	0.5	0.0
91.25	0.0	0.0	5.0	0.0	0.0	26.1	0.0	0.0	0.0	0.0	0.0	0.0	0.8	4.2	0.0	20.6	0.0	0.0	0.0	0.0	0.0	2.5	0.0	2.1	0.0	0.0	0.0	0.0	0.0	0.0	0.0	0.0	0.0	0.0	2.5	0.0	10.1	0.0	1.7	0.0	0.0	0.0	0.4	1.3	0.0
94.35	0.0	0.0	0.4	0.0	0.0	11.2	0.0	0.0	0.0	0.0	0.8	0.0	0.0	2.0	0.4	34.1	0.0	0.0	0.0	0.0	0.0	0.0	0.0	0.0	0.0	0.0	0.0	0.0	0.0	0.0	0.0	0.0	0.4	0.0	0.4	0.8	4.0	0.0	12.9	0.0	0.0	0.0	0.0	0.4	0.0
97.65	0.0	0.0	2.2	0.0	0.0	9.4	0.0	0.0	0.0	0.0	0.6	0.0	0.0	2.8	0.0	8.9	0.0	0.0	0.0	0.0	0.0	0.0	0.0	7.8	0.0	0.0	0.0	0.0	0.0	0.0	0.0	0.0	0.0	0.0	1.7	0.0	11.7	0.0	11.1	0.0	0.0	0.0	0.6	1.1	0.0
98.20	0.0	0.0	1.4	0.0	0.0	20.9	0.0	0.0	0.0	0.0	0.7	0.0	0.0	4.3	0.0	26.6	0.0	0.0	0.0	0.0	0.0	0.0	0.0	3.6	0.0	0.0	0.0	0.0	0.0	0.0	0.0	0.0	0.0	0.0	4.3	0.0	3.6	0.0	3.6	0.0	0.0	0.0	0.0	3.6	0.0
99.20	0.0	0.0	0.9	0.0	0.9	23.7	0.4	0.9	0.0	1.3	0.9	0.4	0.0	5.3	0.0	36.4	0.0	0.0	0.0	0.0	0.0	2.2	1.3	0.0	0.0	0.0	0.4	0.0	0.0	0.0	0.9	0.4	0.0	0.0	0.0	0.9	0.0	0.0	3.5	0.0	0.0	0.0	0.0	0.9	0.0
101.70	0.0	0.0	2.6	0.5	0.0	14.4	0.0	0.0	0.5	0.0	0.5	0.0	0.0	6.7	2.1	30.9	0.0	0.0	0.0	0.0	0.0	2.1	1.0	3.6	0.5	0.0	0.5	0.0	0.0	0.0	0.0	0.5	0.0	0.0	0.5	0.5	2.6	0.0	5.2	0.0	0.0	0.0	0.0	0.0	0.0
103.15	0.0	0.0	0.4	0.0	0.0	18.3	0.0	0.8	0.4	0.0	0.4	0.0	0.0	5.4	3.7	41.1	0.0	0.0	0.0	0.0	0.0	0.8	0.4	0.4	0.0	0.0	0.0	0.0	0.0	0.0	0.0	0.0	0.0	0.4	0.8	0.0	0.0	0.0	9.1	0.0	0.0	0.0	0.0	2.1	0.0
108.10	0.0	0.0	1.0	0.0	1.0	3.9	0.0	0.5	0.0	0.0	0.0	0.0	0.0	0.5	0.0	52.4	0.0	0.0	0.0	0.0	0.0	1.0	0.0	0.5	0.0	0.0	0.0	0.0	0.0	0.0	0.0	0.0	0.0	0.0	0.0	0.5	0.0	0.0	15.5	0.0	0.0	0.0	0.0	0.5	0.0
109.40	0.0	0.0	1.6	0.0	0.0	4.9	0.0	0.0	0.0	0.0	0.0	0.0	0.0	3.3	0.0	29.7	0.0	0.0	0.0	0.0	0.0	0.0	0.0	0.5	0.0	0.0	0.0	0.0	0.0	0.0	0.0	0.0	0.0	0.0	0.5	2.2	11.0	0.0	7.7	0.0	0.0	0.0	0.0	1.1	0.0
110.60	0.0	0.0	0.4	0.0	0.0	4.4	0.0	0.0	0.0	0.0	0.4	0.0	0.0	3.1	0.0	57.3	0.0	0.0	0.0	0.0	0.0	0.0	0.0	0.9	0.0	0.0	0.4	0.0	0.4	0.0	0.0	0.0	0.0	0.4	0.9	1.8	4.4	0.0	8.4	0.0	0.0	0.0	0.0	0.4	0.0
112.70	0.0	0.0	0.6	0.0	0.0	14.4	0.0	0.0	0.0	0.0	1.1	0.6	0.0	4.4	0.0	50.8	0.0	0.0	0.0	0.0	0.0	1.7	0.6	0.0	0.0	0.0	0.0	0.6	0.0	0.0	0.0	0.0	0.0	0.0	1.7	0.0	1.1	0.0	1.7	0.0	0.0	0.0	0.0	0.6	0.0
119.50	0.0	0.0	0.5	0.0	0.0	5.1	0.0	0.0	0.0	0.0	0.0	0.0	0.0	2.3	0.0	63.1	0.0	0.0	0.0	0.0	0.0	1.4	0.9	0.0	0.0	0.0	0.0	0.0	0.0	0.0	0.0	0.0	0.0	0.0	0.0	0.9	0.9	0.0	9.3	0.0	0.0	0.0	0.0	0.5	0.0
120.60	0.0	0.0	1.0	0.0	0.0	0.0	0.0	0.0	0.0	0.0	0.0	0.0	0.0	0.5	0.0	28.3	0.0	0.0	0.0	0.0	0.0	0.0	0.0	0.5	0.0	0.0	0.0	0.5	0.0	0.0	0.0	0.0	0.0	0.0	0.0	0.0	0.0	0.0	12.1	0.0	0.0	0.0	0.0	0.5	0.0
122.85	0.0	0.0	0.0	0.0	0.0	0.0	0.0	0.0	0.0	0.0	0.0	0.0	0.0	0.0	0.0	30.8	0.0	0.0	0.0	0.0	0.0	0.8	0.0	0.0	0.0	0.0	0.0	0.0	0.0	0.0	0.0	0.0	0.0	0.0	0.0	0.0	0.8	0.0	13.5	0.0	0.0	0.0	0.0	0.8	0.0
124.40	0.0	0.0	1.0	0.0	0.0	2.5	0.0	0.0	0.0	0.5	0.0	0.0	0.0	1.5	0.0	33.3	0.0	0.0	0.0	0.0	0.0	1.0	0.0	0.0	0.0	0.0	0.0	1.0	0.0	0.0	0.0	0.0	0.0	0.0	0.0	1.0	3.5	0.0	7.6	0.0	0.0	0.0	0.0	0.0	0.0
124.67	0.0	0.0	0.4	0.0	0.0	3.5	0.0	0.0	0.0	0.0	0.0	0.0	0.0	3.5	0.0	27.6	0.0	0.0	0.0	0.0	0.0	0.9	0.4	0.0	0.0	0.0	0.0	0.0	0.0	0.0	0.0	0.0	0.0	0.0	0.4	0.0	9.2	0.0	14.9	0.0	0.0	0.0	0.0	0.0	0.0
128.10	0.0	0.0	1.7	0.0	0.0	3.8	0.4	0.0	0.0	0.0	0.4	0.0	0.0	1.3	0.0	64.4	0.0	0.0	0.0	0.0	0.0	0.4	0.0	0.4	0.0	0.0	0.0	0.0	0.0	0.0	0.0	0.0	0.0	0.0	0.0	1.3	0.0	0.0	8.4	0.0	0.0	0.0	0.0	0.4	0.4
130.55	0.0	0.0	0.6	0.0	0.0	3.7	0.0	0.0	0.0	0.0	0.0	0.0	0.0	0.6	0.0	31.8	0.0	0.0	0.0	0.0	0.0	2.5	0.0	0.3	0.0	0.0	0.0	0.0	0.0	0.0	0.0	0.0	0.0	0.0	0.0	0.3	0.8	0.0	5.9	0.0	0.0	0.0	0.0	0.3	0.0
134.45	0.0	0.0	1.1	0.0	0.0	2.9	0.0	0.0	0.0	0.0	0.0	0.0	0.0	0.7	0.0	33.7	0.0	0.0	0.0	0.0	0.0	0.0	0.0	0.4	0.0	0.0	0.4	0.0	0.0	0.0	0.0	0.0	0.4	0.0	0.0	0.7	0.0	0.0	13.8	0.0	0.0	0.0	0.0	0.4	0.0
135.75	0.0	0.0	0.0	0.0	0.0	3.2	0.0	0.0	0.0	0.0	0.0	0.0	0.0	1.1	0.0	4.3	0.0	0.0	0.0	0.0	0.0	1.6	0.5	12.4	0.0	0.0	0.0	0.0	0.0	0.0	0.0	0.0	0.0	0.0	0.0	0.0	8.1	0.0	8.1	0.0	0.0	0.0	0.0	0.0	0.0
146.10	0.0	0.0	1.3	0.0	0.0	16.4	0.4	0.0	0.0	0.0	2.7	0.0	0.0	3.1	0.0	14.6	0.0	0.0	0.0	0.0	0.0	5.8	0.4	0.0	0.0	0.0	0.0	0.0	0.0	0.0	0.0	0.0	0.0	0.0	0.0	0.9	0.4	0.0	11.9	0.0	0.0	0.0	0.0	0.4	0.0
157.15	0.0	0.0	1.9	0.0	0.0	26.5	0.5	0.0	0.0	0.0	2.8	0.0	0.0	9.3	0.0	22.3	0.0	0.0	0.0	0.0	0.0	4.2	0.0	0.0	0.0	0.9	0.0	0.0	0.0	0.0	0.0	0.0	0.0	0.0	0.0	0.9	0.0	0.0	1.9	0.0	0.5	0.0	0.0	1.9	0.0
160.35	0.0	0.0	0.8	0.0	0.4	13.0	0.4	0.0	1.3	0.0	1.3	0.0	0.0	3.4	0.0	13.9	0.0	0.0	0.0	0.0	0.0	5.5	0.0	0.0	0.0	0.0	0.0	0.0	0.0	0.0	0.0	0.0	0.4	0.0	0.0	0.4	0.0	0.0	26.1	0.0	0.0	0.0	0.0	0.4	0.0
167.25	0.0	0.0	0.0	0.0	0.0	9.0	0.3	0.0	0.0	0.0	0.3	0.0	0.0	2.1	0.0	12.1	0.0	0.0	0.0	0.0	0.0	0.7	0.0	0.0	0.0	0.0	0.0	0.0	0.0	0.0	0.0	0.0	0.0	0.0	0.0	0.7	2.8	0.0	23.2	0.0	0.0	0.0	0.0	0.3	0.0
170.43	0.3	0.0	0.3	0.0	0.0	6.5	0.0	0.0	0.3	0.0	0.3	0.0	0.0	2.5	0.0	17.6	0.0	0.0	0.0	0.0	0.0	5.3	0.3	0.3	0.0	0.0	0.0	0.0	0.0	0.0	0.0	0.0	0.0	0.0	0.0	0.3	8.0	0.0	10.2	0.0	0.0	0.3	0.0	0.0	0.0
178.56	0.0	0.0	0.0	0.0	0.0	12.0	0.5	0.0	0.0	0.0	0.5	0.0	0.0	1.4	0.0	31.5	0.0	0.0	0.0	0.0	0.0	1.4	0.9	0.0	1.4	0.0	0.0	0.0	0.0	0.0	0.0	0.0	0.0	0.0	0.9	0.0	2.3	0.5	17.1	0.0	0.0	0.0	0.0	0.9	0.0
182.06	0.0	0.0	0.4	0.0	0.0	5.4	0.0	0.0	0.0	0.0	0.0	0.0	0.0	2.5	0.0	35.3	0.0	0.0	0.0	0.0	0.0	0.8	0.4	0.0	0.0	0.0	0.0	0.0	0.0	0.0	0.0	0.0	0.0	0.0	0.0	0.8	0.4	0.0	18.7	0.0	0.0	0.0	0.0	0.4	0.0
182.60	0.0	0.0	0.0	0.0	0.0	2.4	0.5	0.0	0.0	0.0	0.5	0.0	0.0	3.9	0.0	52.7	0.0	0.0	0.0	0.0	0.0	2.4	0.0	0.0	0.0	0.0	0.0	0.0	0.0	0.0	0.0	0.0	0.0	0.0	0.0	0.0	0.0	0.0	29.3	0.0	0.0	0.0	0.0	0.5	0.0
189.80	0.0	0.0	0.5	0.0	0.0	18.0	0.0	0.0	0.0	0.0	0.0	0.0	0.0	2.6	0.0	53.1	0.0	0.0	0.0	0.0	0.0	0.5	2.6	0.0	0.5	0.0	0.0	0.0	0.0	0.0	0.0	0.0	0.0	0.0	1.0	1.5	0.0	0.0	2.6	0.0	0.0	0.0	0.0	0.5	0.5
190.75	0.0	0.0	0.3	0.0	0.0	4.9	0.0	0.0	0.0	0.0	0.3	0.0	0.0	0.3	0.0	24.6	0.0	0.0	0.0	0.3	0.0	0.3	0.0	0.0	0.0	0.0	0.0	0.0	0.0	0.0	0.0	0.0	0.0	0.0	0.0	0.6	0.0	0.0	4.6	0.0	0.0	0.0	0.0	0.6	0.0
200.68	0.0	0.0	0.0	0.0	0.0	3.5	0.0	0.0	0.0	0.0	0.0	0.0	0.0	1.5	0.0	78.4	0.0	0.0	0.0	0.0	0.0	1.0	0.0	0.0	0.0	0.0	0.0	0.0	0.0	0.0	0.0	0.0	0.0	0.0	1.5	0.0	0.0	0.0	10.1	0.0	0.0	0.0	0.0	0.0	0.0
202.37	0.0	0.0	0.0	0.0	0.0	3.4	0.0	0.0	0.0	0.0	0.0	0.0	0.0	1.7	0.0	72.3	0.0	0.0	0.0	0.6	0.0	2.3	0.0	0.0	0.0	0.0	0.0	0.0	0.0	0.0	0.0	0.0	0.0	0.0	0.0	0.0	0.0	0.0	7.3	0.0	0.0	0.0	0.0	1.7	0.0
205.35	0.0	0.0	0.0	0.0	0.0	5.6	0.0	0.0	0.0	0.0	0.0	0.0	0.0	4.1	0.5	64.8	0.0	0.0	0.0	0.0	0.0	1.5	0.5	0.0	0.0	0.0	0.0	0.0	0.0	0.0	0.0	0.0	0.0	0.0	0.5	0.0	0.0	0.0	10.2	0.0	0.0	0.0	0.0	0.0	0.0
207.80	0.0	0.0	0.0	0.0	0.0	8.2	0.0	0.0	0.0	0.0	0.0	0.0	0.0	2.2	0.7	57.5	0.0	0.0	0.0	0.0	0.0	5.2	0.0	0.0	0.0	0.0	0.0	0.0	0.0	0.0	0.0	0.0	0.0	0.0	3.0	0.0	0.0	0.0	6.0	0.0	0.0	0.0	0.0	1.5	0.0
211.85	0.0	0.0	0.0	0.0	0.0	8.7	0.5	0.0	0.0	0.0	0.5	0.0	0.0	2.4	0.0	67.1	0.0	0.0	0.0	0.0	0.0	1.9	1.4	0.0	0.0	0.5	0.0	0.0	0.0	0.0	0.0	0.0	0.0	0.0	1.0	1.0	0.0	0.0	1.9	0.0	0.0	0.0	0.0	3.4	0.0
214.75	1.0	0.0	0.3	0.0	0.0	0.7	0.0	0.0	0.0	0.0	0.3	0.0	0.0	0.7	0.0	53.1	0.0	0.0	0.0	0.0	0.0	0.3	0.0	2.1	0.0	0.0	0.0	0.0	0.0	0.0	0.0	0.0	0.7	0.0	1.0	0.0	4.9	0.0	0.0	0.0	0.0	0.0	0.0	0.0	0.0
217.00	0.0	0.0	0.0	0.0	0.0	6.4	0.0	0.0	0.0	0.0	0.0	0.0	0.0	1.5	0.0	82.2	0.0	0.0	0.0	0.0	0.0	1.0	0.0	0.0	0.0	0.0	0.0	0.0	0.0	0.0	0.0	0.0	0.0	0.0	0.5	1.0	0.0	0.0	1.5	0.0	0.0	0.0	0.0	1.5	0.0
222.00	0.0	0.0	0.0	0.0	0.0	2.4	0.0	0.0	0.0	0.0	0.5	0.0	0.0	0.5	0.0	83.3	0.0	0.0	0.0	0.0	0.0	1.0	0.5	0.0	0.0	0.0	0.0	0.0	0.0	0.0	0.0	0.0	0.0	0.0	0.0	1.0	0.0	0.0	6.7	0.0	0.0	0.0	0.0	0.0	0.0
222.25	0.0	0.0	0.0	0.0	0.5	3.1	0.0	0.0	0.0	0.0	0.0	0.0	0.0	1.5	0.0	81.5	0.0	0.0	0.5	0.0	0.0	0.0	0.0	0.0	0.0	0.0	0.0	0.0	0.0	0.0	0.0	0.0	0.0	0.0	0.0	0.0	0.0	0.0	7.2	0.0	0.0	0.0	0.0	0.5	0.0
224.60	0.0	0.0	0.0	0.0	0.0	0.6	0.0	0.0	0.0	0.0	0.0	0.0	0.0	0.6	0.0	93.9	0.0	0.0	0.0	0.0	0.0	0.6	0.0	0.0	0.0	0.0	0.0	0.0	0.0	0.0	0.0	0.0	0.0	0.0	0.6	0.0	0.0	0.0	1.8	0.0	0.0	0.0	0.0	0.0	0.0
227.10	0.0	0.0	0.8	0.0	1.2	1.6	0.0	0.0	0.0	0.0	0.4	0.0	0.0	0.8	0.0	72.3	0.0	0.0	0.0	0.0	0.0	0.4	0.4	0.0	0.0	0.0	0.4	0.0	0.0	0.0	0.0	0.0	0.0	0.0	0.4	1.2	0.0	0.0	0.8	0.0	0.0	0.0	0.0	1.2	0.0
232.90	0.5	0.0	0.0	0.0	0.0	4.0	0.0	0.0	0.0	0.0	0.0	0.0	0.0	1.5	0.0	88.6	0.0	0.0	0.0	0.0	0.0	0.0	0.0	0.0	0.0	0.0	0.0	0.0	0.0	0.0	0.0	0.0	0.0	0.0	0.0	0.0	0.0	0.0	4.0	0.0	0.0	0.0	0.0	0.5	0.0
237.60	0.0	0.0	0.0	0.0	0.0	1.9	0.0	0.0	0.0	0.0	0.0	0.0	0.0	1.9	0.0	80.8	0.0	0.0	0.0	0.0	0.0	0.5	0.0	0.0	0.0	0.0	0.0	0.0	0.0	0.0	0.0	0.0	0.0	0.0	0.0	0.0	0.0	0.0	12.5	0.0	0.0	0.0	0.0	0.5	0.0
237.70	0.0	0.0	0.0	0.0	0.0	1.0	0.0	0.0	0.0	0.0	0.0	0.0	0.0	1.0	0.0	87.6	0.0	0.0	0.0	0.0	0.0	1.0	0.0	0.0	0.0	0.0	0.0	0.0	0.0	0.0	0.0	0.0	0.0	0.0	2.9	0.0	0.0	0.0	1.0	0.0	0.0	0.0	0.0	1.0	0.0
239.75	0.0	0.0	0.0	0.0	0.0	4.8	0.0	0.0	0.0	0.0	0.5	0.0	0.0	1.9	0.0	85.1	0.0	0.0	0.0	0.0	0.0	1.0	0.5	0.0	0.0	0.0	0.0	0.0	0.0	0.0	0.0	0.0	0.0	0.0	0.0	0.0	0.0	0.0	2.9	0.0	0.0	0.0	0.0	0.5	0.0
240.65	0.0	0.0	0.0	0.0	0.0	1.7	0.0	0.0	0.0	0.0	0.0	0.0	0.0	1.3	0.0	75.6	0.0	0.0	0.0	0.0	0.0	0.8	0.0	0.0	0.0	0.0	0.4	0.0	0.0	0.0	0.0	0.0	0.0	0.0	0.0	0.0	0.0	0.0	2.5	0.0	0.0	0.0	0.0	0.4	0.0
241.25	0.0	0.0	0.0	0.0	0.0	0.0	0.0	0.0	0.0	0.0	0.0	0.0	0.0	0.0	0.0	22.5	0.0	0.0	0.0	0.0	0.0	2.5	0.0	0.0	0.0	0.0	0.0	0.0	0.0	0.0	0.0	0.0	0.0	0.0	0.0	0.0	17.5	0.0	55.0	0.0	0.0	0.0	0.0	0.0	0.0
243.95	0.0	0.0	0.0	0.0	0.0	2.9	0.0	0.0	0.0	0.0	0.0	0.0	0.0	0.5	0.0	90.8	0.0	0.0	0.0	0.0	0.0	0.5	0.0	0.0	0.0	0.0	0.0	0.0	0.0	0.0	0.0	0.0	0.0	0.0	0.0	0.0	0.0	0.0	1.5	0.0	0.0	0.0	0.0	0.5	0.0

DEPH (m)	*Klukisporites foveolatus*	*Klukisporites pseudoreticulatus*	*Klukisporites* spp.	*Leisphaeridia* sp.	*Leptolepidites psarosus*	*Matonisporites silvai*	Megaspores	*Microfoveolatosporis daukiensis*	*Microfoveolatus daukiensis*	*Odontochitina operculata*	*Oligosphaeridium albertenses*	*Oligosphaeridium complex*	*Oligosphaeridium irregulare*	*Oligosphaeridium pocolum*	*Oligosphaeridium pulcherrimum*	*Oligosphaeridium* spp.	*Oligosphaeridium totum*	*Palaeoperidinium cretaceum*	*Perotriletes* spp.	*Pilosisporites trichopapillosus*	*Prolixumsphaeridium parvispinum*	*Pseudoceratium* spp.	*Quadricolpites reticulatus*	*Reticulosporis foveolatus*	*Reticulosporis reticulatus*	*Retitricolpites* spp.	*Retitriletes* sp. 3 (Regali, 1989)	*Rousea georgensis* ?	*Schrankpollis reticulatus* ?	*Sergipea naviformis*	*Sergipea simplex*	*Sergipea* spp.	*Sergipea variverrucata*	*Spiniferites ancoriferas* ?	*Spiniferites bejuii*	*Spiniferites chebca*	*Spiniferites lenzi* ?	*Spiniferites* spp.	*Steevesipollenites* spp.	*Stellatopollis barghoorni*	*Stellatopollis dubius*	*Stellatopollis* spp.	*Striatopollis reticulatus*	*Subtilisphaera senegalensis*	*Systematophora* spp.
13.25	0.0	0.0	0.0	0.0	0.0	8.5	0.0	0.0	0.0	0.0	0.0	0.0	0.0	0.0	0.0	0.0	0.0	0.0	0.0	1.4	0.0	0.0	0.0	0.0	0.0	0.0	0.0	0.0	0.0	0.0	0.0	0.0	0.0	0.0	0.0	0.0	0.0	0.0	0.0	0.0	0.0	0.0	0.0	54.9	0.0
15.78	0.0	0.0	0.0	0.0	0.0	0.0	0.0	0.0	0.0	0.0	0.0	0.0	0.0	0.0	0.0	2.1	0.0	0.0	0.0	0.0	0.0	26.0	0.0	0.0	0.0	0.0	0.0	0.0	0.0	0.0	0.0	0.0	0.0	0.0	0.0	13.5	0.0	5.2	0.0	0.0	0.0	0.0	0.0	0.0	0.0
16.00	0.0	0.0	0.0	0.0	1.1	0.0	0.0	0.0	0.0	0.0	0.0	0.0	0.0	0.0	0.0	1.1	2.3	0.0	0.0	0.0	0.0	6.8	0.0	0.0	0.0	0.0	1.1	0.0	0.0	0.0	0.0	0.0	0.0	0.0	3.4	11.4	0.0	6.8	1.1	0.0	0.0	0.0	0.0	4.5	0.0
16.45	0.0	0.0	0.0	0.0	0.0	0.0	0.8	0.0	0.0	0.0	0.0	0.8	0.0	0.0	0.0	2.3	0.0	0.0	0.0	0.0	0.0	0.0	0.0	0.0	0.0	0.0	0.0	0.0	0.0	0.0	0.0	0.0	0.0	0.0	0.0	0.8	0.0	0.0	1.6	0.0	0.0	0.8	0.0	0.8	0.0
16.65	0.0	0.0	0.0	0.0	0.0	4.1	0.0	0.0	0.0	0.0	0.0	10.2	0.0	0.0	0.0	2.0	0.0	0.0	0.0	0.0	0.0	2.0	0.0	0.0	0.0	0.0	0.0	0.0	0.0	0.0	0.0	0.0	0.0	0.0	0.0	2.0	0.0	16.3	0.0	0.0	0.0	0.0	0.0	0.0	0.0
17.30	0.0	0.0	0.0	0.0	0.0	0.0	0.0	0.0	0.0	0.0	0.0	0.0	0.0	0.0	0.0	0.0	0.0	0.0	0.0	0.0	0.0	1.8	0.0	0.0	0.0	0.0	0.0	0.0	0.0	0.0	0.0	0.0	0.0	0.0	0.0	0.0	0.0	0.0	0.0	0.0	0.0	0.0	0.0	0.0	0.0
18.63	0.0	0.0	0.0	0.0	0.0	0.7	0.0	0.0	0.0	0.0	0.0	0.0	0.0	0.0	0.0	0.0	0.0	0.0	0.0	0.0	0.0	8.5	0.0	0.0	0.0	0.0	0.0	0.0	0.0	0.0	0.0	0.0	0.0	0.0	0.0	6.3	0.0	19.0	0.0	0.0	0.0	0.0	0.0	2.1	0.0
19.24	0.0	0.0	0.0	0.0	0.0	0.0	0.0	0.0	0.0	0.0	0.0	0.0	0.0	0.0	0.0	0.0	0.0	0.0	0.0	0.0	0.0	0.0	0.0	0.0	0.0	0.0	0.0	0.0	0.0	0.0	0.0	0.0	0.0	0.0	0.0	8.6	0.0	0.0	0.0	0.0	0.0	0.0	0.0	0.0	0.0
19.35	0.0	0.0	0.0	0.0	0.0	0.0	0.0	0.0	0.0	0.0	2.4	0.0	0.0	0.0	0.0	0.0	0.0	0.0	0.0	0.0	0.0	0.0	0.0	0.0	0.0	0.0	0.0	0.0	0.0	0.0	0.0	0.0	0.0	0.0	0.0	17.1	0.0	4.9	0.0	0.0	0.0	0.0	0.0	4.9	0.0
19.85	0.0	0.0	0.0	0.0	0.0	0.0	0.0	0.0	0.0	0.0	0.0	0.0	0.0	0.0	0.0	1.6	0.0	0.0	0.0	0.0	0.0	0.0	0.0	0.0	0.0	0.0	0.0	0.0	0.0	0.0	0.0	0.0	0.0	0.0	0.0	3.2	0.0	0.0	0.0	0.0	0.0	0.0	0.0	9.5	0.0
20.53	0.0	0.0	0.0	0.0	0.0	0.0	0.0	0.0	0.0	0.0	0.0	0.0	0.0	0.0	0.0	0.0	0.0	0.0	0.0	0.0	0.0	0.0	0.0	0.0	0.0	0.0	0.0	0.0	0.0	0.0	0.0	0.0	0.0	0.0	0.0	2.2	0.0	0.0	0.0	0.0	0.0	0.0	0.0	39.1	0.0
20.85	0.0	0.0	0.0	0.0	0.0	0.0	0.0	0.0	0.0	0.0	0.0	0.0	0.0	0.0	0.0	0.0	0.0	0.0	0.0	0.0	0.0	1.6	0.0	0.0	0.0	0.0	0.0	0.0	0.0	0.0	0.0	0.0	0.0	0.0	0.0	0.0	0.0	6.3	0.0	0.0	0.0	0.0	0.0	7.9	0.0
22.80	0.0	0.0	0.0	0.0	0.0	0.0	0.0	0.0	0.0	0.0	1.1	0.0	0.0	0.0	0.0	0.0	0.0	0.0	0.0	0.0	0.0	0.0	0.0	0.0	0.0	0.0	0.0	0.0	0.0	0.0	0.0	0.0	0.0	0.0	0.0	9.8	0.0	1.1	0.0	0.0	0.0	0.0	0.0	53.3	0.0
22.88	0.0	0.0	0.0	0.0	9.0	0.5	0.0	0.0	0.0	0.0	0.0	0.0	0.0	0.0	0.0	0.0	0.0	0.0	0.0	0.0	0.0	0.5	0.0	0.0	0.0	0.0	3.0	0.0	0.0	0.5	0.0	0.0	0.0	0.0	0.5	7.5	0.5	4.5	0.0	0.0	0.0	0.0	0.0	4.5	0.0
23.55	0.0	0.0	0.0	0.0	0.0	0.0	0.0	0.0	0.0	0.0	0.0	0.0	0.0	0.0	0.0	0.0	0.0	0.0	0.0	0.0	0.0	3.1	0.0	0.0	0.0	0.0	0.0	0.0	0.0	0.0	0.0	0.0	0.0	0.0	0.0	6.3	0.0	3.1	0.0	0.0	0.0	0.0	0.0	3.1	0.0
24.05	0.0	0.0	0.0	0.0	0.0	0.0	0.0	0.0	0.0	0.0	0.0	0.0	0.0	0.0	0.0	0.0	0.0	0.0	0.0	0.0	0.0	0.0	0.0	0.0	0.0	0.0	0.0	0.0	0.0	0.0	0.0	0.0	0.0	0.0	0.0	0.0	0.0	0.0	0.0	0.0	0.0	0.0	0.0	0.0	0.0
26.23	0.0	0.0	0.0	0.0	0.0	0.0	0.0	0.0	0.0	0.0	0.0	0.0	0.0	0.0	0.0	0.7	0.0	0.0	1.3	0.0	0.0	3.3	0.0	0.0	0.0	0.0	1.3	0.0	0.0	0.0	0.0	0.0	0.0	0.0	0.0	1.3	0.0	5.9	0.0	0.0	0.0	0.7	0.0	5.3	0.0
26.83	0.0	0.0	0.0	0.0	1.0	0.0	0.0	0.0	0.0	0.5	0.0	0.0	0.0	0.0	0.0	0.0	0.0	0.0	0.5	0.0	0.0	0.0	0.0	0.0	0.0	0.0	0.0	0.0	0.0	0.0	0.0	0.0	0.0	0.0	0.0	0.5	0.0	7.9	0.0	0.0	0.0	0.0	0.0	20.3	0.0
28.00	0.0	0.0	0.0	0.0	0.5	0.0	0.0	0.0	0.0	0.0	0.5	0.0	0.0	0.0	0.0	1.0	0.0	0.0	0.0	0.0	0.0	2.5	0.0	0.0	0.0	0.0	0.0	0.0	0.0	0.0	0.0	0.0	0.0	0.0	6.0	8.5	0.0	22.0	0.0	0.0	0.0	0.0	0.0	0.0	0.0
30.60	0.0	0.0	0.0	0.0	0.0	0.0	0.0	0.0	0.0	0.0	0.0	0.0	0.0	0.0	0.0	0.6	0.0	0.0	0.0	0.0	0.0	0.0	0.0	0.0	0.0	0.0	0.6	0.0	0.0	0.0	0.0	0.0	0.0	0.0	0.6	7.4	0.0	3.7	0.0	0.0	0.0	0.0	0.0	0.6	0.0
32.25	0.0	0.0	0.0	0.0	0.0	0.0	0.0	0.0	0.0	0.0	0.0	0.0	0.0	0.0	0.0	0.0	0.0	0.0	0.0	0.0	0.0	2.2	0.0	0.0	0.0	0.0	0.0	0.0	0.0	0.0	0.0	0.0	0.0	0.0	4.5	0.0	0.0	43.6	0.0	0.0	0.0	0.0	0.0	9.5	0.0
33.20	0.0	0.0	0.0	0.0	0.0	0.0	0.0	0.0	0.0	0.0	0.0	0.0	0.0	0.0	0.0	0.0	0.0	0.0	0.0	0.0	0.0	3.9	0.0	0.0	0.0	0.0	0.0	0.0	0.0	0.0	0.0	0.5	0.0	0.0	0.0	6.8	0.0	24.2	0.0	0.0	0.0	0.0	0.0	1.4	0.0
35.95	0.0	0.0	0.0	0.0	0.0	0.0	0.0	0.0	0.0	0.0	0.0	0.0	0.0	0.0	0.0	1.1	0.0	0.0	0.0	0.0	0.0	2.2	0.0	0.0	0.0	0.0	1.1	0.0	0.0	0.0	0.0	0.0	0.0	0.0	0.0	4.3	0.0	0.0	0.0	0.0	0.0	0.0	0.0	6.5	0.0
37.55	0.0	0.0	0.0	0.0	0.0	0.0	0.0	0.0	0.0	0.0	0.0	0.0	0.0	0.0	0.0	0.0	0.0	0.0	0.0	0.0	0.0	1.5	0.0	0.0	0.0	0.0	0.0	0.0	0.0	0.0	0.0	0.0	0.0	0.0	3.5	14.4	0.0	22.4	0.0	0.0	0.0	0.0	0.0	10.4	0.0
40.10	0.0	0.0	0.0	0.0	0.0	0.0	0.0	0.0	0.0	0.0	0.0	0.0	0.0	0.0	0.0	0.0	0.0	0.0	0.5	0.0	0.0	0.0	0.0	0.0	0.0	0.0	0.0	0.0	0.0	0.0	0.5	0.0	0.0	0.0	0.0	15.7	0.0	15.7	0.5	0.0	0.0	0.0	0.0	3.9	0.0
42.25	0.0	0.0	0.0	0.0	0.0	0.0	0.0	0.0	0.0	0.0	0.0	0.0	0.0	0.0	0.0	0.6	0.0	0.0	0.0	0.0	0.0	0.0	0.0	0.0	0.0	0.0	0.0	0.0	0.0	0.0	0.0	0.0	0.0	0.0	0.0	2.9	0.0	0.6	0.0	0.0	0.0	0.0	0.0	52.4	0.0
42.65	0.0	0.0	0.0	0.0	1.0	0.0	0.0	0.0	0.0	0.0	0.0	0.0	0.0	0.0	0.5	0.5	0.0	0.0	0.0	0.0	0.0	0.0	0.0	0.0	0.0	0.0	0.0	0.0	0.0	0.0	0.0	0.0	0.0	0.0	0.0	12.5	0.0	2.5	0.0	0.0	0.0	0.0	0.0	0.5	0.0
44.15	0.0	0.0	0.0	0.0	0.0	0.0	0.0	0.0	0.0	0.0	0.0	0.0	0.0	0.0	0.0	0.0	0.0	0.0	0.0	0.0	0.0	0.0	0.0	0.0	0.0	0.0	0.0	0.0	0.0	0.0	0.0	0.0	0.0	0.0	0.0	0.0	0.0	0.0	2.6	0.0	0.0	0.0	0.0	0.0	0.0
46.35	0.0	0.0	0.0	0.0	1.0	0.0	0.0	0.0	0.0	0.0	0.0	0.0	0.0	0.0	0.0	0.0	0.0	0.0	1.0	0.0	0.0	0.0	0.0	0.0	0.0	0.0	0.5	0.0	0.0	1.0	0.0	0.0	0.0	0.0	0.0	4.5	0.0	14.9	0.5	0.0	0.0	0.0	0.0	0.5	0.0
47.90	0.0	0.0	0.0	0.0	0.0	0.0	0.0	0.0	0.0	0.0	0.0	0.0	0.0	0.0	0.0	1.0	1.0	0.0	0.0	0.0	0.0	0.0	0.0	0.0	0.0	0.0	0.5	0.0	0.0	0.0	0.0	0.0	0.0	0.0	0.0	4.4	0.0	6.4	0.0	0.0	0.0	0.0	0.0	0.0	0.0
48.60	0.0	0.0	0.0	0.0	0.0	0.0	0.0	0.0	0.0	0.0	0.0	0.0	0.0	0.0	0.0	0.0	0.0	0.0	0.0	0.0	0.0	1.0	0.0	0.0	0.0	0.0	0.0	0.0	0.0	0.0	0.0	0.0	0.0	0.0	0.0	26.5	0.0	0.5	0.0	0.0	0.0	0.0	0.0	3.4	0.0
49.70	0.0	0.0	0.0	0.0	1.0	0.0	0.0	0.0	0.0	0.0	0.0	0.0	0.0	0.0	0.0	0.0	0.0	0.0	0.0	0.0	0.0	0.5	0.0	0.0	0.0	0.0	1.0	0.0	0.0	0.0	0.0	0.0	0.0	0.0	0.0	6.0	0.0	13.6	0.5	0.0	0.0	0.0	0.0	1.5	0.0
50.60	0.0	0.0	0.0	0.0	1.6	0.0	0.0	0.0	0.0	0.5	0.0	0.0	0.0	0.0	0.0	0.0	0.0	0.0	0.5	0.0	0.0	1.0	0.0	0.0	0.0	0.0	0.0	0.0	0.0	0.5	0.0	0.0	0.5	0.0	0.0	2.6	0.0	4.7	0.0	0.0	0.0	0.0	0.0	0.0	0.0
51.80	0.0	0.0	0.5	0.0	4.2	0.0	0.0	0.0	0.0	0.5	0.0	0.0	0.0	0.0	0.0	0.0	0.0	0.0	0.5	0.0	0.0	0.0	0.0	0.0	0.0	0.0	2.6	0.0	0.5	0.0	0.0	0.5	0.0	0.0	0.0	10.5	0.0	4.7	0.5	0.0	0.0	0.0	0.0	2.1	0.0
52.35	0.0	0.0	1.0	0.0	2.0	0.0	0.0	0.0	0.0	0.0	5.4	0.5	0.0	0.5	0.5	4.9	0.5	0.0	0.0	0.0	0.0	0.0	0.0	0.0	0.0	0.0	0.0	0.0	0.0	0.5	0.0	0.0	0.0	0.0	0.0	8.8	0.0	0.5	0.0	0.0	0.0	0.0	0.0	16.2	0.5
54.50	0.0	0.0	0.0	0.0	0.8	0.0	0.0	0.0	0.0	0.0	0.0	0.0	0.0	0.0	0.0	0.0	0.0	0.0	0.0	0.0	0.0	0.0	0.0	0.0	0.0	0.0	0.0	0.0	0.0	0.0	0.0	0.0	0.0	0.0	0.0	9.2	0.0	3.1	0.0	0.0	0.0	0.0	0.0	7.7	0.0
56.10	0.0	0.0	0.6	0.0	0.0	0.0	0.0	0.0	0.0	0.0	0.0	0.0	0.6	0.0	0.6	1.8	0.0	0.0	0.0	0.0	0.6	0.6	0.0	0.0	0.0	0.0	0.0	0.0	0.0	0.0	0.0	0.0	0.0	0.0	0.0	14.7	0.0	0.6	0.0	0.0	0.0	0.0	0.0	3.5	0.0
56.95	0.0	0.0	0.0	0.0	1.6	1.6	0.0	0.0	0.0	0.0	1.6	0.0	0.0	0.0	0.0	0.0	0.0	0.0	0.0	0.0	0.0	0.0	0.0	0.0	0.0	0.0	0.0	0.0	0.0	0.0	0.0	0.0	0.0	0.0	0.0	3.3	0.0	0.0	0.0	0.0	0.0	0.0	0.0	1.6	0.0
57.60	0.0	0.0	0.0	0.0	0.0	0.0	0.0	0.0	0.0	0.0	0.0	0.0	0.0	0.0	0.0	0.0	0.0	0.0	0.0	0.0	0.0	0.0	0.0	0.0	0.0	0.0	0.0	0.0	0.0	0.0	0.0	0.0	0.0	0.0	0.0	15.5	0.0	0.9	0.0	0.0	0.0	0.0	0.0	1.7	0.0
57.80	0.0	0.0	0.0	0.0	0.0	0.0	0.0	0.0	0.0	0.0	0.0	2.8	0.0	0.0	0.0	0.0	0.0	0.0	0.0	0.0	0.0	0.0	0.0	0.0	0.0	0.0	0.0	0.0	0.0	0.0	0.0	0.0	0.0	0.0	0.0	5.6	0.0	0.9	0.0	0.0	0.0	0.0	0.0	27.1	0.0
58.70	0.0	0.0	1.4	0.0	0.7	0.7	0.0	0.0	0.0	0.0	2.8	0.0	0.0	0.0	0.0	4.2	0.0	0.0	0.0	0.0	0.0	0.0	0.0	0.0	0.0	0.0	0.0	0.0	0.0	0.0	0.0	0.0	0.7	0.0	0.0	15.4	0.0	0.0	0.0	0.0	0.0	0.0	0.0	1.4	0.0
59.30	0.0	0.0	0.0	0.0	0.0	0.0	0.0	0.0	0.0	0.0	0.0	0.0	0.0	0.0	0.0	0.0	0.0	0.0	0.0	0.0	0.0	0.0	0.0	0.0	0.0	0.0	0.0	0.0	0.0	0.0	0.0	0.0	0.0	0.0	0.0	0.0	0.0	5.3	0.0	0.0	0.0	0.0	0.0	7.5	0.0
60.70	0.0	0.0	0.0	0.0	0.0	0.0	0.0	0.0	0.0	0.0	0.0	0.0	0.0	0.0	0.0	1.1	0.0	0.0	0.0	0.0	0.0	3.7	0.0	0.0	0.0	0.0	0.0	0.0	0.0	0.0	0.0	0.0	0.5	0.0	0.0	9.0	0.0	5.8	0.0	0.0	0.0	0.0	0.0	3.7	0.0
65.45	0.0	0.0	0.0	0.0	0.0	0.0	0.0	0.0	0.0	0.0	1.5	0.5	0.0	0.0	0.0	4.5	0.0	0.0	0.0	0.0	0.0	0.0	0.0	0.0	0.0	0.0	0.5	0.0	0.0	0.0	0.0	0.0	0.0	0.0	0.0	20.9	0.0	2.5	0.0	0.0	0.0	0.0	0.0	2.0	0.5
65.90	0.0	0.0	0.0	0.0	0.0	0.0	0.0	0.0	0.0	0.0	2.9	0.0	0.0	1.4	1.4	2.9	1.4	0.0	0.0	0.0	0.0	0.0	0.0	0.0	0.0	0.0	0.0	0.0	0.0	0.0	0.0	0.0	0.0	0.0	0.0	1.4	0.0	0.0	0.0	0.0	0.0	0.0	0.0	7.2	1.4
67.00	0.0	0.0	0.0	0.0	0.0	0.0	0.0	0.0	0.0	3.6	0.0	0.0	0.0	0.0	0.0	0.0	0.0	0.0	0.0	0.0	0.0	1.2	0.0	0.0	0.0	0.0	0.0	0.0	0.0	0.0	0.0	0.0	0.0	0.0	0.0	4.8	0.0	3.6	0.0	0.0	0.0	0.0	0.0	22.6	0.0
67.40	0.0	0.0	0.0	0.0	0.0	0.0	0.0	0.0	0.0	0.0	0.0	0.0	0.0	0.0	0.0	0.0	0.0	0.0	0.0	0.0	0.0	1.4	0.0	0.0	0.0	0.0	0.0	0.0	0.0	0.0	0.0	0.0	0.0	0.0	0.0	15.7	0.0	4.3	0.0	0.0	0.0	0.0	0.0	4.3	0.0
71.60	0.0	0.0	0.0	0.0	0.0	0.0	0.0	0.0	0.0	0.0	0.0	0.0	0.0	0.0	0.0	0.0	0.0	0.0	0.0	0.0	0.0	1.2	0.0	0.0	0.0	0.0	2.4	0.0	0.0	0.0	0.0	0.0	0.0	0.0	0.0	3.6	0.0	2.4	0.0	0.0	0.0	0.0	0.0	3.6	0.0
72.25	0.0	0.0	0.0	0.0	0.0	0.0	0.0	0.0	0.0	0.0	0.0	0.0	0.0	0.0	0.0	0.0	0.0	0.0	0.0	0.0	0.0	2.3	0.0	0.0	0.0	0.0	1.5	0.0	0.0	0.0	0.0	0.0	0.0	0.0	0.0	18.5	0.0	3.8	0.0	0.0	0.0	0.0	0.0	0.8	0.0
75.40	0.0	0.0	0.0	0.0	0.0	0.0	0.0	0.0	0.0	0.0	0.0	0.0	0.0	0.0	0.0	0.0	0.0	0.0	0.0	0.0	0.0	0.0	0.0	0.0	0.0	0.0	0.0	0.0	0.0	0.0	0.0	0.0	0.0	0.0	0.0	0.6	0.0	1.3	0.0	0.0	0.0	0.0	0.0	23.7	0.0
77.20	0.0	0.0	0.0	0.0	0.0	0.0	0.0	0.0	0.0	0.0	0.0	0.0	0.0	0.0	0.0	0.0	0.0	0.0	0.0	0.0	0.0	0.0	0.0	0.0	0.0	0.0	0.0	0.0	0.0	0.0	0.0	0.0	0.0	0.0	0.0	0.0	0.0	0.0	0.0	0.0	0.0	0.0	0.0	25.6	0.0
80.40	0.0	0.0	0.0	0.0	0.6	0.0	0.0	0.0	0.0	0.0	0.0	0.0	0.0	0.0	0.0	0.0	0.6	0.0	1.1	0.0	0.0	2.2	0.0	0.0	0.0	0.0	0.6	0.0	0.0	0.0	0.0	0.0	0.0	0.0	0.0	8.3	0.0	1.1	0.0	0.0	0.0	0.0	0.0	21.0	0.0
82.55	0.0	0.0	0.0	0.0	1.3	0.0	0.0	0.0	0.0	0.0	0.0	0.0	0.0	0.0	0.0	0.0	0.0	0.0	0.0	0.0	0.0	0.0	0.0	0.0	0.0	0.0	0.0	0.0	0.0	0.0	0.0	0.0	0.0	0.0	0.0	4.5	0.0	1.9	0.0	0.0	0.0	0.0	0.0	21.7	0.0
83.00	0.0	0.0	0.0	0.0	1.0	0.0	0.0	0.0	0.0	0.0	0.0	0.0	0.0	0.0	0.0	0.0	0.0	0.0	0.0	0.0	0.0	1.0	0.0	0.0	0.0	0.0	1.0	0.0	0.0	0.0	0.0	0.0	0.0	0.0	0.0	32.7	0.0	2.0	0.0	0.0	0.0	0.0	0.0	3.0	0.0
84.90	0.0	0.0	0.0	0.0	0.0	0.0	0.5	0.0	0.0	0.0	0.0	0.0	0.0	0.0	0.0	0.0	0.0	0.0	0.0	0.0	0.0	0.0	0.0	0.0	0.0	0.0	1.1	0.0	0.0	0.0	0.0	0.0	0.0	0.0	0.0	0.5	0.0	0.0	0.0	0.0	0.0	0.0	0.0	13.2	0.0
86.70	0.0	0.0	0.0	0.0	0.0	0.0	0.0	0.0	0.0	0.0	0.0	0.0	0.0	0.0	0.0	0.0	0.0	0.0	0.0	0.0	0.0	0.0	0.0	0.0	0.0	0.0	0.0	0.0	0.0	0.0	0.0	0.0	0.0	0.0	0.0	5.3	0.0	9.8	0.0	0.0	0.0	0.0	0.0	0.0	0.0
88.40	0.0	0.0	0.0	0.0	0.0	0.0	0.0	0.0	0.0	0.0	0.0	0.0	0.0	0.0	0.0	0.0	0.0	0.0	0.5	0.0	0.0	1.0	0.0	0.0	0.0	0.0	1.0	0.0	0.0	0.0	0.0	0.0	0.0	0.0	0.0	0.0	0.0	1.0	0.0	0.0	0.0	0.0	0.0	14.5	0.0
91.25	0.0	0.0	0.0	0.0	2.1	0.0	0.0	0.0	0.0	0.0	0.0	0.0	0.0	0.0	0.0	0.0	0.0	0.0	0.4	0.8	0.0	0.0	0.0	0.0	0.0	0.0	2.1	0.0	0.0	0.0	0.0	0.0	0.0	0.0	0.0	3.4	0.0	0.0	0.0	0.0	0.0	0.0	0.0	9.2	0.0
94.35	0.0	0.0	0.0	0.0	0.8	0.0	0.0	0.0	0.0	0.0	0.0	0.0	0.0	0.0	0.0	0.0	0.0	0.0	0.0	0.0	0.0	0.4	0.0	0.0	0.0	0.0	0.4	0.0	0.0	0.0	0.0	0.0	0.0	0.0	0.0	0.0	0.0	0.0	0.0	0.0	0.0	0.0	0.0	30.1	0.0
97.65	0.0	0.0	0.0	0.0	0.6	0.0	0.6	0.0	0.0	0.0	0.6	0.0	0.0	0.0	0.0	0.0	0.0	0.0	0.0	0.0	0.0	0.6	0.0	0.0	0.0	0.0	1.1	0.0	0.0	0.0	0.0	0.0	0.0	0.0	0.0	15.6	0.0	12.8	0.0	0.0	0.0	0.0	0.0	0.6	0.0
98.20	0.0	0.0	0.0	0.0	0.0	0.0	0.0	0.0	0.0	0.0	0.0	0.0	0.0	0.0	0.0	0.0	0.0	0.0	0.0	3.6	0.0	0.0	1.4	0.0	0.0	0.0	0.0	0.0	0.0	0.0	0.0	0.0	0.0	0.0	0.0	6.5	0.0	7.9	0.0	0.0	0.0	0.7	0.0	1.4	0.0
99.20	0.0	0.0	1.3	0.0	0.0	0.0	0.0	0.0	0.0	0.0	0.0	0.0	0.0	0.0	0.0	0.0	0.0	0.0	0.0	0.9	0.0	0.0	0.0	0.0	0.0	0.4	0.4	0.0	0.0	0.0	0.0	0.0	0.0	0.0	0.0	0.9	0.0	1.8	0.4	0.0	0.0	0.0	0.0	10.1	0.0
101.70	0.0	0.0	0.0	0.0	9.3	0.5	0.0	0.5	0.0	0.0	0.0	0.0	0.0	0.0	0.0	0.0	0.0	1.0	0.0	1.5	0.0	0.5	0.0	0.0	0.0	0.0	0.0	0.0	0.0	0.0	0.0	0.0	0.0	0.0	0.0	3.6	0.0	3.1	0.0	0.0	0.0	0.0	0.0	2.6	0.0
103.15	0.0	0.0	0.0	0.0	0.4	0.0	0.4	0.0	0.0	0.0	0.0	0.0	0.0	0.0	0.0	0.0	0.0	0.0	0.4	0.4	0.0	1.7	0.0	0.0	0.0	0.0	0.4	0.0	0.0	0.0	0.0	0.0	0.0	0.0	0.0	1.2	0.0	2.9	0.8	0.0	0.0	0.0	0.0	5.0	0.0
108.10	0.0	0.0	0.0	0.0	0.0	0.0	0.0	0.0	0.0	0.0	0.0	0.0	0.0	0.0	0.0	0.0	0.0	0.0	0.0	0.0	0.0	4.4	0.0	0.0	0.0	0.0	0.0	0.0	0.0	0.0	0.0	0.0	0.0	0.0	0.0	0.0	0.0	1.5	0.0	0.0	0.0	0.0	0.0	17.0	0.0
109.40	0.0	0.0	0.0	0.0	3.3	0.0	0.0	0.0	0.0	0.0	0.0	0.0	0.0	0.0	0.0	0.0	0.0	0.0	0.0	3.3	0.0	0.0	0.0	0.0	0.0	0.0	1.6	0.0	0.0	0.0	0.0	0.0	0.5	0.0	0.0	2.7	0.0	10.4	0.0	0.0	0.0	0.0	0.0	0.5	0.0
110.60	0.0	0.0	0.0	0.0	0.9	0.0	0.0	0.0	0.0	0.0	0.0	0.0	0.0	0.0	0.0	0.0	0.0	0.0	0.0	0.0	0.0	0.0	0.0	0.0	0.0	0.0	1.3	0.0	0.0	0.0	0.0	0.0	0.0	0.0	0.0	0.0	0.0	0.0	0.0	0.0	0.0	0.0	0.0	12.9	0.0
112.70	0.0	0.0	0.0	0.0	0.0	0.0	0.0	0.0	0.0	0.0	0.0	0.0	0.0	0.0	0.0	0.0	0.0	0.0	0.0	0.6	0.0	0.0	0.0	0.0	0.0	0.0	0.0	0.0	0.0	0.0	0.0	0.0	0.0	0.6	0.0	2.2	0.0	13.8	0.0	0.6	0.0	0.0	0.0	0.6	0.0
119.50	0.0	0.0	0.0	0.0	0.9	0.0	0.0	0.0	0.0	0.0	0.0	0.0	0.0	0.0	0.0	0.0	0.0	0.5	0.0	0.5	0.0	0.0	0.0	0.0	0.0	0.0	0.0	0.0	0.0	0.0	0.0	0.0	0.0	0.0	0.0	6.5	0.0	2.8	0.0	0.0	0.0	0.0	0.0	2.8	0.0
120.60	0.0	0.0	0.0	0.0	0.5	0.0	0.0	0.0	0.0	0.0	0.0	0.0	0.0	0.0	0.0	0.0	0.0	0.0	0.0	0.0	0.0	0.0	0.0	0.0	0.0	0.0	0.0	0.0	0.0	0.0	0.0	0.0	0.0	0.0	0.0	1.0	0.0	0.5	0.0	0.0	0.0	0.0	0.0	52.5	0.0
122.85	0.0	0.0	0.0	0.0	0.0	0.0	0.0	0.0	0.0	0.0	0.0	0.0	0.0	0.0	0.0	0.0	0.0	0.0	0.0	0.0	0.0	0.0	0.0	0.0	0.0	0.0	0.0	0.0	0.0	0.0	0.0	0.0	0.0	0.0	0.0	12.8	0.0	2.3	0.0	0.0	0.0	0.0	0.0	38.3	0.0
124.40	0.0	0.0	0.0	0.0	0.5	0.0	0.0	0.0	0.0	0.0	0.0	0.0	0.0	0.0	0.0	0.0	0.0	9.1	0.0	0.0	0.0	2.0	0.0	0.0	0.0	0.0	0.0	0.0	0.0	0.0	0.0	0.0	0.0	0.0	0.0	22.7	0.0	4.0	0.5	0.0	0.0	0.0	0.0	3.0	0.0
124.67	0.0	0.0	0.0	0.0	0.0	0.0	0.0	0.0	0.0	0.0	0.0	0.0	0.0	0.0	0.0	0.0	0.0	0.0	0.0	0.0	0.0	0.9	0.0	0.0	0.0	0.0	0.0	0.0	0.0	0.0	0.0	0.0	0.0	0.0	0.0	19.7	0.0	8.3	0.0	0.0	0.0	0.0	0.0	0.4	0.0
128.10	0.0	0.0	0.0	0.0	0.8	0.0	0.0	0.0	0.0	0.0	0.0	0.0	0.0	0.0	0.0	0.0	0.0	0.0	0.0	0.0	0.0	0.8	0.0	0.0	0.0	0.0	0.0	0.0	0.0	0.0	0.0	0.0	0.0	0.0	0.0	2.9	0.0	3.3	0.0	0.0	0.0	0.4	0.0	2.1	0.0
130.55	0.0	0.0	0.0	0.0	0.3	0.3	0.0	0.0	0.0	0.0	0.0	0.0	0.0	0.0	0.0	0.0	0.0	0.0	0.6	0.0	0.0	0.0	0.0	0.0	0.0	0.0	0.0	0.0	0.0	0.0	0.0	0.0	0.0	0.0	0.3	6.5	0.0	4.2	0.0	0.0	0.0	0.0	0.0	0.3	0.0
134.45	0.0	0.0	0.0	0.0	0.7	0.0	0.0	0.0	0.4	0.0	0.0	0.0	0.0	0.0	0.0	0.0	0.0	0.0	0.0	0.0	0.0	0.0	0.0	0.0	0.0	0.0	0.0	0.0	0.0	0.0	0.0	0.0	0.4	0.0	0.0	1.4	0.0	0.0	0.0	0.0	0.0	0.0	0.0	41.3	0.0
135.75	0.0	0.0	0.0	0.0	1.1	0.5	0.0	0.0	0.0	0.0	0.0	0.0	0.0	0.0	0.0	0.0	0.0	0.0	0.0	0.0	0.0	4.9	0.0	0.0	0.0	0.0	0.0	0.0	0.0	0.0	0.0	0.0	0.0	0.0	0.0	5.9	0.0	8.1	0.0	0.0	0.0	0.0	0.0	0.0	0.0
146.10	0.0	0.0	0.0	0.0	2.2	0.0	0.0	0.0	0.0	0.0	0.0	0.0	0.0	0.0	0.0	0.0	0.0	0.0	0.4	0.0	0.0	0.0	0.0	0.0	0.0	0.0	0.0	0.0	0.0	0.0	0.0	0.0	0.0	0.0	0.0	19.9	0.0	4.4	0.0	0.0	0.0	0.0	0.0	0.4	0.0
157.15	0.0	0.0	0.5	0.0	1.4	0.5	0.5	0.0	0.0	0.0	0.0	0.0	0.0	0.0	0.0	0.0	0.0	0.0	0.5	0.0	0.0	0.0	0.0	0.0	0.0	0.0	5.6	0.5	0.0	0.5	0.0	0.0	0.0	0.0	0.0	6.0	0.0	0.5	0.0	0.0	0.0	0.0	0.5	3.3	0.0
160.35	0.0	0.0	0.8	0.0	0.4	0.0	0.0	0.0	0.0	0.0	0.0	0.0	0.0	0.0	0.0	0.0	0.0	0.0	0.0	0.0	0.0	0.0	0.0	0.0	0.4	0.0	2.9	0.0	0.0	0.0	0.0	0.0	0.4	0.0	0.0	19.3	0.0	4.2	0.0	0.0	0.0	0.4	0.4	2.5	0.0
167.25	0.0	0.0	0.0	0.0	0.7	0.0	0.0	0.0	0.0	0.0	0.0	0.0	0.0	0.0	0.0	0.0	0.0	0.0	0.3	0.0	0.0	0.0	0.0	0.0	0.0	0.0	0.0	0.0	0.0	0.0	0.0	0.0	0.0	0.0	0.0	2.1	0.0	6.9	0.0	0.0	0.0	0.0	0.0	36.0	0.0
170.43	0.0	0.0	0.0	0.0	1.2	0.0	0.0	0.0	0.0	0.0	0.0	0.0	0.0	0.0	0.0	0.0	0.0	0.0	0.0	0.3	0.0	0.0	0.0	0.0	0.0	0.0	3.1	0.0	0.0	0.0	0.0	0.0	0.0	0.0	0.3	11.5	0.0	23.5	0.0	0.0	0.3	0.0	0.0	0.3	0.0
178.56	0.0	0.0	0.5	0.0	7.4	0.5	0.0	0.0	0.0	0.0	0.0	0.0	0.0	0.0	0.0	0.0	0.0	0.0	0.0	0.5	0.0	0.0	0.0	0.0	0.0	0.0	0.5	0.0	0.0	0.0	0.0	0.0	0.0	0.0	0.0	1.9	0.0	10.6	0.0	0.0	0.0	0.9	0.0	0.5	0.0
182.06	0.0	0.0	0.4	0.0	1.2	0.0	0.0	0.0	0.0	0.0	0.0	0.0	0.0	0.0	0.0	0.0	0.0	0.0	0.0	0.4	0.0	0.0	0.0	0.0	0.0	0.0	0.0	0.0	0.0	0.0	0.0	0.0	0.0	0.0	0.0	0.0	0.0	4.1	0.0	0.0	0.0	0.0	0.0	27.8	0.4
182.60	0.0	0.0	0.5	0.0	1.5	0.0	0.0	0.0	0.0	0.0	0.0	0.0	0.0	0.0	0.0	0.0	0.0	0.0	0.0	4.9	0.0	0.0	0.0	0.0	0.0	0.0	0.5	0.0	0.0	0.0	0.0	0.0	0.0	0.0	0.0	0.5	0.0	0.0	0.0	0.0	0.0	0.0	0.0	0.0	0.0
189.80	0.0	0.0	0.0	0.0	1.5	0.5	0.0	0.0	0.0	0.0	0.0	0.0	0.0	0.0	0.0	0.0	0.0	0.0	0.0	0.0	0.0	0.0	0.0	0.0	0.0	0.0	0.0	0.0	0.0	0.0	0.0	0.0	0.0	0.0	0.0	0.5	0.0	1.0	0.0	0.5	0.0	0.0	0.0	10.3	0.0
190.75	0.0	0.0	0.3	0.0	0.3	0.0	0.0	0.0	0.0	0.0	0.0	0.0	0.0	0.0	0.0	0.0	0.0	0.3	0.0	0.0	0.0	0.0	0.0	0.0	0.0	0.0	0.6	0.0	0.0	0.0	0.0	0.0	0.0	0.0	0.0	3.7	0.0	0.0	0.0	0.3	0.0	0.0	0.0	56.3	0.0
200.68	0.0	0.0	0.5	0.0	0.5	0.0	0.0	0.0	0.0	0.0	0.0	0.0	0.0	0.0	0.0	0.0	0.0	0.0	0.0	0.0	0.0	0.0	0.0	0.0	0.0	0.0	0.5	0.0	0.0	0.0	0.0	0.0	0.0	0.0	0.0	0.5	1.0	1.0	0.0	0.0	0.0	0.0	0.0	0.0	0.0
202.37	0.0	0.0	0.0	0.0	0.0	0.0	0.0	0.0	0.0	0.0	0.0	0.0	0.0	0.0	0.0	0.0	0.0	0.0	0.0	0.0	0.0	0.0	0.0	0.0	0.0	0.0	1.1	0.0	0.0	0.0	0.0	0.0	0.0	0.0	0.0	2.3	2.3	0.6	0.0	0.0	0.0	0.0	0.0	4.5	0.0
205.35	0.0	0.0	0.0	0.0	1.0	0.0	0.0	0.0	0.0	0.0	0.0	0.0	0.0	0.0	0.0	0.0	0.0	0.0	0.0	0.0	0.0	0.0	0.0	0.0	0.0	0.0	1.0	0.0	0.0	0.0	0.0	0.0	0.0	0.0	0.0	2.6	0.0	1.0	0.0	0.0	0.0	0.0	0.0	6.1	0.0
207.80	0.0	0.7	0.0	0.0	0.7	6.0	0.0	0.0	0.0	0.0	0.0	0.0	0.0	0.0	0.0	0.0	0.0	0.0	0.0	0.0	0.0	0.0	0.0	0.0	0.0	0.0	2.2	0.0	0.0	0.0	0.0	0.0	0.7	0.0	0.0	3.0	0.0	0.7	0.0	0.0	0.0	0.0	0.0	0.0	0.0
211.85	0.5	0.0	0.5	0.0	1.4	1.4	0.0	0.0	0.0	0.0	0.0	0.0	0.0	0.0	0.0	0.0	0.0	0.0	1.0	0.0	0.0	0.0	0.0	0.0	0.0	0.0	1.0	0.0	0.0	0.0	0.0	0.0	0.0	0.0	0.0	0.0	1.4	0.0	0.0	0.5	0.5	0.0	0.0	0.0	0.0
214.75	0.0	0.3	0.0	0.3	0.3	0.3	1.0	0.0	0.0	0.0	0.0	0.0	0.0	0.0	0.0	0.0	0.0	0.0	0.0	0.7	0.0	0.0	0.0	0.0	0.0	0.0	0.0	0.0	0.0	0.0	0.3	0.0	0.0	0.0	0.0	0.0	0.0	2.1	0.0	0.0	0.0	0.0	0.0	28.0	0.0
217.00	0.0	0.0	0.0	0.0	2.5	0.0	0.0	0.0	0.0	0.0	0.0	0.0	0.0	0.0	0.0	0.0	0.0	0.0	0.0	0.5	0.0	0.0	0.0	0.0	0.0	0.0	0.5	0.0	0.0	0.0	0.0	0.0	0.0	0.0	0.0	0.5	0.0	0.0	0.0	0.0	0.0	0.0	0.0	0.0	0.0
222.00	0.0	0.0	0.0	0.0	0.5	0.0	0.0	0.0	0.0	0.0	0.0	0.0	0.0	0.0	0.0	0.0	0.0	0.0	0.0	0.5	0.0	0.0	0.0	0.0	0.0	0.0	0.5	0.0	0.0	0.0	0.0	0.0	0.0	0.0	0.0	2.4	0.0	0.0	0.0	0.0	0.0	0.0	0.0	0.5	0.0
222.25	0.0	0.5	0.0	0.0	0.5	0.5	0.5	0.0	0.0	0.0	0.0	0.0	0.0	0.0	0.0	0.0	0.0	0.0	0.0	0.0	0.0	0.0	0.0	0.0	0.0	0.0	0.0	0.0	0.0	0.0	0.0	0.0	0.0	0.0	0.0	0.0	0.0	0.0	0.0	0.0	0.0	0.0	0.0	2.6	0.0
224.60	0.0	0.0	0.0	0.0	0.6	0.0	0.0	0.0	0.0	0.0	0.0	0.0	0.0	0.0	0.0	0.0	0.0	0.0	0.0	0.0	0.0	0.0	0.0	0.0	0.0	0.0	0.0	0.0	0.0	0.0	0.0	0.0	0.0	0.0	0.0	0.0	0.0	0.0	0.0	0.0	0.0	0.0	0.0	0.0	0.0
227.10	0.0	0.0	0.0	0.0	4.3	0.4	0.0	0.0	0.0	0.0	0.0	0.0	0.0	0.0	0.0	0.0	0.0	0.0	0.0	0.0	0.0	0.0	0.0	0.0	0.0	0.0	0.0	0.0	0.0	0.0	0.0	0.0	0.0	0.0	0.0	1.6	0.0	0.0	0.0	0.0	0.0	0.0	0.0	11.3	0.0
232.90	0.0	0.0	0.0	0.0	0.0	0.0	0.0	0.0	0.0	0.0	0.0	0.0	0.0	0.0	0.0	0.0	0.0	0.0	0.0	0.0	0.0	0.0	0.0	0.0	0.0	0.0	0.5	0.0	0.0	0.0	0.0	0.0	0.0	0.0	0.0	0.5	0.0	0.0	0.0	0.0	0.0	0.0	0.0	0.0	0.0
237.60	0.0	0.0	0.0	0.0	0.0	0.5	0.0	0.0	0.0	0.0	0.0	0.0	0.0	0.0	0.0	0.0	0.0	0.0	0.0	0.0	0.0	0.0	0.0	0.0	0.0	0.0	0.0	0.0	0.0	0.0	0.0	0.0	0.0	0.0	0.0	1.0	0.0	0.0	0.0	0.0	0.0	0.0	0.0	0.0	0.0
237.70	0.0	0.0	0.0	0.0	1.0	0.0	0.0	0.0	0.0	0.0	0.0	0.0	0.0	0.0	0.0	0.0	0.0	0.0	0.0	0.0	0.0	0.0	0.0	0.0	0.0	0.0	1.9	0.0	0.0	0.0	0.0	1.0	0.0	0.0	0.0	0.0	0.0	0.0	0.0	0.0	0.0	0.0	0.0	0.0	0.0
239.75	0.0	0.0	0.0	0.0	0.0	0.5	0.0	0.0	0.0	0.0	0.0	0.0	0.0	0.0	0.0	0.0	0.0	0.0	0.0	0.0	0.0	0.0	0.0	0.0	0.0	0.0	0.5	0.0	0.0	0.0	0.0	0.0	0.0	0.0	0.0	1.9	0.0	0.0	0.0	0.0	0.0	0.0	0.0	0.0	0.0
240.65	0.0	0.0	0.0	0.0	0.0	0.0	0.0	0.0	0.0	0.0	0.0	0.0	0.0	0.0	0.0	0.0	0.0	0.0	0.0	0.0	0.0	0.0	0.0	0.0	0.0	0.0	0.8	0.0	0.0	0.0	0.0	0.0	0.0	0.0	0.0	2.5	0.0	1.7	0.0	0.0	0.0	0.0	0.0	10.9	0.0
241.25	0.0	0.0	0.0	0.0	0.0	0.0	0.0	0.0	0.0	0.0	0.0	0.0	0.0	0.0	0.0	0.0	0.0	0.0	0.0	0.0	0.0	0.0	0.0	0.0	0.0	0.0	0.0	0.0	0.0	0.0	0.0	0.0	0.0	0.0	0.0	2.5	0.0	0.0	0.0	0.0	0.0	0.0	0.0	0.0	0.0
243.95	0.0	0.0	0.0	0.0	0.0	0.0	0.0	0.0	0.0	0.0	0.0	0.0	0.0	0.0	0.0	0.0	0.0	0.0	0.0	0.0	0.0	0.0	0.0	0.0	0.0	0.0	0.0	0.0	0.0	0.0	0.0	0.0	0.0	0.0	0.0	0.0	0.0	0.0	0.0	0.0	0.0	0.0	0.0	3.4	0.0

DEPH (m)	Acritarca	*Afropollis operculatus*	*Afropollis* spp.	*Antulsporites baculatus*	*Apteodinium granulatum*	*Araucariacites australis*	*Bennettitaepollenites regaliae*	Bisaccate forms	*Botryococcus* spp.	*Brenneripollis peroreticulatus*	*Callialasporites segmentatus*	*Cicatricosisporites microstriatus*	*Cicatricosisporites microstriatus*	*Cicatricosisporites* spp.	*Circulodinium* spp.	*Classopolis classoides*	*Clavatriletes* spp.	*Collarisporites fuscus*	*Complicatisaccus cearensis* ?	*Cribroperidinium edwardsii*	*Crybelosporites pannuceus*	*Cyathidites* spp.	*Cycadopites* spp.
247.00	0.0	0.0	0.0	0.0	0.0	2.0	0.0	0.0	0.0	0.0	0.0	0.0	0.0	1.5	0.0	91.6	0.0	0.0	0.0	0.0	0.0	0.0	0.5
249.10	0.0	0.0	0.5	0.0	0.0	0.0	0.0	0.0	0.0	0.0	0.0	0.0	0.0	1.0	0.0	94.4	0.0	0.0	0.0	0.0	0.0	1.0	0.0
252.60	0.0	0.0	1.5	0.0	0.0	2.5	0.0	0.0	0.0	0.0	0.0	0.0	0.0	0.5	0.0	85.6	0.0	0.0	0.0	0.0	0.0	1.0	0.5
254.60	0.0	0.0	0.0	0.0	0.0	3.0	0.0	0.0	0.0	0.0	0.0	0.0	0.0	0.0	0.0	66.7	0.0	0.0	0.0	0.0	0.0	0.0	1.5
255.65	0.0	0.0	0.0	0.0	0.0	1.0	0.0	0.0	0.0	0.0	0.0	0.0	0.0	1.9	0.0	83.1	0.0	0.0	0.0	0.0	0.0	0.0	0.0
256.10	0.0	0.0	0.0	0.0	0.0	0.4	0.4	0.0	0.0	0.0	0.0	0.0	0.0	0.0	0.0	73.8	0.0	0.0	0.0	0.0	0.0	1.3	0.4
258.50	0.0	0.0	0.0	0.0	0.0	3.5	0.0	0.0	0.0	0.0	0.0	0.0	0.0	0.5	0.0	87.4	0.0	0.0	0.0	0.0	0.0	2.0	1.0
259.05	0.0	0.0	0.0	0.0	0.0	6.6	0.0	0.0	0.0	0.0	0.0	0.0	0.0	1.9	0.0	51.9	0.0	0.0	0.0	0.0	0.0	0.0	0.0
262.95	0.0	0.0	0.0	0.0	0.0	5.2	0.0	0.0	0.0	0.0	0.0	0.0	0.0	0.0	0.0	88.9	0.0	0.0	0.0	0.0	0.0	0.0	0.7
265.10	0.0	0.0	0.0	0.0	0.0	0.0	0.0	0.0	0.0	0.0	0.0	0.0	0.0	1.1	0.0	87.6	0.0	0.0	0.0	0.0	0.0	1.1	0.5
268.05	0.0	0.0	0.4	0.0	0.0	0.4	0.0	0.0	0.0	0.0	0.0	0.0	0.0	2.8	0.0	11.3	0.0	0.0	0.0	0.0	0.0	0.0	0.4
268.30	0.0	0.0	0.0	0.0	0.0	3.1	0.5	0.0	0.0	0.0	0.0	0.0	0.0	0.5	0.0	85.0	0.0	0.0	0.0	0.0	0.0	1.0	0.5
268.50	0.0	0.0	0.0	0.0	0.0	4.1	0.0	0.0	0.0	0.0	0.0	0.0	0.0	1.0	0.0	15.2	0.0	0.0	0.0	0.0	0.0	1.0	0.0
272.55	0.0	0.0	0.0	0.0	0.0	21.5	3.5	0.0	0.0	0.0	0.0	0.0	0.0	0.0	0.0	55.5	0.0	0.0	0.0	0.0	0.0	1.0	2.5
277.70	0.0	0.0	0.0	0.0	0.0	16.3	0.5	0.0	0.0	0.0	0.0	0.0	0.0	1.5	0.0	74.3	0.0	0.0	0.5	0.0	0.0	1.0	0.5
289.60	0.0	0.0	0.5	0.0	0.0	35.0	0.5	0.0	0.0	0.0	0.0	0.0	0.0	3.9	0.0	49.3	0.0	0.5	0.0	0.0	0.0	1.5	0.5
291.50	0.0	0.0	0.5	0.0	0.0	54.7	0.5	0.0	0.0	0.0	0.0	0.0	0.0	1.5	0.0	34.8	0.0	0.0	0.0	0.0	0.0	2.0	0.5
295.10	0.0	0.0	0.5	0.0	0.0	38.5	0.0	0.0	0.0	0.0	0.0	0.0	0.0	2.2	0.0	52.2	0.0	0.0	0.0	0.0	0.0	1.1	2.2
299.30	0.0	0.0	0.5	0.0	0.0	29.0	0.5	0.0	0.0	0.0	0.0	0.0	0.0	3.5	0.0	59.0	0.0	0.0	0.0	0.0	0.0	2.0	0.0
300.60	0.0	0.0	0.0	0.0	0.0	61.0	0.0	0.0	0.0	0.0	0.0	0.0	0.6	1.2	0.0	26.7	0.0	0.0	0.0	0.0	0.0	2.9	0.6
304.05	0.0	0.0	0.0	0.0	0.0	62.3	1.0	0.0	0.0	0.0	0.0	0.0	0.0	2.5	0.0	15.6	0.0	0.0	0.0	0.0	0.0	5.5	1.5
308.95	0.0	0.0	0.5	0.0	0.0	47.7	2.0	0.0	0.0	0.0	0.0	0.0	0.0	1.5	0.0	33.0	0.0	0.0	0.0	0.0	0.0	0.5	4.6
309.53	0.5	0.0	1.0	0.0	0.0	32.5	3.0	0.0	0.0	0.0	0.0	0.0	0.0	3.5	0.0	40.0	0.0	0.0	0.0	0.0	0.0	1.0	2.5
313.25	0.0	0.0	1.1	0.0	0.0	37.9	0.5	0.0	0.0	0.0	0.5	0.0	0.0	1.1	0.0	45.8	0.0	0.0	0.0	0.0	0.0	0.0	0.5
318.00	0.0	0.0	0.0	0.0	0.0	25.7	0.7	0.0	0.0	0.0	0.7	0.0	0.0	0.7	0.0	66.9	0.0	0.0	0.0	0.0	0.0	0.0	0.7
318.65	0.0	0.0	0.0	0.0	0.0	21.1	0.0	0.0	0.0	0.0	1.1	0.0	0.0	0.6	0.0	72.8	0.6	0.0	0.0	0.0	0.0	0.6	0.0
322.25	0.0	0.0	0.0	0.0	0.0	10.2	0.0	0.0	0.0	0.0	0.5	0.0	0.0	0.5	0.0	69.9	0.0	0.0	0.0	0.0	0.5	1.1	2.7
326.45	0.0	0.0	0.0	0.0	0.0	7.0	0.0	0.0	0.0	0.0	0.0	0.0	0.0	0.0	0.0	93.0	0.0	0.0	0.0	0.0	0.0	0.0	0.0
327.43	0.0	0.0	0.0	0.0	0.0	27.6	0.0	0.0	0.0	0.0	0.0	0.0	0.0	0.6	0.0	71.2	0.0	0.0	0.0	0.0	0.0	0.6	0.0
331.30	0.0	0.0	0.0	0.0	0.0	20.1	0.0	0.0	0.0	0.0	0.0	0.0	0.0	0.6	0.0	60.4	0.0	0.0	0.0	0.0	3.2	0.6	5.2
336.20	0.0	0.0	0.0	0.0	0.0	23.6	0.0	0.0	0.0	0.0	0.0	0.0	0.0	0.6	0.0	71.3	0.0	0.0	0.0	0.0	0.0	0.6	1.9
337.45	0.0	0.0	0.0	0.0	0.0	19.4	0.0	0.0	0.0	0.0	0.0	0.0	0.0	0.0	0.0	77.4	0.0	0.0	0.0	0.0	0.0	0.0	3.2
339.30	0.0	0.0	0.0	0.0	0.0	27.2	0.0	0.0	0.0	0.0	0.0	0.0	0.0	1.9	0.0	51.9	0.0	0.0	0.0	0.0	0.0	0.6	3.1
342.05	0.0	0.0	0.0	0.0	0.0	21.5	0.0	0.0	0.0	0.0	0.7	0.0	0.7	2.0	0.0	50.3	0.0	0.0	0.0	0.0	0.7	1.3	4.7
349.18	0.0	0.0	0.0	0.0	0.0	12.6	0.0	0.0	0.0	0.0	0.0	0.0	0.0	1.9	0.0	53.4	0.0	0.0	0.0	0.0	0.0	0.0	4.9
357.50	0.0	0.0	3.0	0.0	0.0	2.4	0.0	0.0	0.0	0.0	0.0	0.0	0.6	0.0	0.0	88.8	0.0	0.0	0.0	0.0	0.0	0.0	0.0
364.90	0.0	0.0	0.0	0.0	0.0	0.0	0.0	0.0	0.0	0.0	0.0	0.0	0.0	0.0	0.0	100.0	0.0	0.0	0.0	0.0	0.0	0.0	0.0
367.65	0.0	0.0	0.0	0.0	0.0	2.6	0.0	0.0	0.0	0.0	0.0	0.0	0.0	2.6	0.0	94.7	0.0	0.0	0.0	0.0	0.0	0.0	0.0
377.65	0.0	0.0	0.6	0.0	0.0	6.8	0.0	0.0	0.0	0.0	0.0	0.0	0.0	0.0	0.0	91.9	0.0	0.0	0.0	0.0	0.0	0.0	0.0
384.60	0.0	0.0	0.0	0.0	0.0	0.8	0.0	0.0	0.0	0.0	0.0	0.0	0.0	0.0	0.0	85.4	0.0	0.0	0.0	0.0	0.0	0.0	0.8
387.35	0.0	0.0	0.0	0.0	0.0	0.0	0.0	0.0	0.0	0.0	0.0	0.0	0.0	0.0	0.0	96.2	0.0	0.0	0.0	0.0	0.0	0.0	0.0
393.05	0.0	0.0	0.0	0.0	0.0	3.0	0.0	0.0	0.0	0.0	0.0	0.0	0.0	1.5	0.0	86.6	0.0	0.0	0.0	0.0	0.0	0.0	0.0
398.05	0.0	0.0	0.0	0.0	0.0	0.0	0.0	0.0	0.0	0.0	0.0	0.0	0.0	3.9	0.0	79.6	0.0	0.0	0.0	0.0	0.0	0.0	0.0
400.53	0.0	0.0	0.0	0.0	0.0	0.0	0.0	0.0	0.0	0.0	0.0	0.0	0.0	6.6	0.0	74.4	0.0	0.0	0.0	0.0	0.0	0.0	0.0
403.75	0.0	0.0	0.0	0.0	0.0	0.0	0.0	0.0	0.0	0.0	0.0	0.0	0.0	0.0	0.0	84.5	0.0	0.0	0.0	0.0	0.0	0.0	0.0
409.90	0.0	0.0	0.0	0.0	0.0	0.0	0.0	0.0	0.0	0.0	0.0	0.0	0.0	1.3	0.0	78.8	0.0	0.0	0.0	0.0	0.0	0.0	0.0
414.95	0.0	0.0	0.0	0.0	0.0	0.0	0.0	0.0	0.0	0.0	0.0	0.0	0.0	0.9	0.0	93.1	0.0	0.0	0.0	0.0	0.9	1.7	0.0

DEPH (m)	*Cyclonephelium* spp.	*Dejaxpollenites foveoreticulatus*	*Dejaxpollenites microfoveolatus* ?	*Dejaxpollenites* spp.	*Dinopterigium* ? spp.	*Echinatisporis varispinosus*	*Elaterosporites klaszi* ?	*Equisetosporites albertenses*	*Equisetosporites concinnus*	*Equisetosporites maculosus*	*Equisetosporites ovatus*	*Equisetosporites* spp.	*Equisetosporites* spp.	*Exochosphaeridium* spp.	*Florentina mantelli*	Foraminiferal linings	*Foveosporites canalis*	*Gnetaceaepollenites chlatratus*	*Gnetaceaepollenites diversus*	*Gnetaceaepollenites jansonii*	*Gnetaceaepollenites* spp.	*Gnetaceaepollenites uesugui*	*Klukisporites foveolatus*	*Klukisporites pseudoreticulatus*
247.00	0.0	0.0	0.0	0.0	0.0	0.0	0.0	0.0	0.0	0.0	0.0	1.0	0.0	0.0	0.0	0.5	0.0	0.0	0.0	0.0	1.5	0.0	0.0	0.0
249.10	0.0	0.0	0.0	0.0	0.0	0.0	0.0	0.0	0.0	0.0	0.0	0.5	0.5	0.0	0.0	0.5	0.0	0.0	0.0	0.0	0.5	0.0	0.0	0.0
252.60	0.0	0.0	0.0	0.0	0.0	0.0	0.0	0.0	0.0	0.0	0.0	1.0	1.0	0.0	0.0	2.0	0.0	0.0	0.0	0.0	0.5	0.0	0.0	0.0
254.60	0.0	0.0	0.0	0.0	0.0	0.0	0.0	0.0	0.0	0.0	0.0	0.0	0.0	0.0	0.0	25.8	0.0	0.0	0.0	0.0	0.0	0.0	0.0	0.0
255.65	0.0	0.0	0.0	0.0	0.0	0.0	0.0	0.0	0.0	0.0	0.0	0.0	0.0	0.0	0.0	12.1	0.0	0.0	0.0	0.0	0.5	0.0	0.0	0.0
256.10	0.0	0.0	0.0	0.0	0.0	0.0	0.0	0.0	0.0	0.0	0.0	0.4	0.0	0.0	0.0	3.0	0.0	0.0	0.0	0.0	0.0	0.0	0.0	0.0
258.50	0.0	0.0	0.0	0.0	0.0	0.0	0.0	0.0	0.0	0.0	0.0	0.0	0.0	0.0	0.0	1.0	0.0	0.0	0.0	0.0	0.5	0.0	0.5	0.0
259.05	0.0	0.0	0.0	0.0	0.0	0.0	0.0	0.0	0.0	0.0	0.0	0.0	0.0	0.0	0.0	15.1	0.0	0.0	0.0	0.0	0.9	0.0	0.0	0.0
262.95	0.0	0.0	0.0	0.0	0.0	0.0	0.0	0.0	0.0	0.0	0.0	0.7	0.0	0.0	0.0	4.6	0.0	0.0	0.0	0.0	0.0	0.0	0.0	0.0
265.10	0.0	0.0	0.0	0.0	0.0	0.0	0.0	0.0	0.0	0.0	0.0	0.0	0.0	0.0	0.0	8.1	0.0	0.0	0.0	0.0	0.5	0.0	0.0	0.0
268.05	0.0	0.0	0.0	0.0	0.0	0.0	0.0	0.0	0.0	0.4	0.0	0.0	0.0	0.0	0.0	27.8	0.0	0.0	0.0	0.0	0.0	0.0	0.0	0.0
268.30	0.0	0.0	0.0	0.0	0.0	0.0	0.0	0.0	0.0	0.0	0.0	0.0	0.0	0.0	0.0	5.2	0.0	0.0	0.0	0.0	1.0	0.0	0.0	0.0
268.50	0.0	0.0	0.0	0.0	0.0	0.0	0.0	0.0	0.0	0.0	0.0	0.0	0.0	0.0	0.0	19.3	0.0	0.0	0.0	0.0	1.5	0.0	0.0	0.0
272.55	0.0	0.0	0.0	0.0	0.0	0.0	0.0	0.0	0.0	2.5	0.0	4.0	5.5	0.0	0.0	0.0	0.0	0.0	0.0	0.0	2.0	0.0	0.0	0.0
277.70	0.0	0.0	0.0	0.0	0.0	0.0	0.0	0.0	0.0	0.0	0.0	0.5	0.0	0.0	0.0	0.0	0.0	0.0	0.0	0.5	0.0	0.0	1.0	0.0
289.60	0.0	0.0	0.0	0.0	0.0	0.0	0.0	0.0	0.0	1.5	0.0	1.5	2.5	0.0	0.0	0.0	0.0	0.0	0.0	0.0	1.0	0.5	0.0	0.0
291.50	0.0	0.0	0.5	0.0	0.0	0.5	0.0	0.0	0.0	0.0	0.0	0.0	0.0	0.0	0.0	0.0	0.0	0.0	0.0	0.0	2.0	0.0	0.0	0.0
295.10	0.0	0.0	0.0	0.0	0.0	0.0	0.0	0.0	0.0	0.0	0.0	0.5	0.0	0.0	0.0	0.0	0.0	0.0	0.0	0.0	2.2	0.0	0.0	0.0
299.30	0.0	0.5	0.0	0.0	0.0	0.0	0.0	0.0	0.0	0.0	0.0	0.5	1.0	0.0	0.0	0.0	0.0	0.0	0.0	0.0	0.5	0.0	0.0	0.0
300.60	0.0	0.0	0.0	0.0	0.0	0.0	0.0	0.0	0.6	0.0	0.0	0.0	0.6	0.0	0.0	0.0	0.0	0.0	0.0	0.0	0.0	0.0	0.6	0.0
304.05	0.0	0.0	0.0	0.0	0.0	0.5	0.0	0.0	0.0	0.0	0.0	0.0	1.5	0.0	0.0	0.0	0.0	0.0	0.0	0.0	2.5	0.0	0.0	0.5
308.95	0.0	0.0	0.0	0.0	0.0	0.0	0.0	0.0	0.0	0.0	0.0	0.0	6.1	0.0	0.0	0.0	0.0	0.0	0.0	0.0	3.6	0.0	0.0	0.0
309.53	0.0	0.0	0.0	0.0	0.0	0.0	0.0	0.0	0.0	0.0	0.0	0.0	5.0	0.0	0.0	0.0	0.0	0.0	0.0	0.0	5.5	0.0	0.0	0.0
313.25	0.0	0.0	0.0	0.0	0.0	0.0	0.0	0.0	0.0	1.6	0.0	0.5	0.5	0.0	0.0	0.0	0.0	0.0	0.0	0.0	6.3	0.0	0.0	0.0
318.00	0.0	0.0	0.0	0.0	0.0	0.0	0.0	0.0	0.0	0.0	0.0	0.0	0.7	0.0	0.0	0.0	0.0	0.0	0.0	0.0	1.4	0.0	0.7	0.0
318.65	0.0	0.0	0.0	0.0	0.0	0.0	0.0	0.0	0.0	0.6	0.0	1.1	1.1	0.0	0.0	0.0	0.0	0.0	0.0	0.0	0.0	0.0	0.0	0.0
322.25	0.0	0.0	0.0	0.0	0.0	0.0	0.0	0.0	0.0	1.1	0.0	0.0	4.3	0.0	0.0	0.0	0.5	0.0	0.0	0.0	2.2	0.0	0.0	0.0
326.45	0.0	0.0	0.0	0.0	0.0	0.0	0.0	0.0	0.0	0.0	0.0	0.0	0.0	0.0	0.0	0.0	0.0	0.0	0.0	0.0	0.0	0.0	0.0	0.0
327.43	0.0	0.0	0.0	0.0	0.0	0.0	0.0	0.0	0.0	0.0	0.0	0.0	0.0	0.0	0.0	0.0	0.0	0.0	0.0	0.0	0.0	0.0	0.0	0.0
331.30	0.0	0.0	0.6	0.0	0.0	0.0	0.0	0.0	0.0	0.6	0.0	1.3	1.3	0.0	0.0	0.0	0.0	0.0	0.0	0.0	2.6	0.0	1.3	0.0
336.20	0.0	0.0	0.0	0.6	0.0	0.0	0.0	0.0	0.0	0.0	0.0	0.6	0.6	0.0	0.0	0.0	0.0	0.0	0.0	0.0	0.0	0.0	0.0	0.0
337.45	0.0	0.0	0.0	0.0	0.0	0.0	0.0	0.0	0.0	0.0	0.0	0.0	0.0	0.0	0.0	0.0	0.0	0.0	0.0	0.0	0.0	0.0	0.0	0.0
339.30	0.0	0.0	0.0	0.0	0.0	0.0	0.0	0.0	0.0	1.2	0.0	2.5	0.6	0.0	0.0	0.0	0.0	0.0	0.0	0.0	7.4	0.0	0.0	0.0
342.05	0.0	0.0	0.0	0.0	0.0	0.0	0.0	0.0	0.0	2.0	0.0	2.0	8.7	0.0	0.0	0.0	0.0	0.0	0.0	0.0	2.0	0.0	0.7	0.0
349.18	0.0	0.0	0.0	0.0	0.0	0.0	0.0	0.0	0.0	1.9	0.0	9.7	10.7	0.0	0.0	0.0	0.0	0.0	0.0	0.0	1.9	0.0	0.0	0.0
357.50	0.0	0.0	0.0	0.0	0.0	0.0	0.0	0.0	0.0	0.0	0.0	0.0	0.0	0.0	0.0	0.0	0.0	0.0	0.0	0.0	1.2	0.0	0.0	0.0
364.90	0.0	0.0	0.0	0.0	0.0	0.0	0.0	0.0	0.0	0.0	0.0	0.0	0.0	0.0	0.0	0.0	0.0	0.0	0.0	0.0	0.0	0.0	0.0	0.0
367.65	0.0	0.0	0.0	0.0	0.0	0.0	0.0	0.0	0.0	0.0	0.0	0.0	0.0	0.0	0.0	0.0	0.0	0.0	0.0	0.0	0.0	0.0	0.0	0.0
377.65	0.0	0.0	0.0	0.0	0.0	0.0	0.0	0.0	0.0	0.0	0.0	0.6	0.0	0.0	0.0	0.0	0.0	0.0	0.0	0.0	0.0	0.0	0.0	0.0
384.60	0.0	0.0	0.0	0.0	0.0	0.0	0.0	0.0	0.0	0.0	0.0	0.0	0.0	0.0	0.0	0.0	0.0	0.0	0.0	0.0	12.2	0.0	0.0	0.0
387.35	0.0	0.0	0.0	0.0	0.0	0.0	0.0	0.0	0.0	0.0	0.0	0.0	0.0	0.0	0.0	0.0	0.0	0.0	0.0	0.0	0.0	0.0	0.0	0.0
393.05	0.0	0.0	0.0	0.0	0.0	0.0	0.0	0.0	0.0	0.0	0.0	0.0	0.0	0.0	0.0	0.0	0.0	0.0	0.0	0.0	0.0	0.0	0.0	0.0
398.05	0.0	0.0	0.0	0.0	0.0	0.0	0.0	0.0	0.0	0.0	0.0	0.0	0.0	0.0	0.0	3.9	0.0	0.0	0.0	0.0	0.0	0.0	0.0	0.0
400.53	0.0	0.0	0.0	0.0	0.0	0.0	0.0	0.0	0.0	0.8	0.0	0.0	0.8	0.0	0.0	9.1	0.0	0.0	0.0	0.0	0.8	0.0	0.0	0.0
403.75	0.0	0.0	0.0	0.0	0.0	0.0	0.0	0.0	0.0	0.5	0.0	0.0	0.5	0.0	0.0	13.4	0.0	0.0	0.0	0.0	0.0	0.0	0.0	0.0
409.90	0.0	0.0	0.0	0.0	0.0	0.0	0.0	0.0	0.0	0.0	0.0	0.0	0.0	0.0	0.0	17.5	0.0	0.0	0.0	0.0	0.0	0.0	0.0	0.0
414.95	0.0	0.0	0.0	0.0	0.0	0.0	0.0	0.0	0.0	2.6	0.0	0.9	0.0	0.0	0.0	0.0	0.0	0.0	0.0	0.0	0.0	0.0	0.0	0.0

DEPH (m)	*Klukisporites* spp.	*Leisphaeridia* sp.	*Leptolepidites psarosus*	*Matonisporites silvai*	Megaspores	*Microfoveolatosporis daukiensis*	*Microfoveolatus daukiensis*	*Odontochitina operculata*	*Oligosphaeridium albertenses*	*Oligosphaeridium complex*	*Oligosphaeridium irregulare*	*Oligosphaeridium pocolum*	*Oligosphaeridium pulcherrimum*	*Oligosphaeridium* spp.	*Oligosphaeridium totum*	*Palaeoperidinium cretaceum*	*Perotriletes* spp.	*Pilosisporites trichopapillosus*	*Prolixumsphaeridium parvispinum*	*Pseudoceratium* spp.	*Quadricolpites reticulatus*	*Reticulosporis foveolatus*	*Reticulosporis reticulatus*
247.00	0.0	0.0	0.5	0.5	0.0	0.0	0.0	0.0	0.0	0.0	0.0	0.0	0.0	0.0	0.0	0.0	0.0	0.0	0.0	0.0	0.0	0.0	0.0
249.10	0.0	0.0	0.0	0.0	0.0	0.0	0.0	0.0	0.0	0.0	0.0	0.0	0.0	0.0	0.0	0.0	0.0	0.0	0.0	0.0	0.0	0.0	0.0
252.60	0.0	0.0	0.0	0.0	0.0	0.0	0.0	0.0	0.0	0.0	0.0	0.0	0.0	0.0	0.0	0.0	0.0	0.0	0.0	0.0	0.0	0.0	0.0
254.60	0.0	0.0	0.0	0.0	0.0	0.0	0.0	0.0	0.0	0.0	0.0	0.0	0.0	0.0	0.0	0.0	0.0	0.0	0.0	0.0	0.0	0.0	0.0
255.65	0.0	0.0	0.0	0.0	0.5	0.0	0.0	0.0	0.0	0.0	0.0	0.0	0.0	0.0	0.0	0.0	0.0	0.0	0.0	0.0	0.0	0.0	0.0
256.10	0.0	0.0	0.0	0.4	0.0	0.0	0.0	0.0	0.0	0.0	0.0	0.0	0.0	0.0	0.0	0.0	0.0	0.0	0.0	0.0	0.0	0.0	0.0
258.50	0.0	0.0	0.0	0.0	0.0	0.0	0.0	0.0	0.0	0.0	0.0	0.0	0.0	0.0	0.0	0.0	0.0	0.0	0.0	0.0	0.0	0.0	0.0
259.05	0.0	0.0	0.0	0.9	0.0	0.0	0.0	0.0	0.0	0.0	0.0	0.0	0.0	0.0	0.0	0.0	0.0	0.0	0.0	0.0	0.0	0.0	0.0
262.95	0.0	0.0	0.0	0.0	0.0	0.0	0.0	0.0	0.0	0.0	0.0	0.0	0.0	0.0	0.0	0.0	0.0	0.0	0.0	0.0	0.0	0.0	0.0
265.10	0.0	0.0	0.0	0.0	0.0	0.0	0.0	0.0	0.0	0.0	0.0	0.0	0.0	0.0	0.0	0.0	0.0	0.0	0.0	0.0	0.0	0.0	0.0
268.05	0.0	0.0	0.0	0.0	0.0	0.0	0.0	0.0	0.0	0.0	0.0	0.0	0.0	0.0	0.0	0.0	2.0	0.0	0.0	0.0	0.0	0.0	0.0
268.30	0.0	0.0	0.0	0.0	0.0	0.0	0.0	0.0	0.0	0.0	0.0	0.0	0.0	0.0	0.0	0.0	0.5	0.0	0.0	0.0	0.0	0.0	0.0
268.50	0.0	0.0	0.0	1.0	0.0	0.0	0.0	0.0	0.0	0.0	0.0	0.0	0.0	0.0	0.0	0.0	0.0	0.0	0.0	0.0	0.0	0.0	0.0
272.55	0.0	0.0	1.0	0.0	0.5	0.0	0.0	0.0	0.0	0.0	0.0	0.0	0.0	0.0	0.0	0.0	0.0	0.0	0.0	0.0	0.0	0.0	0.0
277.70	0.0	0.0	0.0	0.0	0.0	0.0	0.0	0.0	0.0	0.0	0.0	0.0	0.0	0.0	0.0	0.0	0.0	0.0	0.0	0.0	0.0	0.0	0.0
289.60	0.0	0.0	0.0	0.0	0.0	0.0	0.0	0.0	0.0	0.0	0.0	0.0	0.0	0.0	0.0	0.0	0.0	0.0	0.0	0.0	0.0	0.5	0.0
291.50	0.0	0.0	0.0	0.0	0.0	0.0	0.0	0.0	0.0	0.0	0.0	0.0	0.0	0.0	0.0	0.0	0.0	0.0	0.0	0.0	0.0	0.0	0.0
295.10	0.0	0.0	0.0	0.0	0.0	0.0	0.0	0.0	0.0	0.0	0.0	0.0	0.0	0.0	0.0	0.0	0.0	0.0	0.0	0.0	0.0	0.0	0.0
299.30	0.0	0.0	0.0	0.0	0.0	0.0	0.0	0.0	0.0	0.0	0.0	0.0	0.0	0.0	0.0	0.0	0.0	0.0	0.0	0.0	0.0	0.0	0.0
300.60	0.6	0.0	0.0	0.0	0.0	0.0	0.0	0.0	0.0	0.0	0.0	0.0	0.0	0.0	0.0	0.0	0.0	0.0	0.0	0.0	0.0	0.0	0.0
304.05	0.0	0.0	0.0	0.0	0.0	0.0	0.0	0.0	0.0	0.0	0.0	0.0	0.0	0.0	0.0	0.0	0.0	0.0	0.0	0.0	0.0	0.0	0.0
308.95	0.0	0.0	0.0	0.0	0.0	0.0	0.0	0.0	0.0	0.0	0.0	0.0	0.0	0.0	0.0	0.0	0.0	0.0	0.0	0.0	0.0	0.0	0.0
309.53	0.0	0.0	1.5	2.5	0.0	0.0	0.0	0.0	0.0	0.0	0.0	0.0	0.0	0.0	0.0	0.0	0.0	0.0	0.0	0.0	0.0	0.0	0.0
313.25	0.0	0.0	0.5	0.5	0.0	0.0	0.0	0.0	0.0	0.0	0.0	0.0	0.0	0.0	0.0	0.0	0.0	0.0	0.0	0.0	0.0	0.0	0.0
318.00	0.0	0.0	0.0	0.7	0.0	0.0	0.0	0.0	0.0	0.0	0.0	0.0	0.0	0.0	0.0	0.0	0.0	0.0	0.0	0.0	0.0	0.0	0.0
318.65	0.0	0.0	0.6	0.0	0.0	0.0	0.0	0.0	0.0	0.0	0.0	0.0	0.0	0.0	0.0	0.0	0.0	0.0	0.0	0.0	0.0	0.0	0.0
322.25	0.0	0.0	1.6	0.5	0.0	0.0	0.0	0.0	0.0	0.0	0.0	0.0	0.0	0.0	0.0	0.0	0.0	0.0	0.0	0.0	0.0	0.0	0.0
326.45	0.0	0.0	0.0	0.0	0.0	0.0	0.0	0.0	0.0	0.0	0.0	0.0	0.0	0.0	0.0	0.0	0.0	0.0	0.0	0.0	0.0	0.0	0.0
327.43	0.0	0.0	0.0	0.0	0.0	0.0	0.0	0.0	0.0	0.0	0.0	0.0	0.0	0.0	0.0	0.0	0.0	0.0	0.0	0.0	0.0	0.0	0.0
331.30	0.0	0.0	0.0	0.0	0.0	0.0	0.0	0.0	0.0	0.0	0.0	0.0	0.0	0.0	0.0	0.0	0.0	0.0	0.0	0.0	0.0	0.0	0.0
336.20	0.0	0.0	0.0	0.0	0.0	0.0	0.0	0.0	0.0	0.0	0.0	0.0	0.0	0.0	0.0	0.0	0.0	0.0	0.0	0.0	0.0	0.0	0.0
337.45	0.0	0.0	0.0	0.0	0.0	0.0	0.0	0.0	0.0	0.0	0.0	0.0	0.0	0.0	0.0	0.0	0.0	0.0	0.0	0.0	0.0	0.0	0.0
339.30	0.0	0.0	0.6	2.5	0.0	0.0	0.0	0.0	0.0	0.0	0.0	0.0	0.0	0.0	0.0	0.0	0.0	0.0	0.0	0.0	0.0	0.0	0.0
342.05	0.0	0.0	0.7	0.0	0.0	0.0	0.0	0.0	0.0	0.0	0.0	0.0	0.0	0.0	0.0	0.0	0.0	0.0	0.0	0.0	0.0	0.0	0.0
349.18	0.0	0.0	0.0	1.9	0.0	0.0	0.0	0.0	0.0	0.0	0.0	0.0	0.0	0.0	0.0	0.0	0.0	0.0	0.0	0.0	0.0	0.0	0.0
357.50	0.6	0.0	1.2	2.4	0.0	0.0	0.0	0.0	0.0	0.0	0.0	0.0	0.0	0.0	0.0	0.0	0.0	0.0	0.0	0.0	0.0	0.0	0.0
364.90	0.0	0.0	0.0	0.0	0.0	0.0	0.0	0.0	0.0	0.0	0.0	0.0	0.0	0.0	0.0	0.0	0.0	0.0	0.0	0.0	0.0	0.0	0.0
367.65	0.0	0.0	0.0	0.0	0.0	0.0	0.0	0.0	0.0	0.0	0.0	0.0	0.0	0.0	0.0	0.0	0.0	0.0	0.0	0.0	0.0	0.0	0.0
377.65	0.0	0.0	0.0	0.0	0.0	0.0	0.0	0.0	0.0	0.0	0.0	0.0	0.0	0.0	0.0	0.0	0.0	0.0	0.0	0.0	0.0	0.0	0.0
384.60	0.0	0.0	0.0	0.8	0.0	0.0	0.0	0.0	0.0	0.0	0.0	0.0	0.0	0.0	0.0	0.0	0.0	0.0	0.0	0.0	0.0	0.0	0.0
387.35	0.0	0.0	0.0	0.0	0.0	0.0	0.0	0.0	0.0	0.0	0.0	0.0	0.0	0.0	0.0	0.0	0.0	0.0	0.0	0.0	0.0	0.0	0.0
393.05	0.0	0.0	0.0	0.7	0.0	0.0	0.0	0.0	0.0	0.0	0.0	0.0	0.0	0.0	0.0	0.0	0.0	0.0	0.0	0.0	0.0	0.0	0.0
398.05	0.0	0.0	0.0	0.0	0.0	0.0	0.0	0.0	0.0	0.0	0.0	0.0	0.0	0.0	0.0	0.0	0.0	0.0	0.0	0.0	0.0	0.0	0.0
400.53	0.0	0.0	0.0	0.8	0.0	0.0	0.0	0.0	0.0	0.0	0.0	0.0	0.0	0.0	0.0	0.0	0.0	0.0	0.0	0.0	0.0	0.0	0.0
403.75	0.0	0.0	0.0	0.0	0.0	0.0	0.0	0.0	0.0	0.0	0.0	0.0	0.0	0.0	0.0	0.0	0.0	0.0	0.0	0.0	0.0	0.0	0.0
409.90	0.0	0.0	0.0	0.0	0.0	0.0	0.0	0.0	0.0	0.0	0.0	0.0	0.0	0.0	0.0	0.0	0.0	0.0	0.0	0.0	0.0	0.0	0.0
414.95	0.0	0.0	0.0	0.0	0.0	0.0	0.0	0.0	0.0	0.0	0.0	0.0	0.0	0.0	0.0	0.0	0.0	0.0	0.0	0.0	0.0	0.0	0.0

DEPH (m)	*Retitricolpites* spp.	*Retitriletes* sp. 3 (Regali, 1989)	*Rousea georgensis* ?	*Schrankpollis reticulatus* ?	*Sergipea naviformis*	*Sergipea simplex*	*Sergipea* spp.	*Sergipea variverrucata*	*Spiniferites ancoriferas* ?	*Spiniferites bejuii*	*Spiniferites chebca*	*Spiniferites lenzi* ?	*Spiniferites* spp.	*Steevesipollenites* spp.	*Stellatopollis barghoorni*	*Stellatopollis dubius*	*Stellatopollis* spp.	*Striatopollis reticulatus*	*Subtilisphaera senegalensis*	*Systematophora* spp.
247.00	0.0	0.5	0.0	0.0	0.0	0.0	0.0	0.0	0.0	0.0	0.0	0.0	0.0	0.0	0.0	0.0	0.0	0.0	0.0	0.0
249.10	0.0	0.5	0.0	0.0	0.0	0.0	0.0	0.0	0.0	0.0	0.0	0.0	0.0	0.0	0.0	0.0	0.0	0.0	0.0	0.0
252.60	0.0	1.0	0.0	0.0	0.0	0.0	0.0	0.0	0.0	0.0	0.5	0.0	1.5	0.0	0.0	0.0	0.0	0.0	0.0	0.0
254.60	0.0	0.0	0.0	0.0	0.0	0.0	0.0	0.0	0.0	0.0	1.5	0.0	1.5	0.0	0.0	0.0	0.0	0.0	0.0	0.0
255.65	0.0	0.0	0.0	0.0	0.0	0.0	0.0	0.0	0.0	0.0	0.0	0.0	0.0	0.0	0.0	0.0	0.0	0.0	1.0	0.0
256.10	0.0	0.4	0.0	0.0	0.0	0.0	0.0	0.0	0.0	0.0	3.0	0.0	0.9	0.0	0.0	0.0	0.0	0.0	15.5	0.0
258.50	0.0	1.5	0.0	0.0	0.0	0.0	0.0	0.0	0.0	0.0	1.5	0.5	0.0	0.0	0.0	0.0	0.0	0.0	0.0	0.0
259.05	0.0	0.0	0.0	0.0	0.0	0.0	0.0	0.0	0.0	0.0	3.8	0.0	0.0	0.0	0.0	0.0	0.0	0.0	16.0	0.0
262.95	0.0	0.0	0.0	0.0	0.0	0.0	0.0	0.0	0.0	0.0	0.0	0.0	0.0	0.0	0.0	0.0	0.0	0.0	0.0	0.0
265.10	0.0	0.0	0.0	0.0	0.0	0.0	0.0	0.0	0.0	0.0	0.0	0.0	1.1	0.0	0.0	0.0	0.0	0.0	0.0	0.0
268.05	0.0	0.0	0.0	0.0	0.0	0.0	0.0	0.0	0.0	0.0	0.0	39.5	8.1	0.0	0.0	0.0	0.0	0.0	3.6	0.0
268.30	0.0	0.5	0.0	0.0	0.0	0.0	0.0	0.0	0.0	0.0	2.1	0.0	0.0	0.0	0.0	0.0	0.0	0.0	0.0	0.0
268.50	0.0	1.5	0.0	0.0	0.0	0.0	0.0	0.0	0.0	0.0	7.1	0.0	47.7	0.0	0.0	0.0	0.0	0.0	0.0	0.0
272.55	0.0	0.5	0.0	0.0	0.0	0.0	0.0	0.0	0.0	0.0	0.0	0.0	0.0	0.0	0.0	0.0	0.0	0.0	0.0	0.0
277.70	0.0	2.5	0.0	0.0	0.0	0.0	0.0	0.0	0.0	0.0	0.0	0.0	0.0	0.0	0.0	0.0	0.0	0.0	0.0	0.0
289.60	0.0	1.0	0.0	0.0	0.0	0.0	0.0	0.0	0.0	0.0	0.0	0.0	0.0	0.0	0.0	0.0	0.0	0.0	0.0	0.0
291.50	0.0	1.5	0.0	0.0	0.0	0.0	0.0	0.0	0.0	0.0	0.0	0.0	0.0	0.0	0.0	0.0	0.0	0.0	0.0	0.0
295.10	0.0	0.5	0.0	0.0	0.0	0.0	0.0	0.0	0.0	0.0	0.0	0.0	0.0	0.0	0.0	0.0	0.0	0.0	0.0	0.0
299.30	0.0	3.0	0.0	0.0	0.0	0.0	0.0	0.0	0.0	0.0	0.0	0.0	0.0	0.0	0.0	0.0	0.0	0.0	0.0	0.0
300.60	0.0	4.1	0.0	0.0	0.0	0.0	0.0	0.0	0.0	0.0	0.0	0.0	0.0	0.0	0.0	0.0	0.0	0.0	0.0	0.0
304.05	0.0	4.0	0.0	0.0	0.0	0.0	0.0	0.0	0.0	0.0	0.0	0.0	0.0	1.0	0.0	0.0	0.0	0.0	0.0	0.0
308.95	0.0	0.0	0.0	0.0	0.0	0.0	0.0	0.0	0.0	0.0	0.0	0.0	0.0	0.5	0.0	0.0	0.0	0.0	0.0	0.0
309.53	0.0	0.5	0.0	0.0	0.0	0.0	0.0	0.0	0.0	0.0	0.0	0.0	0.0	0.5	0.0	0.0	0.0	0.0	0.0	0.0
313.25	0.0	0.0	0.0	0.0	0.0	0.0	0.0	0.5	0.0	0.0	0.0	0.0	0.0	0.5	0.0	0.0	1.1	0.0	0.0	0.0
318.00	0.0	0.0	0.0	0.0	0.0	0.0	0.0	0.0	0.0	0.0	0.0	0.0	0.0	0.0	0.0	0.0	0.0	0.0	0.0	0.0
318.65	0.0	0.0	0.0	0.0	0.0	0.0	0.0	0.0	0.0	0.0	0.0	0.0	0.0	0.0	0.0	0.0	0.0	0.0	0.0	0.0
322.25	0.0	0.5	0.0	0.0	0.0	0.0	0.5	0.0	0.0	0.0	0.0	0.0	0.0	0.0	0.0	0.0	0.0	0.0	0.0	0.0
326.45	0.0	0.0	0.0	0.0	0.0	0.0	0.0	0.0	0.0	0.0	0.0	0.0	0.0	0.0	0.0	0.0	0.0	0.0	0.0	0.0
327.43	0.0	0.0	0.0	0.0	0.0	0.0	0.0	0.0	0.0	0.0	0.0	0.0	0.0	0.0	0.0	0.0	0.0	0.0	0.0	0.0
331.30	0.0	0.0	0.0	0.0	0.0	0.0	0.0	0.0	0.0	0.0	0.0	0.0	0.0	1.3	0.0	0.0	0.0	0.0	0.0	0.0
336.20	0.0	0.0	0.0	0.0	0.0	0.0	0.0	0.0	0.0	0.0	0.0	0.0	0.0	0.0	0.0	0.0	0.0	0.0	0.0	0.0
337.45	0.0	0.0	0.0	0.0	0.0	0.0	0.0	0.0	0.0	0.0	0.0	0.0	0.0	0.0	0.0	0.0	0.0	0.0	0.0	0.0
339.30	0.0	0.6	0.0	0.0	0.0	0.0	0.0	0.0	0.0	0.0	0.0	0.0	0.0	0.0	0.0	0.0	0.0	0.0	0.0	0.0
342.05	0.0	0.7	0.0	0.0	0.7	0.0	0.0	0.0	0.0	0.0	0.0	0.0	0.0	0.0	0.7	0.0	0.0	0.0	0.0	0.0
349.18	0.0	0.0	0.0	0.0	0.0	0.0	0.0	0.0	0.0	0.0	0.0	0.0	0.0	0.0	0.0	0.0	1.0	0.0	0.0	0.0
357.50	0.0	0.0	0.0	0.0	0.0	0.0	0.0	0.0	0.0	0.0	0.0	0.0	0.0	0.0	0.0	0.0	0.0	0.0	0.0	0.0
364.90	0.0	0.0	0.0	0.0	0.0	0.0	0.0	0.0	0.0	0.0	0.0	0.0	0.0	0.0	0.0	0.0	0.0	0.0	0.0	0.0
367.65	0.0	0.0	0.0	0.0	0.0	0.0	0.0	0.0	0.0	0.0	0.0	0.0	0.0	0.0	0.0	0.0	0.0	0.0	0.0	0.0
377.65	0.0	0.0	0.0	0.0	0.0	0.0	0.0	0.0	0.0	0.0	0.0	0.0	0.0	0.0	0.0	0.0	0.0	0.0	0.0	0.0
384.60	0.0	0.0	0.0	0.0	0.0	0.0	0.0	0.0	0.0	0.0	0.0	0.0	0.0	0.0	0.0	0.0	0.0	0.0	0.0	0.0
387.35	0.0	0.0	0.0	0.0	0.0	0.0	0.0	0.0	0.0	0.0	0.0	0.0	0.0	0.0	0.0	0.0	3.8	0.0	0.0	0.0
393.05	0.0	0.0	0.0	0.0	0.0	0.0	0.0	0.0	0.0	0.0	0.0	0.0	7.5	0.0	0.0	0.0	0.0	0.0	0.7	0.0
398.05	0.0	0.0	0.0	0.0	0.0	0.0	0.0	0.0	0.0	0.0	0.0	0.0	0.0	0.0	0.0	0.0	0.0	0.0	10.7	0.0
400.53	0.0	0.0	0.0	0.0	0.0	0.0	0.0	0.0	0.0	0.0	0.8	0.0	3.3	0.8	0.0	0.0	0.0	0.0	1.7	0.0
403.75	0.0	0.0	0.0	0.0	0.0	0.0	0.0	0.0	0.0	0.0	0.0	0.0	0.0	0.0	0.0	0.0	0.0	0.0	0.0	0.0
409.90	0.0	0.0	0.0	0.0	0.0	0.0	0.0	0.0	0.0	0.0	1.3	0.0	0.0	0.0	0.0	0.0	0.0	0.0	1.3	0.0
414.95	0.0	0.0	0.0	0.0	0.0	0.0	0.0	0.0	0.0	0.0	0.0	0.0	0.0	0.0	0.0	0.0	0.0	0.0	0.0	0.0

DEPH (m)	*Tanyosphaeridium* spp.	*Trichodinium castanea*	*Tricolpites* spp.	*Uesuguipollenites callosus*	*Verrucosisporites* spp.	*Vitreisporites pustulosus*	Total
13.25	0.0	0.0	0.0	0.0	1.4	0.0	71
15.78	0.0	0.0	0.0	0.0	2.1	0.0	96
16.00	0.0	0.0	0.0	0.0	2.3	0.0	88
16.45	0.0	0.0	0.0	0.0	0.8	0.0	128
16.65	0.0	0.0	0.0	0.0	0.0	0.0	49
17.30	0.0	0.0	0.0	0.0	3.5	0.0	57
18.63	0.0	14.1	0.0	0.0	0.0	0.0	142
19.24	0.0	0.0	0.0	0.0	2.9	0.0	35
19.35	0.0	0.0	0.0	0.0	0.0	0.0	41
19.85	0.0	0.0	0.0	0.0	1.6	0.0	63
20.53	0.0	0.0	0.0	0.0	0.0	0.0	46
20.85	0.0	0.0	0.0	0.0	0.0	0.0	63
22.80	0.0	0.0	0.0	0.0	1.1	0.0	92
22.88	0.0	0.0	0.0	0.0	5.0	0.0	200
23.55	0.0	0.0	0.0	0.0	0.0	0.0	32
24.05	0.0	0.0	0.0	0.0	0.0	0.0	62
26.23	0.0	0.0	0.0	0.0	0.7	0.0	152
26.83	0.0	0.0	0.0	0.0	0.5	0.0	202
28.00	0.0	1.5	0.0	0.0	0.0	0.0	200
30.60	0.0	0.0	0.0	0.0	3.1	0.0	163
32.25	0.0	0.0	0.0	0.0	0.6	0.0	179
33.20	0.0	0.0	0.0	0.0	1.9	0.0	207
35.95	0.0	0.0	0.0	0.0	2.2	0.0	92
37.55	0.0	0.0	0.0	0.0	0.5	0.0	201
40.10	0.0	5.9	0.0	0.0	0.5	0.0	204
42.25	0.0	0.0	0.0	0.0	2.4	0.0	170
42.65	0.0	0.5	0.0	0.0	0.5	0.0	200
44.15	0.0	0.0	0.0	0.0	0.0	0.0	39
46.35	0.0	6.5	0.0	0.0	0.5	0.0	201
47.90	0.0	1.5	0.0	0.0	2.9	0.0	204
48.60	0.0	0.5	0.0	0.0	1.5	0.0	204
49.70	0.0	1.0	0.0	0.0	2.0	0.0	199
50.60	0.0	0.0	0.0	0.0	1.0	0.0	191
51.80	1.6	2.6	0.0	0.0	3.1	0.0	191
52.35	0.0	0.0	0.0	0.0	0.5	0.0	204
54.50	0.0	0.0	0.0	0.0	0.0	0.0	130
56.10	0.0	0.0	0.0	0.0	0.6	0.0	170
56.95	0.0	0.0	0.0	0.0	1.6	0.0	61
57.60	0.0	0.0	0.0	0.0	1.7	0.0	116
57.80	0.0	0.0	0.0	0.0	0.0	0.0	107
58.70	0.0	0.0	0.0	0.0	3.5	0.0	143
59.30	0.0	0.0	0.0	0.0	0.0	0.0	133
60.70	0.5	0.0	0.0	0.0	0.0	0.0	189
65.45	0.0	0.0	0.0	0.0	0.5	0.0	201
65.90	0.0	0.0	0.0	0.0	0.0	0.0	69
67.00	0.0	0.0	0.0	0.0	2.4	0.0	84
67.40	0.0	0.0	0.0	0.0	1.4	0.0	70
71.60	0.0	0.0	0.0	0.0	6.0	0.0	84
72.25	0.0	0.0	0.0	0.0	3.1	0.0	130
75.40	0.0	0.0	0.0	0.0	1.3	0.0	156
77.20	0.0	0.0	0.0	0.0	0.0	0.0	86
80.40	0.0	0.0	0.0	0.0	0.6	0.0	181
82.55	0.0	0.0	0.0	0.6	0.0	0.0	157
83.00	0.0	5.9	0.0	0.0	1.0	0.0	101
84.90	0.0	0.0	0.0	0.0	1.6	0.0	189
86.70	0.0	0.0	0.0	0.0	0.0	0.0	133
88.40	0.0	0.0	0.0	0.0	1.0	0.0	200
91.25	0.0	0.0	0.0	0.0	4.6	0.0	238
94.35	0.0	0.0	0.0	0.8	0.0	0.0	249
97.65	0.0	6.7	0.0	0.0	3.3	0.0	180
98.20	0.0	0.7	0.0	0.0	5.0	0.0	139
99.20	0.0	0.0	0.0	0.0	2.2	0.0	228
101.70	0.0	0.0	0.0	0.0	2.1	0.0	194
103.15	0.0	0.0	0.0	0.0	1.7	0.0	241
108.10	0.0	0.0	0.0	0.0	0.0	0.0	206
109.40	0.0	14.3	0.0	0.0	0.5	0.0	182
110.60	0.4	0.0	0.0	0.0	0.4	0.0	225
112.70	0.0	1.7	0.0	0.0	0.6	0.0	181
119.50	0.0	0.0	0.0	0.0	0.9	0.0	214
120.60	0.0	0.0	0.0	0.0	2.0	0.0	198
122.85	0.0	0.0	0.0	0.0	0.0	0.0	133
124.40	0.0	5.1	0.0	0.0	0.0	0.0	198
124.67	0.0	9.2	0.0	0.0	0.4	0.0	228
128.10	0.0	5.4	0.0	0.8	0.0	0.0	239
130.55	0.0	40.8	0.0	0.0	0.0	0.0	355
134.45	0.0	1.1	0.0	0.4	0.4	0.0	276
135.75	0.0	40.0	0.0	0.0	0.0	0.0	185
146.10	0.4	11.5	0.0	1.3	0.9	0.0	226
157.15	0.0	0.0	0.0	5.1	1.4	0.0	215
160.35	0.0	0.0	0.0	1.3	0.0	0.0	238
167.25	0.0	0.3	0.0	1.4	0.7	0.0	289
170.43	0.0	5.9	0.0	0.3	0.6	0.0	323
178.56	0.0	5.1	0.0	0.5	0.0	0.0	216
182.06	0.0	0.0	0.0	0.0	0.0	0.4	241
182.60	0.0	0.0	0.0	0.0	0.0	0.0	205
189.80	0.0	0.0	0.0	1.5	0.0	0.0	194
190.75	0.0	0.0	0.0	1.2	0.0	0.0	325
200.68	0.0	0.0	0.0	0.0	0.0	0.0	199
202.37	0.0	0.0	0.0	0.0	0.0	0.0	177
205.35	0.0	0.5	0.0	0.0	0.0	0.0	196
207.80	0.0	1.5	0.0	0.0	0.0	0.0	134
211.85	0.0	0.0	0.0	1.4	0.0	0.0	207
214.75	0.0	0.0	0.0	1.0	0.0	0.0	286
217.00	0.0	0.0	0.0	0.5	0.0	0.0	202
222.00	0.0	0.0	0.0	0.0	0.0	0.0	209
222.25	0.0	0.0	0.0	0.0	0.5	0.0	195
224.60	0.0	0.0	0.6	0.0	0.6	0.0	163
227.10	0.0	0.0	0.0	0.4	0.0	0.0	256
232.90	0.0	0.0	0.0	0.0	0.0	0.0	202
237.60	0.0	0.0	0.0	0.0	0.0	0.0	208
237.70	0.0	0.0	0.0	0.0	1.0	0.0	105
239.75	0.0	0.0	0.0	0.0	0.0	0.0	208
240.65	0.0	0.0	0.0	0.0	1.3	0.0	238
241.25	0.0	0.0	0.0	0.0	0.0	0.0	40
243.95	0.0	0.0	0.0	0.0	0.0	0.0	206

DEPH (m)	*Tanyosphaeridium* spp.	*Trichodinium castanea*	*Tricolpites* spp.	*Uesuguipollenites callosus*	*Verrucosisporites* spp.	*Vitreisporites pustulosus*	Total
247.00	0.0	0.0	0.0	0.0	0.0	0.0	202
249.10	0.0	0.0	0.0	0.0	0.5	0.0	195
252.60	0.0	0.0	0.0	0.0	1.0	0.0	201
254.60	0.0	0.0	0.0	0.0	0.0	0.0	66
255.65	0.0	0.0	0.0	0.0	0.0	0.0	207
256.10	0.0	0.0	0.0	0.0	0.0	0.0	233
258.50	0.0	0.0	0.0	0.0	0.0	0.0	199
259.05	0.0	0.0	0.0	0.0	0.0	0.0	106
262.95	0.0	0.0	0.0	0.0	0.0	0.0	153
265.10	0.0	0.0	0.0	0.0	0.0	0.0	185
268.05	0.0	0.0	0.0	0.0	0.0	0.0	248
268.30	0.0	0.0	0.0	0.0	0.0	0.0	193
268.50	0.0	0.0	0.0	0.0	0.5	0.0	197
272.55	0.0	0.0	0.0	0.0	0.0	0.0	200
277.70	0.0	0.0	0.0	0.0	1.0	0.0	202
289.60	0.0	0.0	0.0	0.0	0.0	0.0	203
291.50	0.0	0.0	0.0	0.0	1.0	0.0	201
295.10	0.0	0.0	0.0	0.0	0.0	0.0	182
299.30	0.0	0.0	0.0	0.0	0.0	0.0	200
300.60	0.0	0.0	0.0	0.0	0.6	0.0	172
304.05	0.0	0.0	0.0	0.0	1.5	0.0	199
308.95	0.0	0.0	0.0	0.0	0.0	0.0	197
309.53	0.0	0.0	0.0	0.5	0.0	0.0	200
313.25	0.0	0.0	0.0	0.5	0.0	0.0	190
318.00	0.0	0.0	0.0	0.0	1.4	0.0	148
318.65	0.0	0.0	0.0	0.0	0.0	0.0	180
322.25	0.0	0.0	0.0	3.2	0.0	0.0	186
326.45	0.0	0.0	0.0	0.0	0.0	0.0	185
327.43	0.0	0.0	0.0	0.0	0.0	0.0	170
331.30	0.0	0.0	0.0	0.0	0.6	0.0	154
336.20	0.0	0.0	0.0	0.0	0.0	0.0	157
337.45	0.0	0.0	0.0	0.0	0.0	0.0	31
339.30	0.0	0.0	0.0	0.0	0.0	0.0	162
342.05	0.0	0.0	0.0	0.0	0.0	0.0	149
349.18	0.0	0.0	0.0	0.0	0.0	0.0	103
357.50	0.0	0.0	0.0	0.0	0.0	0.0	169
364.90	0.0	0.0	0.0	0.0	0.0	0.0	22
367.65	0.0	0.0	0.0	0.0	0.0	0.0	38
377.65	0.0	0.0	0.0	0.0	0.0	0.0	161
384.60	0.0	0.0	0.0	0.4	0.0	0.0	123
387.35	0.0	0.0	0.0	0.0	0.0	0.0	26
393.05	0.0	0.0	0.0	0.0	0.0	0.0	134
398.05	0.0	0.0	0.0	0.0	1.9	0.0	103
400.53	0.0	0.0	0.0	0.0	0.0	0.0	121
403.75	0.0	0.0	0.0	0.0	1.0	0.0	194
409.90	0.0	0.0	0.0	0.0	0.0	0.0	80
414.95	0.0	0.0	0.0	0.0	0.0	0.0	116

Depth (m)	AOM	Re	O-Eq	O-La	Fh	Wp	Cu	Ww	Mb	Zoo	Sp	FTL	Df
18.00	0.0	0.6	20.6	59.8	0.0	0.4	3.4	4.6	0.0	0.0	10.6	0.0	0.0
25.10	0.0	0.0	33.0	54.0	0.0	0.0	2.0	11.0	0.0	0.0	0.0	0.0	0.0
31.85	3.0	0.0	20.0	69.0	0.0	0.0	1.0	2.0	0.0	0.0	3.0	0.0	2.0
34.75	3.0	0.2	3.8	43.4	0.2	1.0	3.4	29.6	0.0	0.8	13.8	0.8	0.0
36.80	3.0	0.0	37.0	55.0	0.0	0.0	0.0	5.0	0.0	0.0	0.0	0.0	0.0
51.15	2.0	0.0	13.0	59.7	0.0	1.0	6.0	14.0	0.0	0.0	4.0	0.0	0.3
51.70	0.7	0.0	13.0	66.7	0.0	1.0	6.3	11.7	0.0	0.0	0.7	0.0	0.0
57.30	0.6	0.6	14.6	60.4	0.2	0.0	1.6	7.4	0.0	0.4	13.2	0.2	0.8
58.95	0.8	0.8	8.6	67.0	0.0	0.2	0.4	7.6	0.2	1.0	10.8	1.8	0.8
61.05	0.2	0.2	8.4	56.2	0.0	0.6	7.0	19.6	0.0	0.0	3.2	0.0	4.6
61.70	2.0	0.0	2.3	26.7	0.0	0.0	20.3	33.0	0.0	0.3	5.3	0.0	10.0
63.50	1.7	0.0	36.3	55.0	0.0	0.0	0.3	6.3	0.0	0.0	0.3	0.0	0.0
65.80	1.0	0.0	18.4	50.6	0.0	0.6	0.6	18.2	0.0	0.2	10.0	0.0	0.4
68.95	0.3	0.7	29.0	63.3	0.0	0.0	1.7	4.0	0.0	0.0	1.0	0.0	0.0
70.60	0.8	0.8	5.6	59.4	0.0	1.2	2.0	20.2	0.0	0.0	10.0	0.0	0.0
82.15	2.4	0.8	14.6	41.0	0.0	0.8	1.6	24.2	0.0	0.4	11.4	0.0	2.8
85.70	3.0	1.0	10.8	47.8	0.0	0.4	3.8	16.6	0.0	1.0	15.2	0.2	0.2
93.90	2.6	0.2	9.8	37.2	0.0	0.0	3.8	22.4	0.0	0.4	18.8	0.8	4.0
96.00	0.6	0.2	22.6	45.8	0.2	0.6	0.6	12.0	0.0	0.0	16.8	0.0	0.6
100.90	1.2	1.4	13.0	67.2	0.0	0.8	1.0	4.2	0.0	0.0	10.8	0.2	0.2
103.30	4.8	0.2	5.0	28.0	0.0	0.2	1.0	9.8	0.0	1.8	32.0	10.2	7.0
109.00	6.0	0.0	14.0	59.0	0.0	0.0	10.0	11.0	0.0	0.0	0.0	0.0	0.0
119.50	2.0	1.2	8.6	29.2	0.0	0.2	2.0	21.2	0.0	0.8	15.6	3.0	16.2
131.70	0.4	0.4	25.8	37.4	0.0	0.4	0.4	11.2	0.0	2.0	19.8	0.2	2.0
133.55	0.3	0.0	25.0	62.3	0.0	0.7	0.3	10.0	0.0	0.0	1.3	0.0	0.0
137.70	3.4	0.4	13.8	33.8	0.2	0.6	1.2	19.6	0.0	1.0	21.4	1.6	3.0
141.60	1.2	0.4	18.6	38.6	0.0	0.0	1.2	13.4	0.0	0.0	26.4	0.2	0.0
143.97	0.0	0.4	22.6	37.6	0.0	0.2	3.2	21.2	0.4	0.0	14.4	0.0	0.0
147.06	0.0	0.0	48.3	43.3	0.0	0.0	3.0	4.7	0.0	0.0	0.7	0.0	0.0
149.90	17.4	0.0	43.0	36.4	0.0	0.0	0.6	0.4	0.0	0.0	2.2	0.0	0.0
155.70	1.4	0.2	34.6	43.8	0.0	1.2	2.4	6.0	0.0	0.0	8.6	0.0	1.8
158.30	1.0	1.4	10.2	47.6	0.2	1.8	2.4	24.6	0.4	0.0	10.2	0.2	0.0
159.43	1.4	0.2	8.2	32.6	0.2	0.2	5.4	21.2	0.0	0.0	30.6	0.0	0.0
167.70	0.6	0.4	28.4	41.8	0.0	0.4	2.2	8.8	0.2	0.0	16.8	0.0	0.4
174.06	1.6	0.0	19.2	49.4	0.0	0.2	1.0	11.4	0.2	0.0	16.8	0.0	0.2
182.10	3.2	0.2	4.4	32.6	2.2	2.0	3.0	38.8	1.2	0.0	11.6	0.0	0.8
184.00	0.6	0.4	18.2	35.8	0.4	0.2	2.6	16.6	0.2	0.0	24.8	0.2	0.0
209.50	3.2	0.4	6.2	50.0	0.4	0.6	5.4	15.2	0.0	0.2	18.4	0.0	0.0
210.55	2.0	1.4	8.0	48.0	0.2	0.6	3.2	25.2	0.0	0.4	10.4	0.2	0.4
215.05	0.0	0.0	21.6	29.6	0.0	0.2	1.0	11.8	0.0	0.2	35.4	0.2	0.0
216.60	1.0	0.2	9.6	50.4	0.4	0.8	5.4	19.0	0.0	0.2	12.2	0.2	0.6
218.10	0.8	0.2	8.4	46.8	0.0	0.0	1.2	17.4	0.0	0.0	25.0	0.2	0.0
225.15	1.2	0.2	4.0	53.4	0.0	0.4	2.2	21.4	0.0	0.0	17.0	0.2	0.0
230.50	0.6	0.4	4.0	53.4	0.2	1.4	2.8	21.6	0.2	0.0	14.4	0.0	1.0
233.27	0.8	1.0	4.0	47.6	0.6	0.8	9.0	18.2	0.2	0.6	14.8	0.8	1.6
233.70	0.2	0.8	6.8	41.4	0.2	0.2	2.4	29.4	0.6	1.8	15.6	0.2	0.4
242.05	0.4	0.4	17.0	48.6	0.6	0.4	1.0	12.6	0.0	0.0	18.8	0.2	0.0
244.35	1.0	0.2	5.0	52.0	0.6	0.4	6.4	20.8	0.6	0.0	13.0	0.0	0.0
246.75	1.2	1.4	6.8	54.6	0.0	0.0	3.6	20.0	0.6	0.0	11.4	0.2	0.2
248.40	0.8	1.4	7.4	49.6	0.6	0.8	3.6	23.0	0.0	0.4	11.4	0.4	0.6
250.73	1.0	2.0	8.2	48.0	0.0	1.4	1.4	26.8	0.0	0.0	10.6	0.0	0.6
252.75	0.2	0.6	8.0	51.8	0.2	0.2	2.2	14.6	0.0	0.2	19.4	0.2	2.4
254.83	0.4	0.4	3.6	38.0	0.2	0.8	2.4	31.6	0.2	0.2	21.8	0.0	0.4
255.57	0.6	0.8	2.4	43.0	1.2	0.4	4.6	33.8	0.4	0.0	12.2	0.2	0.4
257.65	0.4	0.8	4.6	51.4	0.8	1.0	2.8	25.2	0.4	0.0	12.4	0.0	0.2
259.87	0.2	0.2	4.4	49.2	0.0	0.8	3.6	28.2	0.0	0.0	13.0	0.2	0.2
261.70	0.4	0.4	4.8	48.6	0.2	0.2	8.6	25.4	0.0	0.2	10.4	0.2	0.6
263.32	0.6	0.4	2.4	47.0	0.2	1.0	6.6	22.8	0.8	0.0	17.6	0.0	0.6

Appendix 3a. Palynofacies distribution (percentages) of well GTP-17-SE (continued).

Depth(m)	AOM	Re	O-Eq	O-La	Fh	Wp	Cu	Ww	Mb	Zoo	Sp	FTL	Df
265.78	0.8	0.4	5.0	41.4	0.2	1.6	5.0	31.8	0.0	0.0	13.2	0.4	0.2
268.40	0.4	0.6	3.4	45.0	0.4	1.0	12.6	25.2	0.0	0.0	11.4	0.0	0.0
271.48	0.6	0.8	2.2	27.0	0.2	0.4	14.2	30.4	0.0	0.6	23.6	0.0	0.0
273.20	0.8	0.6	1.8	57.4	0.6	1.6	1.0	25.8	0.0	0.2	9.6	0.2	0.4
275.72	1.8	1.0	4.4	52.6	0.4	0.4	1.2	24.6	0.0	0.0	11.2	0.4	2.0
277.75	1.0	2.0	5.6	63.8	0.0	1.2	2.6	12.2	0.0	0.4	11.0	0.2	0.0
283.83	0.6	0.2	3.6	37.0	0.0	0.2	2.0	27.2	0.0	0.4	26.0	1.2	1.6
285.83	25.6	0.2	3.6	28.2	0.0	0.4	1.6	21.0	0.0	0.2	15.6	0.0	3.6
287.02	13.6	0.4	2.6	25.8	0.2	0.4	1.8	32.6	0.0	0.6	17.4	0.2	4.4
292.25	0.8	0.4	22.6	36.4	0.0	1.0	0.8	25.4	0.0	0.6	9.8	1.4	0.8
294.75	0.2	0.2	13.2	37.8	0.0	0.8	2.0	16.2	0.0	0.8	27.2	1.0	0.6
298.30	1.0	0.0	12.0	43.6	0.2	0.2	2.6	14.6	0.2	0.0	25.4	0.2	0.0
300.93	0.2	0.2	13.0	42.2	0.2	0.6	4.8	17.6	0.0	0.8	19.4	0.8	0.2
302.25	1.4	0.4	5.6	44.6	0.2	0.2	2.2	31.0	0.8	0.6	12.8	0.2	0.0
304.18	1.2	0.6	9.6	43.4	0.2	1.0	3.6	25.2	0.0	0.6	13.0	1.0	0.6
306.00	1.2	0.0	9.0	35.6	0.4	0.2	1.0	39.6	0.6	0.8	10.6	0.6	0.4
309.05	43.8	0.0	3.6	22.6	0.2	0.2	0.2	8.4	0.0	0.4	18.6	0.4	1.6
315.23	1.6	0.2	6.8	43.8	0.0	1.4	6.2	27.4	0.0	0.4	11.8	0.0	0.4
317.75	2.0	0.0	4.2	42.2	0.4	1.4	3.4	32.6	0.0	0.6	11.8	0.6	0.8
318.00	1.2	0.0	11.2	46.8	0.6	0.8	2.8	26.4	0.0	0.6	9.6	0.0	0.0
322.95	0.6	0.2	4.8	47.8	0.4	0.4	3.4	29.2	0.2	0.8	11.8	0.2	0.2
325.80	60.0	0.0	1.8	16.4	0.0	0.2	0.2	9.0	0.0	0.6	10.8	0.8	0.2
327.31	57.8	0.0	0.6	10.4	0.2	0.0	0.2	10.4	0.0	0.2	16.2	3.0	1.0
328.67	20.2	0.0	1.8	17.0	0.0	0.6	0.4	29.4	0.0	0.4	22.6	4.6	3.0
329.50	18.2	0.0	2.6	37.2	0.0	0.6	0.6	25.8	0.0	0.0	12.6	1.6	0.8
331.50	43.8	0.0	2.4	30.2	0.0	0.0	2.6	10.6	0.0	0.0	10.4	0.0	0.0
339.80	67.0	0.2	1.2	8.2	0.0	0.2	0.2	4.2	0.0	0.0	17.0	1.6	0.2
340.40	29.4	0.4	2.2	47.4	0.4	0.6	0.8	7.8	0.2	0.2	10.6	0.0	0.0
341.30	26.0	0.2	4.2	44.6	0.6	0.6	0.8	12.0	0.0	0.4	10.6	0.0	0.0
350.50	14.4	1.2	2.0	63.0	0.0	0.0	0.6	7.2	0.0	0.0	11.6	0.0	0.0
351.50	31.4	0.4	2.8	33.6	0.0	0.4	2.0	14.8	0.6	0.0	14.0	0.0	0.0
362.72	13.4	0.2	2.8	59.6	0.0	0.0	1.2	9.6	0.2	1.0	12.0	0.0	0.0
363.83	53.0	0.0	1.8	23.6	0.4	1.6	0.0	9.2	0.0	0.4	10.0	0.0	0.0
368.30	20.0	0.2	2.0	50.2	0.4	0.4	2.0	12.2	0.8	1.2	10.6	0.0	0.0
369.23	28.6	0.0	2.6	35.2	0.0	0.2	2.2	19.6	0.0	0.0	11.6	0.0	0.0
372.95	39.4	0.0	2.4	32.4	0.0	0.2	1.0	8.2	0.0	0.0	16.4	0.0	0.0
374.15	1.0	0.2	10.4	52.0	0.8	0.6	1.2	18.2	0.0	0.0	15.6	0.0	0.0
378.77	37.6	0.0	3.0	29.2	0.2	0.4	0.4	17.8	0.0	0.0	11.4	0.0	0.0
384.15	6.4	0.2	4.4	49.6	0.0	0.0	3.0	13.6	0.0	0.0	22.8	0.0	0.0
385.27	2.6	0.2	6.2	51.2	0.2	0.4	4.6	24.6	0.0	0.0	10.0	0.0	0.0
386.86	37.8	0.2	1.0	32.0	0.4	0.0	1.4	12.8	0.0	0.0	14.4	0.0	0.0
389.35	32.8	0.4	1.2	38.8	0.0	0.2	0.0	4.0	0.0	0.0	22.6	0.0	0.0
393.25	1.2	0.4	4.8	60.4	0.4	0.6	1.6	15.0	0.4	0.2	15.0	0.0	0.0
396.62	0.8	0.2	4.8	46.4	0.0	1.0	0.2	23.4	0.0	0.2	23.0	0.0	0.0
409.50	56.0	0.0	6.0	18.0	0.0	0.0	0.0	5.0	0.0	0.0	15.0	0.0	0.0
415.88	32.6	0.2	4.0	30.0	0.0	0.4	0.2	12.6	0.0	0.2	19.8	0.0	0.0
440.65	64.4	0.0	0.2	14.2	0.0	0.0	0.2	6.6	0.0	0.0	13.2	1.2	0.0
443.20	0.2	0.4	6.4	61.6	0.0	0.2	0.0	11.4	0.0	1.2	12.6	5.2	0.8
444.17	12.0	0.0	14.2	53.0	0.0	0.2	0.4	10.2	0.0	0.0	9.0	0.6	0.4
451.40	74.2	0.0	0.0	10.0	0.0	0.0	0.0	1.2	0.0	0.6	7.4	6.6	0.0
456.25	32.4	0.0	6.6	42.0	0.0	0.2	0.0	5.6	0.0	0.0	11.6	1.4	0.2
467.40	47.2	0.0	4.0	22.8	0.0	1.4	1.4	12.2	0.0	0.2	10.6	0.2	0.0
469.25	0.4	0.0	22.4	53.2	0.0	0.8	0.8	12.2	0.0	0.0	10.2	0.0	0.0
470.10	20.0	1.4	4.8	32.8	0.0	0.6	0.8	10.4	0.0	0.0	28.8	0.4	0.0
470.95	13.4	0.0	5.8	46.0	0.0	0.2	1.4	7.4	0.0	0.0	25.8	0.0	0.0
Mean	*10.5*	*0.4*	*9.9*	*43.3*	*0.2*	*0.5*	*2.6*	*17.0*	*0.1*	*0.3*	*13.8*	*0.5*	*0.8*

Appendix 3a. Palynofacies distribution (percentages) of well GTP-17-SE (continued).

Depth (m)	AOM	Re	O-Eq	O-La	Fh	Wp	Cu	Ww	Mb	Zoo	Sm	FTL	Df
12.64	9.8	1.6	28.4	47.8	0.8	1.2	1.2	7.0	1.0	0.0	0.4	0.0	0.8
13.25	25.2	2.6	8.6	41.6	1.0	1.4	3.0	7.0	3.2	0.0	2.0	0.0	4.4
15.55	70.4	1.0	3.6	10.6	0.6	0.4	3.2	4.4	0.2	0.0	4.0	0.2	1.4
15.78	63.2	0.2	4.0	8.4	0.0	0.8	1.8	7.0	0.8	0.0	5.4	0.2	8.2
16.00	42.0	2.0	11.0	16.2	0.6	0.6	2.2	6.4	2.8	0.0	5.6	0.4	10.2
16.45	44.2	0.0	5.0	15.2	0.0	1.4	3.8	4.2	2.2	0.0	22.6	0.2	1.2
16.65	28.6	0.0	5.8	9.4	0.0	0.6	1.6	48.0	1.0	0.0	2.0	0.0	3.0
17.90	63.4	0.2	3.4	9.2	0.6	2.0	1.2	6.4	0.8	0.0	12.2	0.0	0.6
18.63	25.4	0.4	8.4	21.2	0.4	1.8	0.8	18.6	3.6	0.0	3.4	1.2	14.8
19.24	46.8	1.2	3.0	19.0	1.2	1.2	6.4	9.2	3.4	0.0	6.0	0.0	2.6
19.35	44.2	0.4	2.4	19.8	2.0	0.2	2.4	15.8	2.6	0.0	4.4	0.0	5.8
19.85	50.2	0.6	1.8	17.4	0.6	0.8	3.8	9.6	4.2	0.0	9.8	0.0	1.2
20.53	52.2	2.4	1.8	15.0	0.2	0.2	4.0	7.6	5.0	1.4	5.2	0.2	4.8
20.85	26.0	1.4	7.0	18.4	0.0	1.2	1.2	23.8	3.4	0.4	1.8	0.6	14.8
22.80	59.8	0.8	1.2	13.0	0.2	0.0	0.8	5.6	2.8	0.4	5.4	0.2	9.8
22.88	16.6	0.0	5.8	22.6	0.0	1.2	0.6	33.6	0.0	0.0	9.0	0.6	10.0
23.55	52.2	0.2	6.4	12.0	0.0	0.8	1.2	17.4	0.2	0.4	5.6	1.8	1.8
24.05	50.8	0.4	3.8	18.8	0.4	0.0	1.0	7.4	0.8	0.0	15.4	0.4	0.8
25.30	39.6	0.2	8.6	23.2	0.0	0.4	1.6	19.6	0.6	0.6	2.4	1.4	1.8
26.23	44.4	3.6	3.6	10.4	3.2	1.4	0.8	12.8	0.8	0.0	14.4	0.0	4.6
26.83	30.0	2.4	3.6	15.2	1.0	2.2	1.0	26.0	0.0	0.4	16.6	0.4	1.2
28.00	10.2	7.8	10.4	24.0	0.4	0.6	0.6	20.6	0.0	0.6	7.8	7.2	9.8
30.60	38.0	2.6	4.6	11.6	1.4	1.0	0.4	25.6	0.8	0.0	12.2	0.2	1.6
32.25	21.0	2.0	5.8	16.2	0.4	0.6	0.0	17.2	0.4	0.6	6.6	2.0	27.2
33.20	25.0	1.2	18.4	18.0	0.2	0.4	0.0	10.2	0.0	1.8	6.4	11.2	7.2
35.10	60.4	3.2	4.8	10.4	2.2	0.2	0.8	9.8	3.8	0.2	3.4	0.2	0.6
35.95	49.2	0.8	3.0	7.0	1.4	0.4	0.4	14.0	0.0	1.4	10.4	1.2	10.8
37.55	7.0	2.8	10.0	22.8	0.0	0.4	0.0	25.2	0.8	0.2	6.8	7.6	16.4
39.45	68.2	0.2	2.0	7.4	2.2	0.0	0.0	6.8	0.8	0.0	9.0	1.2	2.2
40.10	41.0	0.8	10.4	11.2	0.0	0.6	1.0	15.2	0.0	0.0	4.6	5.0	10.2
42.25	58.0	0.2	2.6	7.4	1.8	0.0	0.4	13.8	1.0	0.4	8.0	0.8	5.6
42.65	13.0	1.8	10.8	19.2	0.2	0.2	0.0	23.4	0.0	0.0	3.2	2.0	26.2
44.15	53.4	2.2	5.4	10.8	0.8	0.4	0.2	14.2	2.2	0.2	7.2	0.0	3.0
46.35	10.2	2.0	11.8	20.0	0.2	1.0	1.4	30.2	0.0	0.0	4.4	2.2	16.6
47.90	50.0	1.0	4.6	13.2	1.0	0.4	0.6	12.4	0.8	0.0	12.6	0.4	3.0
48.60	46.0	0.8	2.8	12.0	0.4	1.0	0.4	15.2	0.0	0.0	12.2	1.6	7.6
49.70	2.6	0.4	9.8	36.2	0.4	1.0	0.6	29.0	0.0	0.6	4.2	4.2	11.0
50.60	34.8	1.6	9.0	15.4	0.4	0.0	1.0	20.2	0.8	0.0	10.2	0.2	6.4
51.80	8.8	2.4	12.6	27.2	0.4	0.2	0.2	27.0	0.8	0.0	11.4	1.6	7.4
52.35	49.0	1.0	6.2	18.6	0.0	0.2	2.2	11.4	0.4	0.2	7.4	0.2	3.2
54.50	46.4	1.8	5.6	13.2	0.0	0.4	0.6	15.6	0.4	1.2	7.6	0.0	7.2
56.10	46.4	1.0	2.4	16.8	0.0	0.6	1.2	12.0	0.0	0.6	9.2	0.4	9.4
56.95	58.4	0.4	3.6	14.8	0.4	0.0	0.8	4.4	1.8	0.8	13.6	0.8	0.2
57.60	55.6	1.2	3.0	14.6	0.2	0.4	0.4	11.2	0.0	0.6	5.8	0.8	6.2
57.80	67.0	0.4	1.2	5.6	0.6	0.4	0.6	4.2	1.2	0.6	14.2	0.0	4.0
58.70	45.2	0.8	3.0	15.6	0.2	0.2	0.6	18.6	0.0	1.4	4.8	1.0	8.6
59.30	66.2	0.0	2.0	9.0	0.4	0.0	0.0	3.6	0.0	0.8	15.0	1.2	1.8
60.70	13.0	1.6	4.4	36.0	0.4	0.6	0.6	28.8	0.6	0.2	2.0	0.0	11.8
62.25	45.6	1.0	1.4	31.4	0.6	0.4	0.2	12.6	0.8	0.8	4.8	0.0	0.4
64.65	36.6	2.4	1.0	17.8	0.2	0.0	0.6	11.2	0.2	0.4	5.4	1.8	22.4
66.45	60.4	0.2	0.8	17.0	0.2	0.6	0.2	6.0	1.0	0.4	10.6	0.4	2.2
67.00	74.2	0.0	0.4	5.2	0.0	0.0	0.4	6.8	0.0	1.6	5.4	0.8	5.2
67.40	57.0	1.4	0.4	10.0	0.0	0.0	0.4	9.0	0.0	3.0	4.4	5.0	9.4
71.60	56.2	0.4	1.6	10.8	0.6	0.2	0.0	12.4	1.6	0.4	10.0	0.2	5.6
72.25	31.0	1.0	0.8	18.6	0.0	0.0	2.0	26.2	0.8	0.0	5.2	1.2	13.2
75.40	55.6	1.4	2.4	8.4	0.6	0.2	0.2	12.4	0.6	0.4	14.4	0.8	2.6
77.20	55.4	1.0	1.0	12.6	0.4	0.0	0.6	11.8	0.6	0.0	12.0	1.2	3.4
80.40	20.8	0.4	1.4	36.4	0.0	0.6	0.6	21.4	0.2	0.2	5.0	1.2	11.8
82.55	66.8	0.0	1.4	14.4	0.4	0.0	0.0	4.6	0.0	0.6	8.8	0.2	2.8

Appendix 3b. Palynofacies distribution (percentages) of well GTP-24-SE (continued).

Depth(m)	AOM	Re	O-Eq	O-La	Fh	Wp	Cu	Ww	Mb	Zoo	Sm	FTL	Df
83.00	23.4	0.4	2.2	42.6	0.0	0.6	1.8	15.4	0.0	0.8	2.6	2.0	8.2
84.90	45.2	0.2	1.2	17.0	0.2	0.4	0.6	7.2	0.0	0.6	19.0	1.4	7.0
86.70	13.2	0.2	5.0	43.2	0.6	0.0	0.6	8.6	0.0	1.0	7.6	3.8	16.2
88.40	21.0	0.2	2.4	29.6	0.2	0.4	1.6	12.6	1.2	0.4	25.0	0.8	4.6
91.25	13.4	0.4	1.2	52.6	0.4	0.6	0.6	11.8	0.2	0.2	16.6	0.6	1.4
94.35	47.0	0.0	1.6	14.4	0.4	0.4	0.2	12.4	0.0	0.2	19.0	1.6	2.8
97.65	2.8	0.4	4.0	57.6	0.6	0.4	0.6	15.2	0.0	0.0	5.6	3.2	9.6
98.20	1.6	1.6	6.8	64.4	0.4	1.4	1.2	11.6	0.0	0.0	8.6	0.4	2.0
99.20	23.8	0.2	2.8	38.8	1.0	0.8	1.2	10.4	0.0	0.0	19.4	0.8	0.8
101.70	8.0	1.2	5.8	42.2	0.0	1.2	0.4	18.6	0.0	0.2	17.8	0.8	3.8
103.15	20.6	0.2	3.0	32.8	1.2	0.0	0.4	12.6	0.0	0.2	22.6	2.8	3.6
108.10	48.6	0.2	2.6	9.8	1.0	0.6	0.2	9.0	0.0	0.4	21.6	4.4	1.6
109.40	1.4	1.2	4.4	61.2	0.0	1.6	0.8	15.0	0.0	0.0	9.6	1.4	3.4
110.60	34.2	0.4	1.8	22.0	0.4	0.4	0.4	10.0	0.0	0.0	26.0	1.4	3.0
112.70	0.8	0.4	11.2	56.2	0.6	1.8	2.0	12.0	0.0	0.4	12.2	0.0	2.4
119.50	25.2	0.6	5.0	26.6	0.4	0.8	0.4	14.8	0.0	1.2	15.2	4.2	5.6
120.60	20.6	0.4	5.0	33.8	1.0	0.6	0.2	13.4	0.0	0.2	16.4	0.2	8.2
122.85	20.2	0.8	4.0	51.8	0.4	0.2	0.6	8.0	0.0	1.8	6.6	2.8	2.8
124.40	13.8	0.4	3.8	41.4	0.0	1.2	0.6	13.0	0.0	0.4	16.0	0.8	8.6
124.67	0.8	0.4	5.6	53.4	0.2	0.6	0.0	22.6	0.0	0.8	6.2	3.0	6.4
128.10	14.6	0.2	5.4	26.6	0.2	0.6	0.6	20.6	0.0	0.0	25.4	5.0	0.8
130.55	0.0	3.2	8.6	40.4	0.4	0.4	0.6	24.0	0.0	0.0	16.0	1.4	5.0
134.45	25.4	0.8	3.6	36.6	1.2	0.2	0.2	16.4	0.0	0.2	10.4	4.8	0.2
135.75	1.6	0.0	5.6	51.4	0.0	0.8	0.2	8.8	0.0	0.4	5.0	3.6	22.6
146.10	0.4	1.2	5.2	52.2	0.0	1.8	1.0	26.6	0.0	0.0	7.6	2.6	1.4
157.15	0.0	1.6	3.0	42.6	0.2	1.4	1.6	38.0	0.0	0.0	9.8	0.6	1.2
160.35	32.2	0.6	2.8	20.2	0.4	0.2	0.4	19.6	0.0	0.6	12.2	8.8	2.0
167.25	19.4	0.2	7.2	20.8	1.4	0.2	0.2	15.2	0.0	0.2	18.2	12.0	5.0
170.43	0.0	3.0	7.0	45.8	0.2	0.2	0.4	20.2	0.0	0.0	17.0	3.0	3.2
178.56	0.6	1.0	11.2	48.0	1.0	1.0	0.2	20.6	0.0	0.2	10.2	3.2	2.8
182.06	44.6	0.0	3.6	18.8	0.0	0.0	0.0	14.0	0.0	0.0	14.0	4.8	0.2
182.60	58.2	0.4	2.6	12.8	0.4	0.2	0.2	10.4	0.0	0.2	11.0	2.6	1.0
189.80	3.4	1.8	4.8	45.4	0.0	1.0	4.0	29.2	0.0	0.2	9.6	0.0	0.6
190.75	35.0	0.0	2.0	11.2	0.8	0.0	0.2	12.8	0.0	0.4	30.0	1.8	5.8
200.68	30.0	0.6	9.4	28.4	0.6	0.4	0.2	16.0	0.0	0.0	12.0	2.0	0.4
202.40	47.8	0.0	2.4	18.2	0.4	0.2	0.2	12.8	0.0	0.4	16.8	0.6	0.2
205.85	53.0	0.0	2.6	17.8	0.4	0.0	0.2	10.8	0.0	0.6	13.0	0.6	1.0
207.80	32.2	1.0	8.0	26.0	0.0	0.8	0.2	19.4	0.0	0.2	10.2	0.8	1.2
211.85	0.0	0.8	6.4	46.2	0.6	0.6	0.8	27.2	0.0	1.0	14.6	1.6	0.2
214.75	13.4	0.2	5.2	18.0	0.2	0.6	0.0	26.8	0.0	0.0	31.8	1.6	2.2
217.00	5.2	0.6	5.6	40.2	0.4	1.0	0.0	35.0	0.0	0.2	11.4	0.4	0.0
222.00	22.4	0.2	4.6	26.0	0.4	0.0	0.2	16.2	0.0	0.0	28.0	2.0	0.0
222.25	25.4	0.0	4.2	22.8	0.6	0.0	0.4	15.4	0.0	0.0	28.4	1.6	1.2
224.60	5.8	0.2	4.4	42.0	0.0	1.4	0.8	33.4	0.0	1.2	9.8	0.8	0.2
227.10	22.4	0.4	2.8	15.6	0.2	0.2	0.0	19.0	0.0	0.0	38.4	0.2	0.8
227.70	22.2	0.8	7.6	33.4	0.0	0.4	0.0	25.2	0.0	0.0	10.2	0.2	0.0
232.90	48.0	0.0	2.0	12.2	0.4	0.4	0.0	9.4	0.0	0.4	25.2	1.6	0.4
237.60	38.6	0.0	1.8	16.4	0.2	0.4	0.0	7.6	0.0	0.0	31.8	2.8	0.4
237.70	6.6	0.0	5.4	35.4	0.2	1.2	0.8	35.4	0.0	0.4	13.8	0.8	0.0
239.75	30.4	0.0	1.0	8.8	0.6	0.0	0.0	14.0	0.0	0.0	43.4	0.4	1.4
240.65	20.8	0.2	2.4	17.2	0.0	0.0	0.0	15.2	0.0	0.2	43.2	0.0	0.8
241.25	32.0	0.0	3.3	31.7	0.0	1.7	0.0	17.0	0.0	1.0	2.3	6.7	4.3
243.95	34.6	0.2	3.0	15.6	1.4	0.0	0.0	13.8	0.0	0.2	30.0	0.2	1.0
247.00	12.8	0.0	1.6	19.4	1.0	1.4	0.6	14.0	0.0	0.0	48.8	0.0	0.4
249.10	23.2	0.0	2.6	18.6	0.4	0.8	0.0	12.0	0.0	0.0	42.2	0.0	0.2
252.60	34.4	0.2	0.8	20.0	0.4	0.8	0.2	19.8	0.0	0.2	22.4	0.6	0.2
254.60	49.0	0.2	2.4	18.6	0.0	0.8	0.6	18.2	0.0	0.0	8.2	1.6	0.4
255.65	52.6	0.2	2.2	11.6	1.6	0.4	0.2	9.6	0.0	0.2	20.8	0.0	0.6
256.10	41.4	0.6	1.2	20.6	0.2	1.0	1.0	6.2	0.0	0.0	24.6	1.0	2.2

Appendix 3b. Palynofacies distribution (percentages) of well GTP-24-SE (continued).

Depth(m)	AOM	Re	O-Eq	O-La	Fh	Wp	Cu	Ww	Mb	Zoo	Sm	FTL	Df
258.50	46.4	0.0	1.8	25.4	0.0	0.4	0.8	4.4	0.0	0.4	19.4	0.4	0.6
259.05	49.4	0.0	1.8	15.8	0.0	0.8	1.2	20.4	0.0	0.0	7.4	1.0	2.2
262.95	61.8	0.2	0.6	10.4	0.0	0.2	0.2	9.4	0.0	0.0	17.0	0.2	0.0
265.10	49.0	0.2	0.4	15.4	0.0	0.0	0.2	6.8	0.0	0.0	26.4	1.2	0.4
268.05	12.6	0.2	1.0	19.2	0.2	1.6	0.0	30.0	0.0	0.8	9.4	11.2	13.8
268.30	55.8	0.0	0.8	14.4	0.4	0.6	0.2	4.8	0.0	0.0	22.0	0.6	0.4
268.75	22.4	0.2	1.6	33.0	0.0	1.6	1.4	23.8	0.0	1.6	4.8	3.0	6.6
272.55	4.2	0.4	3.8	30.8	0.0	1.4	3.2	43.4	0.0	1.2	11.6	0.0	0.0
277.70	47.2	0.2	0.4	17.0	0.4	0.6	0.4	10.4	0.0	0.6	22.8	0.0	0.0
289.60	5.8	0.0	6.2	57.4	0.0	0.8	0.8	18.8	0.0	0.0	10.2	0.0	0.0
291.50	4.6	0.2	4.8	55.2	0.2	0.6	2.8	21.2	0.0	0.2	10.2	0.0	0.0
295.10	9.2	0.0	3.8	55.8	0.0	0.6	2.6	16.2	0.0	0.0	11.8	0.0	0.0
299.30	25.0	0.2	2.8	45.0	0.2	1.4	1.2	12.8	0.0	0.0	11.4	0.0	0.0
300.60	51.2	0.2	1.0	22.2	0.0	1.2	1.0	11.0	0.0	0.0	12.2	0.0	0.0
304.05	0.0	0.8	1.2	44.8	0.0	2.8	1.8	34.8	0.0	0.0	13.8	0.0	0.0
308.95	4.2	0.0	0.8	30.8	0.0	1.2	1.6	36.2	0.0	0.0	25.2	0.0	0.0
309.53	0.4	0.2	1.6	38.8	0.6	2.2	1.8	29.2	0.0	0.0	25.2	0.0	0.0
313.25	1.2	0.0	6.2	48.4	0.4	0.4	0.6	23.8	0.0	0.0	19.0	0.0	0.0
318.00	59.6	0.0	1.6	18.2	0.2	0.2	0.4	8.2	0.0	0.0	11.6	0.0	0.0
318.65	52.6	0.0	2.4	14.8	0.6	0.4	0.6	9.6	0.0	0.0	19.0	0.0	0.0
322.25	1.6	1.0	6.0	30.8	0.0	0.6	0.2	25.2	0.0	0.0	34.6	0.0	0.0
326.45	62.8	0.0	1.0	18.2	0.2	0.2	0.0	7.2	0.0	0.0	10.4	0.0	0.0
327.43	36.0	1.4	1.6	33.8	0.0	0.4	0.8	16.0	0.0	0.0	10.0	0.0	0.0
331.30	1.0	0.0	7.0	37.8	1.0	1.0	1.8	28.0	0.6	0.0	21.8	0.0	0.0
336.20	26.8	0.2	4.4	25.8	0.4	0.4	0.8	18.2	0.0	0.2	22.6	0.2	0.0
337.45	54.3	0.0	0.7	20.0	0.3	0.3	0.0	6.7	0.0	0.0	17.7	0.0	0.0
339.30	2.6	2.2	10.0	27.8	0.4	1.4	1.6	36.8	0.0	0.2	17.0	0.0	0.0
342.05	3.2	0.2	10.8	46.2	0.4	0.6	1.0	21.8	0.0	0.0	15.8	0.0	0.0
349.18	39.2	0.4	5.8	22.0	0.8	0.6	3.0	16.4	0.0	1.4	10.4	0.0	0.0
357.50	7.4	0.0	17.0	40.0	0.2	0.0	0.8	19.0	0.0	0.0	15.4	0.0	0.2
364.90	75.3	0.0	0.7	14.0	0.0	0.0	0.3	3.0	0.0	0.0	6.7	0.0	0.0
367.65	66.0	0.0	4.0	12.5	0.5	0.0	0.0	10.5	0.0	0.0	6.5	0.0	0.0
377.65	11.6	0.8	5.8	38.0	0.4	0.4	0.2	15.6	0.0	0.0	27.2	0.0	0.0
382.75	33.0	0.0	0.2	28.0	0.0	0.4	0.2	6.4	0.0	0.0	31.8	0.0	0.0
384.60	2.4	0.6	2.4	48.6	0.2	1.8	0.0	12.0	0.0	0.0	32.0	0.0	0.0
393.05	62.4	0.0	1.2	13.0	0.0	0.0	0.0	5.6	0.0	0.0	16.6	0.0	1.2
398.05	64.8	0.2	0.8	12.6	0.0	0.2	0.0	5.2	0.0	0.0	15.0	0.0	1.2
400.53	45.2	0.0	3.8	28.0	0.6	0.6	0.0	6.8	0.0	1.6	11.2	2.2	0.0
403.75	31.7	0.7	6.3	34.0	0.3	0.3	0.3	10.3	0.0	1.0	12.7	2.3	0.0
409.90	49.0	0.0	3.6	27.8	0.0	0.8	0.2	7.2	0.0	0.0	10.2	1.2	0.0
414.95	40.7	0.0	3.3	27.3	0.7	0.3	0.0	9.3	0.0	1.0	17.3	0.0	0.0
Mean	*32.0*	*0.7*	*4.4*	*25.4*	*0.4*	*0.6*	*0.8*	*15.8*	*0.4*	*0.3*	*13.9*	*1.4*	*3.8*

Appendix 3b. Palynofacies distribution (percentages) of well GTP-24-SE (continued).

Depth (m)	TOC	HI	OI
13.20	1.25	78	121
15.30	3.22	205	60
16.00	3.22	2	25
16.40	3.37	147	59
17.60	3.45	319	57
19.60	4.82	303	47
20.30	0.56	57	118
20.70	3.03	233	46
22.90	1.67	216	61
23.30	0.5	74	114
24.40	2.85	90	64
26.10	3.48	234	49
30.40	1.6	167	53
31.80	3.01	285	52
34.70	1.87	150	57
37.20	0.41	20	132
39.00	4.89	460	44
41.50	2.84	298	46
42.40	1.16	141	92
44.10	2.71	337	56
45.50	1.88	258	60
47.50	2.2	215	53
50.00	1.93	98	56
51.50	1.67	172	56
53.70	2.48	78	58
54.80	0.63	65	140
56.00	3.42	270	47
58.20	2.84	352	52
61.00	2.25	227	76
63.00	4.23	562	51
66.60	1.82	102	57
67.20	0.66	58	112
71.30	1.95	146	57
74.90	1.21	181	76
77.10	2.72	160	53
82.50	1.53	175	69
84.50	0.81	91	79
86.00	0.95	59	62
88.30	1.57	49	64
89.40	1.3	38	68
92.60	0.74	105	155
95.50	1.64	62	61
97.00	0.2	1345	740
99.50	1.6	150	73
102.00	1.8	128	79
105.30	1.41	104	83
108.50	1.61	126	79
110.50	1.52	131	70
112.50	2.33	238	55
116.50	1.02	84	100
118.70	1.71	192	68
119.90	1.83	234	69
121.50	1.9	223	67
123.50	1.41	96	72
124.50	0.85	34	96
125.40	1.35	130	76
128.20	1.51	126	69
132.20	0.28	57	186
134.50	1.92	192	64
141.00	0.92	33	86
146.00	0.58	36	166
160.00	1.16	151	87
166.50	0.82	52	126
182.20	3.02	385	46
190.00	2.26	327	61
191.70	1.05	205	92
192.60	1.14	211	89
202.50	1.68	240	78
204.00	1.9	223	67
205.00	1.52	215	72
213.40	1.22	131	86

Appendix 4. Geochemical data of well GTP-24-SE (continued).

Depth (m)	TOC	HI	OI
215.00	1.78	151	74
218.00	1.08	86	88
222.50	1.99	253	58
226.60	2.86	347	52
226.70	2.9	420	46
232.00	1.83	242	68
234.00	1.7	217	66
236.00	2.63	356	69
240.50	2.2	100	56
243.90	2.69	316	54
246.30	2.03	226	62
250.00	1.4	164	71
251.50	2.7	273	44
253.00	1.61	84	60
253.20	2.38	1	14
256.00	3.26	310	36
257.50	2.79	5	25
261.00	2.35	6	31
264.00	6.64	365	53
265.00	4.47	413	55
266.50	6.94	685	41
287.80	0.82	79	95
291.60	1.52	139	70
294.30	1.96	223	67
297.90	2.5	409	54
305.20	1.02	221	86
315.00	0.74	104	107
317.00	2.32	350	60
321.50	0.98	108	96
323.30	1.12	105	94
324.70	2.33	497	69
336.10	2.44	439	57
337.90	1.82	870	57
343.60	1.76	631	81
346.20	9.59	1234	41
346.50	3.12	831	66
346.80	0.91	478	223
348.10	0.74	328	432
350.40	1.31	331	321
357.30	0.97	232	218
358.60	0.98	137	205
364.00	2.56	509	84
365.70	2.94	745	66
366.30	2.77	685	112
367.50	2.98	755	73
368.80	1.44	533	112
370.30	2.8	702	63
370.65	1.91	605	89
372.60	3.71	824	73
373.20	1.16	417	177
373.70	4.72	812	64
375.60	3	566	87
376.20	1.42	406	184
377.50	2.86	611	97
378.80	0.8	428	218
380.10	0.93	292	306
382.40	4.28	604	27
388.80	3.25	634	74
389.40	5.13	824	23
392.30	6.58	797	45
393.00	4.96	800	29
396.80	7.31	797	43
397.70	7.07	857	41
398.10	8.45	827	62
398.70	4.3	525	84
403.75	0.62	229	363
406.90	0.62	229	345
408.10	1.06	289	232
414.90	0.67	233	364

Appendix 4. Geochemical data of well GTP-24-SE (continued).